Graph-based identification of critical elements in urban water infrastructure

Meijer, D.H.

Important note
To cite this publication, please use the final published version (if applicable).
Please check the document version above.

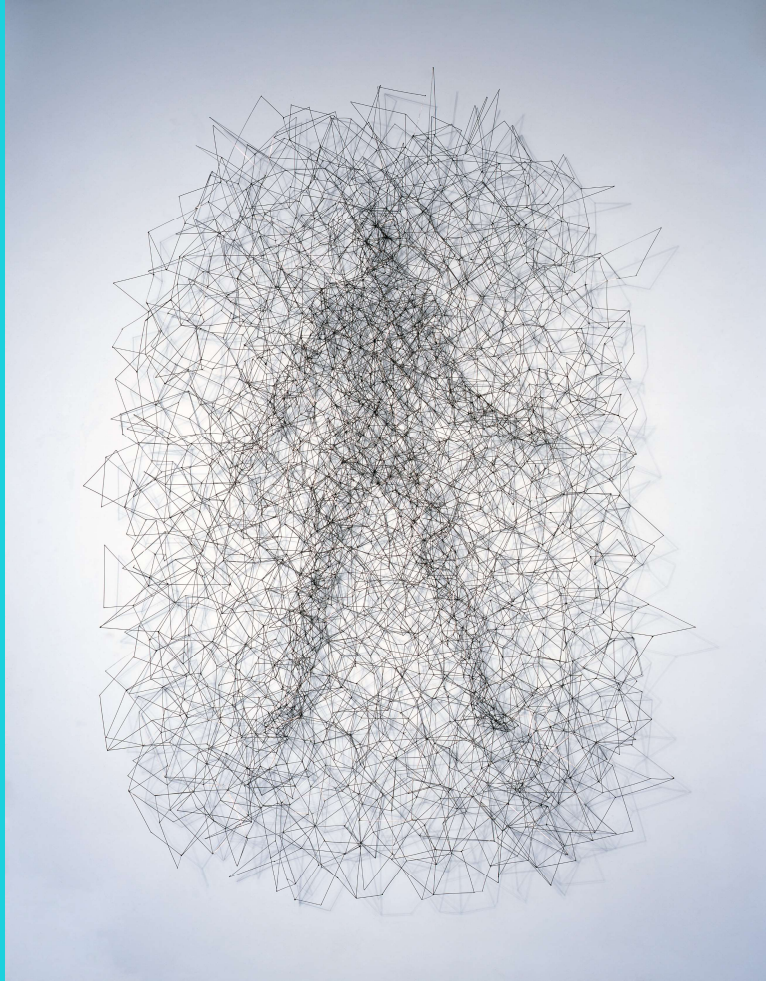# Graph-based identification
# of critical elements
in urban water infrastructure

Mass (Gormley, 2006)

Didrik Meijer

Graph-based identification of critical elements in urban water infrastructure

Didrik Meijer

Graph-based identification of critical elements in urban water infrastructure

Dissertation

for the purpose of obtaining the degree of doctor
at Delft University of Technology
by the authority of the Rector Magnificus, prof.dr.ir. T.H.J.J. van der Hagen
chair of the Board for Doctorates
to be defended publicly on
Tuesday 28 February 2023 at 12:30 o'clock

by

Dirk Hendrik MEIJER
Master of Science in Civil Engineering, University of Twente, the Netherlands
born in Zevenaar, the Netherlands

"Don't judge each day by the harvest you reap
but by the seeds that you plant."

(Stevenson, 1884/2013)

Acknowledgements

During the time I was working on my research, I learned many things and gained a number of insights. Some of these are directly related to this research, and others are not. Examples are:

- In spite of my experience, there is still much to learn.
- Running helps me to organise my thoughts, clear my mind and gain new insights.
- Structured scripting is a skill.
- Combining a full-time job, PhD research and family life is a challenge.
- It is okay to ask for help, and many people are happy to help.
- I don't have to know, or be able, to do everything.
- Preparing for and running a marathon takes less time than a PhD project.
- I enjoy coming up with new ideas and solutions.
- Not all the things I can do well give me energy.
- I get energy from my work when it is of practical use.
- I can build a shelter.
- It is difficult to make a complete list and this list could be much longer ;).

Many people and organisations helped me or gave me the opportunity to go through this PhD process. I would like to thank you all very much!

Because I am fully aware that it is difficult to make complete lists, I will keep the list short: Francois, Hans and Jeroen, thank you for your supervision during my research. Johan and Marco, thanks for the discussions, suggestions and ideas. Deltares, colleagues, thanks for the time provided for this research.

Finally, I would also like to extend my special thanks to the studio of Antony Gormley, Stephen White and the Museum Voorlinden, Wassenaar, Netherlands for allowing me to use the photograph of *Mass*, 2006, on the cover of my thesis.

Didrik Meijer

Summary

The quality of life in urban areas is largely dependent on the functioning of infrastructural networks. Failure of road, water, energy, gas and communication networks, for example, results in inconvenience, nuisance or damage. The failure of one network can cause a negative chain reaction that also impacts the performance of other networks if they are interdependent in a physical, information-related, spatial or other way. This also applies to systems consisting of multiple networks, such as urban drainage systems that include sewers, urban surface water and regional surface water. Without maintenance, network performance decreases over time.

Sewer and water distribution networks consist of many elements. In the Netherlands, the length of the latter network is approximately 120,000 km, and that of the former is 150,000 km. They are essential networks for a healthy environment in urban areas. Increasing urbanisation and population growth, deterioration due to ageing, limited maintenance and climate change, among other things, place the functioning of these networks under pressure. Maintenance and replacement of these networks is necessary. Maintenance and rehabilitation are also challenging due to the need to keep the networks operational, the costs and the possible impact on the environment and the surrounding networks. Because budgets for these activities are limited, network managers must make choices and set priorities regarding what work to do and when to perform it.

Not all elements (connections) in a network are equally important for its performance. Various methods exist to determine the criticality of network elements. However, the existing methods have limitations in terms of either including the network performance or the required calculation effort. Due to these limitations, the methods have been applied either in a limited way or not at all in practice. When these methods are applied, the focus is often on one type of network and not a combination of networks.

The purpose of this thesis was to develop and demonstrate methods for determining the criticality of elements in networks. The impact failures could have on the network performance was its primary focus. A second objective was to determine whether the

developed method could be applied successfully based on network characteristics. To achieve these goals, research was conducted on factors that influence the criticality of an element, on the possibilities of applying simplified hydrodynamic processes in the determination of criticality and on the contribution of different model components to the functioning of water network models.

Three methods are presented to determine the criticality of elements in water distribution networks, sewer networks and urban drainage systems:
1. The Graph Theory Method (GTM) for pressurised systems.
2. The GTM for gravity-driven systems.
3. The Graph-Based Weakest Link Method (GBWLM).

The GTM for pressurised systems and the GTM for gravity-driven systems determine the criticality based on a change in "transport costs" in the network. These methods have been developed to identify the most critical elements but not to evaluate the impact of failures. The methods are only intended to indicate whether the failure of one element affects the performance of the network to a larger extent than the failure of another element.

Criticality depends on the characteristics of the element, its position in the network and the fallback (bypass) options of the network in case of (partial) failure of the element. In the GTM these characteristics are included by combining the network geometry and structure in a Graph. Iterative hydrodynamic calculations have been replaced by a "path analysis". This reduces the required calculation effort considerably. Due to the limited calculation effort, the method enables the analysis of networks consisting of many elements.

With the GTM it is possible to identify the 30–40% of pipes that are most critical in a sewer system. For water distribution networks, the GTM allows the pipes to be divided into groups with a certain degree of importance. Network managers can use this information for prioritising maintenance or rehabilitation works.

The GBWLM was developed to determine both the criticality of elements in urban drainage systems and the impact of a change in the system capacity or the load. With the GBWLM, urban drainage systems consisting of subsystems such as gully pots, storm water or combined sewers and surface water can be analysed with multiyear rainfall series. The combined analysis of systems is necessary because the subsystems have very different storage and drainage capacities. As a result, the systems may react differently to changes in load as a result of climate change or urbanisation.

x

The Network Linearisation Parameter (NLP) was developed to estimate the reliability of the results of the GBWLM in advance. In the GBWLM, hydraulic processes are simplified by linearisation. The simplified hydraulics must provide a sufficiently reliable indication of the actual functioning. With the NLP, the bottlenecks (a bottleneck is a pipe with a larger hydraulic gradient at high flows than the adjacent upstream pipe) in a system can be determined. Depending on the location and size of the pipes with a potentially high water-level gradient and the part of the network affected by these pipes, it can be determined whether the GBWLM can be successfully applied to a network.

The NLPs of seven Urban Drainage Networks (UDNs) with different topological characteristics were determined. The seven UDNs exhibited different characteristics based on the NLP. These UDNs were also analysed with the GBWLM and the results were compared to a reference model. Of the UDNs that matched the reference model well, the bottleneck thresholds were lower and the bottlenecks were not close to outlets.

The developed methods can contribute to "risk-based management", in which network managers balance the risks of failures and the necessity of maintenance and replacement activities. The methods provide network managers with the possibility to adjust maintenance and replacement criteria to the criticality of an element related to the functioning of the entire network. Instead of maintaining all elements with the same frequency and setting the same quality requirements for all elements, the developed methods allow network managers to objectively differentiate maintenance based on the criticality of an element for the functioning of the network.

The GTM, the GBWLM and the NLP have been applied to a limited number of case studies. For these case studies, statistical tests have shown that there is a clear correlation with the methods based on hydrodynamic models. However, more tests are needed before these methods can be widely applied in practice. In addition, there are several applications for graph-based analysis that could be further explored. These include:
- Developing cleaning strategies.
- Developing monitoring strategies.
- Increasing the robustness of (storm water and combined sewer) networks during (re)design by adapting the structure or geometry.
- Impact analyses of hydraulic failure of systems by combining the results of the GTM and GBWLM with GIS analyses.
- Application of the GTM, GBWLM and NLP to other networks.

Samenvatting

De kwaliteit van leven in stedelijke gebieden is sterk afhankelijk van het functioneren van netwerken. Uitval van bijvoorbeeld wegen-, water-, energie-, gas- en communicatienetwerken leidt tot hinder, overlast of schade. Het uitvallen van een netwerk kan een negatieve kettingreactie veroorzaken. Dit kan de prestaties van andere netwerken beïnvloeden als deze van elkaar afhankelijk zijn. Dit geldt ook voor systemen die uit meerdere netwerken bestaan. Een voorbeeld hiervan zijn stedelijke watersystemen die bestaan uit riolering, stedelijk oppervlaktewater en regionaal oppervlaktewater. Zonder onderhoud nemen de prestaties van netwerken na verloop van tijd af.

In Nederland is het rioolnetwerk ongeveer 150.000 km lang en het waterleidingnetwerk 120.000 km. Het zijn essentiële netwerken voor een gezond leefmilieu in stedelijke gebieden. Het functioneren van deze netwerken staat onder druk door toenemende verstedelijking en bevolkingsgroei, veroudering, beperkt onderhoud en klimaatverandering. Onderhoud en vervanging van deze netwerken is noodzakelijk. Dit is een uitdaging omdat de netwerken tijdens de onderhoudswerkzaamheden operationeel moeten blijven en vanwege de kosten. Netwerkbeheerders moeten keuzes maken en prioriteiten stellen met betrekking tot welke werkzaamheden wanneer moeten worden uitgevoerd omdat de budgetten voor onderhoud en vervanging beperkt zijn.

Niet alle elementen (bijvoorbeeld leidingen, putten of gemalen) in een netwerk zijn even belangrijk voor de netwerkprestaties. Er bestaan verschillende methoden om de mate van belangrijkheid van netwerkelementen te bepalen. De bestaande methoden hebben echter beperkingen wat betreft het meenemen van de netwerkprestaties of de vereiste rekeninspanning. Vanwege deze beperkingen worden de methoden in de praktijk niet of slechts beperkt toegepast. Wanneer deze methoden worden toegepast ligt de nadruk vaak op één type netwerk en niet op een combinatie van netwerken.

Het doel van dit proefschrift is het ontwikkelen en demonstreren van methoden voor het bepalen van de mate van belangrijkheid van elementen in netwerken. De impact die storingen zouden kunnen hebben op de prestaties van het netwerk was de primaire focus.

Een tweede doel was op basis van netwerkkenmerken bepalen of de ontwikkelde methoden succesvol kunnen worden toegepast. Om deze doelen te bereiken werd onderzoek gedaan naar factoren die de mate van belangrijkheid van een element beïnvloeden, naar de mogelijkheden om vereenvoudigde hydrodynamische processen toe te passen en naar de bijdrage van verschillende modelcomponenten aan het functioneren van waternetwerken.

Als onderdeel van dit onderzoek zijn drie methoden ontwikkeld en gepresenteerd om de mate van belangrijkheid van elementen in riool- en waterdistributienetwerken en stedelijke watersystemen te bepalen:
1. De grafentheoriemethode (Graph Theory Method [GTM]) voor druksystemen.
2. De grafentheoriemethode voor vrijvervalsystemen.
3. De op de grafentheorie gebaseerd zwakste schakel methode (Graph-Based Weakest Link Method [GBWLM]).

De GTM voor druksystemen en de GTM voor vrijvervalsystemen bepalen de mate van belangrijkheid op basis van een verandering in de 'transportkosten' in het netwerk. Deze methoden zijn ontwikkeld om de meest kritieke elementen te identificeren, maar niet om het effect van falen te evalueren. De methoden zijn alleen bedoeld om aan te geven of het falen van één element de prestaties van het netwerk sterker beïnvloedt dan het falen van een ander element.

De mate van belangrijkheid hangt af van de kenmerken van het element, de positie in het netwerk en de terugval- (bypass)opties van het netwerk in geval van (gedeeltelijke) uitval van het element. In de GTM worden deze kenmerken opgenomen door de netwerkgeometrie en -structuur te combineren in een graaf. Iteratieve hydrodynamische berekeningen zijn vervangen door 'stroompaden-analyses'. Dit vermindert de vereiste berekeningsinspanning. Door de beperktere rekeninspanning kunnen netwerken die uit vele elementen bestaan worden geanalyseerd.

Met de GTM is het mogelijk de 30-40% meest kritieke leidingen in een rioolnetwerk te identificeren. Voor waterdistributienetwerken kunnen met de GTM de leidingen worden ingedeeld in groepen met een bepaalde mate van belangrijkheid. Netwerkbeheerders kunnen deze informatie gebruiken om de onderhouds- of herstelwerkzaamheden te prioriteren.

De GBWLM is ontwikkeld om zowel de mate van belangrijkheid van elementen in stedelijke watersystemen als het effect van een verandering in de systeemcapaciteit of de belasting te bepalen. Met de GBWLM kunnen stedelijke watersystemen bestaande uit

deelsystemen zoals kolken, hemelwaterriolering of gemengde riolering en oppervlaktewater worden geanalyseerd met meerjarige neerslagreeksen. De gecombineerde analyse van systemen is nodig omdat de deelsystemen zeer verschillende berging- en afvoercapaciteiten hebben. Daardoor kunnen de systemen verschillend reageren op veranderingen in de belasting als gevolg van klimaatverandering of verstedelijking. Terugstuwing vanuit de benedenstroomse netwerken kan wateroverlast veroorzaken in de bovenstroomse netwerken.

De netwerk linearisatie parameter (Network Linearisation Parameter, [NLP]) is ontwikkeld om de betrouwbaarheid van de resultaten van de GBWLM vooraf in te schatten. In de GBWLM worden hydraulische processen vereenvoudigd door linearisatie. De vereenvoudigde hydraulica moet een voldoende betrouwbare indicatie geven van het werkelijke functioneren. Met de NLP kunnen de knelpunten (een knelpunt is een leiding met een grotere hydraulische gradiënt bij hoge debieten dan de aangrenzende bovenstroomse leiding) in een systeem worden bepaald. Afhankelijk van de ligging en de grootte van de leidingen met een potentieel grote hydraulische gradiënt en het deel van het netwerk dat door deze leidingen wordt beïnvloed, kan worden bepaald of de GBWLM met succes op een netwerk kan worden toegepast.

De NLP's van zeven rioolsystemen met verschillende topologische kenmerken zijn bepaald. De zeven rioolsystemen vertoonden verschillende kenmerken op basis van het NLP. Deze rioolsystemen zijn ook geanalyseerd met de GBWLM en de resultaten zijn vergeleken met een referentiemodel. Van de rioolsystemen die goed overeenkwamen met het referentiemodel, waren de knelpuntdrempels lager en lagen de knelpunten ver van de lozingspunten.

De ontwikkelde methoden kunnen bijdragen aan 'risicogebaseerd beheer', waarbij netwerkbeheerders de risico's van storingen en de noodzaak van onderhouds- en vervangingsactiviteiten tegen elkaar afwegen. De methoden bieden netwerkbeheerders de mogelijkheid de onderhouds- en vervangingscriteria aan te passen aan de mate van belangrijkheid van een element voor het functioneren van het gehele netwerk. De ontwikkelde methoden stellen de netwerkbeheerders in staat het onderhoud objectief te differentiëren op basis van de mate van belangrijkheid van een element voor het functioneren van het netwerk in plaats van alle elementen met dezelfde frequentie te onderhouden of voor alle elementen dezelfde kwaliteitseisen te gebruiken.

De GTM, de GBWLM en de NLP zijn toegepast op een beperkt aantal casestudies. Voor deze casestudies is uit statistische tests gebleken dat er een duidelijke correlatie is met de op hydrodynamische modellen gebaseerde methoden. Er zijn echter meer analyses nodig

voordat deze methoden op grote schaal in de praktijk kunnen worden toegepast. Bovendien zijn er verschillende toepassingen voor op de graaftheorie gebaseerde analyses die verder kunnen worden onderzocht. Deze omvatten:

- Het ontwikkelen van reinigingsstrategieën.
- Het ontwikkelen van monitoringsstrategieën.
- Het vergroten van de robuustheid van hemelwaterriolering en gemengde riolering tijdens (her)ontwerp door aanpassing van de structuur of geometrie.
- Impactanalyses van hydraulisch falen van systemen door de resultaten van de GTM en GBWLM te combineren met GIS-analyses.
- Toepassing van de GTM, GBWLM en NLP op andere type netwerken.

Contents

1 Introduction

1.1   Infrastructure in urban areas

In 2018, approximately 55% of the world's population lived in cities. This number is increasing and is expected to reach 68% by 2050 (United Nations Department of Economic and Social Affairs, 2019). In the Netherlands, municipalities are responsible for the safety policy in urban areas at the local level (*Gemeentewet, Art. 174 [Municipality act]*, 2021). This responsibility includes providing a safe living environment and maintaining the physical quality of that environment. Physical quality relates to the physical characteristics of the living environment, including the design and management of the public space (Vereniging van Nederlandse Gemeenten [VNG], 2021).

To keep cities liveable, infrastructure is becoming more and more important. Infrastructure is partly situated above ground level (e.g. transport and waste disposal) and partly underground (e.g. sewers, water distribution networks, gas networks, district heating, electricity and telecommunication). The infrastructure consists of different types of networks. Underground networks are often situated close to each other and are normally situated under roads, bicycle paths or sidewalks (Figure 1.1 [van Riel, 2016, p.7]).

1 Introduction
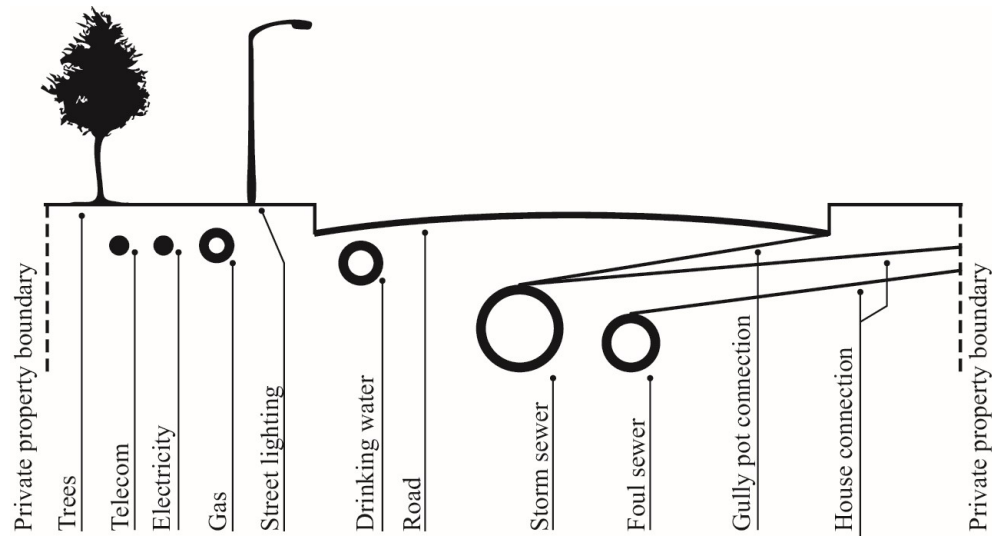
Figure 1.1   Typical layout of networked infrastructures in a Dutch residential street (Note. From On Decision-Making for Sewer Replacement p.7, van Riel, 2016. Copyright 2016 by W. van Riel. Reprinted with permission).

Not all elements in a network are equally important for the functioning of that network. For instance, a transport network consists of sidewalks, bicycle paths, local roads and main roads, and piped water networks include pipes of various diameters. The results of an analysis (see Table 1.1 Mair et al., 2017) of the location and structure of road networks, Water Distribution Networks (WDNs) and a sewer network in three areas in an alpine region shows that the length and structure differ per network and area (Mair et al., 2017).

Table 1.1   Properties of the street network, water distribution network and sewer network of three case studies (CS 1, CS 2, CS 3) in alpine region (Note. Adapted from "Where to find water pipes and sewers? On the correlation of infrastructure networks in the urban environment On Decision" Mair et al. (2017). Water, 9(2), Article 146. https://doi.org/10.3390/w9020146)

	CS 1	CS 2	CS 3
Total street network length (km)	419.48	78.1	67.87
Total water distribution network length (km)	216.75	48.7	52.2
Streets containing water distribution pipes (%)	52	62	77
Looped part of the water distribution network (%)	89	87	88
Total sewer network length (km)	201.93	41.4	46.82
Streets containing sewer pipes (%)	48	53	69
Looped part of the sewer network (%)	71	19	35

What the most important elements are, and what their position is in the network, differ from one network to another. The street network gives an indication of the structure of the networks that lie beneath it, but the network structure depends on the network type. Figure 1.2 represents the transport network, WDN and sewer network of the residential area Tuindorp in Utrecht, the Netherlands. The location of the main roads does not correspond to the pipes with the largest diameters in the WDN and sewer system. Presuming that the diameter of pipes and the type of road is an indication of criticality, then the critical elements of the different networks are scattered over the area.

Transport network
- Bicyle path
- Local road
- Main road
- Sidewalk

UDN pipe diameters (m)
- 0 - 0,45
- 0,45 - 0,9
- 0,9 - 1,35
- 1,35 - 2,25

WDN pipe diameters (mm)
- 25 - 60
- 60 - 90
- 90 - 120
- 120 - 250

Figure 1.2   Location of elements with the main capacity of the transport network, water distribution network and combined sewer system in Tuindorp, Utrecht, the Netherlands.

The performance of networks is threatened by the following (Reyes-Silva et al., 2020):
- Increasing pressure as a result of urbanisation, population growth and densification.
- Deterioration as a result of ageing (and lack of maintenance).
- Terrorist attacks.
- For some networks, climate change.

To adapt networks to changing circumstances and to prevent a decline in performance, maintenance of the networks is necessary. According to Tscheikner-Gratl, Caradot, et al. (2019), in Austria, Germany, France and the Netherlands the actual investments in maintenance and rehabilitation do not meet the expected investment needs, implying that without policy change, the service level in these countries is likely to deteriorate. Because not all elements are equally important for the functioning of a network, network managers could prioritise maintenance and rehabilitation activities if the criticality of the elements is known. However, this is often not the case.

This thesis presents methods and their application to determine the criticality of elements in networks. Network managers can use these methods to optimise maintenance and rehabilitation activities. Because the functioning of a network depends on the type of network and its design, the method must be tailored to the network characteristics. The focus of this study is on the following topics:

- Gravity-driven piped water networks, especially combined and storm sewer systems.
- Pressurised piped water networks, especially water distribution networks.
- Urban drainage systems consisting of gully pots, storm sewers and surface water.

1.2 History of water infrastructure in urban areas

From the Middle Ages onwards, water infrastructure has been developed further and further. During the Middle Ages, water was made available at a central delivery point in urban areas, and the water was then carried by the people to their homes (Mala-Jetmarova et al., 2015). The first designs of WDNs were mainly oriented to minimise transport costs of water to and within the cities (Todini, 2000).

In the 19th century, industrialisation commenced, cities began to grow, and drinking water and sanitation systems were improved. In 1854–1855, an outbreak of cholera was shown by the physician Snow to have resulted from sewage contamination of a public well in London (Hall & Dietrich, 2000; Snow, 1855). Although the importance of high-quality drinking water was already known in ancient times, the importance of good sanitation for health was only recognised in the 19th century. Industrialisation, in combination with the discovery by Snow, initiated the following developments (Kesztenbaum & Rosenthal, 2017; McKeown et al., 1972; Szreter, 1997):

- The concentration of people in urban areas contributed to an increased need for drinking water.

- The availability of drinking water reinforced the demand for sanitation infrastructure to discharge the water.
- Better hygiene due to availability of drinking water and sanitation strongly contributed to a reduction in mortality.
- Extensive population growth led to rapid socio-economic change and the growth of cities.

From the 19th century onwards, designs have moved from relatively simple WDNs to complex networks. In the 19th century, the standard design of a WDN consisted of a relatively large (e.g. 1000 mm) main ring pipe with smaller (e.g. 400 mm) radial pipes. These pipes were connected in the centre to obtain the highest level of water delivery service at any point, even in case of failure of one of the conduits (Todini, 2000). In the present day, water companies deliver water and must comply with water pressure and water quality requirements. For this purpose, they employ complex WDNs that are complex, interconnected collections of sources, pipes and hydraulic control elements (e.g. pumps, valves, regulators, tanks) (Ostfeld, 2015).

The same transition from simple to complex systems can be seen in the development of sewage systems. In the Netherlands, the first households were connected to WDNs in 1850. It took until 1880 for the first households to become connected to the sewer systems. At the end of the 19th century, large-scale sewer systems were constructed to drain the wastewater (Geels, 2006; Preston & van de Walle, 1978) from urban areas to receiving waterbodies, which were preferably downstream.

Figure 1.3 (Langeveld, 2004, p.2) shows that the process of connecting houses to the water infrastructure occurred over a period of more than 100 years. The networks have often "grown organically", following the street plan. During the construction period, there have been changes in, for example, laws and regulations and the related design standards and design criteria, available techniques, costs of manpower and materials and climate. As a result, the networks have become balanced systems, with their own specific characteristics that reflect the dominant dynamics at their specific temporal and spatial scales.

% of connected households to
a sewer system and a drinking water network
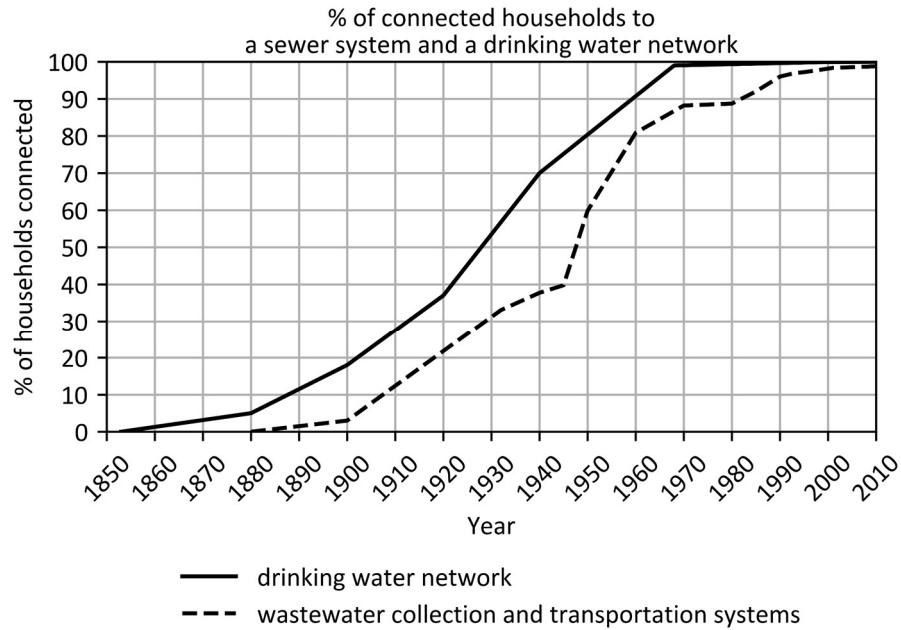
Figure 1.3   Changes in the percentage of households connected to a sewer system and a drinking water network in the Netherlands since 1850. (Note. Adapted from: Interactions within wastewater systems p.2, Langeveld, 2004).

1.3   Asset management

The functioning of networks decreases over time due to wear and tear, contamination and ageing. Therefore, regular maintenance is necessary to ensure a minimum level of functioning and service. For example, calcium carbonate incrustation was already a threat to Roman aqueducts (International Water Association Publishing, n.d.; Kessener, 2017). Regular removal was necessary to prevent blockage of water flow. Modern water systems also need maintenance to ensure the desired service level (International Water Association Publishing, n.d.; Le Gauffre et al., 2007; Wirahadikusumah et al., 2001).

Maintenance and rehabilitation budgets are always limited. Therefore, operators must prioritise these activities. Asset management is increasingly used for this process. Asset management is, according to the definition of Marlow et al. (2010), *"a combination of management, financial, economic, engineering and other practices applied to (physical) assets with the objective of maximising the value derived from an asset stock over a whole life cycle, within the context of delivering appropriate levels of service to customers, communities and the environment, and at an acceptable level of risk"* (p. 1248). Because

the service life of sewer and drinking water conduits is normally at least decades, operating companies are shifting from new designs to redesign and asset management (Tscheikner-Gratl, Caradot, et al., 2019).

For the development of efficient Urban Drainage Network (UDN) and WDN rehabilitation strategies, information is needed about the functioning and condition of the network and the individual elements as well as the consequences of failures (see Section 2.2). However, such information is often not available in sufficient detail. WDNs and UDNs are underground piped infrastructures and have often expanded over decades. The exact characteristics of these networks are often not tracked and therefore are rarely known. Information regarding actual maintenance condition is even more scarce (Tscheikner-Gratl, Caradot, et al., 2019). Because these systems are underground networks in urban areas, it is difficult, time-consuming and costly to collect this information. Therefore, decisions tend to be made based on incomplete management files and documents. The experience of operators and tacit knowledge of the networks play essential roles in decision-making (van Riel, 2016).

Asset management can be implemented as risk-based management. Risk can be defined as the consequences of failure multiplied by the probability of occurrence (Risk = Consequence × Probability) (International Organization for Standardization [ISO], 2014, 2017). The "critical assets" are assets that potentially reduce the possibility of the network to fulfil its objective when these assets fail (ISO, 2014). Ideally, engineers should balance construction costs against failure costs multiplied by the probability of failure. However, this is not possible in practice because of uncertainties in network condition and failure costs. A possible approach is to weigh the construction costs against the effects of failure on the service level of the network.

Dealing with risk in practice is more complex than the aforementioned risk equation . At least two factors complicate risk management (Ale, 2005, 2009):
1. Risk perception: an important phenomenon is that information that strengthens existing ideas is more readily absorbed than information to the contrary. As an example, for a Dutch person, the probability of death due to a flood is equal to the probability of winning the lottery "Staatsloterij" (both are 1×10^{-7} per year), but the probability of winning the lottery is considered by many to be remote but possible, or even likely. At the same time, the probability of losing one's life in a flood is considered to be low.
2. Aversion against large disasters: if large consequence × small probability = small consequence × large probability, the first condition is considered less desirable.

1.4   History of design methods and tools

Designing a (looped) water network requires solving thousands of nonlinear equations to determine the pressures and flows in the systems. Before the computer age, this was impossible. Therefore, rules of thumb and design tables have long been used in the design of networks (Walski, 2006). In the middle of the 19th century, Roe's Table (Table 1.2) was widely used for urban drainage network design. Roe was an engineer and surveyor to the Holborn and Finsbury Sewer Commission in London (Hamlin, 1992). The table indicates the catchment areas that can be drained by sewers of specified diameter and slope. It is based on Roe's empirical observations acquired over approximately 20 years from the London sewers (Burian & Edwards, 2002; Metcalf & Harrison, 1914).

Table 1.2   A portion of Roe's Table, showing the quantity of covered surface from which circular sewers (with junctions properly connected) will convey away the water coming from a fall of rain of 1 inch per hour with house drainage (roofs and courts). First publication was between 1840 and 1845 (1 inch $\approx$ 2.54 cm, 1 acre $\approx$ 4,046.86 m^2).

Diameter of sewer, (inches)	24	30	36	48	60	72	84	96
Level	Acres	Acres	Acres	Acres	Acres	Acres	Acres	Acres
unknown	38.75	67.25	120	277	570	1,020	1,725	2,850
1 in 480	43	75	135	308	630	1,117	1,925	3,025
1 in 240	50	87	155	355	735	1,318	2,225	3,500
1 in 160	63	113	203	460	950	1,692	2,875	4,500
1 in 120	78	143	257	590	1,200	2,180	3,700	5,825
1 in 80	90	165	295	670	1,385	2,486	4,225	6,625
1 in 60	115	182	318	730	1,500	2,675	4,550	7,125

Note. Adapted from John Roe's table, reprinted in Sanitary engineering. a practical treatise on the collection, removal and final disposal of sewage and the design and construction of works of drainage and sewerage. Moore (1898).

During the second half of the 19th century, Mulvany (1851), Kuichling (1889) and Lloyd-Davies (1906) all contributed to concepts that eventually evolved into the Rational Method. The Rational Method is used to determine peak flows in UDNs based on rainfall intensity and the area of the (sub)catchment.

The Hardy Cross method (Cross, 1936) is one of the earliest systematic methods of network analysis. The Hardy Cross method is a specialisation of Newton's method (or the Newton–Raphson method) (Raphson, 1697). It is a numerical analysis method which produces successively better approximations to the roots (or zeroes) of a real-valued

function. The iterative Hardy Cross method is used for determining the flow in pipe network systems based on the inputs and outputs at the boundaries (Cross, 1936).

Other tools used for the design of water networks include design graphs (see Figure 1.4) and sewer slide rules (see Figure 1.5). The design graph is used to estimate the required diameter based on the available hydraulic gradient and discharge and can also be used to check outcomes of calculations. The sewer slide rule is a type of slide rule used to determine the required diameter based on the available hydraulic gradient and discharge (Bos, 1942; Schuitema, 1998).
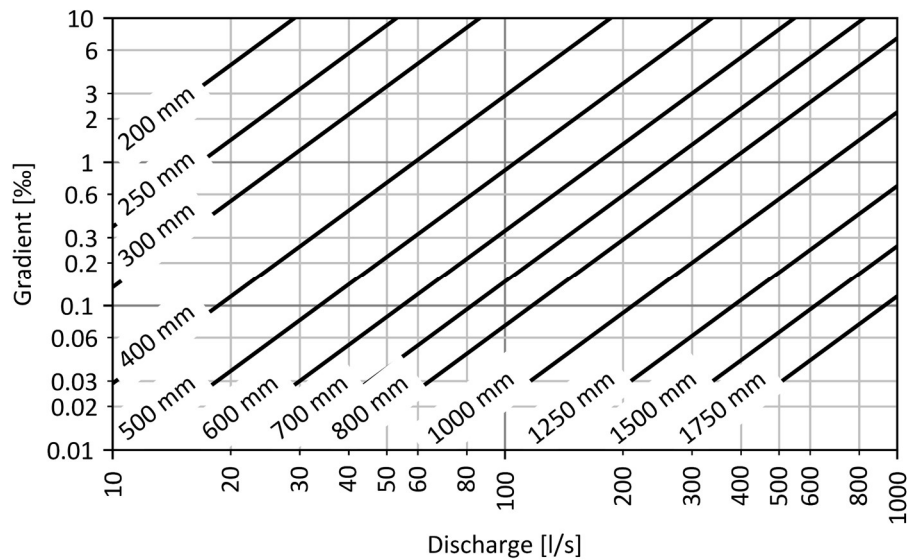
Figure 1.4   Design graph for 100% surcharged capacity.

Figure 1.5   Sewerage rule (Rioolschuif), developed by K. Kaspers (Note. H. van Mameren, personal communication, 23 September 2021. Copyright 2021 by H. van Mameren. Reprinted with permission).

1.4.1 Hydrodynamic models

In the early 1950s, digital computers were first used to solve WDN problems. The development of modern hydraulic UDN models started a few years after the introduction of hydraulic models of WDN in the 1960s (Butler & Davies, 2004; Yen, 1987). From 1960 onwards, computational speed has increased enormously, and new algorithms have been developed to solve the equations. However, the optimal design of networks still requires many calculations. The main elements of a hydrodynamic model are summarised in Table 1.3.

With increasing computational power, the complexity and the level of detail of the hydrodynamic models increased as well. Initially, the calculations were limited to steady-state calculations using simplified geometric descriptions of the networks. In the 1980s, detailed geometric descriptions of the networks were used in combination with time-dependent behaviour of water flows. At present, 1D–2D (one-dimensional–two-dimensional) models are applied to analyse urban drainage systems including drainage, surface water, overland flow and potentially many other details, such as gully pots.

Along with the increasing complexity of models, the number of elements in models has increased as well. In the Netherlands, the average distance between two manholes is approximately 50–60 m. This implies that, in urban areas, there are on average 275–400 manholes per square kilometre and approximately the same number of pipes. This results in networks of thousands of elements for a village and hundreds of thousands of elements for cities.

The calculation effort increases even more when the effects of pipe failure are sought, as the flow distribution in the network will change as a result of a failed pipe. An extensive body of literature exists regarding various system optimisation methods (Walski, 2006). Solutions to optimisation problems have become more comprehensive by including water quality in capacity optimisation in WDN (Walski, 2006). New techniques (e.g. optimisation algorithms and computational speed) have led to new questions and challenges. Combined with the increased size of WDN and UDN, there are still optimisation problems that take too much time to resolve to be addressed in practice (Tscheikner-Gratl, Bellos, et al., 2019).

Table 1.3   The main elements of a hydrodynamic model.

	Water distribution network model	Urban drainage network model
Description of the system. The level of detail of this description varies and consists of:	– the geometry of the components – the mutual relationship of these components (network structure) – the various hydraulic coefficients	– the geometry of the components – the mutual relationship of these components (network structure) – the various hydraulic coefficients – the runoff area – digital terrain model – the mutual relationship between the 1D system and the digital terrain model
Description of the load:	– water demand	– precipitation – dry weather discharge (including extraneous water)
Description of the hydrodynamic processes (the mathematical model):	– 1D flow model	– rainfall runoff model – 1D flow model – 2D flow model

Various approaches can be applied to reduce the calculation effort and keep calculation times within acceptable limits (see Table 1.4). The simplifications applied affect the scope of application of the different model types:

- Reservoir models can be applied for networks in which the storage is more important than the discharge within the network. With these models, information about the spatial resolution is lost.
- Skeleton models focus on the main system and not on its capillaries. For these models, it must be determined which parts do and do not belong to the main system. This cannot always be determined unambiguously. For the parts that do not belong to the main system, information about the spatial resolution is lost. Depending on the size of the main system, storm series or storm events can be applied.
- Full models often use design storm events instead of precipitation series. By simplifying the hydraulic load only, these models describe in detail the functioning of the systems. However, the normative events for determining the recurrence times depend on the storage and drainage capacity of the subsystems. If the dominant process (storage or discharge) is different for any subsystem, it may be necessary to apply storm surge series to determine the recurrence times of flood events.

- Complete networks with simplified process descriptions enable the analysis of complete networks with storm series. However, the results are less accurate than in the case of full networks. Return periods of events can be determined by using storm series.

Table 1.4 Overview of model concepts.

Model concept	Structure	Hydraulic load	Process description
Reservoir model	simplified	series	simplified
Skeleton model	simplified	series / events	full
Full model with events	full	events	full
Complete network simplified process description	full	series	linearised

The model concept applied, influences the results of a criticality analysis. Reservoir models and the skeleton models reduce the number of elements that can be included in the criticality analysis. In addition, changes in network structure can have a major impact on the criticality of elements (see Subsections 5.2.1 and 6.2.2). In full models with events, the characteristics of the storm event influence the calculated criticality of elements. This means that if full models are used, the outcomes depend on the applied event (see Subsection 6.2.1). The criticality quantified by a complete network with simplified process descriptions is only valid for models in which the simplified process description is a sufficiently reliable description of reality. This depends mostly on the linearizability of the process description.

1.4.2   Integral urban water models

UDNs are subsystems of larger systems (e.g. groundwater, water treatment, distribution, sewerage and storm drainage, wastewater treatment, and local or regional surface water systems). They are also situated in complex urban environments and affected by the socio-political environment (Rauch et al., 2012). The Glatt Valley, Switzerland was one of the first locations in which interaction between different components of urban drainage systems was studied in the late 1970's (Gujer et al., 1982).

Bach et al. (2014) have presented an overview of the development of integral modelling and define four levels of integration:
1. Integral Component-Based Models (ICBMs) that integrate components of local urban water systems (e.g. coupling several treatment processes within a wastewater treatment plant).

2. Integral Urban Drainage Models (IUDMs) or integrated water supply models (IWSMs) that integrate subsystems of these systems.
3. Integral Urban Water Cycle Models (IUWCMs) that link these two streams (IUDMs and IWSMs) into a common framework.
4. Integral Urban Water System Models (IUWSMs) that combine the different urban water infrastructures (institutional or physical) and disciplines (e.g. climate, economics, actor behaviour, etc.) of the total urban water cycle.

Every model has an uncertainty. Integrated models consist of either linked sub-models or fully integrated models in one software package, and combining models leads to propagation of uncertainties. This propagation does not necessarily imply an attenuation of this uncertainty. A model should be tailored to the research question, taking into account the uncertainty of each sub-model (Tscheikner-Gratl, Bellos, et al., 2019).

1.5   Objective of the thesis

The general objective of this thesis is to provide and demonstrate a methodology that supports operators of water networks in the optimisation of maintenance and rehabilitation activities by classifying the criticality of elements in their systems. The following research questions have been formulated to meet this objective:
1. Which factors contribute to the criticality of an element in a water network?
2. What are the effects of simplifying hydrodynamic processes when evaluating the criticality of elements in networks?
3. What is the contribution of the network geometry, the network structure, the hydraulic load and the hydrodynamic processes to the functioning of a water network?

1.6   Thesis outline

Figure 1.6 presents the outline of the thesis. Chapter 2 provides an overview of the relevant literature and deals with the criticality of sewer and water distribution networks, the impact of failures in networks and the interactions between networks. Chapter 3 describes three methods to determine the criticality of elements in networks. The first method can be applied on pressurised systems, the second on gravity-driven systems and the third on urban drainage systems. All methods combine graph theory with simplified hydrodynamics. In this chapter, a topological parameter (the network linearisation parameter) has also been included to classify looped storm and combined sewers. Chapter 4 depicts the case studies that have been used to validate and demonstrate the developed

methods. The results of the methods are presented and discussed in Chapters 5, 6 and 7. Each of these chapters focuses on one of the three methods. The application of the network linearisation parameter, to test whether an urban drainage network can be successfully analysed with the GBWLM, is described in Chapter 8. In the final chapter, conclusions are drawn and recommendations for further research are presented.
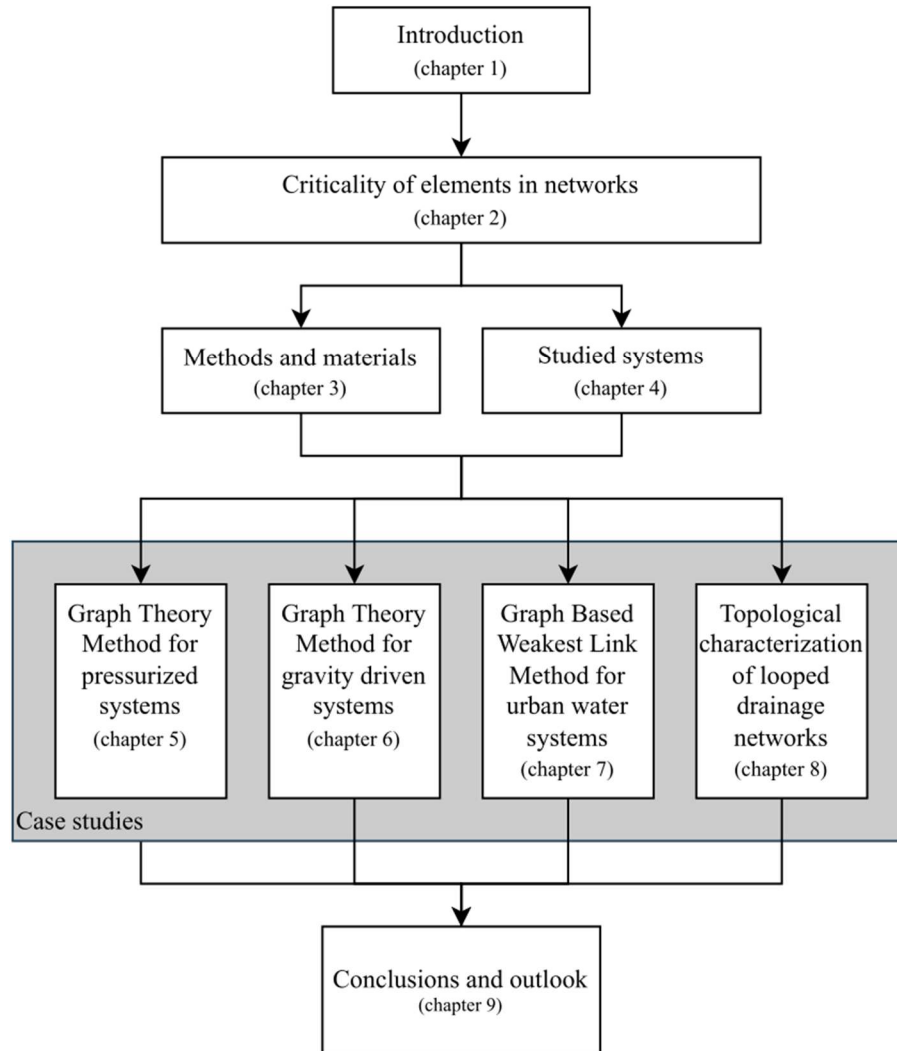
Figure 1.6   Thesis outline. The topological characterisation (Chapter 8) can be used to test whether the graph-based weakest link method (Chapter 7) can be applied successfully to a network.

Chapters 3 and 4 are based on the following studies:

1. Meijer, D., Korving, H., & Clemens-Meyer, F. (2022). A topological characterisation of looped drainage networks. *Structure and Infrastructure Engineering*, 1–14. https://doi.org/10.1080/15732479.2022.2152464

2. Meijer, D., Korving, H., Langeveld, J., Clemens, F. (2023). A method to identify the weakest link in urban drainage systems. (submitted to Water Science & Technology under review)

3. Meijer, D., Post, J., van der Hoek, J.P., Korving, H., Langeveld, J., & Clemens, F. (2020). Identifying critical elements in drinking water distribution networks using graph theory. Structure and infrastructure engineering. doi.org/10.1080/15732479.2020.1751664

4. Meijer, D., Van Bijnen, M., Langeveld, J., Korving, H., Post, J., & Clemens, F. (2018) Identifying Critical Elements in Sewer Networks Using Graph-Theory. Water, 10(2), 136, doi:10.3390/w10020136

Chapter 5 is based on paper 3, Chapter 6 on paper 4, Chapter 7 on paper 2 and Chapter 8 on paper 1.

2 Criticality of elements in networks

2.1 Introduction

This chapter addresses the criticality of sewer and Water Distribution Networks (WDNs), the impact of failures in networks and the interaction between networks. The importance of well-functioning networks for the liveability of urban environments has resulted in numerous studies of networks from various perspectives (e.g. design, maintenance and rehabilitation). Some of the most important network concepts, especially related to the criticality of networks, are summarised in this chapter. Section 2.2 focuses on critical assets. First, the commonly used concepts to determine failure risks, Likelihood of Failure (LoF) and the Consequence of Failure (CoF) are explained. Subsections 2.2.2 and 2.2.1 address three main approaches to determine the failure risks: 1) flow characteristics, 2) hydrodynamic modelling and 3) network analysis. The impact of failure of networks, including some examples, is presented in Subsection 2.2.2. In urban areas, infrastructure networks are often closely situated to each other in a physical sense. Section 2.3 examines the interaction between infrastructure and existing multi-infrastructure rehabilitation methods. Section 2.4 presents an overview of network topology and is divided into four subsections. Subsection 2.4.1 discusses network concepts. Subsection 2.4.2 explains the influence of spatial constraints on these concepts. Subsection 2.4.3 describes the dual graph approach used to transform networks with spatial constraints into networks that can be analysed using methods for networks without spatial constraints. Subsection 2.4.4 summarises topological features used to classify networks. Section 2.5 reflects on the applicability of the of the dual graph approach on Urban Drainage Networks (UDNs). In the last section (2.6), the key points of this chapter are summarised.

2.2 Critical assets

The performance of UDNs and WDNs depends on the functioning of individual elements of these networks. The importance depends on the characteristics of the element, its position in a network and the network characteristics. Critical assets are assets that

potentially reduce the possibility of the network to fulfil its objective when these assets fail (ISO, 2014). Identifying the criticality of elements calls for information about locations at which a reduced capacity of elements has the strongest negative impact on the service level.

Water infrastructure (WDNs and UDNs) needs maintenance to ensure the desired service level (International Water Association Publishing, n.d.; Le Gauffre et al., 2007; Wirahadikusumah et al., 2001). Rehabilitation is necessary to adjust the system to urbanisation and climate change. As mentioned previously, Tscheikner-Gratl, Caradot, et al. (2019) state that because the actual investments in maintenance and rehabilitation do not meet the expected investment needs in various countries, the service level in these countries is likely to deteriorate.

Water infrastructure managers need to prioritise maintenance and rehabilitation activities because means (e.g. budget and human resources) are limited. If the degree of criticality of the elements in a network is known, the maintenance and rehabilitation can be adjusted accordingly instead of maintaining all elements to the same quality level, as is often the case in practice. The difficulty is that networks consist of many elements and criticality depends on many factors. In order to prioritise, the contribution of each element to the functioning of the network should be examined.

The concept of (failure) risks is used in practice for the prioritisation of elements in networks and rehabilitation and maintenance activities. For underground piped infrastructure such as WDNs and UDNs, risk is often defined as a combination of the LoF with the CoF (Anbari et al., 2017; Arthur & Crow, 2007; Arthur et al., 2009; Baah et al., 2015; Laakso et al., 2018; Lukas & Merrill, 2006; Mancuso et al., 2016; McDonald & Zhao, 2001; Pienaar, 2013; Ward & Savić, 2012). Some of these methods focus on the position and characteristics of a network element and others on the contribution of an element to the functioning of the entire network.

2.2.1 Risk analysis based on the contribution of an element to network performance

The methodologies to determine critical assets while taking into account the network performance can be divided into three categories:
1. Methods based on flow characteristics.
2. Methods based on hydrodynamic modelling.
3. Methods based on network analysis.

In UDNs, flow characteristics (e.g. water depth, flow velocity and surcharge capacity) are used to determine the criticality. Arthur and Crow (2007) and Arthur et al. (2009) describe a methodology to identify critical assets in UDNs. Their methodology is based on surcharge capacity combined with surcharging water level and is applicable to gravity systems. Carriço et al. (2012) have used the water depth in a conduit and velocity as indicators for the hydraulic performance.

Hydrodynamic models can be used to quantify the difference in network performance between full capacity and reduced capacity due to failure of a network element (both in WDNs and UDNs). An example is the Achilles approach, which is a planning tool for the identification of weak points during operation and emergency for the urban water infrastructure (Mair et al., 2012; Möderl et al., 2009; Möderl & Rauch, 2011; Sitzenfrei et al., 2011). In a hydraulic model, the capacity of the conduits is reduced one by one to (nearly) zero, and the hydraulic consequences are determined. The larger the system, the larger calculation effort is required. The Achilles approach is based on the percolation theory (Broadbent & Hammersley, 1957; Sahimi, 1994; Stauffer & Aharony, 1991; Stockmayer, 1944). Tscheikner-Gratl et al. (2016) present a method by which the priority of drinking water pipes is based on an estimate of the amount of water discharged in case of failure of a transmission line. These estimates have been made for different failure modes depending on the pipe material (Friedl et al., 2012; Fuchs-Hanusch et al., 2014).

For WDNs, analyses without extensive hydrodynamic calculations are used to determine the criticality with limited computational effort. Graph theory is often used to replace full hydrodynamic calculations. Michaud and Apostolakis (2006) present a methodology to rank elements of a WDN based on water supply and demand. Diao et al. (2014) identified clusters with the strongest external connections and used the number of people left without water as a consequence of failure as criteria to rank elements. Both graph methods focus on the analysis of the main system and discard the capillaries of the system. Balekelayi and Tesfamariam (2019) use four topological graph metrics (betweenness, topological information centrality, eigenvector centrality, and principal component centrality). Each of these four topological metrics provides a hypothesis about the node's importance based on the network topology.

All three methods have their specific limitations. Methods based on flow characteristics are mainly applicable to branched networks, hydrodynamic models require relatively large computational effort, and network analysis methods typically focus on the main system and not on the capillaries of the systems.

2.2.2   Risk analysis based on location and characteristics of elements

The position and characteristics of an element are used as starting point in various risk analysis methods (see e.g. Baah et al., 2015; Laakso et al., 2018; Lukas & Merrill, 2006; Mancuso et al., 2016; McDonald & Zhao, 2001). An analysis of the location and characteristics of an element is used to determine the LoF and the CoF.

The LoF is usually related to the following:
- The soil type.
- The load on the system.
- The material type.
- The age of an element.

The CoF is generally related to the following:
- The conduit geometry (e.g. conduit size and conduit depth).
- The location of the conduits in the urban area (e.g. pipes crossing under railways or roads, pipes close to subway entrances or pipes close to main gas transport lines).
- The number of affected people (e.g. people left without water after a pipe break or people who cannot drain their water in case of a blockage or flooding).
- The impact on ground and surface water bodies.

Weighing factors are used to combine the above parameters influencing the LoF and CoF in decision support systems. Due to the subjectivity present in defining criteria and weights used for the prioritisation of rehabilitation projects, the outcomes of these methods lack reproducibility, hampering their generic applicability (Carriço et al., 2012; Tscheikner-Gratl et al., 2016).

Another limitation of this method is that the consequences of failure may occur at another location in time and space than the failure location. This applies to UDNs in particular. A blockage in a UDN pipe can result in flooding or in unnecessarily spilling of wastewater over a combined overflow structure, hundreds of meters from the actual blockage. These "remote effects" are not included in analyses based on the LoF and CoF, which are only linked to the location and characteristics of the element.

2.2.3   Impact of failure

The impact of failure of water networks depends on various factors, including the network type, the location of failure in the network, the location of failure at street level, weather conditions and time of day. Subsection 2.2.2 has provided an initial overview of the consequences or impact of failure. In this section, the consequences of failures are described in more detail.

The network type influences the impact of the failure. Important differences in characteristics of UDNs and WDNs in that respect are as follows:
- Water quality: WDNs distribute water that is meant to be used by customers. If the water becomes contaminated (due to insufficient pressure in the network), this poses a health risk for users. In case of leakage, the water has no negative impact on the ecosystem. In sewer systems, wastewater is transported. Wastewater poses a risk to surface and groundwater systems.
- System type: UDNs are gravity-driven (and partly pressurised) versus the fully pressurised WDNs. In case of a pipe burst, flooding starts at the location of the break. In the case of blockages, floods may occur in a location other than the location of the blockage itself.
- Demand-driven versus supply-driven: a WDN is driven by the water demand, while a sewer network is supply-driven (storm water runoff or wastewater). In a WDN, the water flows from a limited number of points to many nodes (from water supplier to households). In a sewer system, this condition is exactly the opposite (from gully pots to wastewater treatment plants and combined sewer outfalls).

The impact of a failure also depends on the design of the outdoor space and the affected users of WDNs and UDNs. Salman & Salem (2012) divide the impact of failure of sewer systems into three main categories:
- Economic impact: factors that have a direct impact on operation, maintenance or replacement costs.
- Environmental impact: factors that have the potential to affect the amount of raw sewage discharge and the quality of aquatic life or nature in general.
- Social impact: factors that affect the extent of inconvenience experienced by the public as a result of traffic delays, accidents, health risks and the non-availability of sewer services.

Examples of water distribution network failure consequences
In 2006, an estimated 133 million m3/day (90 million m3/day, excluding non-revenue water) of treated drinking water leaked from WDNs around the world (Kingdom et al.,

2006). Similar estimates of 126 million m3/day (including non-revenue water) were reported for 2015 by LaBrecque (2015). This is on the order of 16 litres per day per person, which is over three times the amount of water consumed by people categorised as lacking access to clean water (United Nations Development Programme , 2006). Kingdom et al. (2006) have estimated the costs of physical drinking water losses at $14.6 billion per year. These numbers illustrate the need for asset managers to take up the challenge of reducing these losses that are, at least in part, due to ageing of existing WDNs.

Table 2.1 integrates the results of studies on the impact of pipe breaks of WDNs and blockage of UDNs, divided based on the three categories above (economic, environment and social) (Halfawy et al., 2008; Le Gauffre et al., 2007; McDonald & Zhao, 2001; Salman & Salem, 2012; Tscheikner-Gratl et al., 2016; Yerri et al., 2017). The following observations can be made:

- The impact of failure is often connected to the location of failure. The location is described, for example, by the infrastructure above the sewer section, the building type connected to the sewer or the neighbourhood type(Salman & Salem, 2012). In case of flooding, this is not necessarily true. This creates the risk of an incorrect relationship between the location of a disturbance and the affected area.
- Weighing factors are used to classify impact factors of greater or lesser importance (Halfawy et al., 2008; Salman & Salem, 2012; Tscheikner-Gratl et al., 2016). The classification is therefore at least partly subjective, and the classification of the effect depends on the weights assigned.

The impact of failure of an element is determined by the characteristics mentioned of the element and the objects present in a certain radius around the element or flooding location. This analysis is often carried out with the help of geographical information systems (Laakso et al., 2018; Salman & Salem, 2012; Tscheikner-Gratl et al., 2016). The principles behind these techniques are comparable. A buffer is drawn around a failed element or flooded area, and it is analysed which objects (buildings, roads etc.) are present in the buffer zone.

Examples of water distribution network failure consequences
In 2006, an estimated 133 million m^3/day (90 million m^3/day, excluding non-revenue water) of treated drinking water leaked from WDNs around the world (Kingdom et al., 2006). Similar estimates of 126 million m^3/day (including non-revenue water) were reported for 2015 by LaBrecque (2015). This is on the order of 16 litres per day per person, which is over three times the amount of water consumed by people categorised as lacking access to clean water (United Nations Development Programme , 2006). Kingdom et al.

(2006) have estimated the costs of physical drinking water losses at \$14.6 billion per year. These numbers illustrate the need for asset managers to take up the challenge of reducing these losses that are, at least in part, due to ageing of existing WDNs.

Table 2.1   Overview of the impact of pipe breaks in water distribution networks and blockages in urban drainage networks.

	WDN	Sewer system
Economic factors		
Repair costs: size of the pipe section	X	X
Repair costs: depth of the pipe section	X	X
Repair costs: type of road pavement (asphalt, paving stones, etc.)	X	X
Repair costs: infrastructure above the pip2s (except roads)	X	X
Repair costs: restricted access for repair	X	X
Repair costs: seismic conditions	X	X
Damage to buildings	X	X
Substitution expenses due to customer outage	X	X
Operational pressure	X	
Lost product	X	
Environmental factors		
Quality of affected surface water		X
Quality of affected groundwater		X
Quality of the water (storm water vs wastewater)		
The landslide potential of the area	X	X
The location of the pipe section relative to the downstream of combined sewer overflow or sanitary overflow locations		X
Social factors		
Traffic disruption depending on the type of roadway that is flooded	X	X
The building type that is flooded by customer outage (e.g. hospitals, schools, houses)	X	X
The land use (business, residential, recreational) in the flooded area	X	X
The number of previous complaints (frequency of failure)	X	X
Nuisances of a "hydraulic" nature service interruption	X	X
Health risk: contamination drinking water	X	
Health risk: contact with wastewater		X
Proximity to other critical infrastructure	X	X

2 Criticality of elements in networks

Member states of the European Union (EU) are obliged to reduce leakage losses. The EU has defined Best Environmental Management Practices (BEMP). One of the proposed targets is an Infrastructure Leakage Index (ILI) lower than 1.5 (Equation 2.1; European Commission, Directorate-General for environment, 2018). Member states must report the ILI of their WDNs by 12 January 2026. Within 2 years, member states must submit an action plan to reduce their leakage rate if the ILI exceeds a threshold (European Parliament, Council of the European Union, 2020).

$$\text{ILI} = \frac{\text{Current Annual Real Losses (CARL)}}{\text{Unavoidable Annual Real Losses (UARL)}} \qquad (2.1)$$

In addition to waste drinking water, the failure of underground (piped) infrastructure can disrupt daily life, especially in cities. An historical example of the impact of failure of a WDN is the flooding of the post office of Chicago, Illinois, US in 1936. A water main break filled the building with two meters of water. Workers managed to rescue most of the mail; however, part of the mail was saturated (Chicago Architecture Editor, 2016). A recent example is the flooding of the basement of the hospital VU Medical Center (VUmc) in Amsterdam, the Netherlands, in 2015. A pipe break in the WDN of Amsterdam, in front of the hospital, resulted in flooding. The damage to the hospital was tens of millions of euros and resulted in the evacuation of 334 patients (Nederlands Instituut Bedrijfshulpverlening, 2016; *Voor Tientallen*, 2015).

According to the American Society of Civil Engineers (2017) there are approximately 240,000 water main breaks per year in the US. Yerri et al. (2017) analysed 20 cases and have provided a damage estimate, including costs related to lost product, repair and return to service, travel delay, customer outage and substitution expenses, health costs and property damage. Overall it was concluded that the costs of a pipe break can be substantial (Table 2.2).

Examples of sewer failure consequences
Sewer blockages occur regularly; the reported rates of blockages are as follows (Post, 2016; ten Veldhuis & Clemens, 2011):
- Main sewers: 0.3–0.7 blockages per 100 km sewer length per year.
- Gully pots: 18–28 blockages per 100 km sewer length per year.
- Lateral house connections: 905 blockages per 100 km sewer length per year.

A well-known example of a sewer blockage is the fatberg in Kingston, London, UK. A 15-ton fatberg almost completely blocked the sewer system. If this had not been discovered

in time, raw sewage could have flooded, spurting out of manholes in large parts of Kingston (Welsh, 2014).

The consequences of UDN blockages are somewhat similar to WDN pipe breaks (floods and service disruption). In addition, the inflow of wastewater into ground or surface water bodies may harm the environment and, most importantly, a reduced capacity due to (partial) blockage of a UDN may result in a significant increase in flooding and associated health risks (de Man & Leenen, 2014; van Bijnen et al., 2018).

Table 2.2   Overview of total costs of 20 water main breaks cases in the United States of America (Yerri et al., 2017).

Case	State	Month and year	Diameter (mm)	Costs (M$)
Metro West Tunnel	Massachusetts	May 2010	3,048	85.3
UCLA Campus	California	Jul. 2014	762	28.8
Connecticut Avenue in Chevy Chase	Maryland	Mar. 2013	1,524	21.9
Denver	Colorado	Feb. 2008	1,676	18.6
Capital Heights	Maryland	Jan. 2011	1,372	16.0
Bethesda	Maryland	Dec. 2008	1,676	11.4
Montgomery County	Alabama	Mar. 1998	2,438	9.8
Manhattan	New York	Jan. 1998	1,220	9.5
Robbinsdale	Minnesota	Sep. 2014	914	7.4
Dundalk	Maryland	Sep. 2009	1,830	7.2
Fort Lauderdale	Florida	Jun. 2011	1,066	4.3
Sunset Boulevard	California	Sep. 2014	914	3.3
DeKalb County	Georgia	Jan. 2015	914	3.0
San Bruno	California	Jul. 2015	1,372	2.5
West Kensington	Pennsylvania	Aug. 2012	1,220	2.2
West Philadelphia	Pennsylvania	Jun. 2015	914	2.2
Frankford	Pennsylvania	Dec. 2013	1,220	2.1
Louisville	Kentucky	Jul. 2011	1,220	1.6
Salt Lake City	Utah	Oct. 2014	1,220	1.1
Old City	Pennsylvania	Oct. 2012	914	1.0

2.3   Interaction between infrastructure networks

In cities, the infrastructure networks are (physically) located close to each other and the failure of one network sometimes results in failure of other urban infrastructure. For example, sinkholes can be caused by infiltration of soil into sewer networks. These sinkholes may lead to the collapse of roads and other underground (piped) networks. This happened twice in 2014 in the city of Apeldoorn, the Netherlands. Due to a break in a

25

water supply main, the soil around a gas pipe was washed away. Due to a loss in support, the gas pipe ruptured and 540 residents were left without gas and water supply for several days during winter *(Hele Week Gasstoring Apeldoorn*, 2014; *Huizen Apeldoorn dagenlang zonder gas,* 2014).

Research has been carried out on the interdependency between (critical) infrastructure networks. Pederson et al. (2006) has defined and examined five main classes of interdependence related to infrastructure networks, which were derived from a classification by Rinaladi (2001):

1. Physical: (often) engineering reliance between components.
2. Informational interdependency: an informational or control requirement between components.
3. Geospatial interdependency: a relationship that exists entirely because of the proximity of components.
4. Policy or procedural interdependency: an interdependency that exists due to a policy or procedure that relates a state or event change in one infrastructure sector component to a subsequent effect on another component.
5. Societal interdependency: the interdependencies or influences that an infrastructure component event may have on societal factors such as public opinion, public confidence, fear and cultural issues.

Only sparse information has been found regarding "collapsing" infrastructure triggering the collapse of other infrastructure. Well-known external factors that influence structural deterioration and collapsing of pipes are increase of the load on pipes and movement of pipes. The main component of surface loading for conduits beneath roads is likely to be that from traffic. Measured bending strains in pipes increase linearly with axle load and tend to decrease with increasing speed of vehicles (Pocock et al., 1980).

Davies et al. (2001) have presented an overview of causes of pipe displacement:

- Water main burst and leakage (WDNs): washing away of soil may cause voids around sewer pipes. This may trigger the final stage in the collapse of a sewer pipe. However, the cause–effect relationship is not clear. A sewer collapse can also cause a water main fracture.
- Ground movements: trench excavations may affect nearby underground infrastructure. The zone of movement along a trench is on each side 2–2.5 times the trench depth (Symons et al., 1982).
- Groundwater level: groundwater may wash away soil and cause voids.
- Ground conditions: shrinkages and swelling of ground may influence the stress on a pipe.

The above-mentioned factors of pipe displacement are all caused by ground movements. According to Papadakis (1999), ground movements are an important cause of pipe failures. On the other hand, ground movements are sometimes caused by pipe failures, such as a water main burst or sand infiltration in a sewer conduit, and can also be caused by maintenance and rehabilitation activities on nearby situated networks.

Operators should consider opportunities and risks for other networks when maintenance is required. Reducing costs by coordination of maintenance may be possible (Tscheikner-Gratl, Caradot, et al., 2019). Maintenance of networks may cause risks of failure of nearby situated networks, especially when ground is moved. This condition also applies when a lack of maintenance may influence the functioning of other networks, for example when sand infiltration in a sewer pipe or the flushing of sand by a leak in a WDN results in movement and burst in other networks.

Tscheikner-Gratl, Caradot, et al. (2019) have presented an overview of applications of multi-infrastructure rehabilitation found in the literature. The authors show that the presented methods or case studies suffer from significant limitations, such as the following:
- A focus on only monetary savings due to coordination.
- Limited available datasets or datasets with poor data quality.
- Hypothetical numerical examples without geographical components.

Although the applications of multi-infrastructure rehabilitation have limitations, some of the case studies show a significant reduction in lifetime costs when compared to replacement without coordination. However, in asset management decisions other considerations than the state of networks or the criticality of elements may have an overpowering impact (Tscheikner-Gratl, Caradot, et al., 2019; van Riel, 2016).

When the criticality of elements of networks is known, operators can use this information during the design and replacement phases. Ideally, the network design should be adjusted so that the fewest possible critical points remain. If that is not possible, the position of critical elements of different networks can be aligned; they can be placed close together or far apart.

There is no known literature on the advantages and disadvantages of those options. When critical elements of different networks are situated in the same street section, these elements can be maintained with a higher frequency to maintain a satisfactory operational condition of these elements. However, critical elements of two networks could be affected in case of failure, resulting in a large impact.

2.4   Network topology

Much literature exists about network models, network topology and failure. Networks have been studied from numerous perspectives, including mathematics, transport, civil engineering (water, energy), computer science, biology, (tele)communication and sociology. The sections below describe the following:

- Important concepts in analyses of complex networks.
- Impact of spatial constraints on networks.
- Topological features to characterise networks.
- The dual graph approach to convert spatial networks to scale-free networks.

Graph theory is often used for the analysis of networks. A graph $G = (V, E)$ is a set V of vertices (nodes) and a set E of edges (links) formed by pairs of nodes (König, 1936) (see Figure 2.1). A path in a graph between a source node and a target node is a route between the source node and the target node without a node occurring more than once (for more details see Section 3.3).

graph

	v1	v2	v3	v4	v5	v6
v1	0	1	1	0	0	0
v2	1	0	1	0	0	0
v3	1	1	0	1	0	0
v4	0	0	1	0	1	1
v5	0	0	0	1	0	1
v6	0	0	0	1	1	0

G = (V,E)
V = v1, v2, v3, v4, v5, v6
E = 12, 13, 23, 34, 45, 45, 56
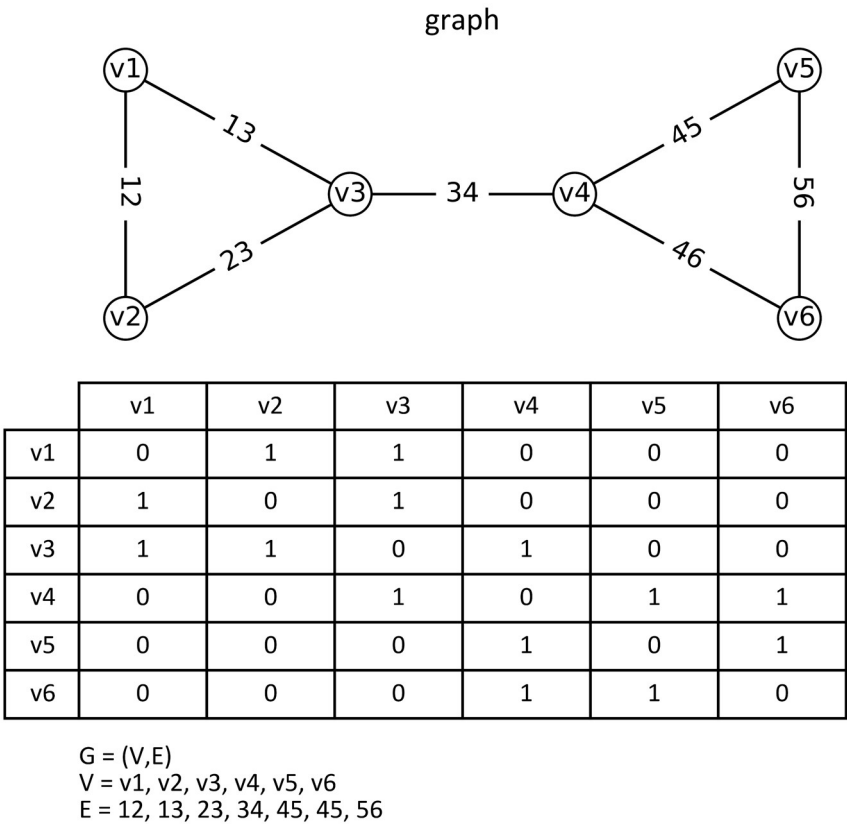
Figure 2.1   A network represented as a graph. On top, a network consisting of nodes v1 to v6 (set *V*) and a number of links (set *E*). This network can also be described mathematically as matrix. For example, node v3 is connected to nodes v1, v2 and v4, which is represented by a 1 in the matrix.

2.4.1   Important concepts in complex network analyses

Albert and Barabási (2002) have presented an overview of the advances in the field of complex networks, focusing on statistical mechanics of network topology and dynamics. They discuss the main models and analytical tools, covering random graphs and small-world and scale-free networks, as well as the interactions between topology and the network's robustness against failures and terrorist attacks.

Until the 1950s, complex networks were mainly studied as regular graphs using graph theory. Since the 1950s, complex networks have been described as random graphs. A widely used model for studying random graphs is the Erdós-Rényi model. This model starts with N nodes and every edge is formed with probability p independently of every other

edge. This results in a graph with approximately $p \frac{N(n-1)}{2}$ edges distributed randomly (Albert & Barabási, 2002).

Albert and Barabási (2002) also observe that since the 1990s, three concepts play an important role in network analyses:
1. The small-world concept: there is a relatively short path between any two nodes, even in large networks. The path length is defined as the number of edges along the shortest path (Watts, 1999; Watts & Strogatz, 1998).
2. Clustering: cliques are common in social networks. In these circles of acquaintances, every member knows every other member. The degree of clustering can be expressed with the clustering coefficient shown in Equation 2.2.

$$C_i = \frac{2E_i}{k_i(k_i - 1)} \qquad (2.2)$$

where k_i is the number of edges connected to node i and E_i is the total number of edges.

3. Scale-free networks and degree distribution (degree is the number of edges that are connected to the node): the distribution of the node degree $P(k)$ for large networks has a power-law tail as shown in Equation 2.3.

$$P(k) \sim k^{-\gamma} \qquad (2.3)$$

where $P(k)$ is the distribution of the node degree and k is the node degree.

The three concepts (small worlds, clustering and scale-free networks) result in three main classes of modelling paradigms (Albert & Barabási, 2002):
1. Random graphs based on the Erdös–Rénvi model serve as benchmarks for modelling and empirical studies.
2. Small-world models are situated between random graphs and highly clustered regular lattices.
3. Scale-free models are used to explain the origin of non-Poisson degree distributions (such as power-law tails) as seen in real systems by focusing on the network dynamics.

The small-world and scale-free models are used to describe real networks. Characteristic differences between real world networks and random networks are as follows:

- The clustering coefficient is typically much larger for (most) real world networks as compared to random networks of equal numbers of nodes and edges (Watts & Strogatz, 1998).
- Scale-free real world networks have a power-law degree distribution, in contrast to random graphs that have a Poison distribution with a peak at $P(\langle k \rangle)$ ($\langle k \rangle$ is the average degree of the network).

Scale-free models are widely used to test the robustness of networks. Albert and Barabási (2002) have shown that networks that meet the criteria of scale-free models display a high degree of robustness against random failure of edges. However, nodes with a high degree (hubs are nodes connected to many other nodes) are crucial for the functioning of scale-free networks. Therefore, the functioning of these networks is susceptible to (terrorist) attacks on hubs.

2.4.2   Impact of spatial constraints on networks

Barthélemy (2011) has presented an overview of the influence of spatial constraints on the structure and properties of networks (transportation and mobility networks, internet, mobile phone networks, power grids and social and contact networks). The topological structure is strongly influenced by space, as an important consequence of space is that costs are associated with the length and location of the edges. Two main categories of spatial networks are planar graphs and non-planar graphs.

"A plane graph is a graph drawn in the plane in such a way that any pair of edges meet only at their end vertices (if they meet at all). A planar graph is a graph which is isomorphic to a plane graph, i.e. it can be (re)drawn as a plane graph" (Clark & Holton, 1991, p. 157). In contrast to planar graphs, non-planar graphs can have intersection links (e.g. rail networks or flyovers, airline networks, cargo ship networks or the internet) (Barthélemy, 2011). Although exceptions are possible, in this research it has been assumed that WDN, UDN and urban drainage systems can be drawn as planar graphs.

Spatial constraints affect the network characteristics of planar graphs in the following ways (Barthélemy, 2011):
- In planar graphs, *P(k)* is peaked because space restricts the existence of high degrees.
- In planar graphs, the length of links is limited, and the distribution is peaked.
- The tendency to connect to hubs is limited, but there is a tendency of cliques to form between spatially close nodes leading to higher clustering coefficients.
- In 2D planar networks, the average shortest paths scale as $\sqrt{\text{No. of nodes}}$.

31

According to Barthélemy (2011), the five most important models of spatial networks are the following:

1. Random geometric graph: the nodes in a plane are connected according to a given geometric rule (e.g. distance).
2. Spatial Erdös-Rénvi graph: the probability to connect two nodes depends on the distance between these nodes.
3. Spatial small-world graph: based on a given probability distribution for their length, random links are added to a d-dimensional lattice.
4. Spatial growth model: a spatial extension of the scale-free models in which new nodes have a preference to be connected to already well-connected nodes.
5. Optimal networks: networks obtained by the minimisation of a certain cost function.

The optimal network model is important in many practical engineering issues related to both the problem of optimal networks and optimal flow through the networks. This has resulted in a large variety of hub-and-spoke networks. In the case of optimal networks, fluctuations and resilience to sabotage attempts naturally lead to the formation of loops. However, loops can also have adverse effects. For example, in WDNs, loops might lead to prolonged stagnation of water, which can have a negative effect on water quality.

2.4.3 Converting spatial networks to scale-free networks with the dual graph approach

Over the past 10–15 years, the dual graph approach has been used to analyse urban road, drainage and water distribution networks. A dual graph or line graph (Harary & Norman, 1960) is a graph in which nodes are replaced by edges and edges by nodes. In a dual graph, each vertex represents an edge of the graph. The dual graph has an edge for each pair of vertices in G that are separated from each other by an edge (Harary & Norman, 1960).

To cluster edges, the dual graph approach is combined with the Intersection Continuity Negotiation model (ICN model) (Porta et al., 2006) or Hierarchical Intersection Continuity Negotiation (HICN) (Masucci et al., 2013). The ICN model is a generalisation model based on the principle of continuity for urban street networks. At each graph node, the two edges forming the largest convex angle are assigned the highest continuity and are coupled together. This is repeated for other edges. In nodes with an odd degree, the remaining edge receives the lowest continuity value (Porta et al., 2006). In the HICN, the roads are first categorised to four hierarchical levels which broadly reflect capacity. The ICN is then applied at each road category (Masucci et al., 2013).

A way of schematising a UDN or WDN as a graph is to assign a node for each manhole or connection point and an edge for each pipe or connection (see Figure 2.1). In the dual graph approach, groups of pipes with, for example, the same diameter are schematised as a node, and the manholes are schematised as connections between the groups of pipes. The diameters are applied as an HICN criterion (Zischg et al., 2017, Zischg et al., 2019). A simple example is shown in Figure 2.2. According to Klinkhamer et al. (2019), high node degrees represent collector pipes in UDNs; however, Zischg et al. (2019) have shown that high node degrees do not necessarily correlate with large pipe diameters.
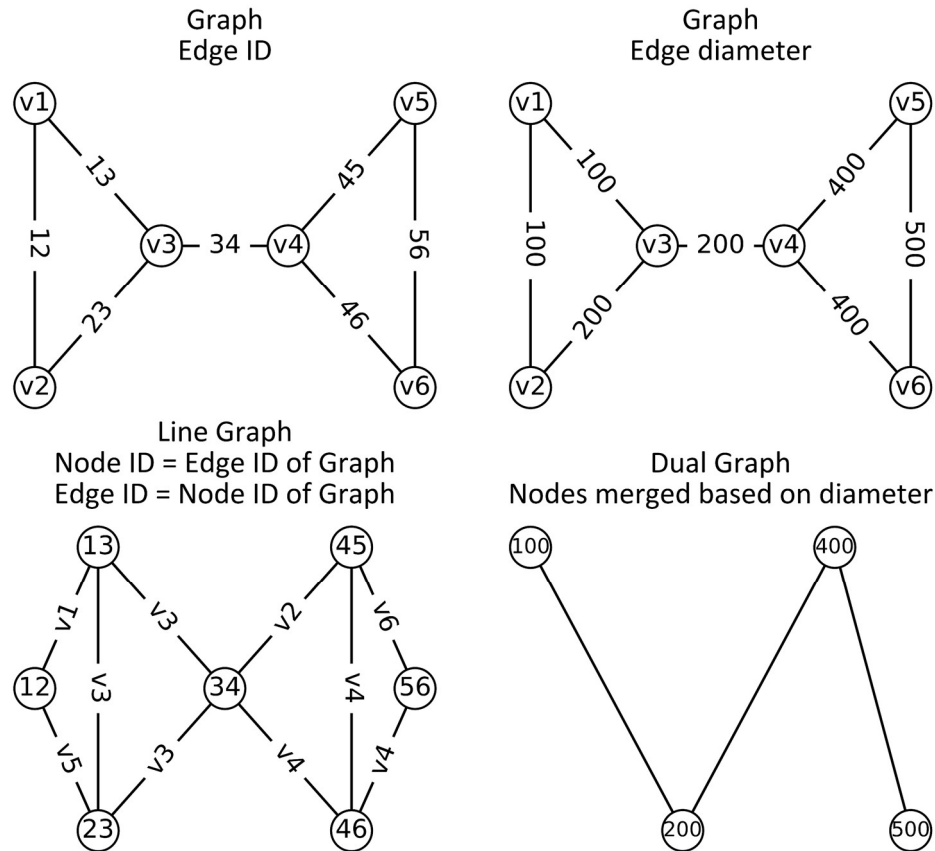
Figure 2.2   Example of the conversion of a graph (top) into a dual graph (bottom-left) and the merging of connections based on the diameters (bottom-right).

According to Krueger et al. (2017), the benefit of dual mapping (based on pipe diameters) of urban water networks is that separate pipes are mapped as "functional pipe units". The node-degree distribution is affected by representing a network as a dual graph. Kalapala

et al. (2006) and Klinkhamer et al. (2019) analysed urban road networks, drainage networks and water supply networks with the dual graph approach and the HICN. They show that the node-degree distribution of these networks changes from a peaked distribution to a highly variable degree distribution with a heavily tailed *P(k)*. They conclude that these properties suggest a robustness against random failures and a vulnerability to the loss of high node-degree hubs. The overlap in locations between the networks introduces the possibility for cascading failures affecting multiple infrastructure networks. Klinkhamer et al. (2017) conclude that co-located large degree elements can be applied as a criterion to allocate resources for maintenance and investment.

2.4.4 Topological features to characterise networks

Networks are usually characterised based on topological features. In this section, commonly used topological characteristics are presented, and the meaning of these characteristics is explained.

Barthélemy (2011) has presented an overview of the main empirical features that can be used to characterise all types of networks with spatial constrains:

- Number of nodes *N.*
- Average (node) degree $\langle k \rangle$ (degree = the number of edges connected to a node).
- Average clustering coefficient *C* (Equation 2.4).
- Average shortest path *l.*
- The degree distributions *P(k)* (scale-free models: broad with a power-law tail; spatial constraints model: peaked).
- The weight distributions of the edges *P(w)* (peaked or broad).
- The scaling of the strength with the degree $s(k) \sim k^{\beta}$.
- The relationship between the centrality (number of shortest paths through a link or node) and the degree.
- Meshedness, shown in Equation 2.4 (Buhl et al., 2004).

$$M = \frac{E - N + 1}{2N - 5} \tag{2.4}$$

where *M* is meshedness, *E* is the number of edges and *N* is the number of nodes.

The trend of describing networks based on topological characteristics has continued over the past 10 years (Giudicianni et al., 2018; Johnson et al., 2019; Johnson et al., 2021; Meng et al., 2018; Metcalfe, 2020; Reyes-Silva et al., 2020; Yazdani et al., 2011). Topological parameters used to describe networks are the following:

- Size:
    - Number of nodes.
    - Number of links.
- Structure:
    - Maximum (node) degree.
    - Average (node) degree.
    - Degree assortativity: the degree variance in a network.
    - Node closeness: the inverse of the sum of shortest paths from a node to every other node.
    - Density: the ratio between the number of edges and the maximal number of edges.
- Redundancy:
    - Meshedness coefficient 1 (Equation 2.4).
    - Meshedness coefficient 2 (meshedness based on the inner nodes degree) (Reyes-Silva et al., 2020).
    - Clustering coefficient (or transitivity), a redundancy measure derived by quantifying the density of triangular loops and the degree to which junctions in a graph tend to be linked (Wasserman & Faust, 1994). In grid-like structures and networks with structural loops different from a simple triangle, the clustering coefficient is normally small (Yazdani et al., 2011).
- Robustness:
    - Algebraic connectivity: the second smallest eigenvalue of the Laplacian matrix. The Laplacian matrix is a matrix with the node degrees minus the adjacency matrix (see Figure 2.3). The adjacency matrix describes the connections between nodes. An eigenvector is a vector for which direction does not change in a transformation. The eigenvalue is the factor by which the eigenvector is scaled. A large algebraic connectivity implies the following (Wang & Van Mieghem, 2010):
        - To generate a bipartition, a relatively large number of links should be deleted.
        - A robust synchronised state.
        - More optimal performance of dynamic processes, e.g. synchronisation of dynamic processes at the nodes of a network and random walks on graphs.
        - Efficient movement and dissemination of random walks.
    - Spectral gap: difference between first and second eigenvalues of a graph's adjacency matrix. A large spectral gap is usually associated with

35

high network performance (Watanabe & Masuda, 2010) and a relatively short distance between nodes (Donetti et al., 2006).

- o Density of bridges: number of bridges (a bridge is an edge that does not belong to any cycle) and the total number of links. The higher the density, the smaller is the meshedness.
- o Density of articulation points: ratio of the number of articulation points (an articulation point is the node variant of bridge) and the total number of nodes. The higher the density, the smaller is the meshedness.
- o Inverse spectral radius: inverse of the largest absolute eigenvalue of the adjacency matrix. The lower the inverse spectral radius, the better is the communication within a network. A low number implies many hubs and many loops (Giudicianni et al., 2018).
- o Central point dominance: the average difference in betweenness centrality of the node with the maximum betweenness centrality and all other nodes. A high value means that one node is much more often in a path than the other nodes of the network.
- Distance measures:
  - o Average path length (*l*).
  - o Network diameter: the maximum eccentricity. Eccentricity of node *n* is the maximum distance from *n* to all other nodes in *G*.
  - o Network radius: the minimum eccentricity.
  - o Average hop count: the average shortest path between all node pairs.
- Centrality, importance:
  - o Node betweenness (max): number of shortest paths through a node.
  - o Link betweenness (max): number of shortest paths through a link.

To clarify the relationship between the structure of a network and the topological features, these values have been calculated for two networks: an unstructured grid of 10 × 10 and the minimum spanning tree of this grid (see Figure 2.4, Figure 2.5 and Table 2.3).

Degree matrix

	v1	v2	v3	v4	v5	v6
v1	2	0	0	0	0	0
v2	0	2	0	0	0	0
v3	0	0	3	0	0	0
v4	0	0	0	3	0	0
v5	0	0	0	0	2	0
v6	0	0	0	0	0	2

Adjacency matrix

	v1	v2	v3	v4	v5	v6
v1	0	1	1	0	0	0
v2	1	0	1	0	0	0
v3	1	1	0	1	0	0
v4	0	0	1	0	1	1
v5	0	0	0	1	0	1
v6	0	0	0	1	1	0

Laplacian matrix

	v1	v2	v3	v4	v5	v6
v1	2	-1	-1	0	0	0
v2	-1	2	-1	0	0	0
v3	-1	-1	3	-1	0	0
v4	0	0	-1	3	-1	-1
v5	0	0	0	-1	2	-1
v6	0	0	0	-1	-1	2
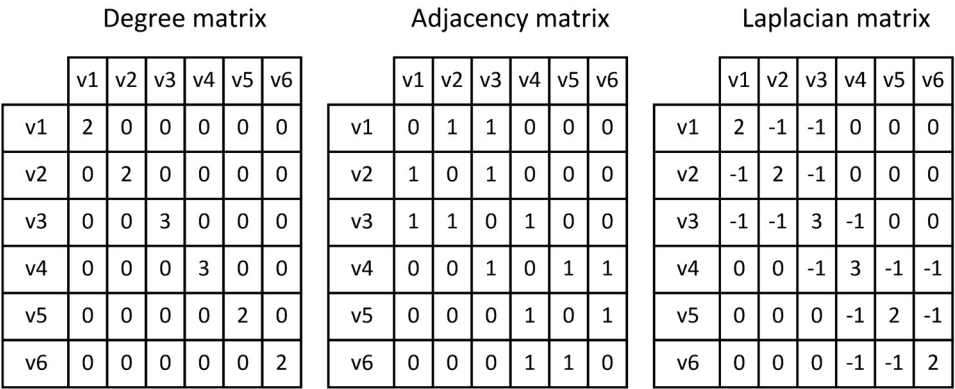
Figure 2.3 Degree, Adjacency and Laplacian matrix of the graph in Figure 2.1.

Grid 10x10

Minimum spanning tree,
grid 10 x 10

300 m

300 m
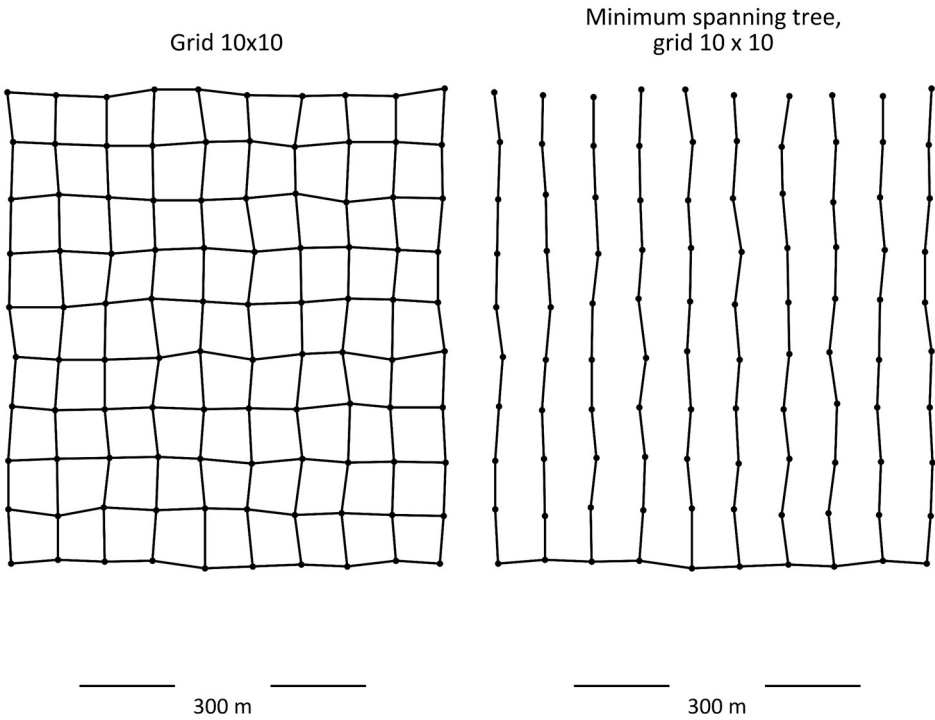
Figure 2.4   Unstructured 10 × 10 grid and its minimum spanning tree.

Table 2.3   Topological features of an unstructured grid (10 × 10), its minimum spanning tree and
the differences between these characteristics for both networks.

Parameter	category	Grid 10 × 10	Minimum spanning tree, grid 10 × 10	Difference
number of nodes	size	100	100	0
number of links	size	180	99	81
maximum degree	structure	4	3	1
average degree	structure	3.6	1.98	1.62
degree assortativity	structure	0.57	0.39	0.18
node closeness	structure	0.15	0.09	0.06
density	structure	0.0364	0.02	0.0164
meshedness coefficient 1	redundancy	0.42	0	0.42
meshedness coefficient 2	redundancy	0.8	0.05	0.75
clustering coefficient	redundancy	0	0	0
algebraic connectivity	robustness	0.0979	0.0076	0.0903
spectral gap	robustness	0.2365	0.1633	0.0732
central point dominance	robustness	0.07	0.47	0.4
density of bridges	robustness	0	1	1
density of articulation points	robustness	0	0.9	0.9
inverse spectral radius	robustness	0.2606	0.4098	0.1492
average path length	distance measures	6.67	11.85	5.18
network diameter	distance measures	18	27	9
network radius	distance measures	10	14	4
average hop count	distance measures	6.67	11.85	5.18
node betweenness (max.)	centrality	616.21	2810	2193.79
link betweenness (max.)	centrality	475	2500	2025
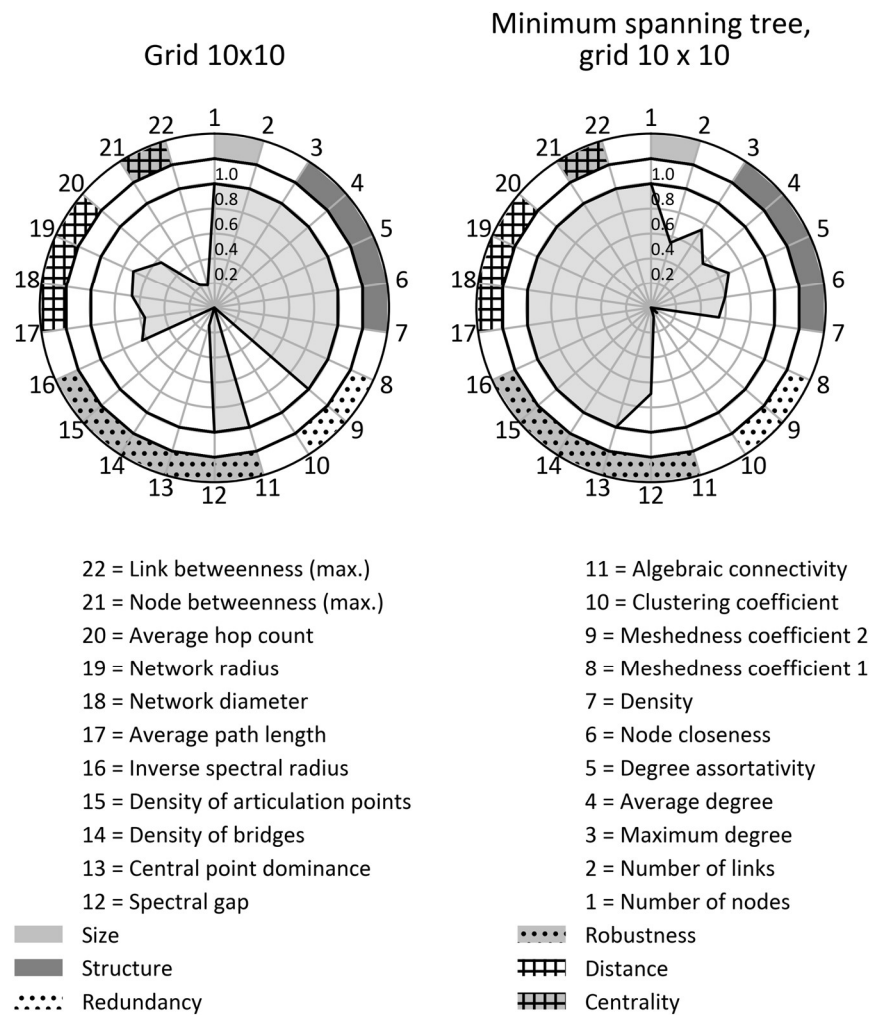
Figure 2.5   Normalised topological features of an unstructured 10 × 10 grid and its minimum spanning tree.

2.5   Reflection on the applicability of the dual graph approach on urban drainage networks

The dual graph approach, in combination with the HICN (based on pipe diameters), is used to convert UDNs into networks with characteristics of small-world and scale-free networks (Zischg et al., 2019). Figure 2.6 shows an example of the UDN of Loenen and its dual graph representation. Loenen's UDN is used as an example because, of the seven UDNs (see section 0), it is the most branched one. The structure of the network is still partly recognisable in this example.

Applying the dual graph approach on the Loenen network has two important consequences. First, the pipes in the looped part of the network have the same diameter and are replaced by one node (rectangles with solid line in Figure 2.6). This node has a central place in the network and has the highest degrees because it is interconnected with many other parts of the network. A part of the network around which water can flow in case of a blockage is therefore represented as one element in the dual graph approach. Second, the part in the dotted rectangle are two branches that come together. Because the diameter of these branches is equal, the branches are also displayed as one node in the dual graph. This means that pipes that drain different parts of the network are represented as one node in the dual graph if the diameter of the pipes is the same.

Graph   Dual Graph

Figure 2.6   Urban drainage network in Loenen, shown as a graph and a dual graph. Larger and darker dots and lines indicate larger pipe diameters. The pipes with the same diameter (colour) in the rectangles are replaced by one node in the dual graph.

The degree distribution *P(k)* of the UDN of Loenen is presented is Figure 2.7. The graph representation shows a peak at a degree of two. The degree distribution of the dual graph representation has a power-law tail for larger degrees. The two nodes in the rectangles in dual graph representation in Figure 2.6 have the highest degree and should, according to the scale-free theory, be crucial for the functioning of the network.
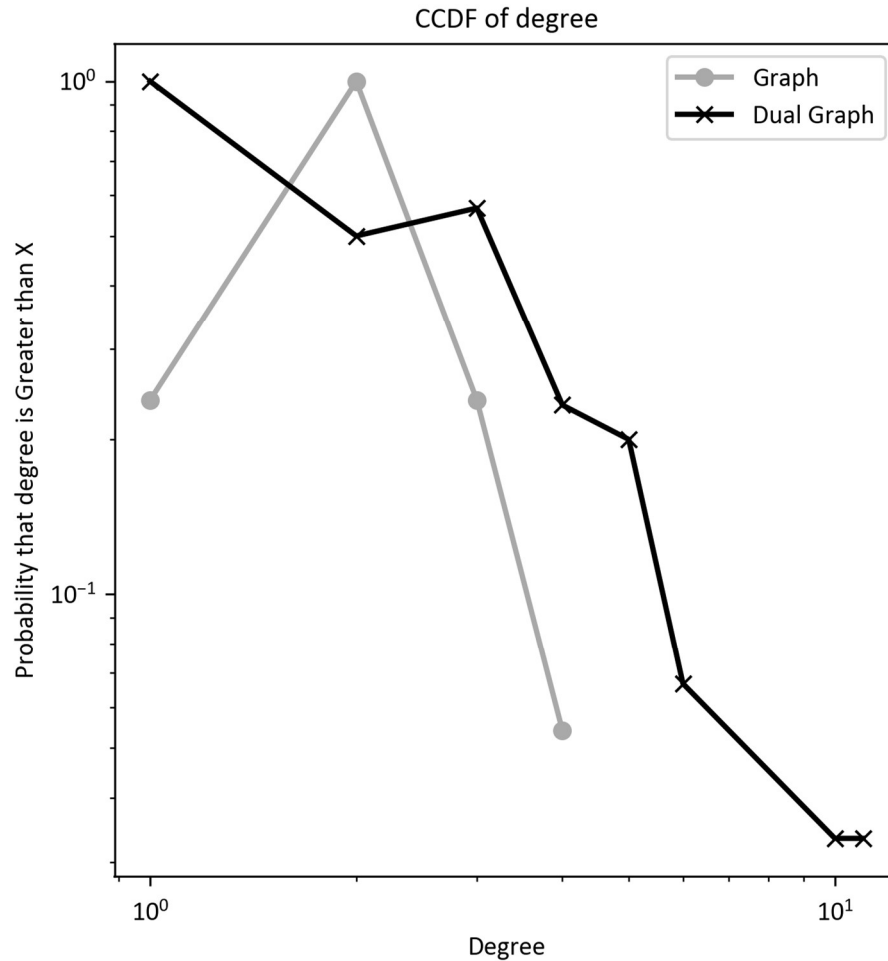
Figure 2.7   The probability of the degree distribution of Loenen's urban drainage network, represented as a graph and a dual graph.

The dual graph approach neglects the fact that these pipes function partially as each other's backup. With the dual graph approach, adjacent pipes with the same diameter are merged into one node. Meshed parts of a network can be merged to one node (see Figure 2.6). It is not plausible that all merged pipes will fail all at the same moment. If a failure occurs in this part of the UDN, it will usually only be a partial failure.

If pipes of the same diameter from different sub-areas converge, the dual graph approach ignores the fact that the consequences of failure depend on the exact failure location. The dual graph approach does not distinguish among upstream areas (see Figure 2.6). Failure

of one branch will lead to other consequences than failure of another branch. This information is lost in the dual graph approach.

These examples show that the assumption of the scale-free network theory, in which nodes with a high degree are crucial for the functioning of scale-free networks, cannot be applied automatically to a dual graph representation of a UDN. Information is lost when the network structure is changed. This could lead to invalid conclusions if the analysis is not carried out carefully, especially for looped networks.

2.6   Overview

Various methods exist to determine critical elements in piped water networks. Most methods use the concepts of LoF, CoF, or a combination of both. Some of these methods focus on the consequences of the failure of an object without considering its impact on the functioning of the network itself. The methods that take the functioning of the network into account are often only applied to the main system and not to the capillaries of the system because of the required computational effort.

Failure impact can be determined by first determining where the failure of a network will lead to negative consequences. Using information from databases of geographical information systems, it is possible to determine which objects are situated at these locations and how they may be affected by the failure of the network.

Very limited literature is known regarding the combined analysis of different underground piped water networks. During the design and replacement phases, operators must decide about the position of the critical elements of their networks in relation to other networks. Situating critical elements of different networks close to each other allows for the option to keep these elements in good condition by a coordinated intensive maintenance programme. By locating critical elements of different networks far from each other, the risk of failure of critical elements of different networks failing simultaneously is reduced.

Networks have been studied from many perspectives, both from different phases of use (construction and management) and from different disciplines. For scale-free networks, the hubs (high node degree) are the most critical elements. For other networks, it is not yet possible to determine the criticality of network elements without (comprehensive) analysis techniques based on hydrodynamic models.

3 Materials and methods

3.1 Introduction

This chapter describes one broadly accepted method and three methods suggested by the author to determine the criticality of network elements. The first method is used as a reference for the suggested methods. All methods are based on the percolation theory. The percolation theory (see Subsection 2.2.1) (Broadbent & Hammersley, 1957; Sahimi, 1994; Stauffer & Aharony, 1991; Stockmayer, 1944) can be used to determine the criticality of all the elements in a network, based on the performance of the network. However, if hydrodynamic models are used to evaluate network performance, the computational effort increases rapidly with the size of the network, as non-linear equations have to be solved. The number of simulations is equal to the number of elements in a network plus one. As the number of elements in a network increases, both the number of simulations required and the duration of each individual simulation increase. The number of equations scales as the number of elements to the power of three.

In order to overcome the drawback of the method based on the combination of percolation theory and hydrodynamic models, three alternative methods are proposed, illustrated and tested using a range of case studies. These methods replace the hydrodynamic calculations by "path analyses" according to graph theory. This reduces the required computing power and allows the method to be applied to larger networks or with longer events. Longer events are necessary when a system consists of subsystems with different characteristics and the time of concentration increases (see Subsection 4.2.3). The duration of the storm event should at least correspond to the maximum time of concentration of the studied (sewer) system (Coördinatiecommissie Integraal Waterbeleid, 2012). The three methods have been developed for:

- Pressurised systems, such as Water Distribution Networks (WDNs).
- Gravity-driven systems, such as storm water or combined sewers.
- Systems consisting of various subsystems, such as urban drainage systems, including gully pots, storm sewers and surface water.

Section 3.2 describes the existing hydrodynamic model-based weakest link method (HBWLM). This method is based on the percolation theory and hydrodynamic models. The HBWLM is used as a reference for the other analyses. The concepts of graph theory that have been used are explained in Section 3.3. The two subsequent sections (3.4 and 3.5) describe the Graph Theory Method (GTM) and the Graph-Based Weakest Link Method (GBWLM) for urban drainage systems, respectively. The section describing the GTM is split into two subsections: 3.4.1 for pressurised systems and 3.4.2 for gravity-driven systems. Section 3.5 describes the GBWLM in detail. The section also includes a subsection (3.5.3) about the linearisation of the hydrodynamics in the GBWLM. To evaluate whether the GBWLM can be applied on a storm or combined sewer network, the Network Linearisation Parameter (NLP) is presented in Subsection 3.5.4. The outcomes of the HBWLM and the GTM and GBWLM have been compared (see Chapter 5, 6 and 7); the applied statistical methods are explained in Section 3.6.

3.2 The Hydrodynamic model-Based Weakest Link Method (HBWLM)

A generally applicable method to determine the criticality of elements in networks is shown in Figure 3.1 This method has been adapted from the Achilles approach (Mair et al., 2012; Möderl et al., 2009) and the percolation theory (Broadbent & Hammersley, 1957; Sahimi, 1994; Stauffer & Aharony, 1991; Stockmayer, 1944). The Achilles approach can be used to determine vulnerable sites of (water) infrastructure. For the identification of vulnerabilities, the outcomes of a hydrodynamic model are used. This method is referred to as the HBWLM.

In the HBWLM, the capacity of network elements is reduced one by one and the effect on the network performance is determined through model simulations. The outcomes of the simulations are compared with the outcomes of the original model in which all elements have their full capacity. The number of simulations is equal to the number of elements plus one. An indicator (e.g. number of flooded manholes, flood volume or water level) for the network performance is used to rank the elements. The most critical element is the one that results in the worst network performance if the capacity of this element is reduced.

Figure 3.1   Process to determine the degree of criticality with the hydrodynamic model-based weakest link method.

The HBWLM was used as a reference for the case studies (see Section 4) because it allows determination of the criticality of all elements in the network based on the performance of the network. The method can be tailored to specific system types and failure mechanisms.

3.2.1   The HBWLM for pressurised systems

The HBWLM can be applied to pressurised systems for the failure mechanism "leakage". A leak can be modelled by adding an outlet pipe with a reservoir of relatively low pressure (head) behind it. The head in the reservoir of the leak is an indication of the leak size. The operational pressure at a connection point depends on the static and the dynamic head. In order to apply similar leaks at different connection points, the head in the leak reservoir must be adjusted to the operational pressure in a connection point; the effect of various pressure drops can be tested. The head for connection point n is set at:

$$H_{\text{leak n}} = H_{\text{connection point n}} - \Delta p \tag{3.1}$$

where $H_{leak\,n}$ is the head of the reservoir connected to connection points n, $H_{connection\,point\,n}$ is the calculated head in the run without leaks for connection point n and Δp is the applied pressure drop.

47

3 Materials and methods

The process of the HBWLM to determine the criticality of an element in a pressurised system is shown in Figure 3.2. The first step is a simulation with the complete original WDN model (run 0). The calculated head (pressure) at every connection point is stored. Thereafter, a pipe and reservoir are added to the network. The new pipe is connected to one of the connection points of the original network and the pressure in the reservoir is set according to the characteristics of the leak location (Equation 3.1). This represents a leak where the water can flow out of the WDN. Then a new simulation is performed. This process is repeated as often as the number of connection points.
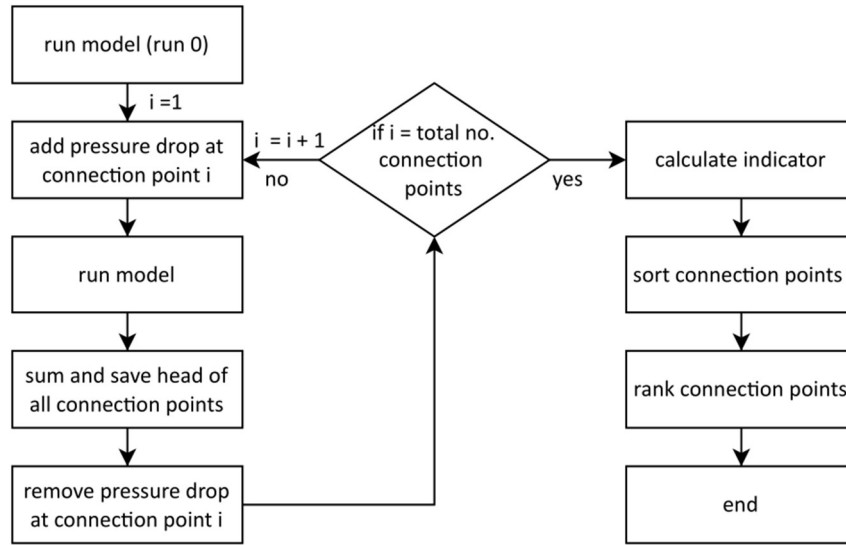
Figure 3.2   Process to determine the degree of criticality with the hydrodynamic model-based weakest link method for pressurised systems.

Two indicators can be tested to rank the elements based on the criticality. In the first method, the connection points are ranked based on total head. The simulation with the lowest total head would indicate that the "leak" is connected to the most critical element. When the sum of the head is low the impact is large, and vice versa. The total head calculation is as follows:

$$H_{\text{total } j} = \sum_{i=0}^{n} \text{head}_i \qquad\qquad (3.2)$$

where $H_{total\,j}$ is the summed head of all connection points for run j, $Head_i$ is the calculated head in connection point i and n is the number of connection points.

48

In the second method, the number of users confronted with a water pressure below a certain threshold are counted for each run ($Users_{p<t}$). The impact increases with an increasing value of $Users_{p<t}$:

$$Users_{p<t\,j} = \sum_{i=0}^{n} Users_i \text{ if } H_{node\,i} < H_{threshold} \tag{3.3}$$

where $Users_{p<t\,j}$ is the number of users with a water pressure below the threshold pressure for run j, $Users_i$ is the number of users connected to connection point i, $H_{connection\ point\ i}$ is the head in connection point i, $H_{threshold}$ is the threshold pressure and n is the number of connection points.

3.2.2   The HBWLM for gravity-driven systems

The HBWLM can be applied to gravity-driven systems for the failure mechanism "blockage" (see Figure 3.3). A blockage can be modelled by removing an element (full blockage) or adjusting the capacity of the element (partial blockage). In the case studies, the diameter was reduced to 10 mm to simulate a nearly complete blockage (in practice, the minimum pipe diameter in the Netherlands is about 250 mm).
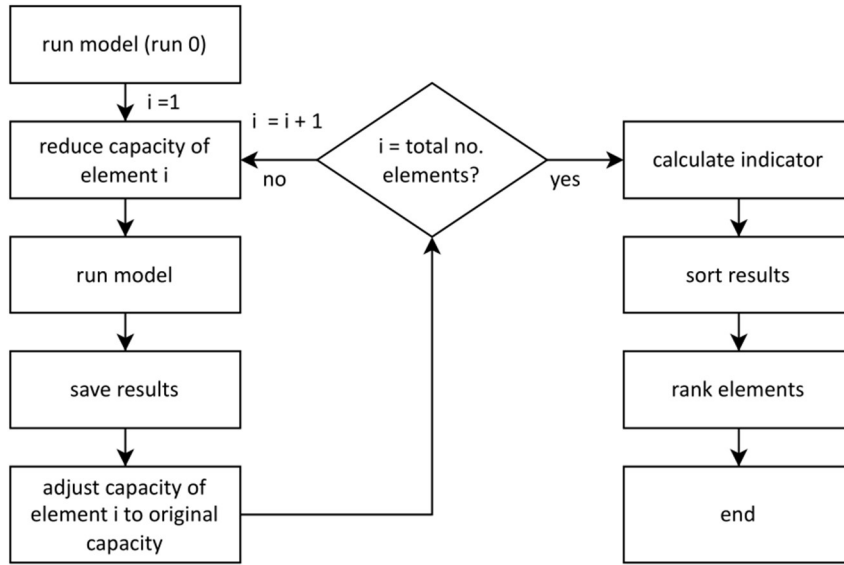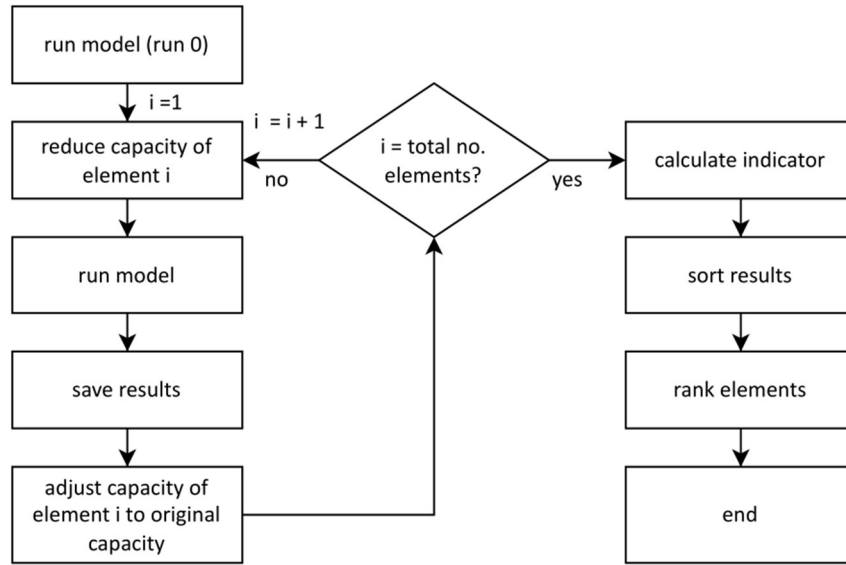

Figure 3.3   Process to determine the degree of criticality with the hydrodynamic model-based weakest link method for gravity-driven systems.

3 Materials and methods

The Achilles approach literature presents two methods to determine the criticality. The first method (Equation 3.4) is a performance indicator based on the maximum ponded volume and the total rainfall runoff (Möderl et al., 2009):

$$PI = 1 - \frac{\sum_{i=1}^{N} \max(V_{P,i})}{\sum_{j=1}^{C} V_{R,j}}$$

(3.4)

where $V_{P,i}$ is the ponded volume of node I and $V_{R,j}$ is the total rainfall runoff volume for catchment j. The main assumption by Möderl et al. (2009) is that the performance indicators are independent of the rainfall events. Method 2 (Equation 3.5) shows a performance indicator for the probability of damage caused by flooding (Mair et al., 2012):

$$F = \frac{\sum_{i=0}^{\#J} \min(x, \max(0, F_i))/x}{No. J}$$

(3.5)

in which x is the threshold flooding volume in m^3 in the simulation period, *No.J* is the total number of junctions and F_i is the probability of damage caused by pluvial flooding.

In order to determine the criticality for storm events without flooding, a slightly different evaluation method can be used. When a part of the network is not connected to an outfall because of a blocked conduit, floods will occur at every storm event of any significance (V_{event} > $V_{storage}$). The severity of the blockage depends on the area that is disconnected from an outfall. The blocked conduits that lead to "unconnected nodes" are ranked based on the runoff surface connected to these nodes. After that, the other conduits are ranked based on the results of the HBWLM.

The links are ranked based on the increase in flood volume and the increase of water level in the system. After each run, these values are determined for each manhole. The results of all manholes are summed, and the links are sorted: first based on the total increase in ponded volume and then on the total increase in water level. The conduit with the largest total increase in the flood volume is ranked as most critical after the conduits that cause "unconnected nodes". If the increase in flood volume is the same for two conduits, the conduits are sorted based on the increase in water level.

3.2.3   The HBWLM for urban drainage systems

The HBWLM can also be used to evaluate the contribution of subsystems or groups of elements to the functioning of the entire system, for example, an urban drainage system consisting of gully pots, storm sewers and surface water. In this case, the main steps taken in the HBWLM are:

- Simulate the functioning of the system.
- Gradually reduce the capacity of (groups of) elements of the urban drainage system.
- Simulate the functioning of the adjusted subsystems of the urban drainage system and take into account the backwater effects.
- Evaluate the performance of the urban drainage system.

The general workflow of the HBWLM for urban drainage systems is shown in Figure 3.4. Flood frequency and flood extent are used as indicators.
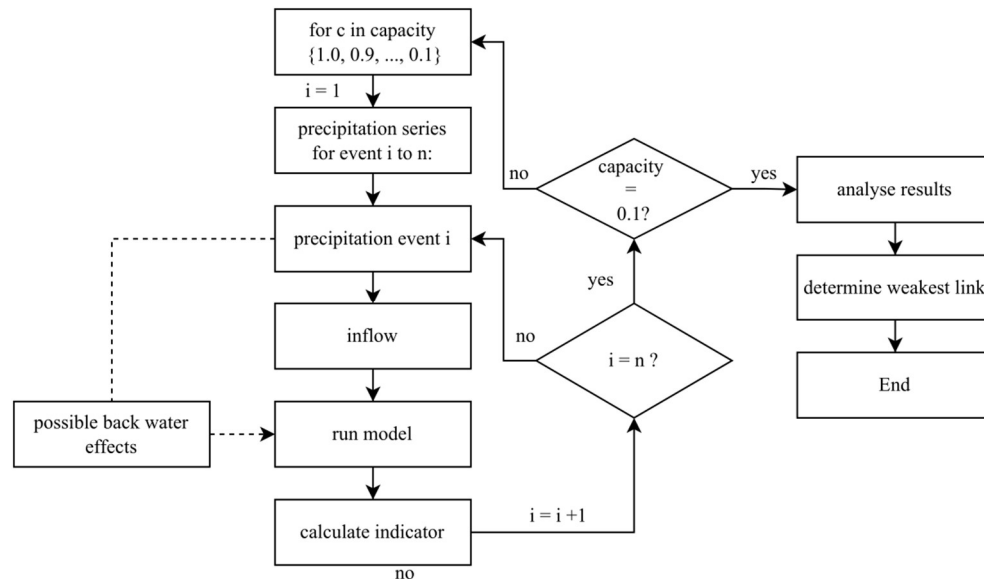
Figure 3.4   General overview of the hydrodynamic model-based weakest link method applied to urban drainage systems.

3.3   Brief introduction to graph theory

Graph theory is used in the developed methods to determine the criticality. Graph theory has been applied to replace the hydrodynamic models of the HBWLM by "flow path

analysis". This eliminates the need for solving non-linear equations and reduces the required computing power. Graph theory is a mathematical theory and is widely used in, for example, route problems, logistic problems and optimisation of flow problems. Leonhard Euler laid the foundation of graph theory in 1736 with the Königsberg bridge problem (Harju, 2012).

A graph can be used to simplify a network and its connectivity in nodes and links (also called edges) (Rodrigue, 2017). Networks such as water supply networks, sewer systems and electricity networks are typical examples of graphs consisting of links (conduits or cables) and nodes (connections or manholes). In hydrodynamic models, graphs are used to represent the structure of the network.

A graph $G = (V, E)$ is a set V of nodes and a set E of links (see Figure 2.1) formed by pairs of nodes (König, 1936). A path in a graph between a source node and a target node is a route between these nodes without a node occurring more than once. Each link can have a weight, cost or penalty. The term most often used is cost and has been adopted here as well.

Costs are a metric for determining the shortest or cheapest paths. For water systems, the necessary amount of energy to transport the water (head loss) is utilised as costs. For the graph in Figure 3.5, a path v1–v6 is v1, v2, v3, v4, v5, v6 (costs = 5) and the shortest path v1–v6 is v1, v3, v4, v6 (costs = 3). There are different kinds of graphs. The upper-left graph in Figure 3.5 is a graph in which v1, v2 = v2, v1. This graph can be used when the costs of opposite flow directions in a conduit are the same; in this example, the costs are 1.

A directed graph or digraph is formed by nodes connected by directed links. In a digraph the link v1, v2 ≠ v2, v1 while in a graph v1, v2 = v2, v1 (see Figure 3.5, digraph). A digraph can be used when the costs of opposite flows are different. In this example, the costs of the links in the positive direction are 1, and those in the negative direction are 2. When all nodes in a directed graph are connected in two directions, it is termed a strongly connected graph (see Figure 3.5 top right). The removal of a conduit can result in one or more strongly connected digraph(s). The graph at the middle-left in Figure 3.5 shows the situation in which the connection v5, v6 and v6, v5 is removed, and the result is a strongly connected digraph. The graph in the middle-right in Figure 3.5 shows the situation in which the connection v3, v4 and v4, v3 is removed, and the result is two connected sub-digraphs.

A layered graph consists of a network and one or more copies of this network (layer-1 = (di)graph-1, layer-2 = (di)graph-2). The layers are connected at the nodes. Each node of

layer-1 is connected with its copy in layer-2. One or two (directed) links can be used for the connection between two nodes of different layers (see lower-left graph in Figure 3.5).
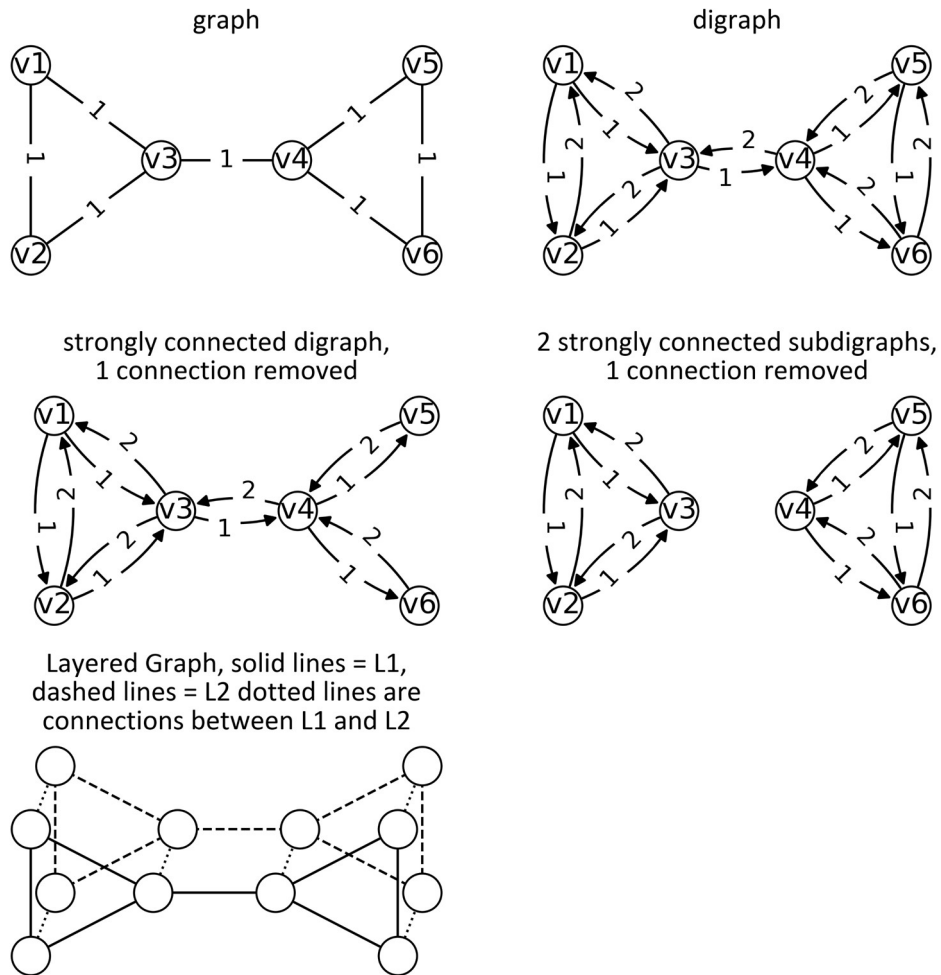
Figure 3.5   Basic principles of graph theory. The numbers along the edges show the costs of the edges. All figures represent the same network. The upper-left figure represents a graph in which v1, v2 = v2, v1; The upper-right figure represents a digraph in which v1, v2 ≠ v2, v1; The graph in the middle-left shows a strongly connected digraph after one connection is removed; the graph in the middle-right shows two strongly connected sub-digraphs after a connection is removed. The lower-left graph shows a layered graph.

3 Materials and methods

3.3.1 The costs of links

The links' costs are derived from the head loss. The head loss is the amount of energy needed to transport water from point A to point B. The head loss comprises two parts. The first part is the static head and is the amount of energy needed to lift water. The amount of energy is equal to the differences in water level at point A and B. The second part is the dynamic head. The amount of energy that is lost due to the resistance of water to flow between A and B is expressed as the dynamic head loss. The dynamic head loss depends on the characteristics of the liquid and the conduit dimension and hydraulic characteristics.

The dynamic head loss is described as

$$\Delta H = \xi \frac{v^2}{2g}$$

(3.6)

where ξ is a resistance factor (-), v is velocity (m/s) and g is gravitational acceleration (m/s²).

In a gravity-driven system, the head loss comprises a dynamic part and two static parts (see Figure 3.6). The first static component (head loss 1 in Figure 3.6) is the height difference between the water level in the connection point or manhole upstream of the conduit and the upstream invert level of a conduit. If the water level in the manhole upstream of the conduit is higher than the upstream invert conduit level, this value is zero. The second static component is the height difference between the upstream and downstream invert levels of the conduit itself (head loss 2 in Figure 3.6). If the water level is higher than the invert level, this value is zero. If the downstream invert level is lower than the upstream invert level, the value is also zero. For the analysis of gravity-driven systems under storm conditions, a water level equal to the lowest Combined Sewer Outflow structure (CSO) in the network, is applied.
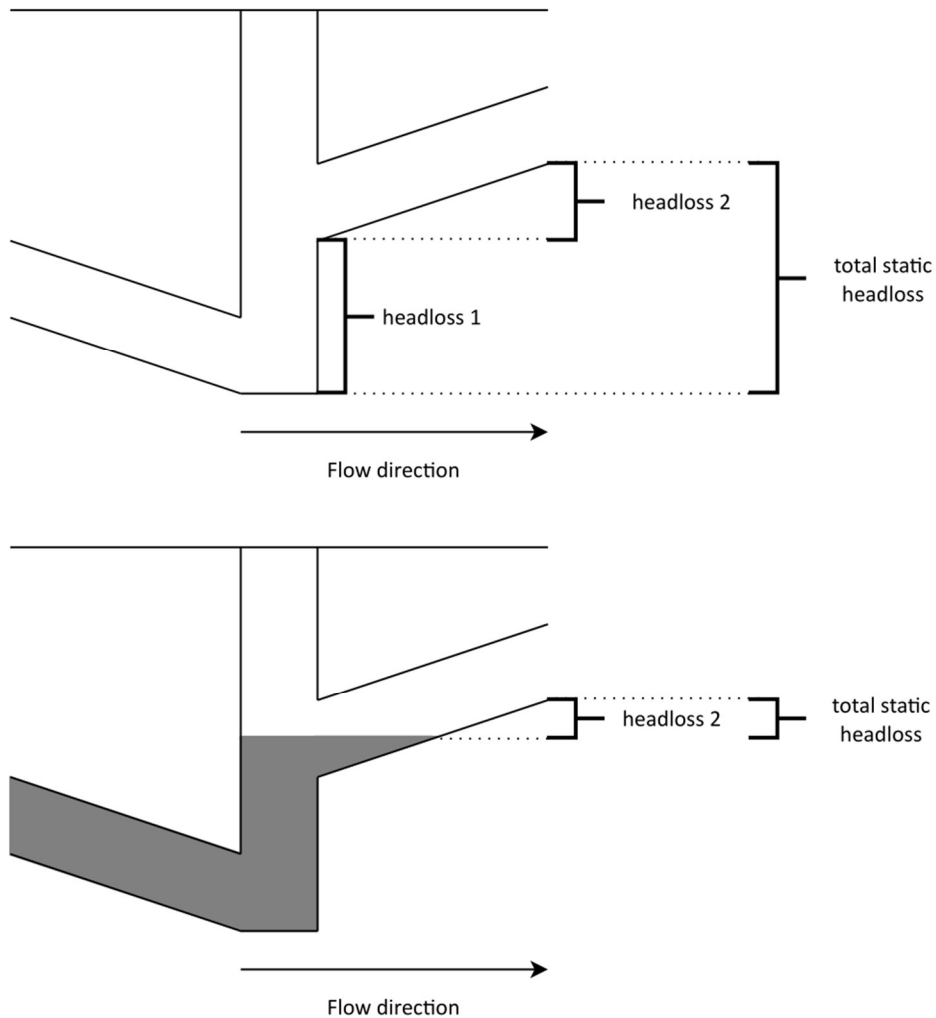
Figure 3.6   Static costs of conduits for an empty system (top) and a system with a certain water level (bottom).

3.3.2   Graph algorithms

The Dijkstra algorithm (Dijkstra, 1959) is a widely used algorithm to calculate the shortest paths in graphs. The general principle is to assign to every node a tentative distance value (source = 0, target = ∞). The source node is marked as active and the other nodes as unvisited. The tentative distances are calculated to all neighbours' nodes from the source node. The smallest of the newly calculated tentative distances and the currently assigned tentative distances are assigned to the node. When all the distances between the source node and the neighbour nodes have been calculated, the source node is marked as visited.

55

The unvisited node with the smallest distance becomes the new active node. The process continues till all unvisited nodes have been visited or the target node is reached.

The minimum cost flow algorithm (Min_Cost_Flow) of the Networkx module in Python (Hagberg et al., 2008; NetworkX Developers, n.d.) is used to evaluate the consequences of a capacity reduction in networks. The algorithm can be applied to a digraph in which the edges have both a cost and a capacity. The nodes desire to send or receive some amount of flow. The algorithm calculates the minimum costs for a flow that satisfies the demands of all nodes. That means that for each node the net inflow or outflow is equal to the demand of that node.

In case of multiple sources in pressurised systems or targets in gravity-driven systems, the algorithms must be applied as often as the number of sources or targets, respectively. This can be prevented by applying a central source or target. For example, in a UDN all targets (outfalls) are connected with the central target (outfall). The edges between the central target and the other targets have identical costs. If the minimum cost flow algorithm is used, the demand of the central target is set equal to the demand of the sources but with an opposite sign (total demand). The edges between the central target and the targets receive the same capacity as the total demand. Applying the algorithms once is sufficient to determine the paths from all nodes to the central target.

3.4   The Graph Theory Method (GTM)

The GTM is a method to determine the criticality of network elements in pressurised and gravity-driven networks. The process is similar to the HBWLM, but the hydrodynamic calculations of the HBWLM are replaced by flow path analysis based on graph theory. This allows determination of the criticality of elements with (substantially) less calculation effort. The GTM analyses the entire network structure and determines the consequences of the failure of each element on network performance.

When applying the GTM, it must be tuned to the network characteristics and failure mechanism. The main differences between a pressurised system and a gravity-driven system are the following:
- A WDN is a pressurised system and driven by the water demand, while a UDN is gravity-driven system and driven by supply (storm water runoff or wastewater). This implies that water in a WDN flows from a limited number of points to many connection points. In an UDN, this is exactly the opposite.

- A WDN is a pressurised system. Normally the drinking water pumping stations maintain an overpressure to prevent the risk of contamination by groundwater. UDNs comprise subsystems with gravity-driven flow and pressurised subsystems. It is common that water is collected in gravity systems and transported by gravity to pumping stations or CSOs, on a regional scale pumping stations transport the wastewater in pressurised systems to Waste Water Treatment Plants (WWTPs).
- For determining the criticality of conduits of UDN, 100% loss of transport capacity (blockage or complete structural collapse) is used as a failure mechanism for conduits. In WDN a pressure-drop result from leakage or a pipe burst is considered as the dominant failure mechanism.

3.4.1   The GTM for pressurised (water) networks

The GTM can be used to determine where leaks have the greatest impact on the performance of WDNs. The most critical location is the one that leads to the greatest decrease in network performance. Leaks are applied at all points at which two or more connections come together (connection points). The criticality of a connection point can be linked to the adjacent connections.

The impact of a leakage depends on the following:
1. The location of the leak relative to a Water Pumping Station (WPS).
2. The position of the leak in the network relative to other connection points in the network.

The location of the leak and the position of the leakage in the network is based on the shortest path from the connection points (source) to the leak location and to the WPS (targets). The shortest paths are determined by the Dijkstra algorithm (see Subsection 3.3.2). The "shortest path" is interpreted as the path with the "least hydraulic resistance". If the costs are low, the source (connection point) is situated close to the target (WPS or leak location); if the costs are high, the connection point is situated far from the target. In the case of multiple WPSs, the costs of all nodes to all WPSs are determined and for each node the costs to the closest WPS is used as shortest path. Figure 3.7 presents the GTM for pressurised (water) and specifically for the situation in which the GTM is applied to a WDN.

3 Materials and methods
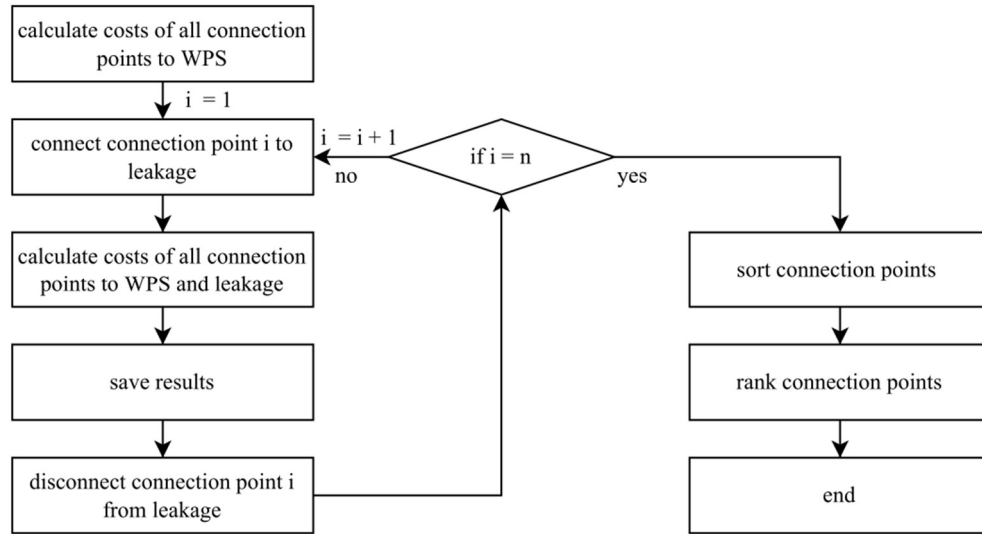
Figure 3.7   Process to determine degree of criticality with the graph theory method for water distribution networks.

The WDN is schematised as a graph. Each connection (valve, pipe) is represented as an edge. The dynamic head loss is used as costs for the edges. The head loss of the elements depends on the applied discharge (q). In the GTM, the discharge functions as scaling factor. The scaling factor is the same for all elements. The applied discharge does not affect the outcome of the GTM as long as the discharge is larger than 0 m^3/s.

Two evaluation methods can be tested to determine the criticality of the connection points:

1. Basic method:
   The number of connection points at which the costs (head loss) to the leak is smaller than the costs to the WPS is counted. This is an indication of the extent of influence of a leak.

2. Weighing method:
   Instead of the number of connection points, the sum of (costs connection point to WPS)$^{-1}$ of connection points at which the costs (head loss) to the leak is smaller than the costs to the WPS, is used ($\sum \frac{1}{\text{costs connection point to WPS}}$). As a result, the connection points close to the WPS are ranked as being more important than the connection points far from the WPS.

The connection points are ranked from the highest counted number of connection points (most important) to the lowest number of connection points (less important). The

58

criticality of the elements of the WDN is first compared for all connection points and second for only the connection points with water users.

3.4.2   The GTM for gravity-driven systems

The GTM can be used to determine where blockage has the greatest impact on the performance of Combined Sewer Systems (CSS) and on Storm Water Systems (SWS). The most critical element is the element that results in the greatest decrease in network performance. A blockage is simulated by removing a pipe from the network.

The decrease in transport capacity to the outflow points as a result of a blockage determines the effect and depends on the following:
- The properties of the pipe that is blocked.
- The position of the blockage in the network.
- The bypass options in the network (e.g. branched or looped structure).

With the GTM, the decrease in transport capacity as a result of a blockage can be tested based on the increase in transport costs. Transport costs are based on the shortest paths from all nodes to the closest outfall and the runoff area of each node. To determine the criticality during dry weather conditions, the outfall is a pumping station; during wet weather conditions, the outfalls are CSOs or rainwater outlets. The transport costs are calculated as follows:

$$C_{graph} = \sum_{i=1}^{n} C_{i-outfall} * A_i \tag{3.7}$$

where C_{graph} represents the total transport costs of the network, *n* is the number of nodes in the network and $C_{i-outfall}$ represents the costs of the shortest path of node *i* to the closest outfall and A_i the runoff area of node *i*.

The CSS or SWS is represented as a digraph. Each manhole is represented as a node and each pipe as a link. Between each pair of nodes two links are used, each with its own costs. The links' costs are derived from the head loss (static and dynamic) in a link (see 3.3.1). This allows identification of the costs of a positive and negative flow direction (see Figure 3.5, digraph). This is necessary because a blockage of a conduit can result in a reversed flow. To reduce calculation time, the calculations are not carried out from the source to the target node but rather from the target(s) to all nodes. The upstream and downstream costs are therefore exchanged.

After calculating the total costs of the complete graph, a connection between a pair of nodes is deleted to simulate a conduit blockage (see middle images in Figure 3.5). This implies that the edges v_x, v_y and v_y, v_x are deleted. When all nodes are connected, the new graph remains a strongly connected digraph (see Figure 3.5, middle-left). Otherwise, the result is two strongly connected sub-digraphs (see Figure 3.5, middle-right). Two situations are possible. In the first, all (sub)digraph(s) contain at least one target node (CSO). In the second, only one of the sub-digraphs contains at least one target node. If the first situation occurs, the total costs of the (sub)digraph(s) are determined. If the second situation occurs, the runoff surface of the nodes that are not connected to a target is summed.

The result is a list of deleted connections with the total costs of each digraph or the runoff surface that is not connected anymore to a target. When a part of the network is not connected to an outfall because of a blocked conduit, floods will occur once the storage is filled. The severity of the blockage depends on the area that is disconnected from the outfall. The blocked conduits that lead to "unconnected nodes" are ranked based on the runoff surface connected to these nodes. The deleted connections are sorted, first by the amount of runoff surface that is not connected to a target and second by the total costs of the digraph from a large to a small amount of runoff surface and from high to low costs. The deleted connections are ranked from 1 (most critical connection) to the total number of edges (less critical). The applied process is shown in Figure 3.8.
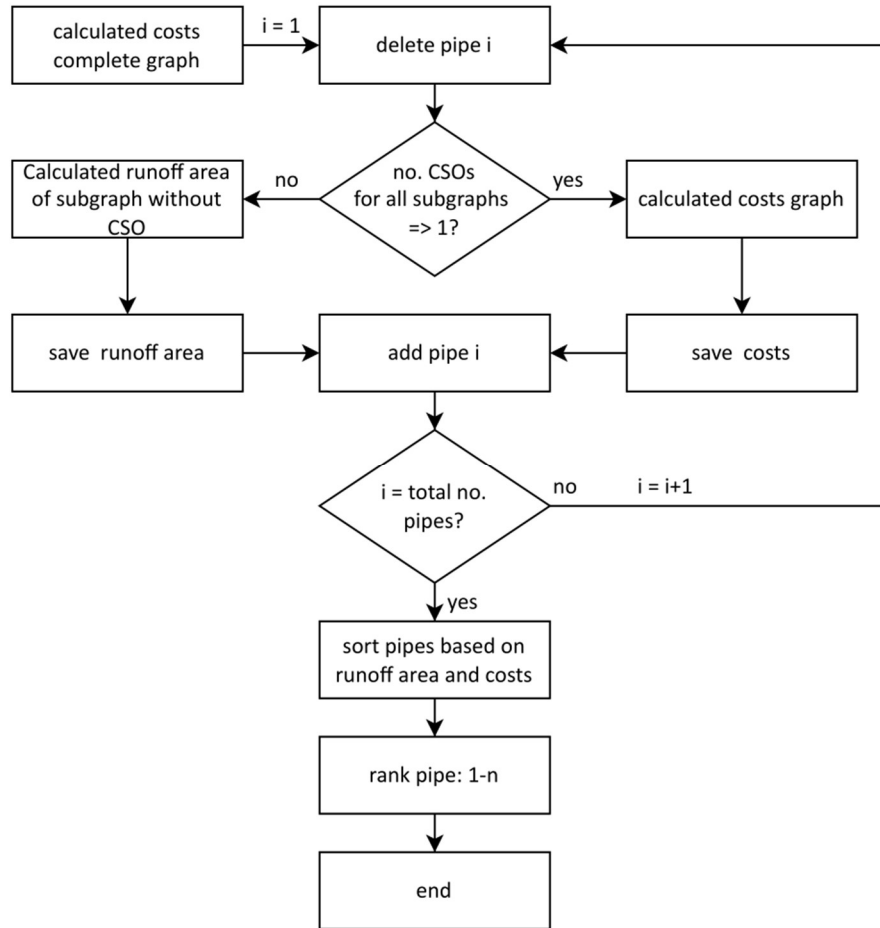
Figure 3.8   Process to determine degree of criticality with graph theory.

3.5   The Graph-Based Weakest Link Method (GBWLM)

The GBWLM has been developed for the analysis of the criticality of (groups) of elements in urban drainage systems. The method can be used to determine which (element of which) subsystem has the largest impact on system performance when the capacity of the subsystem decreases or when the load on the system increases. The system performance is evaluated based on the flood frequency and flooded area.

The impact on the system performance depends on the effect of the change in capacity or load on the subsystem but also on the interaction between subsystems. Because subsystems are designed for different storage and drainage standards, they react

differently to changes in load or capacity. Therefore, an analysis with a long-term time series is necessary to analyse system performance under different conditions. The GBWLM has been developed to analyse comprehensive urban water networks at three levels of subsystems: gully pots, storm sewers and surface water systems, with multi decade precipitation series.

The GBWLM is based on the HBWLM (see Subsection 3.2.3). The hydrodynamic models have been replaced by water balances and flow path analysis. The functioning of urban drainage systems depends on the available discharge and storage capacity. Therefore, both have been included as criteria in the HBWLM (see Figure 3.9).
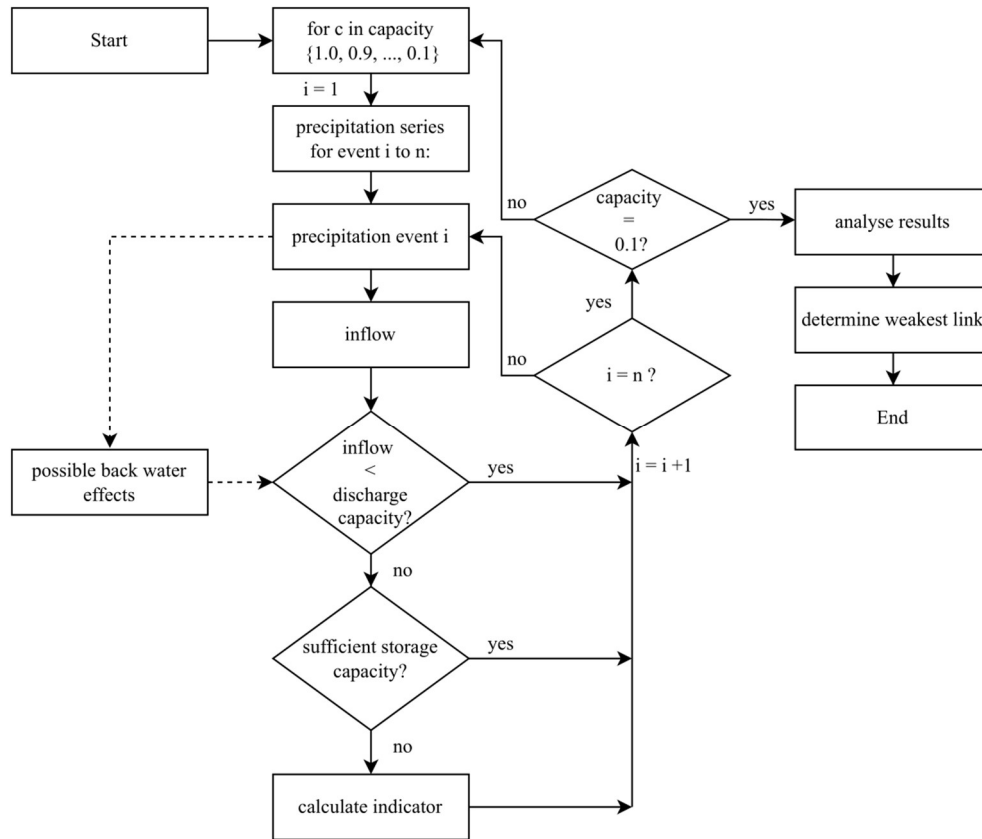
Figure 3.9   General overview of the hydrodynamic model-based weakest link method applied to urban drainage systems.

For the analysis of the flows through the network, the minimum cost flow algorithm (Hagberg et al., 2008) is used (see Subsection 3.3.2). The algorithm calculates the

minimum costs for a flow that satisfies the demands of all nodes. In order to apply the algorithm, a cost and capacity must be determined for each connection.

To estimate the capacity of the connections and the costs of the connections between the layers of the graph (see Subsection 3.5.2), hydrodynamic process descriptions are linearised (see Subsection 3.5.3). The general outline of the GBWLM is shown in Figure 3.10. The various components are described in detail in the following sections, and the main characteristics are summarised in Table 3.1.
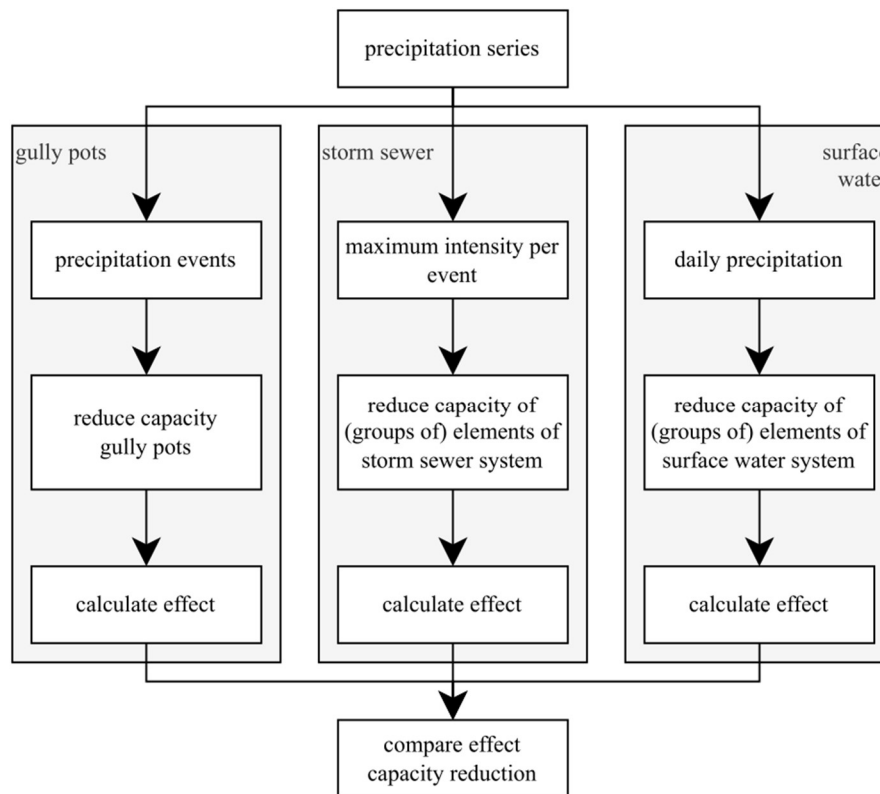
Figure 3.10   The graph-based weakest link method process for urban drainage systems focused on gully pots, storm sewers and surface water systems. For a detailed description see Subsections 3.5.1–3.5.3.

Table 3.1   Characteristics of the graph-based weakest link method for urban drainage systems consisting of gully pots, storm or combined sewer systems and surface water.

	Gully pots	Storm sewer	Surface water
Failure mechanism	Capacity reduction	Capacity reduction	Capacity reduction
Outcome	Flooded area and flood frequency	Flooded area and flood frequency	Flooded area and flood frequency
Network schematisation	Not applicable	Digraph 3 layers	Digraph 2 layers
Costs of edges	Not applicable	Static and dynamic head loss	Static and dynamic head loss
Capacity of edges	Not applicable	Linearised hydraulics	Linearised hydraulics
Evaluation method	Inflow vs capacity	Flow between layers of the graph	Flow between layers of the graph + water balance

3.5.1   Precipitation load on the subsystems

The test load applied is a multiyear precipitation series that is subdivided into mutually independent events (see the precipitation blocks at the top of the three columns in Figure 3.10). A model for rainfall runoff is omitted for the sake of simplicity. As a result, inflow is equal to precipitation volume at all times. Events are considered to be mutually independent when the initial conditions of the system are identical for each event (i.e.: the time for emptying the system after a storm event has to be considered as this determines the initial filling of the system for the next event. These events are considered independent only when the time-gap between time windows in which precipitations occurs is larger than the time needed to empty the system. The characteristic system response times of the gully pots and storm sewers are determined and used to divide the series into separate independent events. The urban drainage system was tested with the full precipitation series. For the individual events, it was determined whether flooding occurred or not.

The critical precipitation load of the subsystems depends on their primary function (storage or discharge). The leading principles (in flat areas) are the following:
- Gully pots: exceeding discharge capacity (rainfall intensity).
- Storm sewers: exceeding discharge capacity (rainfall intensity).
- Surface water systems: exceeding storage capacity (rainfall volume).

The inflow and outflow of subsystems are interdependent. The maximum drainage capacity of gully pots affects the maximum inflow of the storm sewers. In addition, the

cumulative outflow of the storm sewer results in a cumulative inflow of the surface water system (see Figure 3.11 and, for more details, Appendix C.1.).
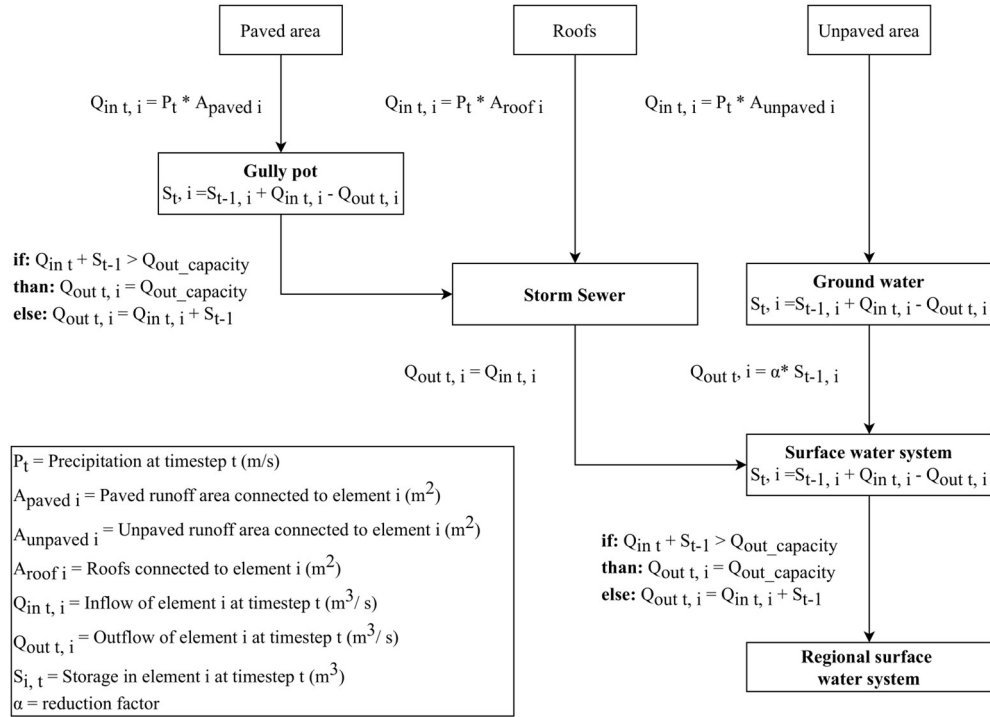
Figure 3.11   Overview of the water balance of graph-based weakest link method subsystems.

3.5.2   Graph schematisation of storm water and surface water networks

The design of the subsystems in the GBWLM can be tuned to the characteristics of the systems and the leading principle (see Subsection 3.5.1). A gully pot is represented as a reservoir with outflow. The storm sewers and surface water systems are described as digraphs (digraph-1; see Figure 3.5). The nodes represent manholes and the edges represent conduits in storm sewer digraphs. In surface water digraphs, the nodes correspond to the watercourses between two structures, and the edges to the structures (weirs, orifices, pumps). All the structures in both the combined or storm sewers and surface water systems are made of multiple sub-connections in order to increase capacity with increasing head loss (see Subsection 3.5.5).

Surface water system

A copy of digraph-1 is created (digraph-2) for the surface water system. The two digraphs when combined form an object referred to as a layered graph (layer-1 = digraph-1, layer-2

3 Materials and methods

= digraph-2; see Figure 3.5, layered graph, and Figure 3.12). Layer-2 is used as a bypass to drain the water if the capacity of layer-1 is insufficient. The bypass is used to ensure that the algorithm used (minimum cost flow algorithm, see Subsection 3.3.2) always finds a solution. The layers are connected at the nodes. Each node of layer-1 is connected with its copy in layer-2. On the outflow location(s) of the network, the direction of the connection between the layers is from layer-2 to layer-1. At the other nodes, the direction between the layers is from layer-1 to layer-2.

For the surface water system, a water balance is used at each node to store the water that cannot be drained via the structures. The available storage is determined for the watercourses between two structures with equation 3.8.

$$
\left.\begin{array}{c}
\Delta t \times Q_{in} + S_{t-1} > \Delta t \times Q_{structure} \rightarrow Q_{out} = Q_{structure}, \\
S_t = S_{t-1} + \Delta t \times Q_{in} - \Delta t \times Q_{out} \\
\\
\Delta t \times Q_{in} + S_{t-1} \leq \Delta t \times Q_{structure} \rightarrow Q_{out} = Q_{in} + \frac{S_{t-1}}{\Delta t}, \\
S_t = S_{t-1} + \Delta t \times Q_{in} - \Delta t \times Q_{out} = 0
\end{array}\right\} \quad (3.8)
$$

where Q_{out} is outflow of surface water node (m³/s), Q_{in} is inflow of surface water node (m³/s) $Q_{structure}$ is maximum discharge capacity structure (m³/s), Δt is time interval (s), and S_t is storage in surface water node at timestep t (m³).
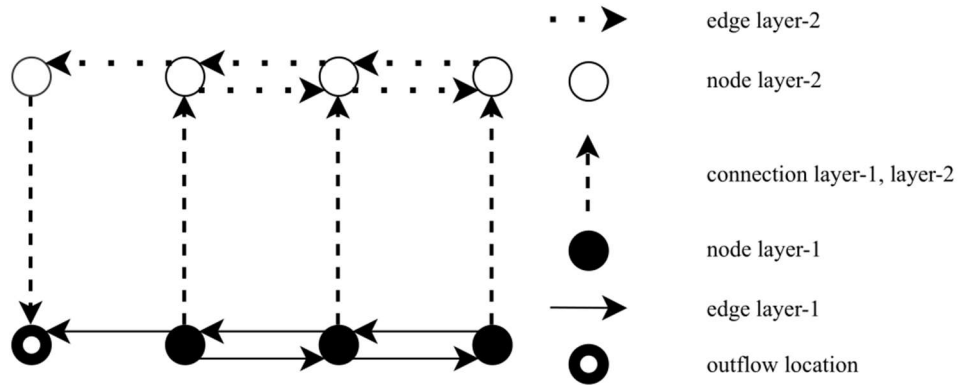
Figure 3.12   Overview of the edge types in the surface water component of the graph-based weakest link method. Layer-1 represents the structure of the network in which the nodes represent manholes watercourses. Edges correspond to the structures. Layer-2 is used when capacity of layer-1 is exceeded and indicates rising water levels in the surface water system.

Storm sewer system

Two copies of digraph-1 are created (digraph-2 and digraph-3) for a combined or storm sewer system. The nodes in layer-1 represent the manholes. The edges represent the

66

conduits of the storm or combined sewer system. Each node (manhole) of layer-1 is linked to the copy of this node in layer-2 (connection L1–L2) and layer-3 (connection L1–L3). The nodes of the layers are connected with an edge in the opposite direction at the outflow locations (connection L2–L1 and connection L3–L1 instead of connection L1–L2 and connection L1–L3). Layer-2 is used to drain the water when the capacity of layer-1 is insufficient. Layer-3 is used as a bypass to drain the water when the capacity of Layer-1 and the connections L1–L2 are insufficient (see Figure 3.13). The use of three layers makes it possible to limit the capacity of the connection L1–L2 and still always arrive at a solution of the minimum cost flow algorithm via layer-3.
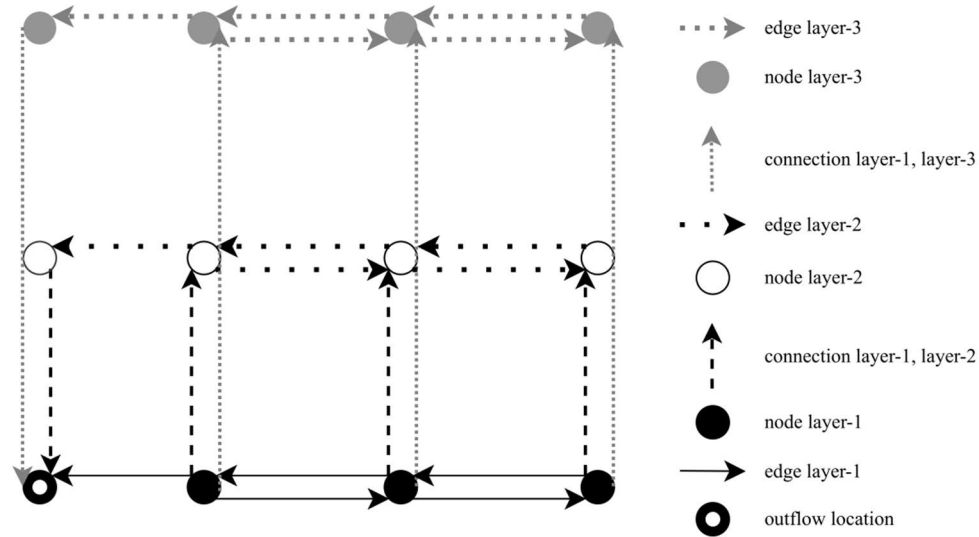
Figure 3.13 Overview of the edge types in the storm or combined sewer component of the graph-based weakest link method. Layer-1 represents the structure of the networks in which the nodes represent manholes. Edges correspond to the pipes and structures. Layer-2 is used when capacity of Layer-1 is exceeded and indicates flooding. Layer-3 is a bypass in case the capacity of the links between Layer-1 and Layer-2 is exceeded.

3.5.3 Linearised hydrodynamics in the GBWLM

Hydrodynamics are linearised to estimate the capacity of the pipes and the costs of the connections between layers of the graph. The quadratic hydraulic gradient equation (Equation 3.9) has been simplified to a linear relationship (Equation 3.10). The maximum capacity of each pipe is computed (Equation 3.9) based on the maximum available hydraulic gradient. α_{linear} is determined for each pipe by linearising the discharge (between zero and the maximum pipe capacity) and the maximum available hydraulic gradient (Equation 3.10):

$$I = \alpha_{quadratic}Q^2 \qquad\qquad (3.9)$$

$$I = \alpha_{linear}|Q| \qquad\qquad (3.10)$$

where I is the hydraulic gradient (-), Q is the discharge (m³/s), $\alpha_{quadratic}$ is a quadratic hydraulic parameter (s²/m⁶) and α_{linear} is a linear hydraulic parameter (s/m³).

The process of linearisation in the GBWLM consists of the following steps:
1. Calculate the costs of the pipes based on the head loss (see 3.3.1).
2. Calculate the available hydraulic gradient. The available gradient for conduits depends on the crest level or surface water level of the outflow point, street level and path length and is determined as follows:
   a. For digraph-1, the shortest paths of all nodes to the closest outflow points are calculated with the Dijkstra algorithm (Dijkstra, 1959).
   b. For each manhole, the minimum available hydraulic gradient is determined by dividing the differences between ground level and crest level by the path length without taking into account the available gradients of the other manholes.
   c. For each manhole (from smallest to largest available hydraulic gradient from step b), the available hydraulic gradient is recalculated, this time taking into account the gradients of the other manholes. If a path crosses a path with a known hydraulic gradient, the hydraulic gradient is computed between the level of the gradient line at junction, the street level and the path length.
3. Calculate the pipe capacity with Equation 3.9.
4. Calculate α_{linear} with Equation 3.10.
5. Determine the runoff area that discharges via a pipe. The paths that include a pipe are selected. The runoff area of all starting nodes (sources) of these paths is summed.
6. Determine costs between connections for layer-1 and layer-2. The costs are equal to the freeboard (ground level minus water level) of all manholes which correspond with the static head loss. The water levels are calculated with an iterative process. The discharge and corresponding hydraulic gradient (Equation 3.10) in every pipe are calculated based on the runoff area that drains via a pipe (step 5) and a low rainfall intensity. Starting at the node with the smallest available hydraulic gradient, the water levels are calculated on the path from the closest outfall (see step 2 c). If the water level is below ground level at all manholes, the rainfall intensity is increased until the water level is above ground

level at one or more manholes. The water levels calculated with the last intensity at which no floods occur are used to calculate the freeboard for every manhole.

3.5.4 Network linearisation parameter: a topology parameter for urban drainage networks

To determine in advance whether the hydrodynamics can be linearised and the GBWLM is suitable for analysing a network, the NLP has been developed as an indicator. The NLP is based on the network geometry, pipe characteristics and the runoff area.

In optimal designed networks, the pipe diameters are matched to the design flow rates. In flat areas, this results in uniform hydraulic gradients, especially in pipes toward outflow locations. In pipes furthest from the outfalls, other design criteria influence the minimum pipe diameter, resulting in lower gradients. At bottlenecks (pipes with larger hydraulic gradients at high flows than adjacent upstream pipes), the gradient increases to allow a larger discharge.

If full hydraulic equations are used, each pipe gets a specific hydraulic gradient in order to use the maximum capacity of the network. In the GBWLM, each pipe has a fixed maximum capacity based on a fixed gradient. The linearisation in the GBWLM is valid when the hydraulic gradients in the network are approximately equal. The degree of homogeneity of the gradients in a catchment draining into an overflow determines whether linearisation can be applied successfully. If there are many bottlenecks, especially in the main pipes to the outfall locations, the outcomes of the GBWLM are less valid.

The hydraulic gradient in the GBWLM depends on the α_{linear} and the discharge (Equation 3.10). The required capacity of each pipe is unknown at the start. To estimate the discharge, the shortest paths between all manholes and the outflow structure are determined. For each pipe, the runoff area that discharges via a pipe (RA_{pipe}) is calculated based on the runoff area of each manhole and the shortest path from the manhole to an outfall. Based on the α_{linear} and RA_{pipe} the NLP is determined by Equation 3.11:

$$\text{NLP} = \frac{1}{\alpha_{linear}\,RA_{pipe}} \tag{3.11}$$

where NLP is the network linearisation parameter (m/s), RA_{pipe} is the runoff area that discharges via a pipe (m^2) and α_{linear} is a hydraulic parameter (s/m^3).
For each pipe, the NLP is quantified along a path from the manhole to the outflow location by calculating the NLP-factor (Equation 3.14). If the NLP-factor of a pipe is larger than 1, the head loss is larger than the head loss of the directly upstream pipe. If the NLP-factor

exceeds a threshold, the pipe is labelled as a "bottleneck". The part of a UDN that drains to an outflow location is defined as an "outflow catchment". For each bottleneck, two parameters are determined:

1. Bottleneck location, Equation 3.13.
2. Percentage of affected manholes, Equation 3.14:

$$\text{NLP-factor} = \frac{\alpha_{lineair}\, RA_{down\,stream\,pipe}}{\alpha_{lineair}\, RA_{up\,stream\,pipe}} \tag{3.12}$$

$$\text{Bottleneck location} = \frac{Pipe\,No.}{Max.path\,length} \tag{3.13}$$

$$\%\text{ affected manholes} = \frac{No.manholes}{Tot.No.manholes} \times 100\% \tag{3.14}$$

where the bottleneck location is the position of the bottleneck in a path relative to the maximum path length of all manholes in an outflow catchment, Pipe No. is the location number of a pipe counted from outflow location (-), Max. path length is the maximum path length to the outfall location of all manholes in an outflow catchment (-), % affected manholes is the percentage of manholes affected by the bottleneck, No. Manholes is the number of manholes with a path to an outlet crossing the bottleneck and Tot. No. Manholes is the total number of manholes in a UDN (see Figure 3.14).

Outflow catchment 17R0204, Almere Waterwijk Noord

Outflow catchment

Max. path length

Bottleneck

Affected manholes
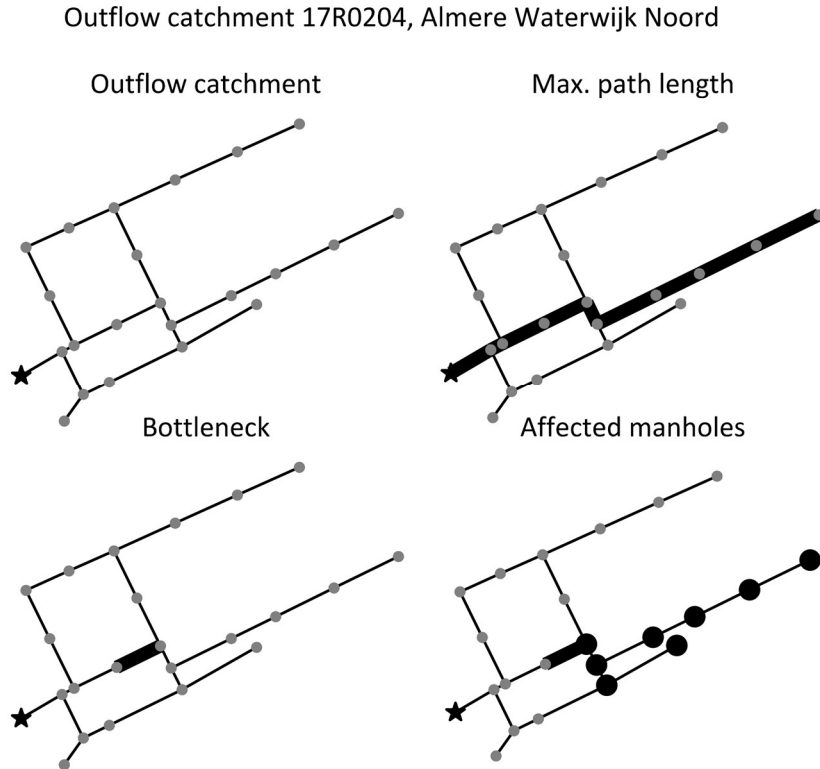
Figure 3.14 Example of the network linearisation parameter for outflow catchment 17R0204 of the urban drainage network of Almere Waterwijk Noord. The upper-left subplot depicts the outflow catchment 17R0204 and the outfall is indicated by a star. The wide black line in the upper-right subplot is the maximum path length. The wide black line in the lower-left figure is the location of the bottleneck. The dots in the lower-right figure are the affected manholes.

3.5.5 The costs and capacity of links in the GBWLM

The costs and capacity of most of the edges in the GBWLM are derived from the head loss. The process to determine the capacity of the pipes is described in the previous section and the costs of the pipes in Subsection 3.3.1. For some edges, an additional operation is carried out or an exception can be made. These are described below.

Bypass edges
The capacity of the bypass edges (see Figure 3.12 surface water: Layer-2, connection L1–L2, connection L2–L1; and Figure 3.13 combined and storm sewer: Layer-3, connection L1–L3, connection L2–L1, connection L3–L1) is equal to the total inflow. This ensures that there is always a path through which all the water can be drained. The bypass (excluding

connection L2–L1, connection L3–L1) may only be used if there is no other outlet route available. Therefore, the cost of the bypass should be equal to the total cost of the non-bypass pipes. The costs of connection L2–L1, connection L3–L1 are zero.

Combined or storm sewer edges L1–L2
The L1–L2-connections of the combined and storm sewers should only be used if the full capacity of layer-1 is used. If the sum of the costs of all edges in layer-1 is used, this is always the case. In addition, a distinction must be made in the costs of the various connections based on the freeboard. The combination of the sum of costs of all edges of layer-1 and the freeboard is used as costs for edges L1–L2.

The capacity of L1–L2 influences the number of flooding locations. If the capacity of layer-1 is insufficient, water will flow via L1–L2 connections to the second layer. The capacity of the L1–L2 connections, in combination with the shortage of drainage capacity in layer-1, determines how many L1–L2 links are required to drain the water. If a L1–L2 link is used, to the location is marked as a flood location. A default value depending on the flood characteristics can be used for the capacity of L1–L2.

Structures
All the structures in both the combined or storm sewers and surface water systems are made of multiple sub-connections in order to increase capacity with increasing head loss. Small changes in head loss can result in large changes in hydraulic capacity of structures (and especially weirs). The relationship between capacity and costs (head loss) of a structure is derived from its characteristics. The head loss is incrementally increased. For each head loss, a sub-connection is added to the graph. The cost of the sub-connection is equal to its head loss. For sub-connection 1, the capacity is equal to the capacity of the corresponding head loss. For the other sub links (i in 2 to n), the capacity is equal to the capacity of corresponding head loss of sub-connection i minus the capacity of the corresponding head loss of sub-connection $i-1$ (see Table 3.2).

Table 3.2   Costs and capacity of structures.

Sub-connection of structure	Head loss (m)	Costs	Total capacity structure (m³/s)	Capacity sub-connection structure (m³/s)
1	0.01	0.01	$Q = \alpha 0.01^\beta$	$Q = \alpha 0.01^\beta$
2	0.02	0.02	$Q = \alpha 0.02^\beta$	$Q = \alpha 0.02^\beta - \alpha 0.01^\beta$
3	0.03	0.03	$Q = \alpha 0.03^\beta$	$Q = \alpha 0.03^\beta - \alpha 0.02^\beta$
Etc.	…	…	…	…

The capacity and costs of all link types of the GBWLM are summarised respectively in Table 3.3 and Table 3.4.

Table 3.3   Overview of the capacity of the edges in the digraphs.

Edge type	Capacity storm sewer	Capacity surface water
layer-1	$Q = \alpha H^\beta$	$Q = \alpha H^\beta$
layer-2	$Q = \alpha H^\beta$	total inflow
layer-3	> total inflow	not applicable
connection L1–L2	default value for more details see Subsection 7.2.3	total inflow
connection L1–L3	total inflow	not applicable
connection L2–L1	total inflow	total inflow
connection L3–L1	total inflow	not applicable

Table 3.4   Overview of the costs of the edges in the digraphs of the graph-based weakest link method.

Edge type	Costs storm sewer	Costs surface water
layer-1	head loss	head loss
layer-2	head loss	head loss
layer-3	head loss	not applicable
connection L1–L2	sum costs of edges in layer-1 + freeboard	sum costs of edges in layer-1
connection L1–L3	sum costs of edges in layer-1 and layer- 2	not applicable
connection L2–L1	0	0
connection L3–L1	0	not applicable

3.5.6   Capacity reduction and effect

Gully pots

The results of a reduction of the discharge capacity of the gully pots can be evaluated (see left column of Figure 3.10 and Figure 3.4). The number of events in which the discharge capacity is less than the rainfall intensity (which is identical to the runoff intensity, as no rainfall runoff model is used) is counted per gully pot and multiplied with the runoff area of the gully pot. This results in an estimation for the flooded area and the flood frequency.

Storm sewers

The consequences of a capacity reduction of the sewer system is evaluated using the function Min_Cost_Flow of the Networkx module in Python (Hagberg et al., 2008). This function determines the flow paths having minimum costs of all nodes to the central outflow point; this is performed for each event (see the centre column of Figure 3.10 and Figure 3.9). Water flows from the nodes of digraph-1 via the edges to the central outflow point. If the water flows through a layer-1–layer-2 edge, the manhole is labelled as flooded. The flooded area is set equal to the runoff area of the connected gully pots.

Surface water system

The effects of a reduction of the surface water system are determined in two steps: 1) the water levels are calculated (see Figure 3.9); 2) if these exceed a threshold, then the impact on the storm sewer is calculated (backwater effect, see Figure 3.15). The inflow in the surface water systems flows, together with the stored water, to the central outflow point (see Figure 3.11). A water level change is calculated by dividing the stored water volume by the storage area. If the level rise exceeds a threshold, the impact on the storm sewer is calculated. The capacity of the sewer conduits is then re-calculated based on the increased water level and the corresponding hydraulic gradients. The event that caused the increased surface water level is selected from the storm sewer event series and recalculated with the GBWLM to determine the flooded area in the storm sewer. If the flooded area has increased compared to the situation of the 100% available sewer capacity, the increase in flooded area and frequency is counted.
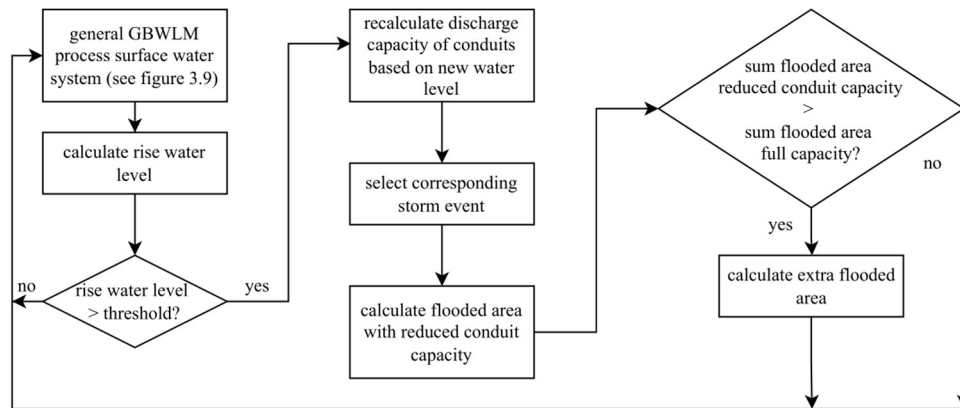
Figure 3.15   Process of the surface water component of the graph-based weakest link method.

3.6   Statistical measures for comparison of outcomes

3.6.1   Kendall's τb coefficient

The Kendall rank correlation coefficient (Kendall, 1945), commonly referred to as Kendall's tau-b coefficient (τ_b) is used to determine the relationship between the outcomes of the HBWLM and the GTM. τ_b is a nonparametric measure of association based on the number of concordances and discordances in paired observations. τ_b is used to compare the relationship of datasets and not of individual conduits. Minus one (−1) implies a 100% negative association; one (1) is a 100% positive association. Equation 3.15 presents this calculation:

$$\tau_b = \frac{(P-Q)}{\left(\sqrt{(P+Q+X_0)*(P+Q+Y_0)}\right)} \tag{3.15}$$

where τ_b is Kendall's tau b coefficient, P is the number of concordant pairs, Q is the number of discordant pairs, X_0 is the number of pairs tied only to the X variable and Y_0 is the number of pairs tied only to the Y variable.

3.6.2   F1 score

The F1 score (or F1 measure) is a measure of the accuracy of a test. It combines the recall and precision in a single measure. The recall is a measure of the critical elements that were correctly identified as such, and the precision represents the proportion of correctly identified critical elements (see Figure 3.16). If recall and precision are of equal weight, the formula is as follows (Chinchor, 1992):

$$F_1 = \frac{2*P*R}{P+R} = \frac{2*TP}{2*TP+FP+FN} \tag{3.16}$$

$$R = \frac{TP}{TP+FN} \tag{3.17}$$

$$P = \frac{TP}{TP+FP} \tag{3.18}$$

where P is precision (-), R is recall (-), TP is true positive (-), FP is false positive (-), FN is false negative (-) and F_1 is F1 score (-).
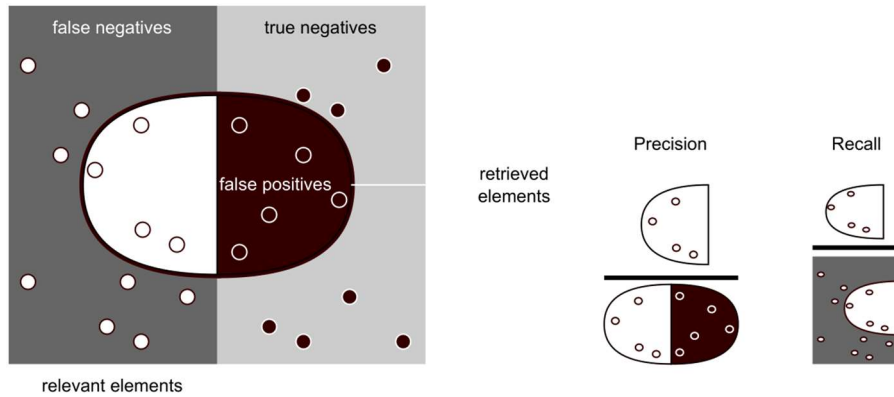
Figure 3.16 Precision and recall (Note. Adapted from "F-Score", (n.d.). CC-BY-NC).

For the GBWLM, precision is the number of correctly identified flooded manholes divided by the total number of flooded manholes identified by the GBWLM. The recall of the GBWLM is the correctly identified number of flooded manholes by the GBWLM divided by all the flooded manholes (in the hydrodynamic model).

For a studied WDN, a percentage of the most critical elements, identified with the hydraulic model method, is selected. The same percentage of most critical elements identified with the graph theory method is also selected. A comparison is made of the true positive, false positive and false negative items. Because the group size is predefined, the number of false positive and false negative elements are the same (unless there are equal rank numbers), and therefore the precision and recall and F1 score are also the same. For maintenance and rehabilitation strategies, the elements of a WDN can be divided into groups. The exact ranking within each group is less important, provided that the overlap between the HBWLM and the GTM is sufficient. The F1 score is a measure of the overlap.

3.6.3   Matthews correlation coefficient

The Matthews Correlation Coefficient (MCC), or phi coefficient, can be used to compare the outcomes of the HBWLM and the GBWLM:

$$MCC = \frac{(TP * TN) - (FP * FN)}{\sqrt{(TP + FP) * (TP + FN) * (TN + FP) * (TN + FN)}} \qquad (3.19)$$

Where TP is true positive (flooded manholes in the hydrodynamic model and the GBWLM), TN is true negative (non-flooded manholes in the hydrodynamic model and the GBWLM), FP is false positive (flooded manholes in the GBWLM but not in the hydrodynamic model) and FN is false negative (flooded manholes in the hydrodynamic model but not in the GBWLM). Unlike F1, the MCC takes into account the number of both correctly and incorrectly predicted positive (flooded) and negative (not flooded) locations.

If any of the four sums in the denominator is zero, the MCC is set to 0. This means that if none or all manholes are flooded in both approaches, the prediction is 100% correct, but the MCC = 0. If only a few manholes are flooded or not flooded, the first term of the numerator is (true positive × true negative) and is relatively small, and therefore the MCC value is relatively low. This happens at the transition point from non-flooding to flooding. Therefore, in addition to the MCC, the percentages FP and FN should also be considered.

3.7　Overview of the presented methods

Three methods have been presented to determine the criticality of elements in networks. The GTM for pressurised systems and gravity-driven systems determines the criticality based on a change in "transport costs" in the network. These GTMs have been developed to identify the most critical elements but not to evaluate the impact of failures. The methods are only intended to indicate whether the failure of one element affects the performance of the network more or less than the failure of another element.

The GBWLM was developed to determine both the criticality of elements in urban drainage systems and the impact of a change in the system, such as a capacity reduction or increase in load. To estimate the reliability of the results of the GBWLM in advance, the NLP was developed.

To clarify the differences among the three methods, their main characteristics are summarised in Table 3.5 and Table 3.6. The tables show that the analysed failure mechanism, the network schematisation, the costs of the edges, the inclusion or exclusion of the capacity of the pipes and the evaluation criteria depend on the network type.

Table 3.5　　Characteristics of the graph theory method for pressurised and gravity-driven systems.

	Pressurised systems	Gravity-driven systems
Failure mechanism	Leakage	Blockage
Outcome	Ranking of the elements	Ranking of the elements
Network schematisation	Graph	Digraph
Costs of edges	Dynamic head loss	Static and dynamic head loss
Capacity of edges	Not applicable	Not applicable
Evaluation method	Costs to leak versus costs to pump stations	Unconnected node and cost to outfalls

Table 3.6   Characteristics of the graph-based weakest link method for urban drainage systems consisting of gully pots, storm or combined sewer systems and surface water.

	Gully pots	Storm sewer	Surface water
Failure mechanism	Capacity reduction	Capacity reduction	Capacity reduction
Outcome	Flooded area and flood frequency	Flooded area and flood frequency	Flooded area and flood frequency
Network schematisation	Not applicable	Digraph 3 layers	Digraph 2 layers
Costs of edges	Not applicable	Static and dynamic head loss	Static and dynamic head loss
Capacity of edges	Not applicable	Linearised hydraulics	Linearised hydraulics
Evaluation method	Inflow vs capacity	Flow between layers of the graph	Flow between layers of the graph + water balance

4 Studied water systems

4.1 Introduction

The methods presented in Chapter 3, the Graph Theory Method (GTM) and the Graph-Based Weakest Link Method (GBWLM) have been applied to multiple case studies. This section describes the case studies and provides some background information on the case studies. These case studies are all located in the Netherlands, most of them are situated in flat areas, and one resides in a mildly sloped region.

The degree of variation in ground level has an influence on the functioning of drainage systems. Therefore, Section 4.2 describes the functioning of urban drainage systems in the Netherlands. Subsections 4.2.1 and 4.2.2 present the characteristics of Urban Drainage Networks (UDNs) and urban surface water systems, respectively. The interactions between these systems are explained in Subsection 4.2.3. The three subsequent sections describe the studied water distribution networks (WDNs; Section 4.3), combined sewer and storm water systems (Section 0) and urban drainage system (Section 4.5). Section 4.6 presents the applied rainfall series.

4.2 Urban drainage systems in the Netherlands

The purpose of urban drainage systems is to supply water in dry periods in order to keep the (ground) water levels at the desired height. In wet periods, the aim is to store and drain water and prevent flooding (see Figure 4.1). For the second purpose, urban drainage systems consist of the anterior part of drainage systems (gully pots and lateral household connections), the storm water or drainage network and the receiving surface water system.

Analysing an entire urban drainage system requires a considerable amount of work because of the large number of components (gully pots, manholes, pipes, pumps, structures, channels, etc.). The interpretation of model results and the translation into practice requires experience and knowledge. Subsystems (e.g. combined sewer systems, storm water systems and local or regional surface water systems) are commonly analysed

separately, and the functioning of some components (e.g. gully pots, household connections) are often neglected.
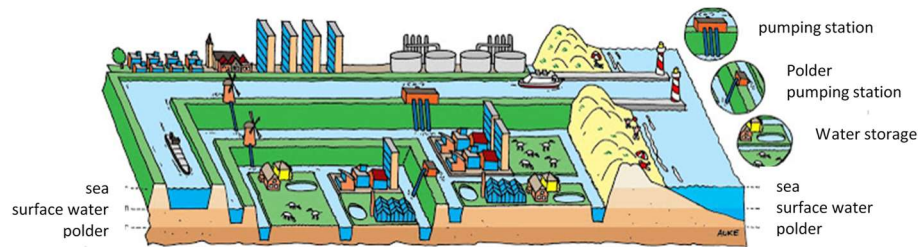
Figure 4.1   Urban drainage and stormwater management systems (Note. Adapted from A. Herrema, personal communication, September 1, 2019. Copyright 2019 by A. Herrema. Reprinted with permission).

4.2.1   Characteristics of urban drainage networks

Because the Netherlands is flat, the distance over which water can be transported by gravity is limited (1–2 km). Specific characteristics of UDNs in flat areas are:

- Looped systems: except for hilly parts in the south-eastern region of the Netherlands, most combined, foul and storm water systems are looped systems. If blockage occurs during dry weather conditions, water can flow through other pipes to the pumping station, preventing blockages from being noticed. During storm events, these blockages, initially not noted, sometimes cause pluvial flooding.
- Low flow velocities: because of the limited hydraulic gradient during both dry weather conditions and storm events, flow velocities are limited. Normal flow velocities vary from < 0.1 m/s during dry weather conditions to 0.7–1 m/s during storm events. These velocities are normally too small for allowing sediment transport of significance, which may result in relatively strong sediment accumulation in the systems (Ashley et al., 2004).
- Many Combined Sewer Outflow (CSO) structures: because of the limited hydraulic gradient, the transport distance to CSO structures is limited. Runoff surface discharging to individual CSOs is in general < 15 ha. Blockages influence the hydraulic gradients. The combination of many CSOs, limited hydraulic gradients and blockage sometimes result in an inversion of hydraulic gradients and a redistribution of the flows over the CSOs. Thus, catchments do not always discharge via the same CSO.

4.2.2 Characteristics of urban surface water systems

Urban surface water systems are designed to store and drain water to regional water systems. Weirs are used to compartmentalise water systems into areas with mutually different water levels, depending on the ground level and land use. In the western part of the Netherlands, pumps are used to drain water to regional systems because a large part is situated below sea level. In urban areas, roads cross the watercourses by bridges or culverts. Therefore, the urban surface water system is subdivided into subsystems by culverts and weirs, each with specific storage and discharge capacities.

Water levels in receiving surface water systems may strongly influence the functioning of UDNs. Therefore, the analysis of entire urban drainage systems is important for the understanding of the functioning of the urban drainage systems (Bolle et al., 2006; Jha et al., 2012). Because the subsystems are often managed by several organisations, the data of the subsystems are also managed by different organisations. Because it is a rather complicated task to combine different models, both from technical and organisational perspective, studies often focus on only one subsystem.

For system analyses, long-term simulations are essential because each system (gully pots, drainage system, surface water system) has its own specific characteristic time scale. A linear relationship between the output and input of various models does not exist. Consequently, the statistics for determining flood return periods (average time between events to occur) calculating the expected annual damage is not straightforward. This is explained in more detail in Subsection 4.2.3. Long-term simulations that require a large computational effort are needed (Vaes et al., n.d., 2009), yielding impractical demands on computation time.

4.2.3 Functioning of urban drainage systems

The functioning of the subsystems (gully pots, storm sewers, and surface water) of an urban drainage system depends on the design capacity. Each subsystem has its own design criteria. Commonly used design criteria in the Netherlands are as follows (see Figure 4.2):
- Gully pots: discharge capacity of 54 mm/h (150 l/(s.ha)).
- Storm sewers: discharge capacity of 21.6 mm/h (60 l/(s.ha)).
- Surface water: storage capacity of 60 mm and a discharge capacity of 0.54–1.08 mm/h (1.5–3 l/(s.ha)).
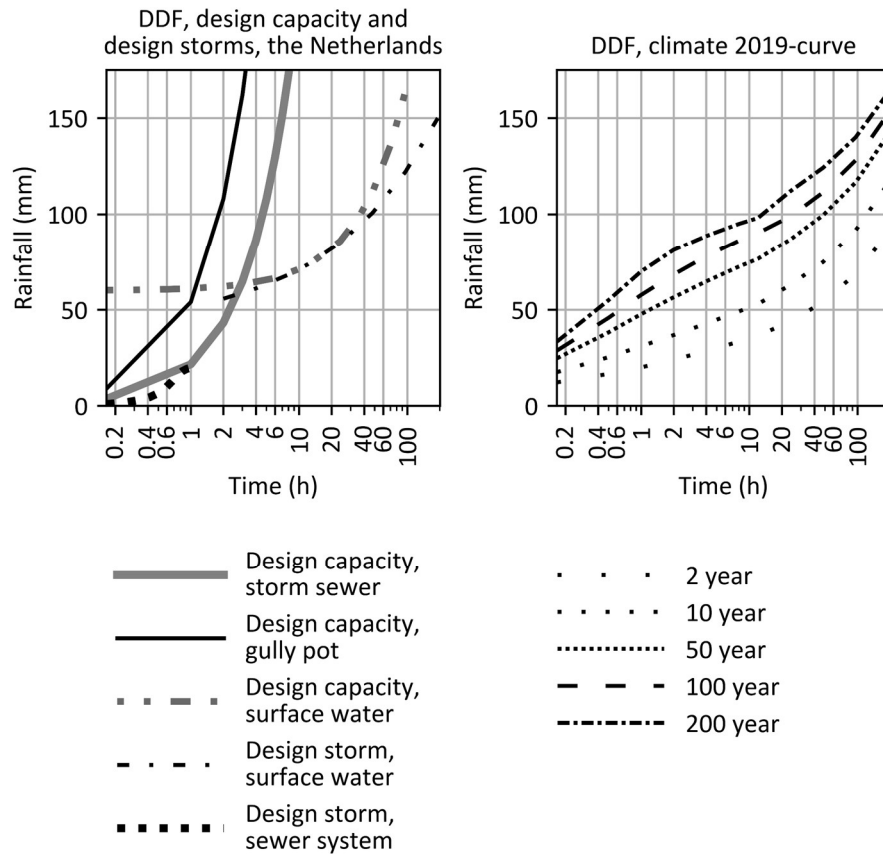
Figure 4.2   Left: design capacity and design storm events (Note. based on: Langeveld & Schilperoort, 2019); right: depth duration frequency curves Beersma et al., 2019).

Shortly after the start of an intense storm event, the subsystems may start to interact with each other. This interaction is seldom included in the design and management of the system. The functioning of the subsystems with and without interaction is presented in Figure 4.3 and Figure 4.4.

The process of draining and storing precipitation without interaction between the subsystems is sketched in Figure 4.3 (based on Langeveld & Schilperoort, 2019). If the storm intensity exceeds 21.6 mm/h and the storm volume is less than approximately 60 mm, flooding occurs due to the limited capacity of the storm sewer system. If the storm intensity exceeds 41.67 mm/h (150 l/(s.ha)) and the volume is less than approximately 60

mm, flooding starts by exceeding the capacity of the gully pots. If the storm volume exceeds approximately 60 mm, flooding occurs by exceeding surface water capacity. The depth duration frequency (DDF) relation with a return period of, for example, T = 50 years (Beersma et al., 2019) exceeds the capacity of the three mentioned subsystems. For this event, Figure 4.3 shows:

- 0 – approximately 0.8 h: T = 50 years event exceeds the capacity of the gully pots and the storm sewer.
- Approximately 0.8 – 3 h: T = 50 years event exceeds the capacity of the storm sewer.
- Approximately 3 – 24 h: T = 50 years event the capacity of the surface water system.
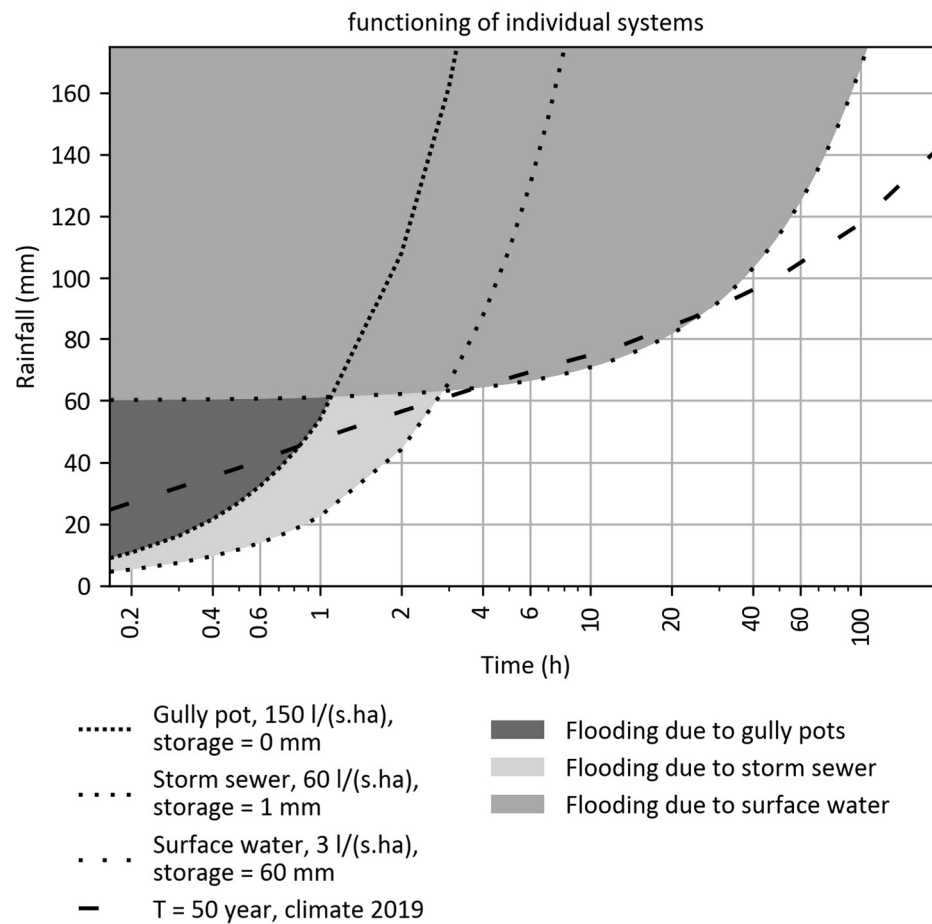
Figure 4.3   The general functioning of the individual subsystems of an urban drainage system, without the interaction between the subsystems (based on: Langeveld & Schilperoort, 2019).

4 Studied water systems

The interaction between the subsystems is dynamic. This is illustrated with a T=25 year event as an example. The functioning of the subsystems, including interaction, is represented in Figure 4.4 (based on the DDF curve; Beersma et al., 2019). In general terms, the following sequence of phases is triggered by a storm event:

- Discharge increases and water level in the storm sewer rises. At critical locations (locations far from the outflow or locations with low ground levels), the water level exceeds the ground level, consequently decreasing the capacity of the gullies due to back-water effects. At those locations, the gully pot inflow capacity becomes equal to the storm sewer's capacity.
- The water level in the surface water rises. The available hydraulic gradient in the storm sewer decreases, and therefore the discharge capacity reduces. This results in more critical locations and flooding. At those locations, the inflow capacity of the gully pots will be reduced.
- When the full storage capacity of the surface water is used, the drainage capacity of the gully pots and storm sewers will be equal to the discharge capacity of the surface water of 3 l/(s.ha).

As a result of the interaction between subsystems, the actual capacity of the subsystems is often lower than the design capacity; instead of the design capacity, the capacity of the subsystems varies in time and place. During a storm event, the discharge ranges between the maximum discharge capacity of the subsystems and the discharge capacity of the downstream-situated subsystems. Well-maintained gully pots and storm sewers close to outfall locations will maintain the design capacity for a longer period of time, in contrast to gully pots and storm sewers far from outfalls where the capacity reduces quickly after the start of the storm event. If the interaction is included in the analysis, the flood duration for a T = 25 year event increases from approximately 2 hours to 4 hours and even longer depending on the location in the network (Figure 4.4). This means that to understand the location and severity of flooding, including a statistically reliable return period, an analysis using an integrated model and a long time precipitation series is needed.

integrated functioning, T = 25
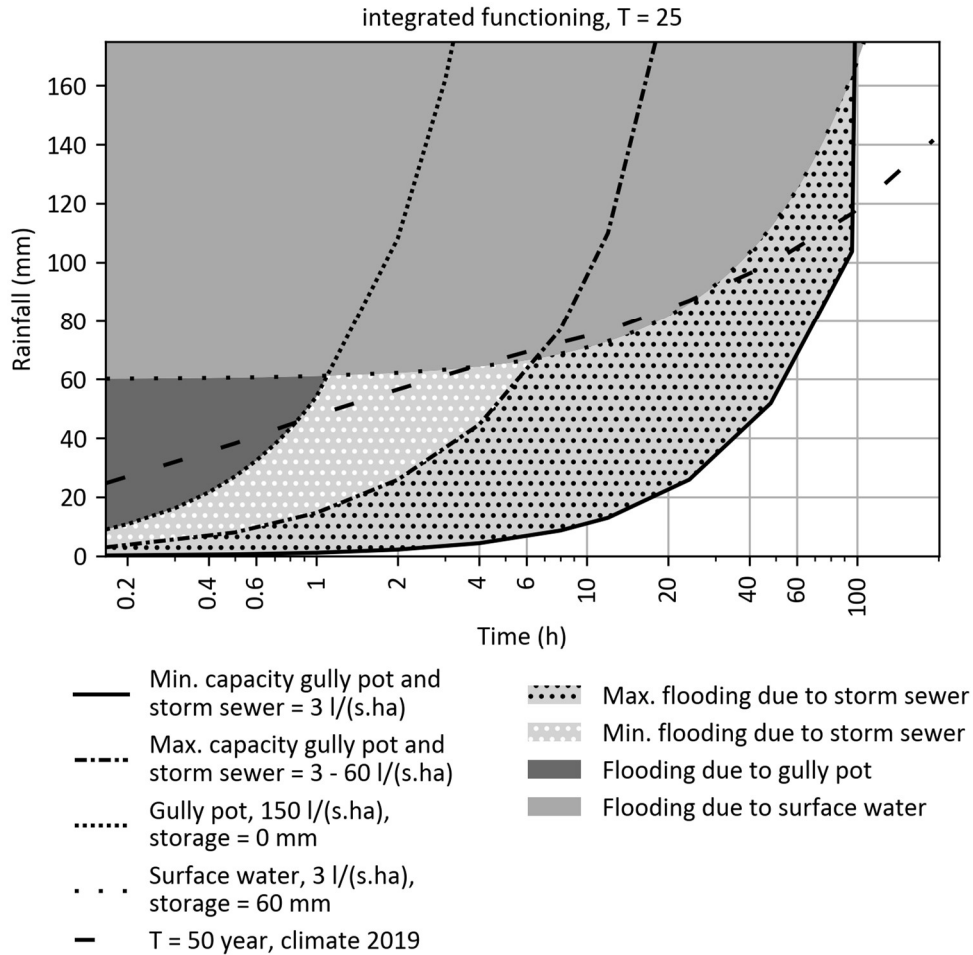
Figure 4.4   The individual subsystems including the interaction between the subsystems for an event with a return period *T* = 25 years.

If the balance between the subsystems is disturbed, the capacity will decrease. The balance between subsystems changes if the capacity of the subsystems changes (e.g. due to ageing, change in run off area or adjustments in one of the subsystems [operational condition]) or if precipitation intensities change (as a result of climate change). It is expected that, due to climate change, the recurrence time of a *T* = 25 event in 2019 will decrease to *T* = 10 in 2050 (Beersma et al., 2019). The effect of above-mentioned changes is shown in Figure 4.5 and Figure 4.6.

Figure 4.5 shows the interaction for a climate scenario of 2050 (Beersma et al., 2019). Climate change is increasing precipitation intensity and volume. As a result, surface water levels will rise faster reducing the capacity of the storm sewer. This is the area hatched with circles in Figure 4.5.
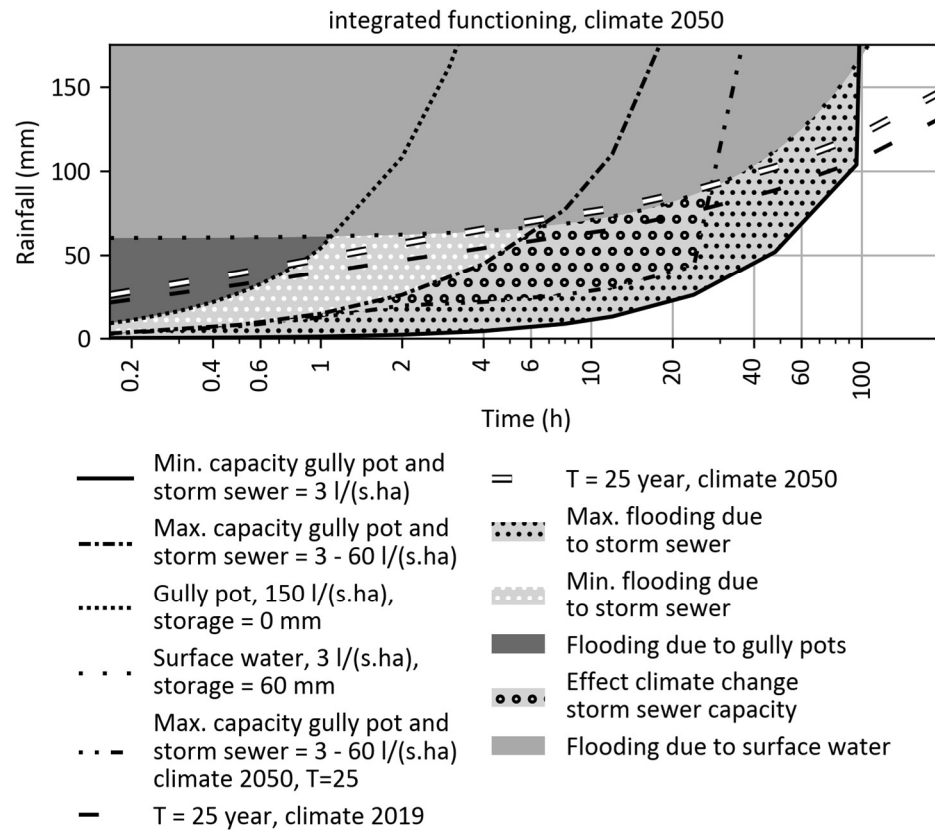
Figure 4.5   Integrated functioning climate 2050: the functioning of the systems with a climate scenario of 2050.

Figure 4.6 shows the effect of a capacity reduction of 33%. The effect of reduced capacity of the gully pots is presented in Figure 4.6 with horizontal and vertical hatch. The effect of reduced capacity of the surface water system is indicated with a diagonal hatch. The storm sewer capacity is also affected by the reduced capacity of the surface water system. The impact of the reduced capacity on the storm sewer is indicated by the star hatch. To quantify the effects of climate change or capacity reduction an analysis of the combined subsystems, an analysis using an integrated model and a multiyear precipitation series is needed.

integrated functioning, reduced capacity

······· Gully pot, 150 l/(s.ha), storage = 0 mm	····· Max. flooding due to storm sewer
· · · Surface water, 3 l/(s.ha), storage = 60 mm	★★★ Extra flooding from storm sewer
=·=· Min. capacity gully pot and storm sewer = 2 l/(s.ha)	░░░ Min. flooding due to storm sewer
=·=·· Max. capacity gully pot and storm sewer = 2 - 40 l/(s.ha)	Flooding due to gully pots
—— Min. capacity gully pot and storm sewer = 3 l/(s.ha)	Extra flooding from gully pot
–·–·· Max. capacity gully pot and storm sewer = 3 - 60 l/(s.ha)	Flooding due to surface water
::::::: Gully pot, 100 l/(s.ha), storage = 0 mm	Extra flooding from surface water

Figure 4.6   Integrated functioning reduced capacity: the functioning of the systems with a capacity reduction of 33%.

4.3 Case studies for water distribution networks

Three WDNs were used as case studies for a demonstration and a comparative analysis of the GTM for pressurised systems with the HBWLM. The first network is the Cavlar WDN. This is a benchmark WDN that is used as test model of the Dutch Watercycle Research Institute (Mesman, 2018). The second network is the WDN of the village of Leimuiden, the Netherlands. This network was chosen because it has been used as a case study in previous research (e.g., Moors et al., 2018); as a result, detailed, validated models are available. The third model is the WDN of Tuindorp in Utrecht, the Netherlands. The Tuindorp WDN is part of the larger WDN of the city of Utrecht and was chosen because detailed information is available on both the WDN and the UDN. This allows for combined analysis of the criticality of both networks in future research.

Figure 4.7 shows the layout of the networks; the details of the networks are presented in Table 4.1. The software tool Wanda (Deltares, Delft, the Netherlands) was used for the hydraulic calculations.

Table 4.1   Main characteristics of the water distribution networks.

Characteristics	Cavlar	Tuindorp	Leimuiden
Drinking water utility	Does not apply	Vitens	Oasen
Area (km^2)	5.7	1.7	1.5
Number of water pumping stations	1	2	1
Number of households	5,817	1,922	1,835
Network length (km)	34.9	37.2	26
Number of pipes + valves	1,054	1,701	3,243
Number of connection points	1,040	1,611	3,218
Number of connection points with water users	747	503	1,438
Minimum diameter (mm)	22	25	32
Maximum diameter (mm)	600	710	315
Loops[1]	15	92	25
Branches	118	174	79

---

[1] A loop is defined as a path with the same start and end of more than two nodes with the least number of nodes with a minimum degree of three.

Cavlar   Leimuiden   Tuindorp

1000 m   1000 m   1000 m

Figure 4.7   The structures of the water distribution networks.

4.4   Case studies for combined sewer and storm sewer systems

Five combined sewer systems and two storm water systems were used as case studies to demonstrate and validate the following:

- The GTM for gravity-driven systems.
- The urban drainage part of the GBWLM.
- The Network Linearisation Parameter (NLP).

The combined sewer systems in the case studies are:

- Loenen, the Netherlands.
- Tuindorp in Utrecht, the Netherlands.
- Drunen, the Netherlands.
- Heusden, the Netherlands.
- Vlijmen, the Netherlands.

The storm sewer networks in the case studies are:

- Waterwijk Zuid in Almere, the Netherlands.
- Waterwijk Noord in Almere, the Netherlands.

The systems of Loenen and Tuindorp have been analysed several times in other studies and are also extensively calibrated (Korving & Clemens, 2005; Langeveld et al., 2005; van Bijnen et al., 2012, 2017). Table 4.2 and Table 4.3 show their characteristics, and Figure 4.8 shows the layout of the systems. For the Loenen catchment, two situations were studied: Loenen-2, including both CSO structures, and Loenen-1, where a weir that only becomes active during storm events with high rainfall intensities is closed. The software tool Sobek (Deltares, Delft, the Netherlands) was used for the hydraulic calculations.

89

Table 4.2   Characteristics of four urban drainage systems.

Characteristics	Waterwijk Zuid	Waterwijk Noord	Loenen	Tuindorp
Catchment area	Flat	Flat	Mildly sloping	Flat
System type	Storm water	Storm water	Combined	Combined
System structure	Looped	Looped	Partly branched	Looped
Contributing area (ha)	9.2	14.6	20.5	56.2
Number of inhabitants (-)	0	0	2,100	10,656
Number of combined sewer overflow structures (-)			2	5
Number of storm sewer outflow structures (-)	4	3		
Number of pumping stations (-)	0	0	1	1
Number of edges (-)	92	118	352	778
Number of nodes (-)	80	102	337	684

Table 4.3   Characteristics of three urban drainage systems.

Characteristics	Vlijmen	Heusden	Drunen
Catchment area	Flat	Flat	Flat
System type	Combined	Combined	Combined
System structure	Looped	Looped	Looped
Contributing area (ha)	208.74	41.34	103.01
Number of inhabitants (-)	15,740	4,786	11,600
Number of combined sewer overflow structures (-)	10	6	4
Number of pumping stations (-)	1	1	2
Number of edges (-)	1,776	787	2,053
Number of nodes (-)	1,556	722	1,843

Almere
Waterwijk
Zuid

Almere
Waterwijk
Noord

750 m

750 m

Loenen

Tuindorp

750 m

750 m

Vlijmen

Heusden

750 m

750 m

Drunen

750 m
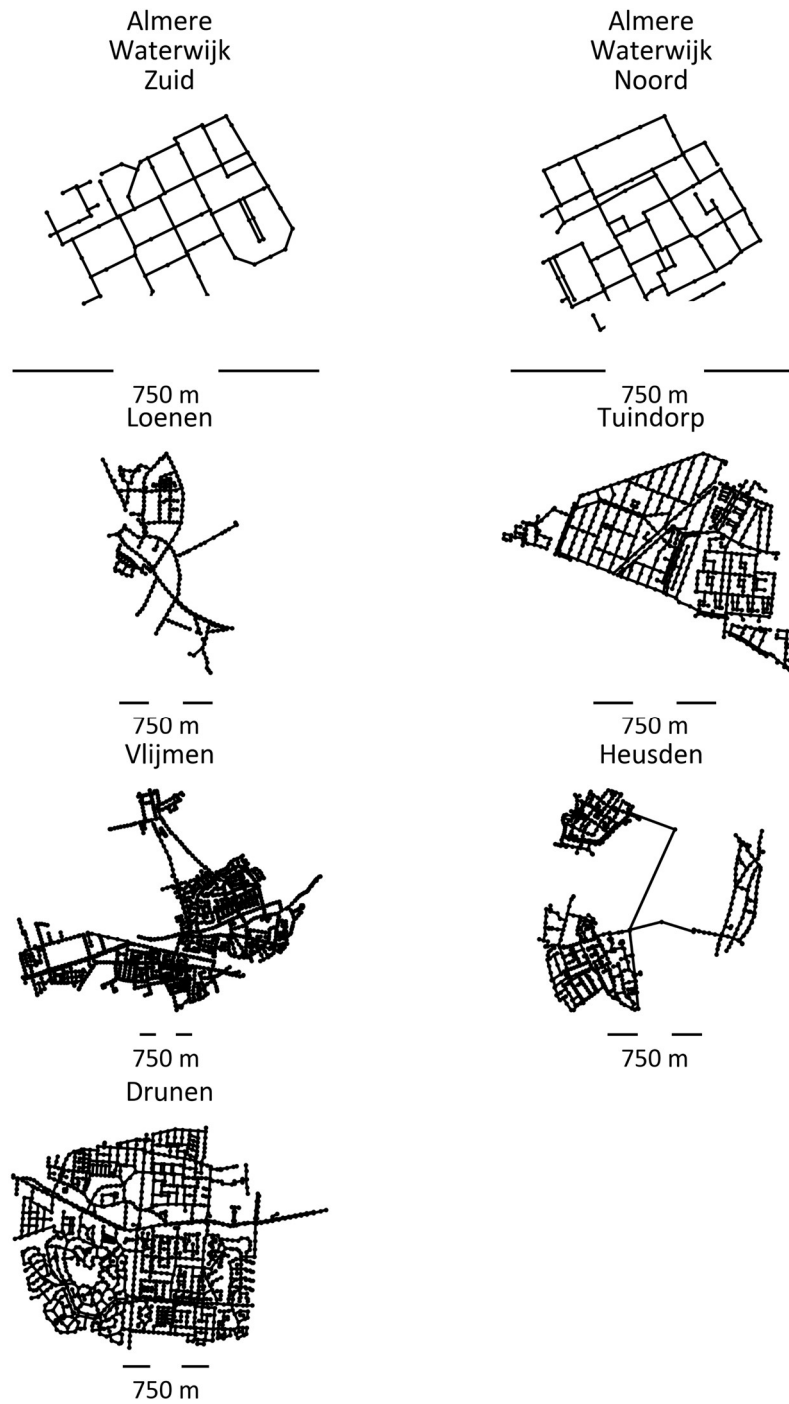
Figure 4.8   Structure (pipes and manholes) of seven urban drainage systems.

4.5   Case study for urban drainage systems

A part of Almere's urban drainage system in the Netherlands was used as case study for the GBWLM. Almere is located in Flevoland, a province that was reclaimed from the former Zuiderzee. It is an entirely human-made and controlled polder system. The case study focused on the surface water system in Almere Centrum (see Figure 4.9) and the storm sewer catchments Waterwijk Oost Noord (referred to as Waterwijk Noord) and Waterwijk Oost Zuid (referred to as Waterwijk Zuid), situated in the north-eastern part of the area (for more details, see Subsection 4.2.1). The pumping station that discharges water to a larger regional surface water system is situated just to the south of Waterwijk Zuid.

The "Weerwater" is a large pond (1.5 km^2) located in the centre of the surface water system; because of its storage capacity, it has a dampening effect on variations in the surface water level. The surface water system is divided into a main system and a smaller subsystem. The water level in the main system, directly connected to the storm water systems, has a –5.5 m reference level. The reference water level in the smaller section in the southwestern part is –4.8 m and functions as a boundary condition for the main system. During storm events, water is discharged from the subsystem to the main system. The characteristics of the surface water system are summarised in Table 4.4. The software tool Sobek (Deltares, Delft, the Netherlands) was used for the hydraulic calculations.
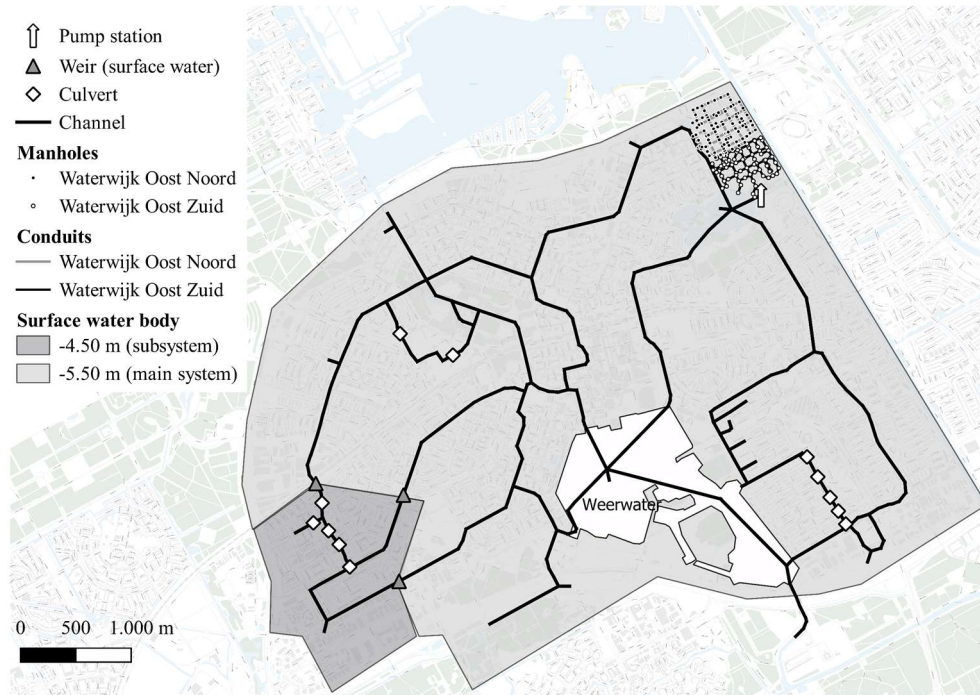
Figure 4.9   The urban drainage system of Almere.

Table 4.4   Characteristics of the surface water system of Almere Centrum.

Characteristics	Surface water system Almere Centrum
Length of channels (km)	39.8
Area surface water (km^2)	2.6
Runoff area unpaved (km^2)	8.0
Runoff area paved (km^2)	12.4
Surface water level (m reference level)	−4.8 and −5.5
Number of weirs	3
Number of culverts	12
Pump capacity (m^3/s)	3.41

Table 4.5 provides an overview of the runoff area per gully pot, determined using the Voronoi triangulation (Voronoï, 1908). In Waterwijk Zuid, a school playground is connected to some gully pots, resulting in a relatively large (119 m^2) average runoff area per gully pot.

Table 4.5   The characteristics of the gully pots in Waterwijk Noord and Waterwijk Zuid.

Characteristics	Waterwijk Noord	Waterwijk Zuid
Number of gully pots	696	461
Average runoff surface per gully pot (m²)	103	119
Maximum runoff surface per gully (m²)	338	486

4.6   Applied rainfall series and events

4.6.1   Applied rainfall events for gravity-driven systems

Precipitation events were used to determine the criticality of elements in urban drainage models with the HBWLM. Different events were used to understand the sensitivity of the criticality to the type of event examined (Table 4.6). First, the most commonly used stationary (homogeneous in space and constant in time) design events in the Netherlands, with an intensity of 40, 60 and 90 l/(s.ha), were used. Loenen, with two CSOs, was tested with a more extensive set of 10 stationary storm events with rainfall intensity ranging from 10–100 l/(s.ha). The duration of all stationary events was 24 hours. Second, 10 design storm events (homogeneous in space and dynamic in time) from the Dutch national guidelines for hydrodynamic modelling of urban drainage systems (Stichting RIONED, 2004) were used[2]. These storm events cover a range of return periods (0.25, 0.50, 1, 2, 5 and 10 years), pattern shapes (peak intensity at the beginning or at the end of the event) and durations (45, 60 and 75 minutes). The storm events varied between 10.5 mm in 75 minutes (maximum intensity 40 l/(s.ha). or 14 mm/h) to 35.7 mm in 45 minutes (maximum intensity 210 l/(s.ha) or 75.6 mm/h). Third, for the Tuindorp catchment, 13 independent storm events were selected from the rainfall series observed by the Royal Dutch Meteorological Institute in De Bilt (period 1955–1964).

Table 4.6   Storm events used to determine criticality with the hydrodynamic model-based weakest link method for gravity-driven systems. CSO = combined sewer outfall.

	Stationary design storm events	Dynamic design storm events	Observed storm events
Loenen 1 CSO	40, 60 and 90 l/(s.ha) (14, 21.6 and 32.4 mm/h)	10	not applicable
Loenen 2 CSOs	10 - 100 l/(s.ha) (3.6-36 mm/h)	10	not applicable
Tuindorp	40, 60 and 90 l/(s.ha) (14, 21.6 and 32.4 mm/h)	10	13 events

---

[2] In 2020, composite storm events were added to the Dutch national guidelines for hydrodynamic modelling (Stichting Rioned, 2020).

Van Bijnen et al. (2012) applied Monte Carlo simulations to systematically study the impact of in-sewer defects on the hydraulic performance of the Tuindorp catchment. Because it was not possible to predict which storm event would result in flooding in the model simulations due to the changes in the characteristics of the network during each run in the Monte Carlo procedure, long-term rainfall series were used instead of predefined storm events. The authors selected 41 independent storm events. The selection criteria required that: 1) the water level reached a level higher than the threshold level 25 cm below ground level or 2) at least two CSOs started working. In addition, a selection of conduits was applied to determine the impacts on hydraulic performance. The conduit locations were chosen based on the system layout and expert judgement. This resulted in a total number of 198 conduits. In the hydraulic simulations regarding pluvial flooding, the diameters of selected conduits were reduced individually to 10% of the original conduit diameters.

The results of the above simulations showed that the number of flooded locations, flood volumes and threshold exceedances in Tuindorp were caused by 13 of the 41 rainfall events. The total calculation time was 273 hours, which is a very time-consuming method for this looped system. For the 13 storm events (homogeneous in space and dynamic in time) that caused flooding, the criticality of conduits was determined. The characteristics of these 13 storm events are presented in Table 4.7.

Table 4.7 Characteristics of the 13 observed storm events.

Storm event	Total volume (mm)	Maximum intensity (mm/15 min)	Duration (dd:hh:mm)
17-7-1955	23.5	7.49	00:17:30
23-8-1956	43.9	3.69	02:20:30
20-9-1957	56.8	6.68	03:06:30
18-8-1958	23.1	10.62	01:12:30
23-6-1960	16.8	12.5	00:10:30
7-10-1960	114.0	3.4	06:06:30
1-12-1960	58.0	3.72	03:07:30
5-6-1961	51.4	16.53	00:20:30
25-7-1962	30.8	6.47	03:09:30
1-10-1962	24.0	8.67	01:06:30
2-8-1963	26.0	14.46	02:04:30
17-8-1963	65.2	5.61	04:15:30
17-8-1964	52.2	4.54	02:06:30

4.6.2   Applied rainfall series for urban drainage systems

For the analysis of urban drainage system networks and to understand the consequences of interaction between the subsystems perennial precipitation series were used. The applied rainfall series is the registered series by the Royal Dutch Meteorological Institute in De Bilt over the period 1955–1979 with a 15 minutes resolution.

The storm event in this rainfall series with the largest impact on surface water system in Almere is an event from October 1960 (108.6 mm in 96 h) with a return period of ~50–100 years (estimated from the DDF curve in Figure 4.2). This implies that, although the rainfall series was relatively short, it included a representative event with a return period close to the design return period (T = 100) of the surface water system.

The GBWLM was validated against the outcomes of a hydrodynamic surface water model and a hydrodynamic sewer model of Almere. For the validation of the surface water part of the GBWLM, the period 1955–1964 of the above-mentioned rainfall series was used. For the validation of the storm and combined sewer component, a storm event with increasing rainfall intensity from 1 mm/h to 30 mm/h in steps of 1 mm/h was used. The duration of each precipitation intensity was 12 hours. Between each of the two consecutive precipitation intensities, a dry period of 5 days was applied. This meant that the initial conditions at the different intensities were the same. For these 30 storm intensities, the results of the GBWLM were compared with the results from a hydrodynamic model.

5 Application of the graph theory method to water distribution networks

5.1 Introduction

To validate and demonstrate the Graph Theory Method (GTM) for pressurised systems (see Table 3.5 in Section 3.7 for main characteristics) it was applied to three Water Distribution Networks (WDN). (Hydraulic) conditions and even the structure of the system of WDNs are dynamic; for instance, when a pipe break is detected, valves are closed to isolate the section with the break in order to prevent losses and to allow for repairs to be performed. Ideally the network, apart from the isolated section, achieves the minimum required service level. In this sense, two operational mode conditions can be distinguished:

1. The complete system is operational.
2. One or more sections are isolated from the rest of the system.

A distinction for both modes must be made when applying the GTM because the network structure changes if valves are closed. This study has focused on the situation directly after a pipe break when all valves are open.

Section 5.2 presents the results and interpretation. The outcomes of the GTM were compared with the outcomes of the HBWLM. For the comparison of the degree of criticality, the Kendall's τ_b and the F1 score were used. The τ_b indicates the similarity in ranking results of the two methods, and the F1 score was used to validate the connection points that are marked as positive (critical) and negative (less critical). The results are discussed in Section 5.3. The conclusions regarding the GTM for pressurised systems are presented in Section 5.4.

5.2   Results and interpretation

The criticality of elements in three WDNs (see Section 4.3) was determined by the Hydrodynamic model-Based Weakest Link Method (HBWLM) and the GTM for pressurised systems, and the results were compared. In the HBWLM, a pressure drop of 20 m was applied. For the comparison of the degree of criticality, Kendall's τ_b and F1 scores were used (see Subsection 3.5.6). The F1 score was used as follows. For the studied WDN, a percentage of the most critical connection points identified with the HBWLM was selected (population). The same percentage of most connection points identified with the GTM was selected (retrieved elements). A comparison was made of the true positive, false positive and false negative items. Because the number of the population was equal to the number of the retrieved elements, the number of false positive and false negative connection points were the same (unless there are equal rank numbers). Therefore, the precision and recall and F1 score were also the same (see Equations 3.18-3.20)

Different comparisons were made for the networks, one in which all connection points were ranked and another in which only the connection points to which water users are connected were ranked. Including all connection points allowed for a more detailed analysis because more connections points were used. When only the connection points with drinking water users were ranked, the ranking was focused on the affected number of users.

5.2.1   Results of the Hydrodynamic model-Based Weakest Link Method (HBWLM) and the Graph Theory Method (GTM) (basic method)

The following three subsections present the results of the comparison between the criticality based on the HBWLM and the GTM (basic method) of the Cavlar, Tuindorp and Leimuiden WDNs.

Results of the HBWLM and the GTM for the Cavlar WDN
Both the τ_b value and the F1 score indicated a correlation between the criticality based on the HBWLM and the GTM for the Cavlar network. On the left side of Figure 5.1 and Figure 5.2, the correlation between the HBWLM and the GTM has been plotted. Rank number 1 is the most critical connection point, and the highest rank number (1040/735) is the least critical. Figure 5.1 depicts a correlation between the outcomes for all connection points (τ_b = 0.81). The results for the case with the connection points with water users (Figure 5.2) were similar (τ_b = 0.79). The right sides of Figure 5.1 and Figure 5.2 present the F1 score. The F1 score was greater than 70%, except when only the 1% of the most important connection points were selected.

In order to quantify the F1 score for the 1% most important connection points, the 10 most important connection points (1% of 1040) according to the HBWLM were selected. A similar approach was attempted for the GTM. However, the GTM ranked the first 18 connection points as equally important (GTM rank = 1, HBWLM rank = 1–16, 22 and 35), and therefore it was not possible to select exactly 1% of the connection points. By calculating the F1 score for the first 1% of the most critical connection points, the recall was 1 (the selected connection points by the GTM included the connection points with the rank 1–10 of the HBWLM); however, the precision was relatively low because 18 connection points were selected instead of the requested 10 connection points.

Cavlar

Figure 5.1   Overview of the correlation between the outcomes and the F1 score of the hydrodynamic model-based weakest link method and the graph theory method for the Cavlar water distribution network, with a pressure drop of 20 m for all connection points.

Cavlar

Figure 5.2   Overview of the correlation between the outcomes and the F1 score of the hydrodynamic model-based weakest link method and the graph theory method for the Cavlar water distribution network, with a pressure drop of 20 m for the connection points with water consumers.

Results of the HBWLM and the GTM for Tuindorp's WDN

The results for Tuindorp's WDN were similar to the results of Cavlar network. Figure 5.3 depicts a correlation (τ_b = 0.75) between the criticality based on the GTM and the HBWLM. The F1 score of 0.73–0.97 illustrates an overlap between the results of the GTM and the HBWLM for the 1–10% most critical connection points. The other F1 scores were greater than 0.8. The results for the case with the connection points with water consumers were similar (see Figure B.1). Analysis of the differences between the criticality based on the HBWLM and the GTM for the WDN of Tuindorp indicated, as was the case for the WDN of Cavlar, an overestimation of the criticality of the branches by the GTM.

Tuindorp

Figure 5.3   Overview of the correlation between the outcomes and the F1 score of the hydrodynamic model-based weakest link method and the graph theory method for the Tuindorp water distribution network, with a pressure drop of 20 m for all connection points.

Results of the HBWLM and the GTM for Leimuiden's WDN

The results of Leimuiden's WDN ($\tau_b = 0.65$) differed from the results of the WDNs of Cavlar and Tuindorp (see Figure 5.4). There was a correlation between the HBWLM and the GTM for the connection points with a rank under 600 (20% most important connection points) and over 2,700 (80% most important connection points). However, for these two sections the point cloud was more dispersed than for the Cavlar and Tuindorp cases. Nevertheless, it was possible to use the GBWLM to indicate which 20% (or 80%) of the pipes are the most important for the functioning of the WDN.

For the connection points with a rank between 600 and 2,700, the differences in criticality of the HBWLM and GTM were large. For these connection points, the results were roughly a point cloud. That means, for example, that a criticality of 600 based on the HBWLM could correspond with a criticality between 600 and 7,400 based on the GTM and vice versa. It was therefore not possible to use the GBWLM to determine, for example, the 30–40% most critical pipes.
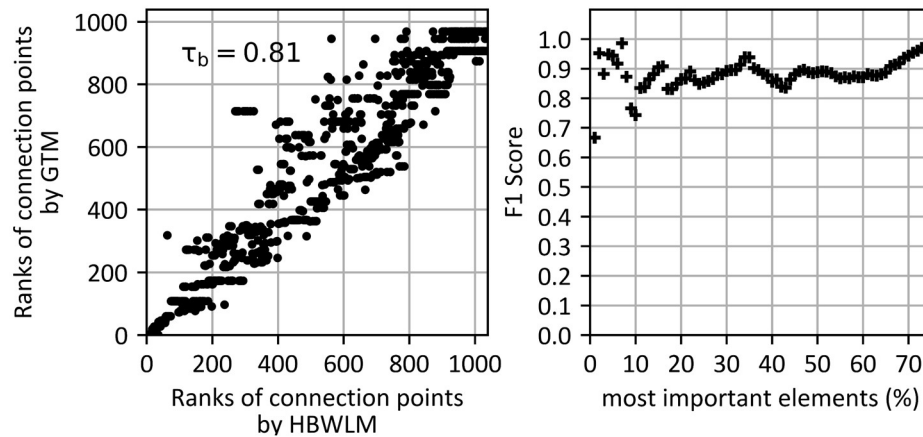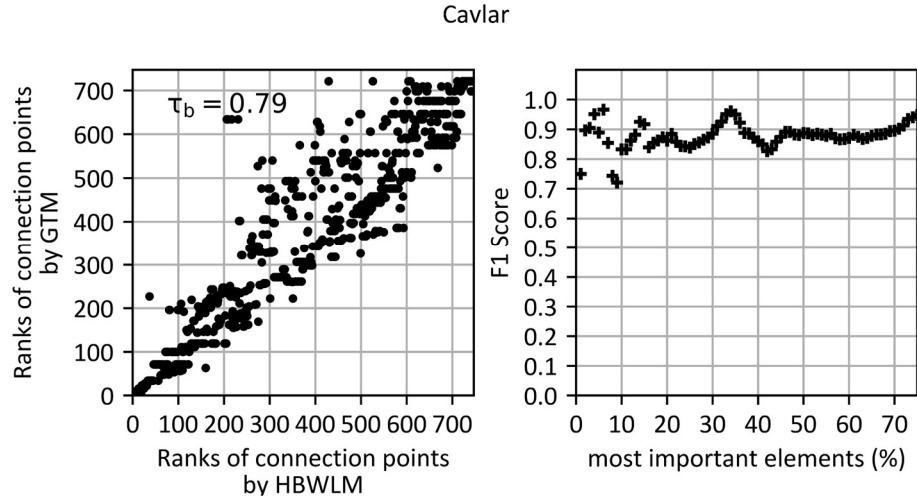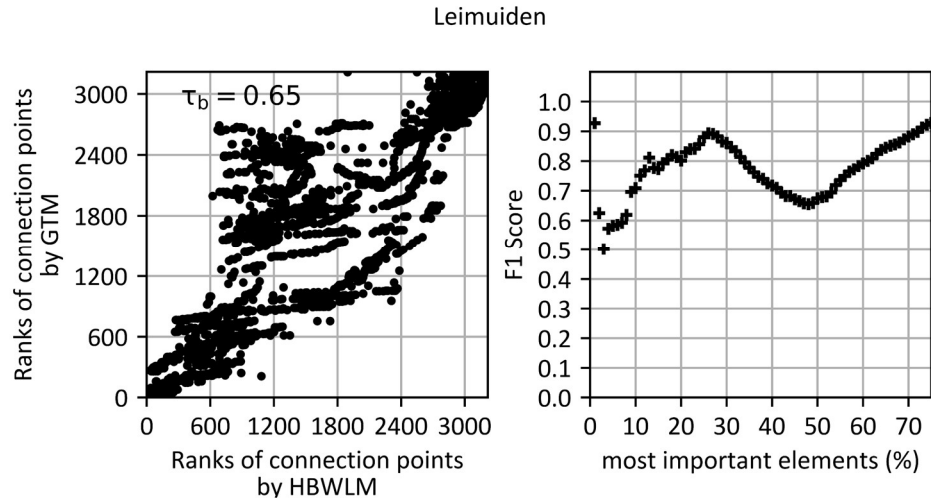
Leimuiden

Figure 5.4   Overview of the correlation between the outcomes and the F1 score of the
               hydrodynamic model-based weakest link method and the graph theory method for the
               Leimuiden water distribution network, with a pressure drop of 20 m for all connection
               points.

The F1 score of the WDN of Leimuiden was also lower than the F1 score of the WDNs of
Tuindorp and Cavlar. The pattern of τ_b values was also visible in the F1 scores because at
the start, the point line was relatively wide, and the F1 score was relatively low. The F1
score varied between 0.50 and 0.93 if the 1–10% most critical connection points were
selected. The F1 score for percentages between 42 and 53 varied between 0.6 and 0.7.
This observation corresponds with the graph at the left side of Figure 5.4, in which the
differences between the HBWLM and GTM are larger. The other F1 scores were greater
than 0.7. The results for the case with the connection points with water consumers were
similar.

Analysis of the difference between the outcomes of the HBWLM and the GTM indicated
that in the WDN of Leimuiden, the importance of the connection points in the loop at the
right side of Leimuiden (see
Figure 4.7) and the branches were overestimated. An underestimation of the criticality
was visible in the centre of the WDN of Leimuiden.

5.2.2 Results of the Hydrodynamic model-Based Weakest Link Method (HBWLM) and the Graph Theory Method (GTM) (weighting method)

The weighting evaluation method (the sum of (costs connection point to water pumping station)$^{-1}$ of connection points at which the costs (head loss) to the leak is smaller than the costs to the WPS [see 3.4.2]) showed a stronger (τ_b = 0.79) correlation between the outcomes of the HBWLM and GTM for the WDN of Leimuiden than the basic method. The points in Figure 5.5 are less dispersed than in Figure 5.4, and the τ_b is 0.14 higher. Figure 5.5 shows that the F1 score was the lowest when the 4% most important items were selected (F1 = 0.48), but all other F1 scores were over 0.57, and for a percentage of 7% and higher, the F1 score was over 0.75.
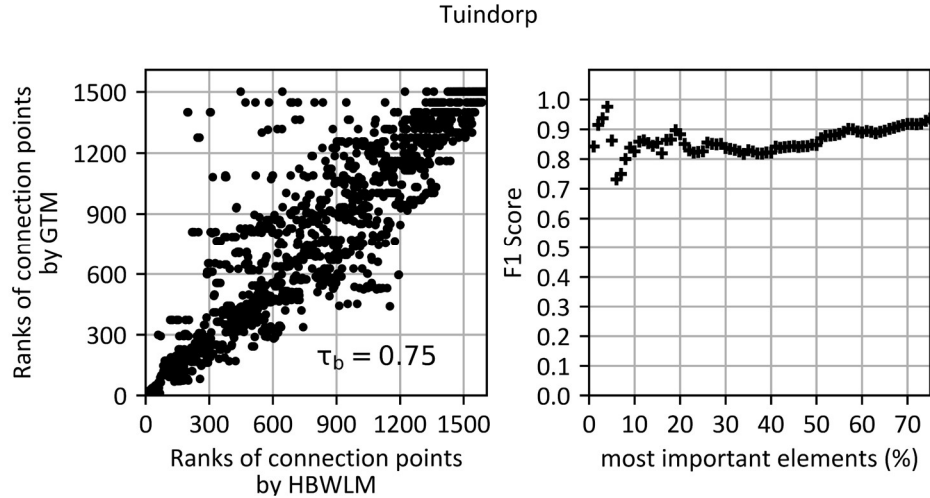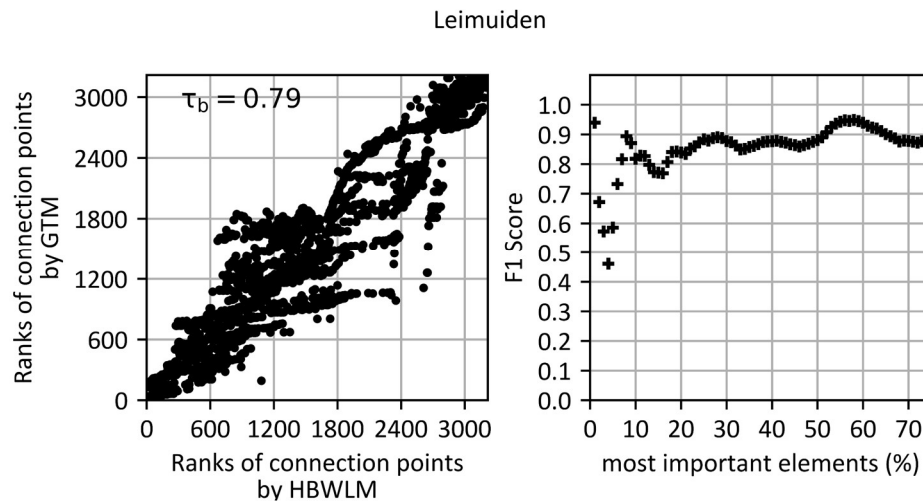
Leimuiden

Figure 5.5   Overview of the correlation between the outcomes and the F1 score of the hydrodynamic model-based weakest link method and the graph theory method for the Leimuiden water distribution network with a pressure drop of 20 m for all connection points. The criticality is based on sum of (costs to water pumping station)$^{-1}$ for the connection points where the costs to the leak are less than to the water pumping station.

5.2.3 Spatial distribution of criticality

The elements of the WDN that are ranked with the GTM are the connection points. For the maintenance of the system, the elements are more important than the connection points. However, the connection points give a clear pattern in the network that can be used to select the most important elements of the network (see Figure 5.6).

Tuindorp 25% most important connection points based
on the hydrodynamic model-based weakest link method

Tuindorp 25% most important connection points based
on the graph theory method

1000 m
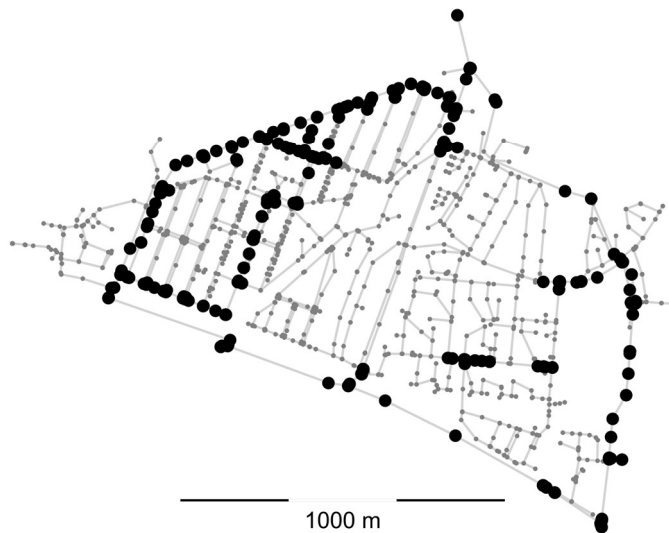
Figure 5.6   Overview of the top 25% in importance connection points (black dots) of the Tuindorp
water distribution network based on the hydrodynamic model-based weakest link
method (top) and the graph theory method (bottom). Those connection points
represent a clear pattern in the network, which can be used to select the most
important elements of the network.

5.2.4 The impact of the head loss on the criticality in the HBWLM

The impact of the applied pressure drop on the criticality was tested with the HBWLM. The degrees of criticality of the connection points for different pressure drops were computed and plotted against each other together with the corresponding τ_b values. If the degree of criticality is independent of the pressure drop, $\tau_b = 1$.

The impact of the applied pressure drop on the criticality was limited, so the pressure drop did not influence the applicability of the GTM. Figure 5.7 shows that the criticality in the Cavlar WDN depended on the size of the pressure drop. However, the differences were limited, and the smallest τ_b was 0.92. Because the correlation between the different pressure drops was high and the size of the pressure drop had almost no influence on the 40–50% most critical connection points, the GTM was not sensitive to pressure drops.

Cavlar, correlation at various pressure drops
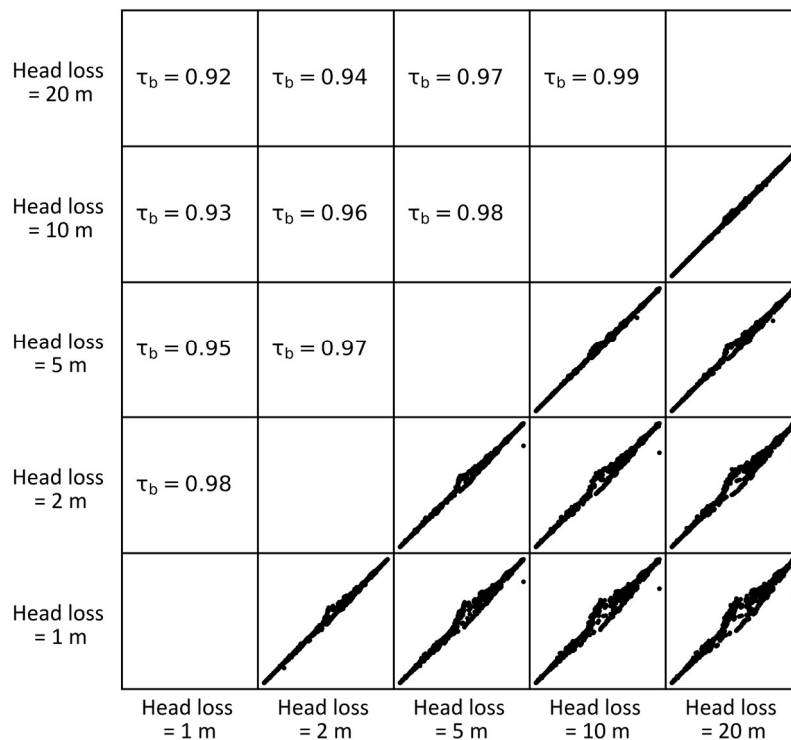
Figure 5.7   Overview of the correlation of criticality of elements based on the hydrodynamic model-based weakest link method by various pressure drops for the Cavlar water distribution network. For example, $\tau_b = 0.96$ in cell head loss = 2 m, head loss = 10 m (0.96), corresponds with the scatter plot in cell head loss = 10 m, head loss = 2 m.

5.2.5 Ranking based on the connections with a pressure below a threshold

A different approach to rank the outcomes of the HBWLM is to count the connection points with a pressure below a certain threshold pressure. Table 5.1 presents an overview of the results in which only the connection points with water users were included.

The following approach was used: the maintained operational pressure head in the WDN was 30 m. A leak was added to the network in the HBWLM with a pressure head of 20 m below the operational pressure, so the pressure on the leak location was 10 m. Criticality was based on the number of water users with an operational pressure below a certain threshold. The process was repeated for four different thresholds. The results were compared with the outcomes of the GTM.

The results show that the larger the differences between the pressure drop and the applied threshold, the higher was the τ_b. When the criticality of the HBWLM was based on connection points with a pressure below the operational pressure minus 19 m (pressure < 11 m) the GTM did not identify the same critical elements. Many connection points received the same ranking in the HBWLM. If the elements in the HBWLM were ranked based on the number of connection points with a threshold pressure of 5 or 10 m below the operational pressure, there was a correlation ($\tau_b > 0.7$) between the outcomes of the HBWLM and the GTM.

Table 5.1   Overview of the τb of the comparison of the results of the hydrodynamic model-based weakest link method ranked on the number of connection points with a pressure below a threshold and the graph theory method.

	Pressure at connection points < operational pressure –19 m	Pressure at connection points < operational pressure –15 m	Pressure at connection points < operational pressure –10 m	Pressure at connection points < operational pressure –5 m
Cavlar	0.45	0.69	0.84	0.82
Tuindorp	0.29	0.57	0.78	0.82
Leimuiden	0.23	0.58	0.73	0.75

The criticality was sensitive to the applied threshold. Figure 5.8 presents the HBWLM result of ranking the connection points based on a threshold value. It shows that the correlation for various thresholds was low. This implies that the result of the method is very sensitive to the criteria applied to the ranking of the elements. Consequently, this criterion may not be useful in practice for determining the criticality of an element.

Leimuiden, correlation at various thresholds

|	Threshold < 11 m	Threshold < 12 m	Threshold < 15 m	Threshold < 20 m	Threshold < 29 m
Threshold < 29 m	$\tau_b = 0.01$	$\tau_b = 0.14$	$\tau_b = 0.31$	$\tau_b = 0.47$	
Threshold < 20 m	$\tau_b = 0.36$	$\tau_b = 0.53$	$\tau_b = 0.77$		
Threshold < 15 m	$\tau_b = 0.51$	$\tau_b = 0.70$			
Threshold < 12 m	$\tau_b = 0.76$				
Threshold < 11 m					
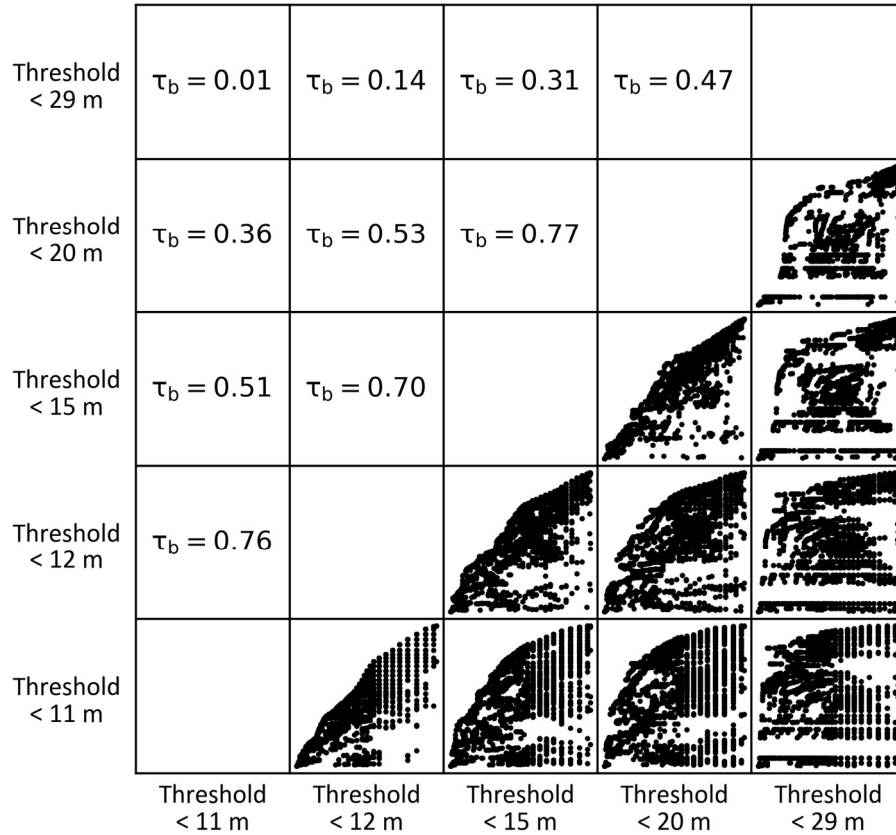
Figure 5.8   Overview of the correlation of criticality of elements based on the hydrodynamic model-based weakest link method by various pressure thresholds for the Leimuiden water distribution network.

5.2.6   Importance of hydraulics versus network structure and geometry

In the GTM, the criticality of a WDN mainly depends on the network structure and the geometry of the network elements. In the HBWLM, the combination of hydraulics, network structure and the geometry of the network elements determines the criticality of elements. To obtain an initial understanding of the importance of network structure and the geometry of the elements versus the hydraulics for the criticality, an analysis was performed. The process of solving the hydrodynamic equations in the HBWLM was limited to examine the contribution of hydrodynamics to the criticality.

5 Application of the graph theory method to water distribution networks

To obtain stable results from the hydrodynamic model, multiple iterations were needed due to the non-linear nature of the equations involved. In each iteration, the discharge in the elements was adjusted until the required precision was met or the maximum number of iterations was reached. The maximum number of iterations was limited to 2, 5, 25 and 100 iterations.

The number of iterations required also depended on the initial conditions and the solver used. For this test, the Wanda solver was used (Deltares, Delft, the Netherlands). The initial conditions consisted of non-flowing water and pressure corresponding to 30 m at the WPS. A leak was added to all connection points in turn with a pressure drop of 20 m (see Subsection 3.2.1).

Figure 5.9 shows that with two iterations, τ_b was 0.76 (comparable with τ_b of the GTM and the HBWLM); with 10 iterations, τ_b increased to 0.97. That τ_b was 0.76 for two iterations implies that in a hydraulic model as well, outcomes depend strongly on the structure of the network. The correlation increased quickly between five and 10 iterations. The Cavlar network showed similar behaviour (see Figure B.7).

It is possible to use differentiated discharges in elements to determine the costs of the elements in the GTM. In this way, one hydraulic aspect can be taken into account more precisely in the GTM. The effect of a differentiated discharge was tested with the GTM. The discharge influences the costs of the elements and therefore the shortest paths.

Tuindorp
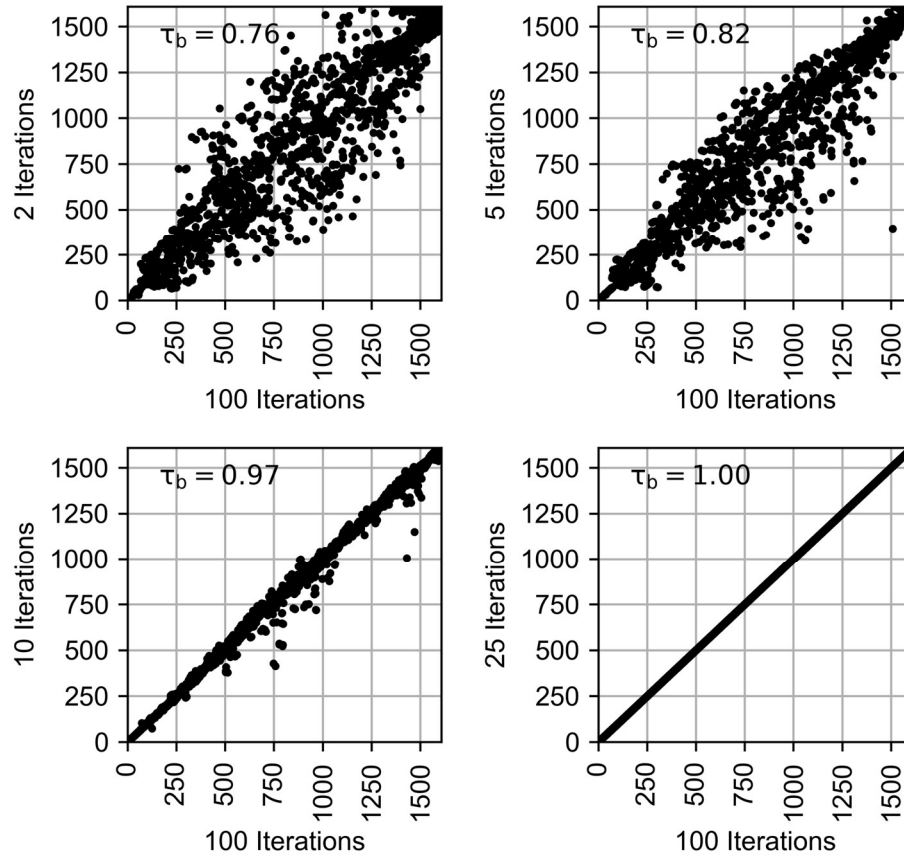
Figure 5.9   Overview of the criticality of the elements of the water distribution network of Tuindorp based on 2, 5, 10 and 25 iterations, respectively, compared with the reference scenario of 100 iterations.

The discharge of each element was determined iteratively and used to determine the costs of the elements. The discharge consisted of a constant part and variable part. For the first iteration, the constant and variable discharge were the same for all elements. This discharge was used to calculate the edge costs for the first run. After the first iteration, the new discharges (see Equation 5.1) were used to determine new costs of the elements and this process was repeated.

$$Q_{tot\ element\ i} = Q_{con} + (Q_{var} * NSP_{element\ i}) \tag{5.1}$$

109

where $Q_{tot\ element\ i}$ is the total discharge in conduit i for run $n + 1$ (m³/s), Q_{con} is the constant discharge (m³/s), Q_{var} is the variable discharge (m³/s) and $NSP_{element\ i}$ is the number of times element i was in the shortest path from all connection points to the closest WPS in run n. The GTM results did not match better with the outcomes of the HBWLM, and therefore this method was not applied further in the GTM.

5.3　Discussion

5.3.1　Ranking criteria in the HBWLM

Two methods were used to determine the criticality with the HBWLM:
1. Criticality based on the sum of the pressure in the connection points.
2. Criticality based on the number of nodes with a pressure below a threshold.

With the first method, the criticality was comparable for various pressure drops. The outcomes of the second method were highly dependent on the chosen threshold and the occurring pressure drop (see Table 5.1 and Figure 5.8). An advantage of the first method is that no threshold is needed, resulting in an objective method. An advantage of the second method is that it provides more information about the number of water users with a pressure below the required service level.

5.3.2　Application of the GTM with the two evaluation methods

When using the standard (non-weighting) evaluation method, there was a relationship (τ_b >= 0.75) between the results of the GTM and the HBWLM for the WDNs of Cavlar and Tuindorp. The correlation of the WDN of Leimuiden was lower, especially for the 35–60% most important elements. If the weighting evaluation method was used, the correlation increased.

In Leimuiden's WDN there are some clusters of connection points relatively far from the WPS. The GTM overestimated the importance of these connection points if the weighting evaluation method was used (sum of 1/[costs connection point to WPS]). As a result, the connection points close to the WPS were ranked as being more important than the connection points far from the WPS. For Leimuiden's WDN, this resulted in a higher F1 score. If the distance from the connection points to the WPS were evenly distributed, summing the connection points would result in a higher F1 score (basic evaluation method).

With both evaluation methods, it was possible to determine the 10% most important elements with an F1 score greater than 0.7. However, the first evaluation method was less accurate for the Leimuiden case if a small percentage (< 10%) of the most important elements was selected. For maintenance and rehabilitation strategies, the elements of a WDN can be divided into groups. The exact ranking within each group is less important as long as the overlap between the HMM and the GTM is sufficient.

The accuracy of the GTM was compared with the method of Balekelayi and Tesfamariam (2019). Balekelayi and Tesfamariam (2019) were able to identify 12 out of the 20 most critical components of the Richmond WDN (836 connection points, 1 reservoir, 6 cascading tanks, 948 pipes, 7 pumps and 1 valve). This corresponds to an F1 score of 0.6. For the WDN analysed with the GTM, the F1 score was over 0.6. Because the test network used by Balekelayi and Tesfamariam (2019) was different from the networks in this research, an exact comparison of the results is not possible. However, for the tested networks the F1 score is on the same order of magnitude as the method of Balekelayi and Tesfamariam (2019) applied to the Richmond WDN.

5.3.3   Consequences of the simplified hydraulics

The correlation measures (τ_b and F1) showed that there was a relatively strong relationship between the results of the GTM and HBWLM, but there were also some differences due to the simplified hydraulics. In the GTM, a fixed discharge (and head loss) is used. In a hydraulic model, the discharge increases for some of the elements in case of a leakage. This effect is not included in the GTM; however, if leakage occurs in or close to an element with a large diameter or high pressure, the impact according to the HBWLM is visible in a large part of the system. The GTM assumes that the impact is limited to the part of the network where the connection points of the costs to the leak are lower than the costs to the WPS. Consequently, the GTM sometimes underestimates the importance of these elements (element with a large diameter or high pressure).

The GTM overestimated the criticality of the branches (see Section 5.2 and Appendix B). The HBWLM classified these elements as less important because they are dead-end parts of the WDN. In case of a leakage, the WDN has enough capacity to compensate for the loss in pressure in the other parts of the network, so the effect of leakage is only locally visible.

5.3.4   Classification of water distribution networks

The evaluation method to be used (basic, weighted) depends on the network properties. Therefore, it would be helpful to objectively classify WDNs. Hoagland et al. (2015) derived

a classification method to distinguish grid, looped and branched networks; however, the differences among the WDNs in the three case studies are very small when applying these criteria. The criteria are as follows (Hoagland et al., 2015):

- Branch configuration: No. of branch pipes / Total no. pipes > 0.5.
- Grid configuration: No. 3-pipe loops + No. 5-pipe loops < No. 4-pipe loops.
- Loop configuration: No. 3-pipe loops + No. 5-pipe loops > No. 4-pipe loops.

The distribution of the distances from the connection points to the WPS differs in the networks. The structure of Cavlar and Tuindorp is such that the central parts of these networks receive water from two sources (pumping stations). In the Leimuiden network, the central part receives water from one source only. Apart from this, there are clusters of connection points in the loop at the east side of Leimuiden and some branches. This is also apparent in the distribution of the distances from the connection points to the WPSs. Figure 5.10 shows the distribution of the distances of the connection points to the WPSs. It depicts a skewed distance distribution in the Leimuiden network.
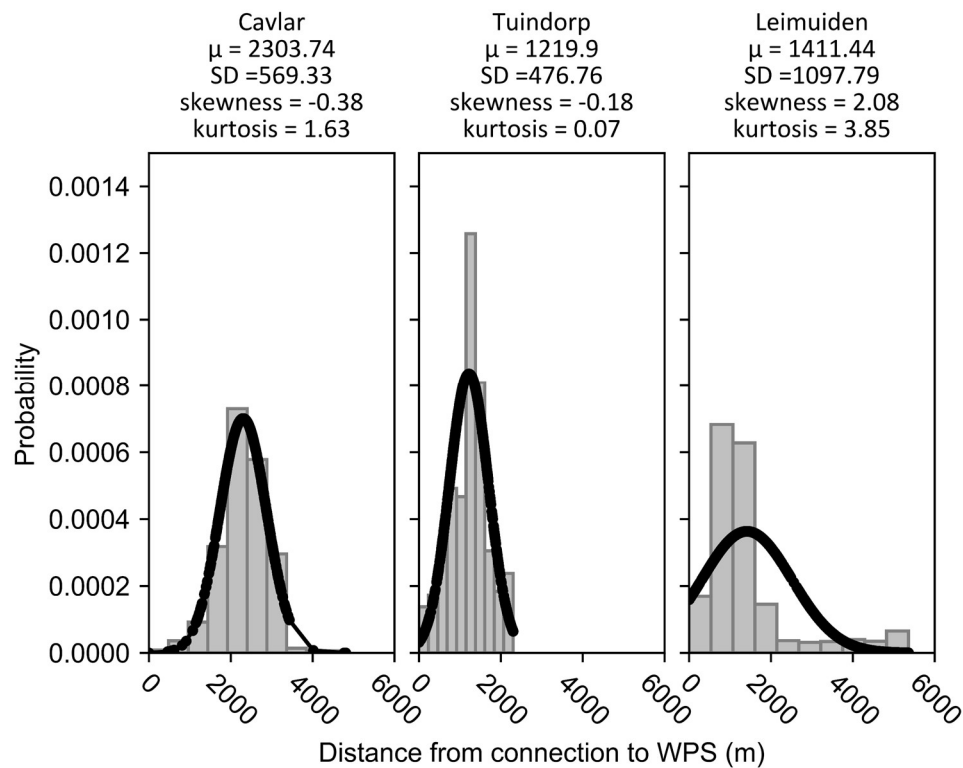
Figure 5.10   Statistical description of the distribution of the distance from the connections to the closest water pumping station of the three analysed water distribution networks.

To compare the distances from the connection points to the WPSs, Q–Q (quantile–quantile) plots were used. A Q–Q plot is a graphical method for comparing two probability distributions. Quantiles are plotted against each other. The distribution of the Cavlar and Tuindorp networks closely resembled the normal distribution (see Figure 5.11), in contrast to the distribution of Leimuiden's WDN, which clearly deviated from a normal distribution. The criterion is objective and easy to apply and therefore suitable for choosing the counting method in GTM. However, to the authors' knowledge, this criterion is not often applied for the classification of WDNs. Therefore, more research is needed to determine the robustness of the criterion "normal distribution". It should be whether the standard deviation or the skewness is the dominant discriminating factor in determining which option of the GTM should be used.

Q-Q plot for norm distribution
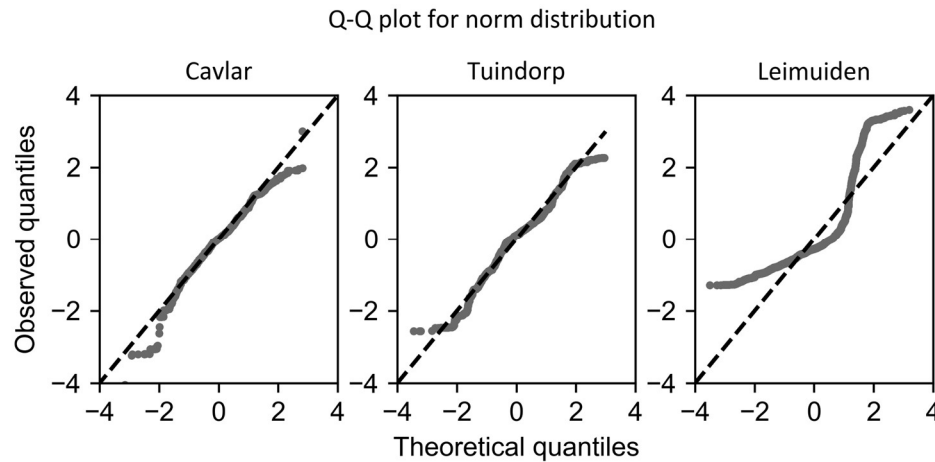
Figure 5.11   Distribution of the distance from the connection points to the water pumping stations.

5.4   Conclusions

The GTM is a network-geometry- and network-structure-based method used to identify the most critical elements in a WDN with respect to malfunctioning of the entire system. The degree of criticality based on the GTM was compared with the degree of criticality obtained using the HBWLM. Results show that the outcomes of the GTM corresponded with the outcomes of the HBWLM, as the F1 score (a measure of the overlap between the HBWLM and the GTM) for the results was over 0.7 for 10% of the most important elements. Thus, the GTM was able to classify the most critical elements correctly for the cases analysed in this research. If the distances from connection points to the WPSs follow a normal distribution, the (non-weighted) evaluation method can be used. If not, the weighing evaluation method can be applied.

With the GTM it is possible, from the perspective of the functioning of the entire system, to divide the elements of a WDN into groups of more important and less important elements. Managers of WDNs can use these groups to prioritise maintenance or rehabilitation activities or differentiate quality requirements to the network. By combining the results of the GTM with the failure probability, managers of a WDN could use the outcomes in a risk-based maintenance approach. In addition, because the GTM can be used to classify the critical elements and the GTM is based on the structure, it is likely that for the studied WDN, the geometrical structure has more influence on the functioning of the WDN than the hydraulics.

6 Application of the graph theory method to urban drainage networks

6.1 Introduction

To validate and demonstrate the Graph Theory Method (GTM) for gravity-driven networks (see Table 3.5 in Section 3.7 for main characteristics), it was applied to three combined sewer networks. Section 6.2 presents the results and interpretation. The outcomes of the GTM were compared with the outcomes of the Hydrodynamic model-Based Weakest Link Method (HBWLM). For the comparison of the degree of criticality, Kendall's τb was used; τb is a measure of similarity in results between the two methods. The results are discussed in Section 6.3; this section shows, among other things, that the results of the GTM were rather insensitive to the parameter values used to determine the costs of the edges (discharge, water level, difference in crest level). Conclusions regarding use of the GTM for gravity-driven systems are presented in Section 6.4.

6.2 Results and interpretation

6.2.1 Degree of criticality based on the Hydrodynamic model-Based Weakest Link Method (HBWLM)

The criticality based on the HBWLM was used as reference for the GTM for gravity-driven systems. With the HBWLM, the criticality of the elements of three combined sewer systems (Loenen with 1 CSO, Loenen with 2 CSOs, Tuindorp) was determined.

To assess the impact of a storm event on the criticality, three types of storm events were used (stationary [homogenous in space and constant in time] and dynamic [homogenous in space and variable in time] design events and observed storm events). For these events, the degree of criticality of the pipes was determined. The results were compared. The degree of criticality was plotted against each other per two events and τ_b was calculated.

τ_b was used because criticality rank was compared. If the degree of criticality was independent of the storm event, the τ_b value was 1.

Figure 6.1 shows an example in which the type of storm event affected the degree of criticality of the conduits. The criticality of the conduits based on the HBWLM of the sewer system Tuindorp was quantified for four measured storm events. The degree of criticality was ranked from most important (1) to least important (778). The removal of a conduit of the network resulted in 188 cases of one or more nodes that were no longer connected to a combined sewer overflow (rank 1–188 in Figure 6.1). These conduits were ranked based on the runoff surface that could no longer drain to a CSO. The degree of criticality of these conduits was therefore storm-independent. The left graph in Figure 6.1 shows a relatively small difference ($\tau_b = 0.91$) in criticality for the events of 18-08-1958 and 23-06-1960. The right graph shows a relatively large difference ($\tau_b = 0.57$) in criticality when the events of 23-08-1956 and 25-07-1956 were used.
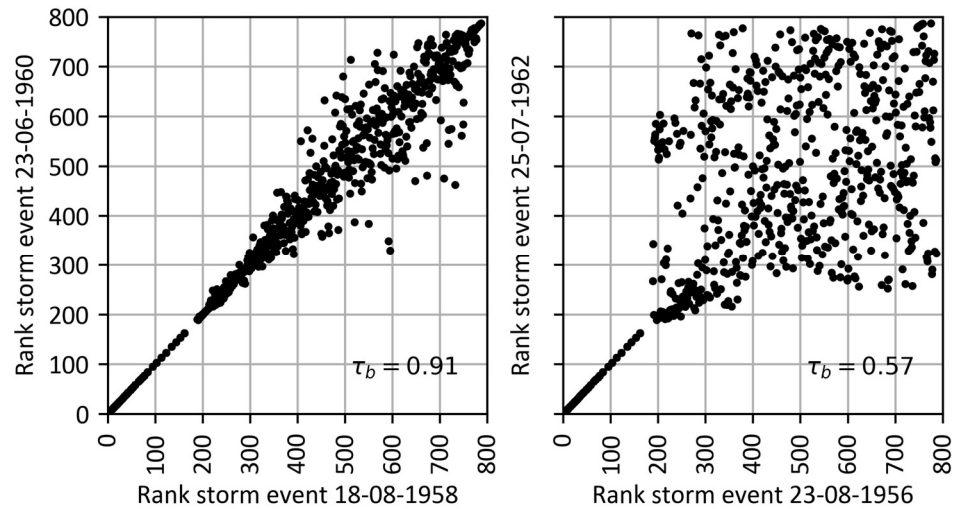
Figure 6.1   Overview of the degree of criticality of the conduits based on the hydrodynamic model-based weakest link method of the Tuindorp sewer system. The left graph shows the results of storm events 18-08-1958 and 23-06-1960. The right graph shows the results of the storm events 23-08-1956 and 25-07-1956.

Figure 6.2–Figure 6.5 illustrate that the type of storm event affected the degree of criticality of the conduits of the other combined sewer networks as well. The extent to which the ranking was affected depended on the differences in the storm events. If the differences in maximum rainfall intensity or shape between the storm events were limited, τ_b approached 1 and the degree of criticality of the individual elements was nearly

identical. If the differences became larger, τ_b dropped below 0.6 (see Figure 6.5) and the degree of criticality of the individual elements changed.

Figure 6.2   Loenen-1: τ_b value of the comparison of the degree of criticality based on the hydrodynamic model-based weakest link method of various stationary storm events. The larger and darker a dot, the higher the value of τ_b.

Figure 6.3   Loenen-2: τ_b value of the comparison of the degree of criticality based on the hydrodynamic model-based weakest link method of various stationary storm events. The larger and darker a dot, the higher the value of τ_b.

	40 l/s.ha (14.4 mm/h)	60 l/s.ha (21.6 mm/h)	90 l/s.ha (32.4 mm/h)
40 l/s.ha (14.4 mm/h)		0.97	0.9
60 l/s.ha (14.4 mm/h)	●		0.9
90 l/s.ha (14.4 mm/h)	●	●	

Figure 6.4   Tuindorp: τ_b value of the comparison of the degree of criticality based on the hydrodynamic model-based weakest link method of various stationary storm events. The larger and darker a dot, the higher the value of τ_b.

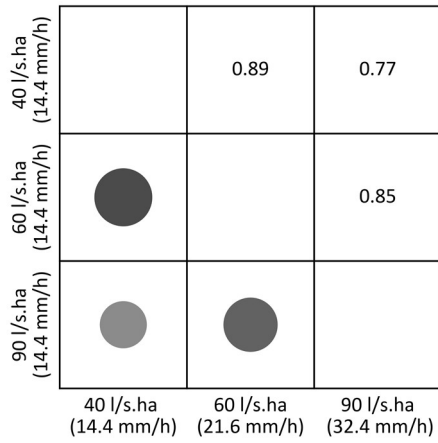|	17-7-1955	23-8-1956	20-9-1957	18-8-1958	23-6-1960	7-10-1960	1-12-1960	5-6-1961	25-7-1962	1-10-1962	2-8-1963	17-8-1963	17-8-1964
17-7-1955		0.62	0.66	0.67	0.68	0.66	0.67	0.66	0.58	0.69	0.67	0.6	0.66
23-8-1956	●		0.64	0.67	0.66	0.6	0.62	0.65	0.57	0.65	0.68	0.58	0.61
20-9-1957	●	●		0.74	0.72	0.66	0.68	0.72	0.61	0.73	0.73	0.61	0.68
18-8-1958	●	●	●		0.91	0.74	0.79	0.84	0.68	0.89	0.87	0.65	0.75
23-6-1960	●	●	●	●		0.74	0.79	0.84	0.67	0.86	0.89	0.64	0.75
7-10-1960	●	●	●	●	●		0.81	0.74	0.67	0.75	0.73	0.64	0.79
1-12-1960	●	●	●	●	●	●		0.83	0.7	0.8	0.79	0.64	0.84
5-6-1961	●	●	●	●	●	●	●		0.65	0.8	0.88	0.61	0.77
25-7-1962	●	●	●	●	●	●	●	●		0.7	0.65	0.64	0.65
1-10-1962	●	●	●	●	●	●	●	●	●		0.83	0.63	0.76
2-8-1963	●	●	●	●	●	●	●	●	●	●		0.63	0.75
17-8-1963	●	●	●	●	●	●	●	●	●	●	●		0.63
17-8-1964	●	●	●	●	●	●	●	●	●	●	●	●	

Figure 6.5   Tuindorp: τ_b value of the comparison of the degree of criticality based on the hydrodynamic model-based weakest link method of various observed storm events. The larger and darker a dot, the higher the value of τ_b. The lowest correlation value τ_b is 0.57.
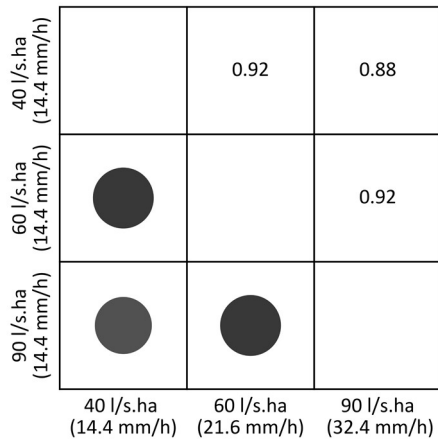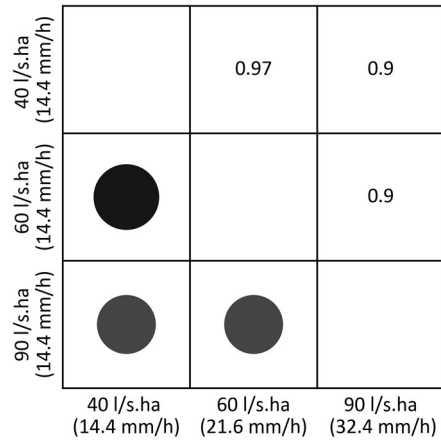
As the dynamics of the hydraulic load are an important factor in the distribution of water flows in networks, it is not feasible to determine a single value for the criticality of an element in a network when applying the HBWLM. The results show that the degree of criticality varied for conduits with both lower and higher degrees of criticality. This was observed for stationary storm events as well as for dynamic design storm events and observed storm events. The effect was present in all tested sewer systems.

Effect of small openings instead of fully blocked pipes

In the HBWLM, conduits were not completely blocked but the internal diameter was reduced to 10 mm. The minimum internal diameter in the tested sewer networks was 151 mm. The assumption was that the effect of a 10 mm conduit instead of a fully closed conduit would be negligible because the remaining area of the cross section was less than 1% of the original area. Figure 6.6 shows the results of the comparison of the degree of criticality based on the HBWLM for the Tuindorp catchment for the two methods (fully blocked vs diameter of 10 mm). The figure shows that the results were not identical but were similar, with τ_b = 0.98. The degree of criticality was ranked from most important (1) to least important (778).
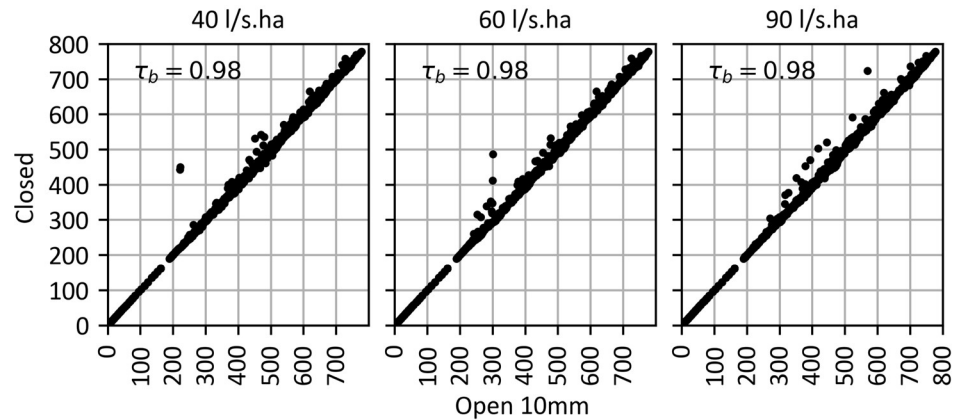
Figure 6.6   Comparison between the degree of criticality based on the hydrodynamic model-based weakest link method in which conduits are completely blocked (closed) and in which the conduit diameter is reduced to 10 mm (open 10 mm).

6.2.2   Comparison of the criticality based on the HBWLM and the Graph Theory Method (GTM)

The degree of criticality based on the GTM was compared with the outcomes of the HBWLM in terms of the Kendall's τ_b. τ_b was used because the criticality is a rank between one and the number of analysed elements of a network. The criticality of the pipes of the

three networks (Loenen with one CSO [Loenen-1], Loenen with two CSOs [Loenen-2] and Tuindorp) was determined and compared to the criticality based on the HBWLM.

For each network, a range of τ_b has been presented. There are two reasons for this:
1. The criticality of the HBWLM depended on the storm event (Subsection 6.2.1).
2. The criticality of the GTM depended on the costs of the conduits. The parameters discharge, water level and crest difference influenced the costs (see Subsection 3.3.1). The impact of the value of these parameters is described in Subsection 6.3.2.

For both versions of Loenen networks, the results indicate a strong relationship between the criticality based on the GTM and HBWLM because all τ_b values were at least 0.80. For Loenen-1 (Loenen with one CSO), τ_b varied between 0.90 and 0.97. This implies a strong relationship in the outcomes for all combinations of all tested storm events with the HBWLM and the GTM. Figure 6.7 shows the results of the comparison with the dynamic and stationary storm events with the highest and lowest τ_b. The Loenen-2 network is more complex than the Loenen-1 network because of the additional CSO. For Loenen-2, τ_b varied between 0.80 and 0.96 (see Figure 6.8). This value is 0.01–0.1 less than the τ_b for Loenen-1.

For the Tuindorp network, Kendall's τ_b varied between 0.46 and 0.78 (see Figure 6.9). The relationship between the results of the HBWLM and the GTM was less strong than for the Loenen catchments. The Tuindorp network is more complex than the Loenen network because the number of conduits and CSO structures is more than twice as large. For the Tuindorp network, it was still possible to identify the 250–300 (30–40%) most important pipes using the GTM.
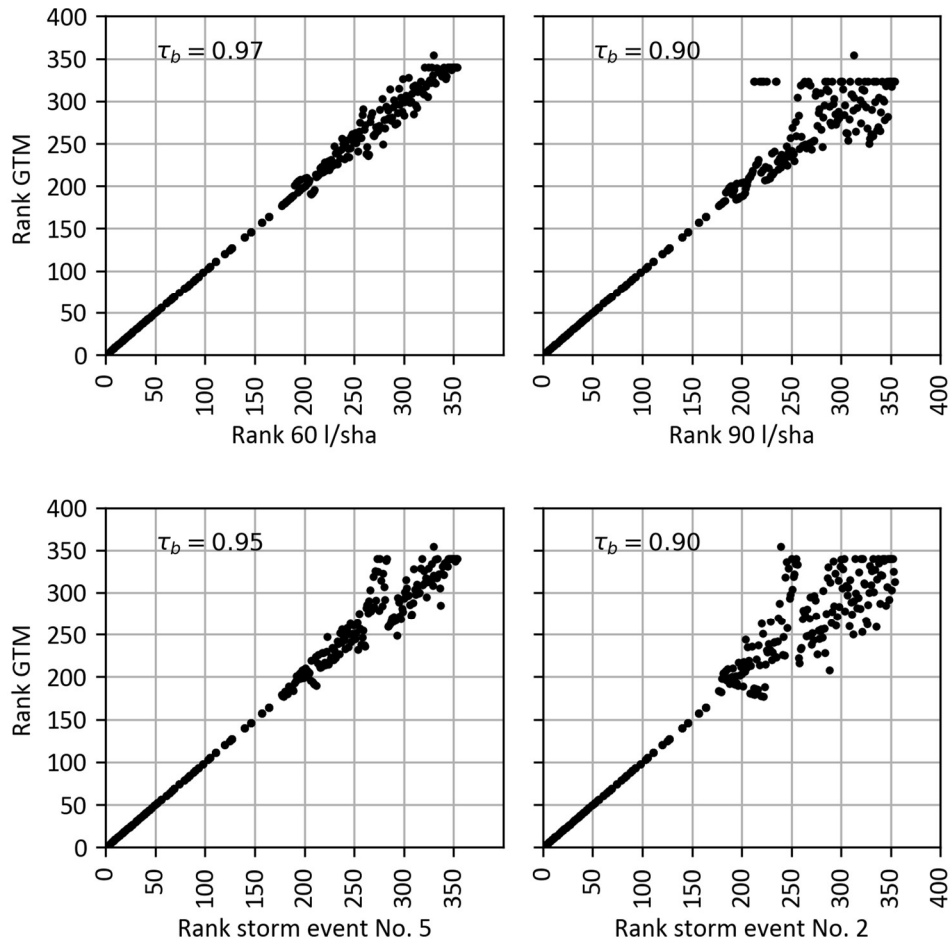
Figure 6.7 Comparison of the degree of criticality of the conduits based on the graph theory method and the hydrodynamic model-based weakest link method. The graphs show the results for Loenen-1. The graphs on the left side show the ranking with the highest τ_b of both the stationary storm events (upper graph) and the dynamic storm events (lower graph). The graphs on the right side show the ranking with the lowest τ_b.
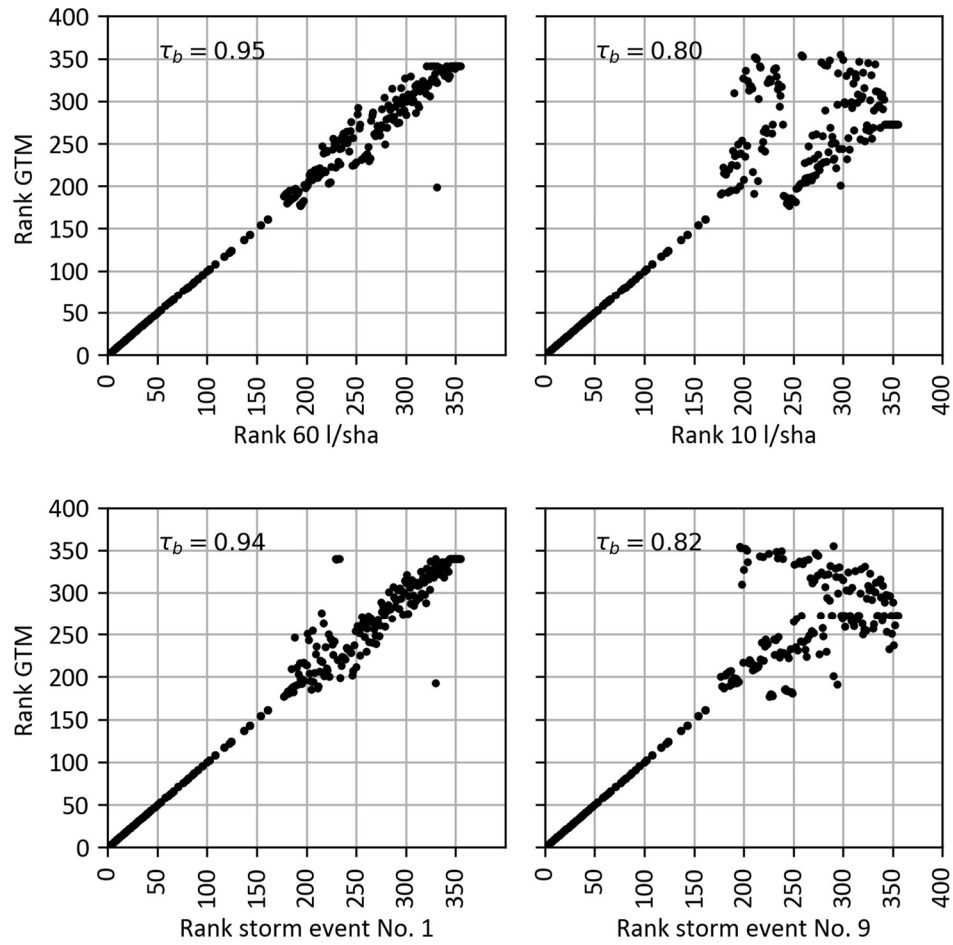
Figure 6.8   Comparison of the degree of criticality of the conduits based on the graph theory method and the hydrodynamic model-based weakest link method. The graphs show the results for Loenen-2. The graphs on the left side show the ranking with the highest τ_b of both the stationary storm events (upper graph) and the dynamic storm events (lower graph). The graphs on the right side show the ranking with the lowest τ_b.
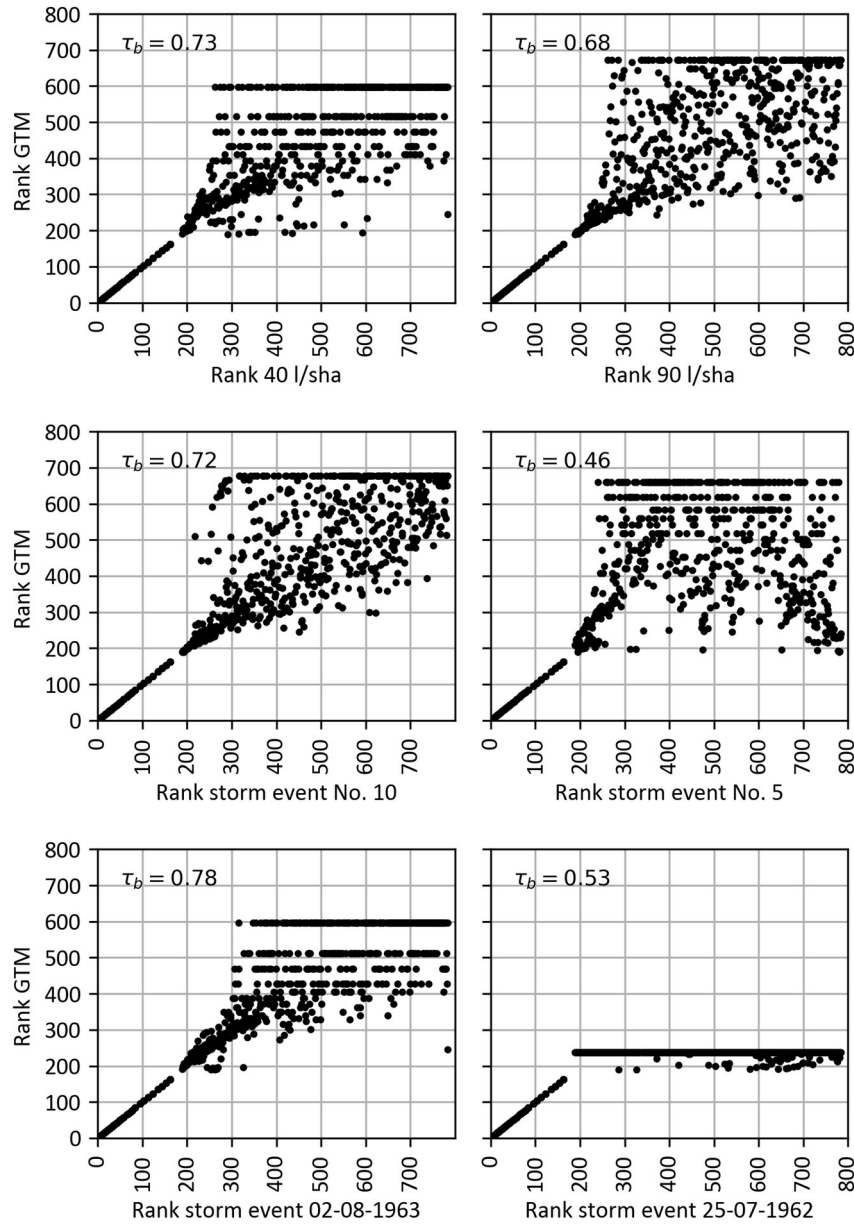
Figure 6.9   Comparison of the rank of importance of the pipes based on the graph theory method and hydrodynamic model-based weakest link method. The graphs show the results for Tuindorp. The graphs on the left side show the ranking based on the graph and hydraulic model outcomes with the highest τ_b of the stationary storm events (upper graph), the dynamic storm events (middle graph) and the observed storm events (lower graph). The graphs at the right side show the ranking based on the graph and hydraulic model outcomes with the lowest τ_b.

6.2.3   Criticality of the pipes shown in space

Figure 6.10 and Figure 6.11 present the results of the criticality of the conduits for Loenen and Tuindorp based on the GTM. The figures show that, as expected, the conduits that would cause a part of the network to be disconnected when these conduits are blocked were classified as important. Other important conduits are the conduits in the direction of the combined overflow structures. For Loenen there was a clear difference between the situations with one and two CSOs (Loenen-1 and Loenen-2). This is also visible in the results of the hydraulic model. For Tuindorp, the links between the CSOs were classified as moderately important by the GTM. These conduits were ranked as more important based on the HBWLM.
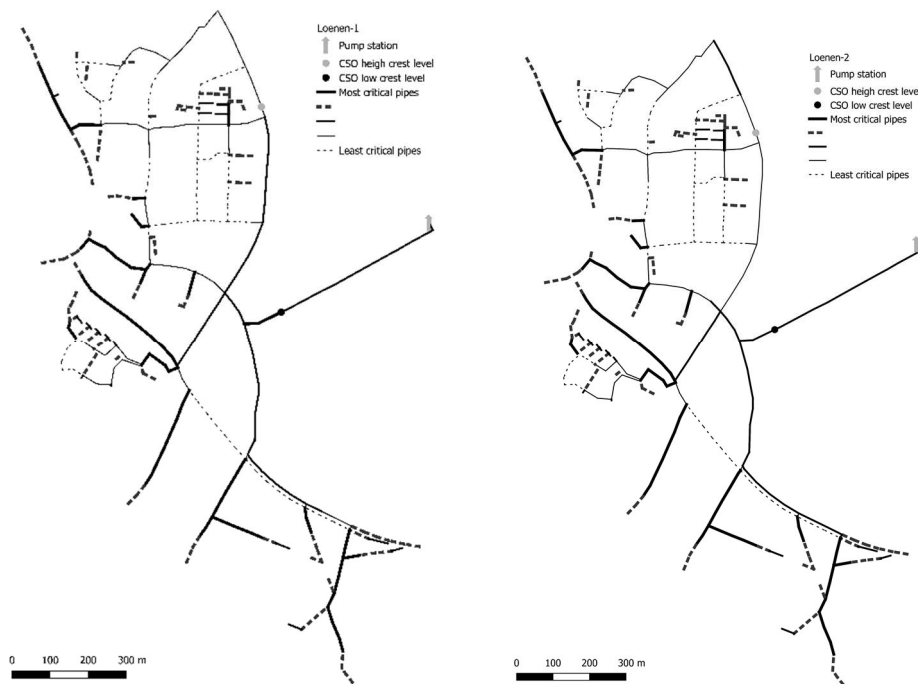
Figure 6.10   Degree of criticality for Loenen-1 (left) and Loenen-2 (right). The darker the lines, the more critical the conduits. Some conduits have the same degree of criticality, but the conduits south of the high overflow structure have a different degree of criticality. In Loenen-2, these conduits are less important because in the case these conduits are blocked the water can flow to the high overflow structure which is not possible in the Loenen-1 system.

Figure 6.11   Degree of criticality of Tuindorp. The darker the lines, the more critical the conduits.

Figure 6.12 and Figure 6.13 show the results of the comparison between the results of the HBWLM and the GTM. The darker the line, the smaller was the difference in criticality rank between the two methods.
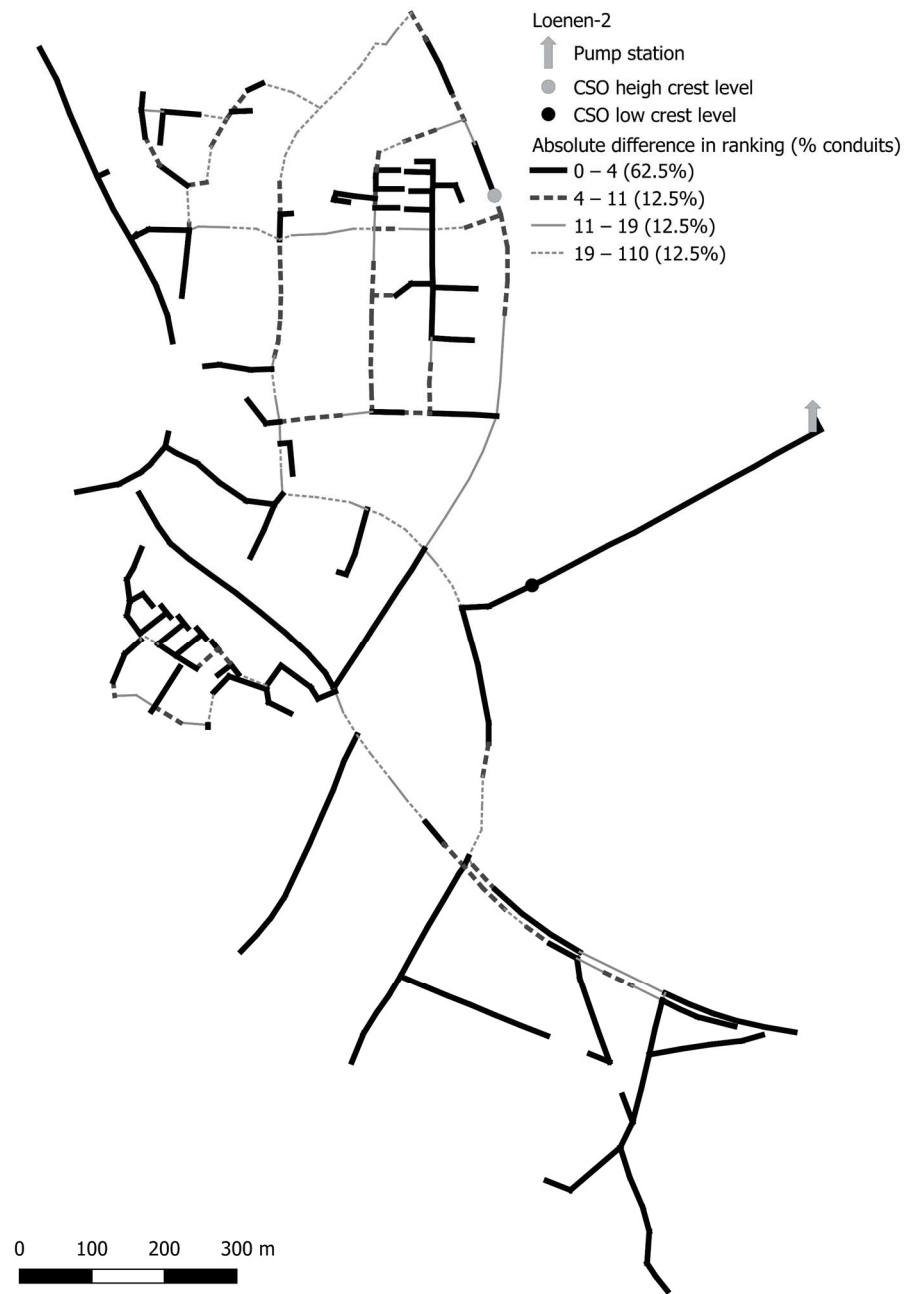
Figure 6.12   Difference in criticality rank between the hydrodynamic model-based weakest link
             method and the graph theory method for Loenen-2.

Figure 6.13   Difference in criticality rank between the hydrodynamic model-based weakest link
method and the graph theory method for Tuindorp. The classification of the groups is
based on the equal count method.

6.3   Discussion

6.3.1   Differences between the HBWLM and the GTM and their consequences

The algorithm in the HBWLM and the GTM is the same, but the hydrodynamic calculations in the HBWLM have been replaced by a "flow path analysis". This leads to a considerable reduction of the required computational effort (see Subsection 6.3.3) but also induces several differences. The most important differences are the following:

1. Change or no change in flow rate due to blockages.
2. Flooding versus transport costs as evaluation criterion.

Change or no change in flow rate due to blockages
In hydrodynamic calculations, flows and water heights are recalculated for each time step in the simulation. If a blockage occurs in the HBWLM, the flow in the network changes. As the flow rate changes, the required head loss to transport the water changes as well, as it is quadratic to the flow velocity (see Equation 3.6).

127

In the GTM, the cost of the pipes is calculated once at the beginning of the analysis. These costs are then used during the entire analysis. If a blockage in one pipe causes the flow velocity in another pipe to increase (sharply), the costs of the pipe in which the flow velocity increases are not adjusted.

Due to the above differences, the GTM results may be less reliable when two pipes run in parallel with approximately the same diameter. In the case of the HBWLM, the velocity in the operating pipe can double, increasing the head loss by a factor of four. This may lead to more flooding locations, and the pipe may be classified as critical. In the case of the GTM, the transport costs due to the pipes running parallel are the same, and the total transport costs will (barely) increase; the pipe will be classified as non-critical.

The same effect is visible when two CSOs are connected by a conduit with a relatively large hydraulic capacity. When a conduit close to one of the CSOs is blocked, water must flow to the other CSO, or flooding will occur. In the HBWLM, water levels at many locations will increase, and the conduit will be ranked as important. Because the costs of a pipe with a large hydraulic capacity are limited in the GTM, the additional transport costs will also be limited, so the conduit will not be ranked as (very) important.

Flooding versus transport costs as evaluation criterion
For the classification of criticality, the HBWLM distinguishes between flooding and rising water levels. The degree of flooding and increase of water levels as a result of a blockage depends on the available overcapacity in a network. The network characteristics and the dynamics of the storm event influence the extent to which the available capacity of a network is utilised. Therefore, the results of the HBWLM depend on the applied storm event. The GTM only determines the increase in costs in case of a blocked conduit. An increase in transport costs is weighted equally everywhere.

If the capacity of a network is already fully in use, a blockage of one of the pipes will always lead to an (increase in) flooding. However, a blockage in a pipe close to a CSO can lead to an increase of flooding at many locations, whereas a blockage in a pipe in the upstream part of a network will have effects on fewer locations. The blockage of the pipe close to the CSO will therefore be classified as more important than the pipe in the upstream part of the network with the HBWLM.

If the capacity of a network is not yet fully used, the consequences of a blockage depend on many factors (e.g. bypass options, degree of overcapacity or location of the blockage). Blockage of a pipe in the upstream part may lead to local flooding, whereas blockage of a

pipe close to a CSO may only lead to a limited increase in water levels. Blockage of the pipe close to the CSO will therefore be classified as less important than blockage of the pipe in the upstream part of the network with the HBWLM.

The above observation also explains why the correlation between the HBWLM and the GTM in the Tuindorp catchment was lower for dynamic storm events 5 and 6 than for the other storm events (Figure 6.14). The maximum water levels for these storm events for the fully operational sewer system were between 0.1 and 0.25 cm below ground level in the most critical parts of the network and even more at the less critical parts. If a blockage of a pipe in the more critical part of the network resulted in a flooding at one or more locations, this pipe was ranked as important. The pipe was ranked as more critical than the pipes in the less critical part of the network even if a blockage there led to higher water level increases at more locations in the network.

6.3.2 Sensitivity of parameters in the graph theory method

In addition to network structure and network geometry, three parameters are used in the GTM to determine the criticality. The costs of the conduits depend on two parameters: discharge and water level. For networks with CSOs with different crest levels, the difference in crest levels is a third parameter.

The discharge influences the dynamic part of the costs of the conduits. If a discharge of 0 m^3/s is used, the dynamic part of the costs of the conduits is zero. With an increasing discharge, the relative importance of the dynamic part of the costs of the conduits increases. However, the ratio of the dynamic part of the costs between the conduits remains the same because the same discharge is used for all conduits.

The water level influences the static parts of the conduit costs. The conduits with both invert levels below the water level have no static costs. If the water level varies between the lowest and highest invert level, the static cost component decreases if the water level increases (and vice versa).

The difference in crest levels of a CSO determine the additional costs of a CSO with a higher crest level. These are the static costs of a CSO link in the network.

A sensitivity analysis was carried out to determine the influence of these parameters on the criticality (Figure 6.14–Figure 6.16). The discharge was varied between 0 and 0.2 m^3/s, and the water level was varied between 0 and 1 m above the lowest crest level; the costs for the differences in crest level were varied between 0 and 0.5 m for the Tuindorp case

and between 0 and 1 m for the Loenen case. For each value, the degree of criticality was determined. The outcomes of the GTM were compared with the outcomes of the HBWLM. Kendall's τb was used to compare of the degree of criticality.

Discharge

Figure 6.14 shows that the variation in the τ_b values was limited for the tested discharges as long as discharge was greater than 0 m^3/s. The graphs show that a discharge of 0.02 m^3/s resulted in a maximum for τ_b. As mentioned above, the discharge influenced the dynamic costs. With a discharge of 0 m^3/s, the dynamic costs are ignored, and with high discharge the static costs increase sharply (because of the power factor in the ratio of discharge to head loss) and become the only determining factor for the outcome of the GTM.

It is important that the dynamic costs have the same order of magnitude as the static costs. Because Loenen is situated in a mildly sloped area, the static costs are more important than the dynamic costs. Due to the variation of the ground level, the height differences in combination with the structure of the network determine the criticality of the conduits to a major extent. The costs to overcome differences in altitude (static costs) are higher than the additional dynamic costs caused by relatively small pipe cross sections (dynamic costs).

Figure 6.14   The results of the sensitivity analysis of the graph theory method. Loenen-1 is the network of Loenen including one combined sewer outfall; Loenen-2 includes two combined sewer outfalls. The *x*-axis shows the discharge and the *y*-axis shows Kendall's τ_b. Note that the scale of the *y*-axis varies.

Water level

For Loenen-1, with one CSO, and Loenen-2, including two CSOs, the effect of the water level was limited (see Figure 6.15) because Loenen is situated in a mildly sloped area; a higher water level affected only a limited number of conduits. For Tuindorp, the effect of the water level was also limited because only less than 10% of the invert levels of the conduits are situated above the lowest weir. A water level equal to the lowest CSO or equal to the design level of the flow over the CSO (0.3 m in the Netherlands) could be used to account for the differences in crest levels.

Difference in crest levels

For sewer systems with CSOs of different crest levels, a small (< 0.1) additional cost for the CSOs with a higher crest level had a positive effect on τ_b, but the effect was limited (< 0.05) (see Figure 6.16). The degree of criticality could change strongly if another crest height were to be used. This means that it is important to select the additional costs for overflows with different crest heights carefully in flat areas. The additional costs for higher crest levels must be on the same order of magnitude as the dynamic costs. Therefore, if a low discharge is used, the additional costs also must be low; if a higher discharge is used, the additional costs can be higher.
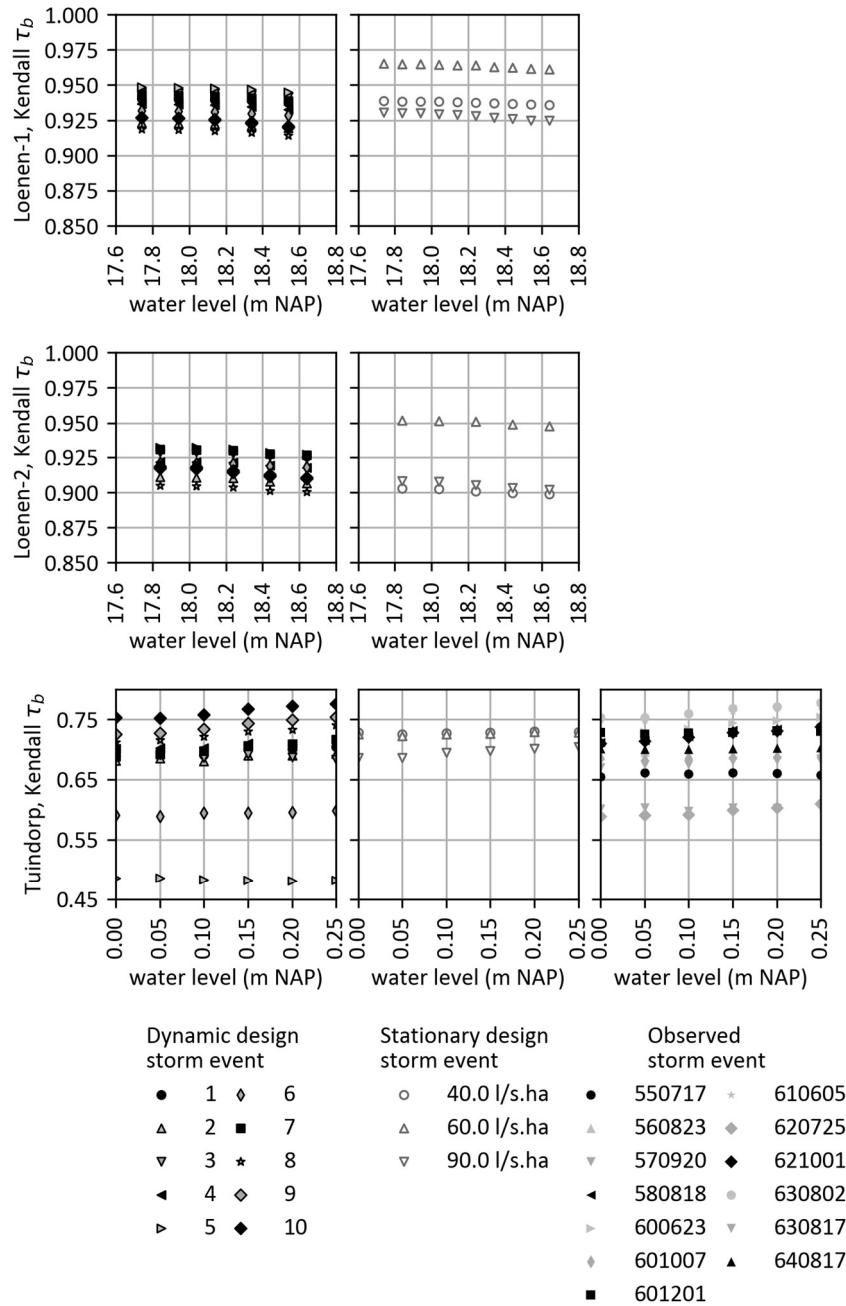
Figure 6.15   The results of the sensitivity analysis of the graph theory method. Loenen-1 is the network of Loenen including one combined sewer outfall, Loenen-2 includes two combined sewer outfalls. The *x*-axis shows the water level, and the *y*-axis shows Kendall's τ_b. Note that the scale of the *y*-axis varies.
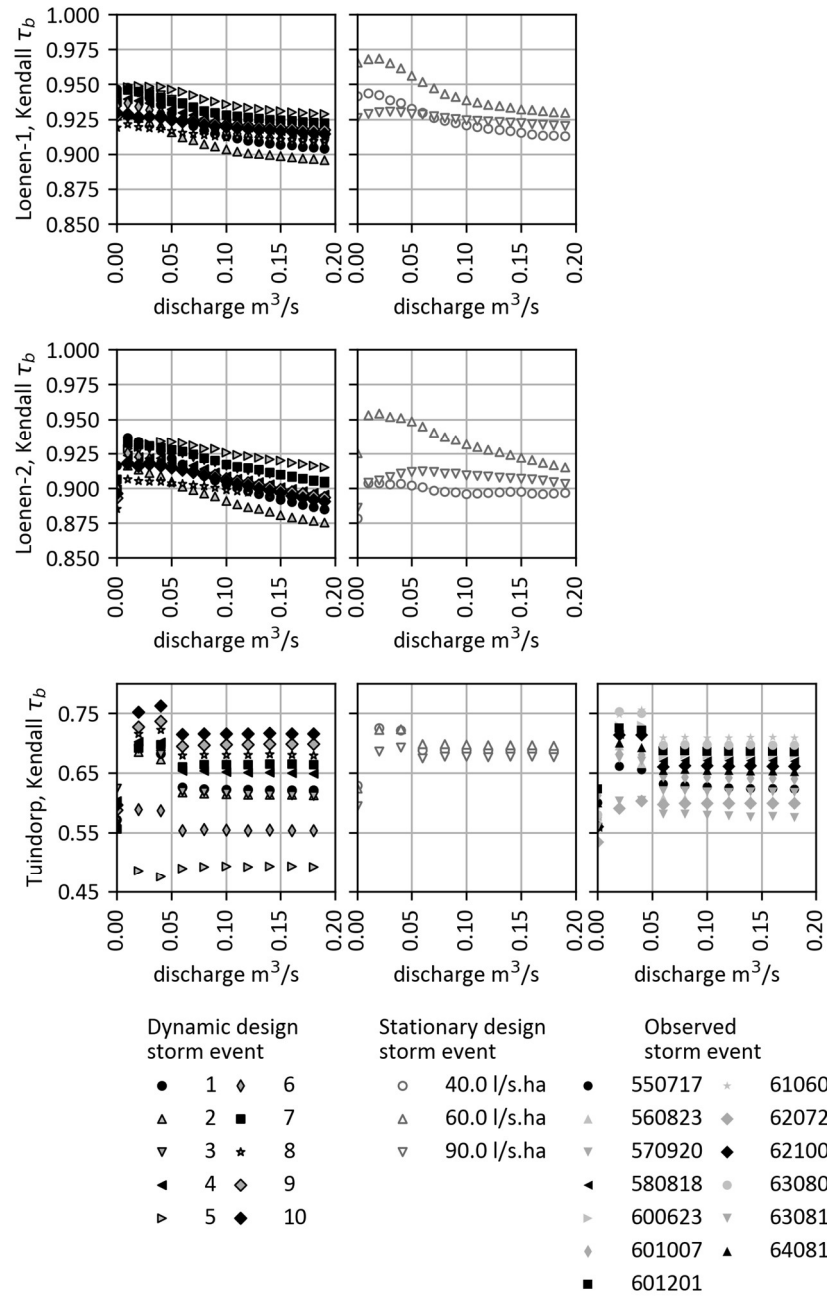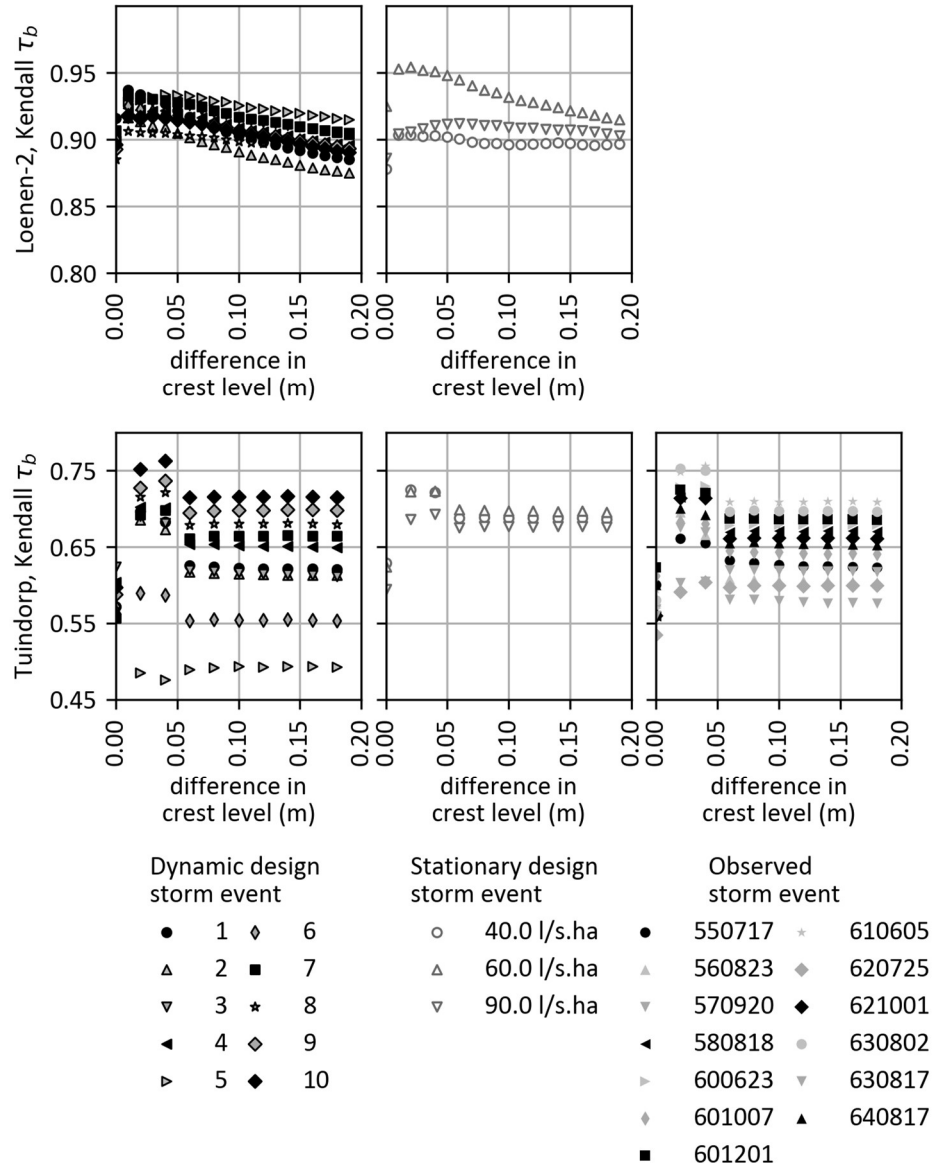
Figure 6.16   The results of the sensitivity analysis of the graph theory method. Loenen-1 is the network of Loenen including one combined sewer outfall, Loenen-2 includes two combined sewer outfalls. The *x*-axis shows the difference in crest levels, and the *y*-axis shows Kendall's τ_b. Note that the scale of the *y*-axis varies.

6.3.3   Performance of the GTM

Table 6.1 shows the performance of the HBWLM and the GTM. All calculations were made on the same computer. The table shows that the GTM based on graph theory was a few hundred to a few thousand times faster than the HBWLM method based on the hydraulic models if one storm event was used in the GTM.

Table 6.1   Comparison of the performance of hydrodynamic based weakest link method and the graph theory. The time of the hydraulic model is based on one storm event.

Network	Number of elements	Computer time for hydraulic model	Computer time for graph methodology	Computational gain factor
Loenen-1*)	337	2 h 45 min	2 s	4950
Loenen-1**)	337	2 h 24 min	2 s	4320
Loenen-2*)	337	2 h 45 min	4 s	2475
Loenen-2**)	337	2 h 24 min	4 s	2160
Tuindorp*)	778	6 h 24 min	38 s	606
Tuindorp**)	778	4 h 12 min	38 s	398

*) Stationary storm event, simulation 24 hours.

**) Dynamic storm event, simulation 2 hours.

6.4   Conclusions

In this chapter, the GTM has been presented as a method to identify the most critical elements in sewer systems with respect to the performance of the network. The method is objective and independent of the type of storm event and requires limited computational effort. The degree of criticality of the conduits was compared with the HBWLM. There was a high correlation (Kendall's $\tau_b > 0.72$) between the GTM and HBWLM results.

The criticality for the partly branched, mildly sloping catchment of Loenen had a stronger correlation with the HBWLM than the results of the looped, flat Tuindorp catchment. Nevertheless, for both catchments, it was possible to identify the 30–40% most critical conduits.

The degree of criticality based on the GTM depends on three parameters: discharge, water level and difference in crest levels of overflow structures. The outcomes of the GTM are not sensitive to the exact value of the variables as long as the variables have values that result in dynamic and static costs on the same order of magnitude. The importance of

135

the dynamic part of the costs of the conduits is limited for sewer systems in (mildly) sloped areas where the overflow is situated in the lower part of the system.

The degree of criticality based on the HBWLM strongly depends on the storm event used. In the HBWLM, the degree of criticality is determined by removing each conduit individually from the network. The links are ranked based on the total increase in flood volume and the increase of water level in the sewer system. Use of different storm events can lead to a different ranking of the elements. Important elements can become less important, and the inverse situation can also occur. Because of this condition, it is impossible to define a single ranking of the degrees of criticality for different rainfall intensities by removing each conduit individually from a network.

Apart from the influence of the storm event, there are two other causes for the differences in the results of the degree of criticality based on the HBWLM and the GTM. The first is that, in the GTM, the same discharge is used for all conduits (except for the blocked pipe), even when a conduit in the system is blocked. The second is that in the GTM, each increase in costs is equally important. In the HBWLM, an increase in water level that causes flooding is weighted as more important than a comparable increase in water level without flooding.

7 Application of the graph-based weakest link method to urban drainage systems

7.1 Introduction

The Graph-Based Weakest Link Method (GBWLM) was validated and demonstrated using the Almere case (see Table 3.6 in Section 3.7 for the main characteristics of the GBWLM). Section 7.2 presents the results and interpretation of the analysis of a capacity reduction of the gully pots, storm sewer and surface water system. The section also includes the validation results of the GBWLM as well as the results for optimisation of the capacity of the connections between the layers of the storm sewer networks. In addition, Subsection 7.2.4 describes the outcomes of the analysis of the added value of hydrodynamics in the GBWLM. The GBWLM is discussed in Section 7.3 and the conclusions about the method are presented in Section 7.4.

7.2 Results and interpretation

7.2.1 Integrated analysis of the urban drainage system of Almere

Flood frequency and flood extent were used to analyse the impact of capacity reduction of the urban drainage system of Almere. The flood frequency and extent were determined for various capacity reductions of the three analysed subsystems: gully pots, storm sewer and surface water. The results are presented in bar charts (Figure 7.1 and Figure 7.2); the horizontal axis shows the capacity reduction (%), the vertical axis shows the flood frequency (number per year), and the bar colour indicates the flood extent (flooded area as a percentage of total paved area).

The results for the surface water network in Figure 7.1 and Figure 7.2 present the increase of flooding compared to the situation in which all three subsystems have full capacity. The total flooding is therefore the sum of the flood in the storm sewer at 0% capacity reduction and the flood due to the surface water system.

Gully pots

The function levels of the gully pots in Waterwijk Zuid and Noord at declining capacity were similar. However, both the flood frequency and flood extent were larger in Waterwijk Zuid. This corresponds with the (approximately 15%) larger average runoff area per gully pot in Waterwijk Zuid (see Table 4.5). The flood frequencies of the gully pots were 0–2 times per year if full capacity was available.

The flood frequency and flood extent increased with a non-linear relationship with decreasing capacity. The impact on the performance was limited for capacity reductions up to 40%. The flood frequency was 5 or 6 times per year and the flood extent was limited to 5% of the area for most events. This implies that the overcapacity for most gullies was approximately 30%. This can be considered a safety factor in the design.

Surface water

A reduction of the discharge capacity of the surface water system had a slightly greater impact on the frequency and extent of flooding in Waterwijk Noord than in Waterwijk Zuid. At the full capacity of the surface water system, the flood frequency was less than once a year. The impact of a capacity reduction of the surface water was relatively limited when the capacity reduction was limited to 70%. Both the flood frequency and flooded area increased strongly with an increased capacity reduction.

The number of times that more than 75% of the surface was flooded was approximately 85 times per year in Waterwijk Noord and 70 times per year in Waterwijk Zuid in case of a capacity reduction of 90%. This is notable because Waterwijk Noord floods less frequent than Waterwijk Zuid for capacity reductions up to 80%.
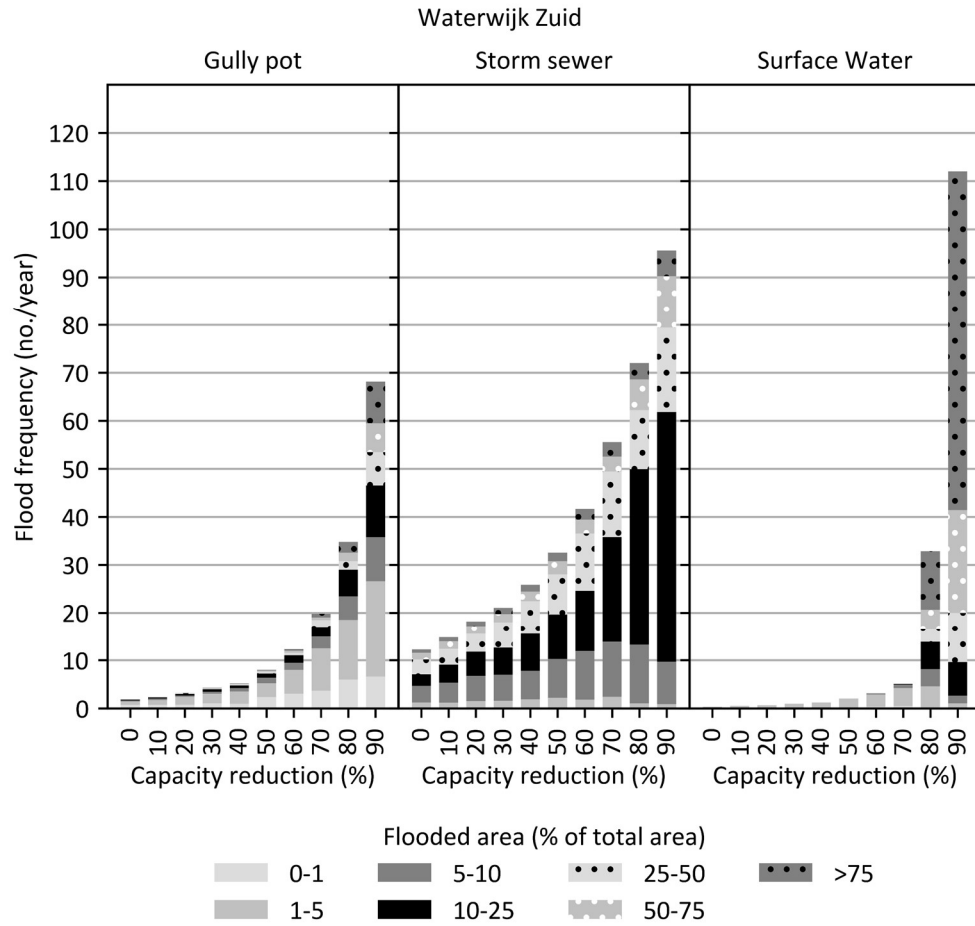
Figure 7.1   Overview of the yearly flood frequency for the various available capacities of gully pots, storm sewers and surface water system in Waterwijk Zuid. If full capacity is available, the flood frequency of the gully pots is 2 times per year the flood frequency of the storm sewer 12 times per year and the flood frequency of the surface water is less than 1 time/year.
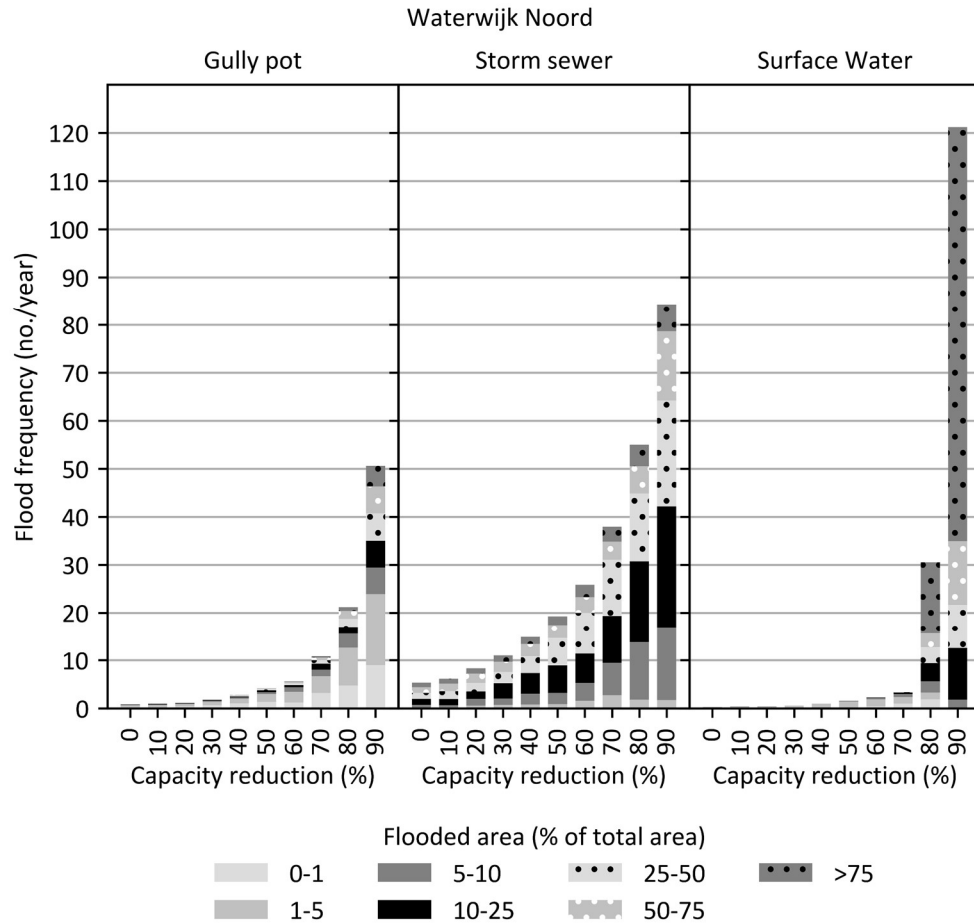
Figure 7.2   Overview of the flood frequency per year for the various available capacities of gully pots, storm sewers and surface water system in Waterwijk Noord. If full capacity is available, the flood frequency of the gully pots is less than 1 times per year the flood frequency of the storm sewer 5 times per year and the flood frequency of the surface water is less than 1 time/year.

Storm sewer

The differences in the performance of the two storm sewer systems were larger than those of the other subsystems in the two catchments. Waterwijk Zuid flooded about 12 times a year and Waterwijk Noord five times a year without capacity reduction. More events with a small flood extent occured in Waterwijk Zuid than in Waterwijk Noord. The flood frequency increased to 96 times per year in Waterwijk Zuid and 85 times per year in Waterwijk Noord if the capacity declined.

The most striking difference was observed in the extent of flooding. A clear increase could be seen in the frequency of events with a flood extent of 10–25% in Waterwijk Zuid if the capacity decreased. In Waterwijk Noord the frequency of all flood extent categories increased. This means that a decrease in the capacity of the storm sewer in Waterwijk Zuid resulted in higher flood frequencies but with a limited extent. In Waterwijk Noord both smaller and larger flood events occurred more frequently.

7.2.2 Validation of the Graph-Based Weakest Link Method (GBWLM)

The results of the GBWLM were validated against the HBWLM. The validation was based on four criteria:
1. Flood volume at system level of the storm sewer.
2. Number of flooded manholes at system level.
3. Locations of flooded manholes.
4. Rise of the surface water level.

A storm event was used with a progressive rainfall intensity ranging from 1 mm/h to 30 mm/h to validate the storm sewer system of the GBWLM. A dry period of 5 days was applied between each of the two consecutive precipitation intensities. Thus, the initial conditions at the different intensities were identical. The results are summarised in Table 7.1 (for more details see Appendix C). The table shows the minimum values of the 30 events.

The correlation between the flood volume of the HBWLM and GBWLM for the storm sewer was significant (R^2 = 0.97–0.98 and τ_b = 0.95–0.96, Figure C.1). This implies that if the flood volume increased according to the HBWLM, it also increased according to the GBWLM.

In the GBWLM, the flooding started at a slightly lower rainfall intensity (2 mm/h) than in the HBWLM, while the GBWLM provided a satisfactory estimate of both the total number of flooded manholes and the locations where the flooding occurred (see Figure C.2 – Figure C.5, Appendix C). The scores for the number of flood locations and the locations of the flooded manholes were lowest at the transition between non-flooded and flooded regions. The indicator for the number of flooded manholes, the percentage correctly classified manholes (flooded, non-flooded) reached the lowest score of 72% correctly classified manholes. In this transition phase, the indicator for the locations of flooded manholes, the F1 score, may drop below 0.3. The F1 score is so low because only a few manholes were flooded in the transitional phase. If some of these manholes are not correctly classified, this results in a low F1 Score. If the rain intensity after the transition

between non-flooded and flooded increased by 2 mm/h, the F1 score also increased rapidly.

The surface water system was validated with a 10-year rainfall event and the water level rises of the GBWLM were compared with the results of the HBWLM. The results of the validation of the surface water part of the GBWLM showed a strong correlation (R^2 = 0.93; see Appendix C, Figure C.6). This means that the GBWLM followed the pattern of surface water level rise in the HBWLM.

Table 7.1 Overview of the validation results for the graph-based weakest link method for a sewer system, based on a storm event with an increasing intensity of 1–30 mm/hr. The values of the flooded manholes and the F1 score are the minimum values of the 30 events.

		Waterwijk	Waterwijk Zuid	Waterwijk Noord
Flood volume	R^2	0.98	0.98	0.97
	τ_b	0.95	0.95	0.96
Flooded manholes	True positive/negative (minimum%)	84	69	82
	False positive (maximum%)	12	21	6
	False negative (maximum%)	6	14	18
F1 (overall)	F1	0.84	0.87	0.80
	Precision	0.78	0.84	0.70
	Recall	0.90	0.90	0.92
F1 (minimum value)	F1	0.21	0.24	0.11
	Precision	0.16	0.19	0.06
	Recall	0.33	0.33	0.84

7.2.3 Optimisation of the capacity of the layer-1 layer-2 connections

As described in Subsection 3.5.2, the combined and storm sewer networks were schematised with three layers. These layers were connected at the location of the manholes with L1–L2 connections and L1–L3 connections. If the capacity of layer-1 was insufficient, water would flow via L1–L2 connections to the second layer. The capacity of the L1–L2 connections, in combination with the shortage of drainage capacity in layer-1, determined how many L1–L2 links were required to drain the water.

As mentioned in Subsection 3.5.5, a default value of 15 m³/h can be used for the L1–L2 connections. However, the capacity of the connections can be adjusted to improve the outcomes of the GBWLM. For seven Urban Drainage Networks (UDNs; see Section 0) the capacity of the L1–L2 connection was optimised based on the outcomes of the HBWLM. The capacity increased from 0 m³/h–50 m³/h in steps of 5 m³/h. Figure 7.3 shows the Matthews Correlation Coefficient (MCC), percentage of False Positives (FP) and percentage of False Negatives (FN) for seven UDNs and 14 storm intensities. Unlike F1, the MCC takes into account both the number of correct and incorrect predicted positive (flooded) and negative (non-flooded) locations. The figure shows that the optimal capacity (the capacity with the highest average MCC score for the tested rainfall intensities) varied between 5 and 30 m³/h.
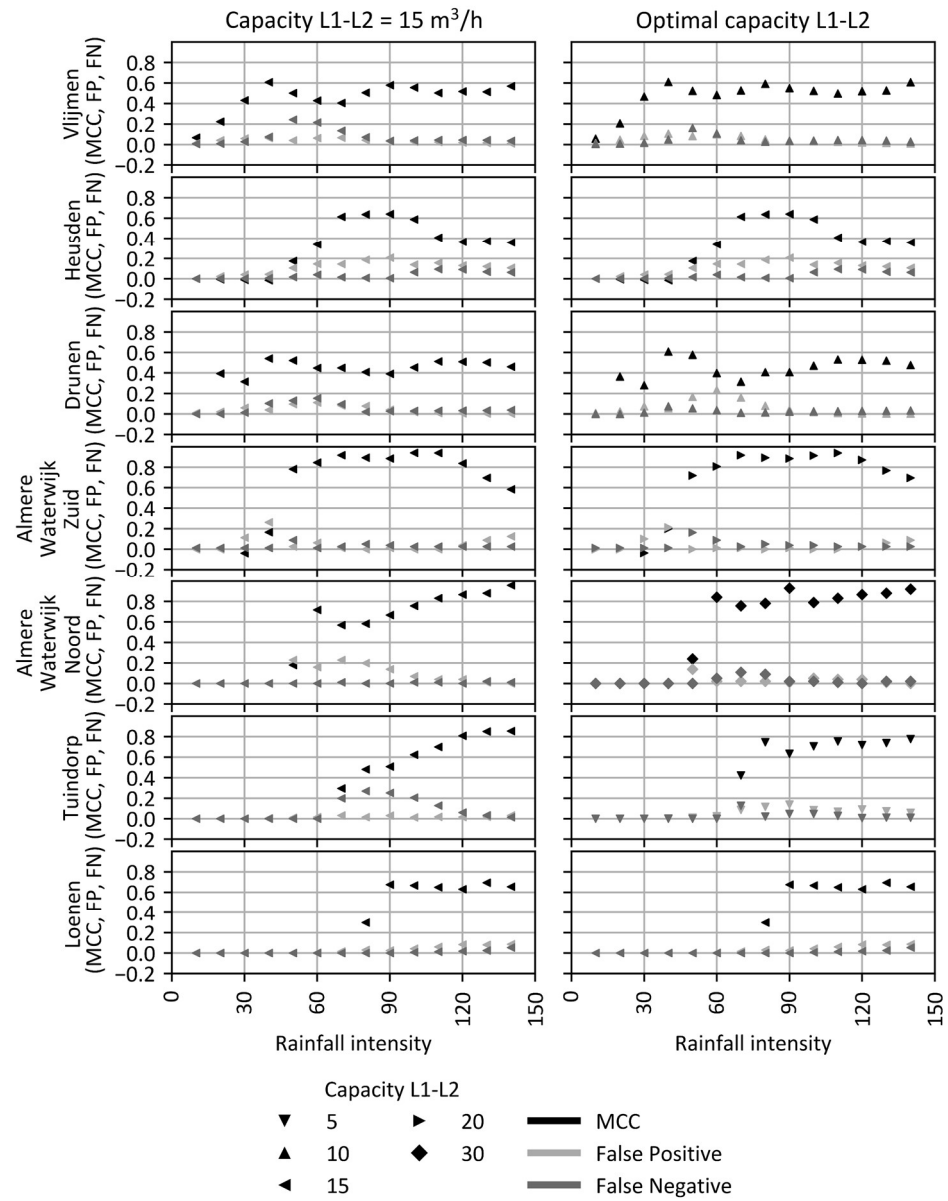
Figure 7.3   Comparison between capacity L1–L2 of 15 m³/h and optimal capacity L1–L2. The graph shows the Matthews Correlation Coefficient (MCC), % False Positive (FP) and % false Negative (FN) for 7 urban drainage networks and 14 storm intensities.

The optimal capacity of L1–L2 can also be derived from the Network Linearisation Parameter (NLP) and the NLP-factor (see Subsection 3.5.4 and Equations 7.1, 7.2 and 7.3). The NLP was developed to test the homogeneity of the hydraulic gradients in a network and whether there are any bottlenecks (pipe with a larger hydraulic gradient at high flows than the adjacent upstream pipe. In this situation the NLP-Factor is larger than 1). If the gradients are homogeneous, the GBWLM can be applied on the network (see Subsection 0).

$$NLP = \frac{1}{\alpha_{linear} \, RA_{pipe}} \qquad (7.1)$$

$$NLP\text{-factor} = \frac{\alpha_{lineair} \, RA_{down \, stream \, pipe}}{\alpha_{lineair} \, RA_{up \, stream \, pipe}} \qquad (7.2)$$

$$\% \text{ affected manholes} = \frac{No.manholes}{Tot.No.manholes} \times 100\% \qquad (7.3)$$

where NLP is the network linearisation parameter (m/s), RA_{pipe} is the runoff area that discharges via a pipe (m²) and α_{linear} is a hydraulic parameter (s/m³).
% affected manholes is the percentage of manholes affected by the bottleneck, No. Manholes is the number of manholes with a path to an outlet crossing the bottleneck and Tot. No. Manholes is the total number of manholes in a UDN (see Figure 3.14).

If the capacity of a downstream pipe is (much) larger than the capacity of a pipe located directly upstream, the GBWLM strongly underestimates the capacity of the upstream pipes. The same gradient is maintained in the hydraulic linearisation for both pipes. In reality, the gradient in the downstream pipe (large cross section) will be smaller than that in the upstream pipe (small cross section); with the steeper gradient, the capacity of the upstream pipe will increase. To compensate for this effect, a larger capacity for the L1–L2 connections can be used.

The locations at which the cross section of a downstream pipe is larger than the capacity of a pipe located directly upstream can be calculated with Equation 7.2. If the NLP-factor of a pipe is larger than 1, the head loss is larger than the head loss of the directly upstream pipe (bottleneck). When the NLP-factor of a pipe is less than 1, the head loss is smaller than the head loss of the directly upstream pipe. So, there is a larger capacity rather than a bottleneck. The percentage of affected manholes can be calculated with Equation 7.3. The optimum capacity for the connection L1–L2 derived from seven tested networks was: Optimal capacity L1–L2 = 3.68 + 0.39 × % affected manholes (see Figure 7.4). More networks must be analysed to determine whether the derived relationship for determining the capacity of the connection L1–L2 can be generally applied.
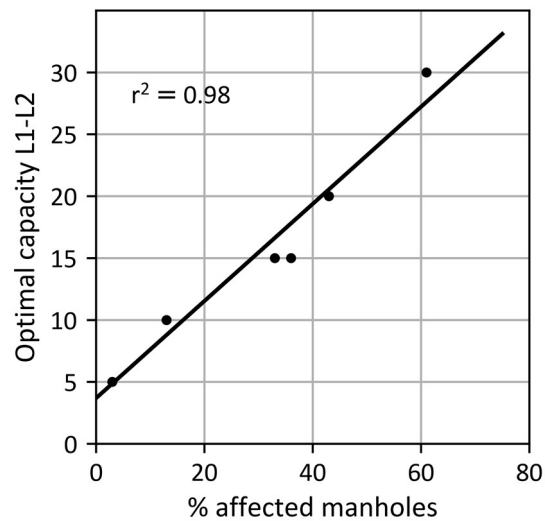
Figure 7.4   Relation between the percentage of affected manholes network with a linearisation
parameter-factor lower than 1 and the optimal capacity of the connection L1–L2.

7.2.4   The added value of linearised hydrodynamics in the GBWLM

•   The added value of including hydraulic information in the network analysis with the GBWLM was tested. Three options to include the costs of edge costs and two options to determine the capacity were analysed (see Table 7.2). The following costs of the pipes were tested:

- Uniform: the costs of all edges in layer-1 and layer-2 were set equal.
- Pipe length: the costs of the edges in layer-1 and layer-2 were equal to the pipe length.
- Head loss: the costs of all edges in layer-1 and layer-2 were equal to the head loss (see Subsection 3.3.1).

The capacity of the pipes was estimated in two ways:

- Cross-sectional area of the pipe multiplied by a constant velocity (velocity x pipe area linearisation).
- Based on linearised hydrodynamics (see Subsection 3.5.3).

146

Table 7.2   Combinations of hydraulic information that were used for the analysis.

Variant	Costs	Capacity
1	Uniform	Velocity x pipe area linearisation
2	Pipe length	Velocity x pipe area linearisation
3	Head loss	Velocity x pipe area linearisation
4	Uniform	Linearised hydrodynamics
5	Pipe length	Linearised hydrodynamics
6	Head loss	Linearised hydrodynamics

The effect of adding hydraulic information depended on network characteristics and storm dynamics. For some networks (e.g. Loenen, Almere Zuid and Almere Noord), the similarity of the results between the HBWLM and the GBWLM increased by adding hydraulic information. For other networks no clear relationship was seen. In any case, adding hydraulic information did not reduce the similarity between the outcomes of the HBWLM and the GBWLM. Figure 7.5 presents the MCC and the percentage of false positives and false negatives for seven networks, six variants of hydraulic information and 14 storm intensities (10–140 l/(s.ha)). The MCC was used because, unlike F1, it accounts for the number of both correct and incorrect predicted positive (flooded) and negative (non-flooded) locations. The following observations were noted:

- The networks reacted differently to adding linearised hydraulic information. For some networks the results improved, and for some networks the results only improved if hydraulic information was added to costs and capacity. For other networks (Tuindorp), the results were more or less similar.

- At the onset of flooding, the results of the GBWLM were generally the least accurate in comparison with the hydrodynamic models. A small difference in water level could cause a manhole to be flooded or not. Minor deviations in both methods may therefore lead to a low MCC value. The percentage of false positives and false negatives also had a peak when flooding started.

- The MCC values were higher in general for more intense storm events. When many manholes were flooded, it was easier to predict flooded manholes correctly.

- The MCC values were higher if linearised hydrodynamics were applied for the capacity of the pipes instead of the velocity x pipe area linearisation. The velocity x pipe area linearization is simpler and more generic than linearised hydrodynamics. The velocity x pipe area linearization only takes into account the pipe diameter, and the linearised hydrodynamics includes the pipe diameter, the invert levels of the pipe and the hydraulic gradient.

147

- Pipe costs based on the head loss resulted in a better match between the results of the GBWLM and the HBWLM than when the pipe costs were uniform or derived from the diameter.
- If the linearised hydrodynamics were used to determine the capacity of the pipes, the MCC values were more constant than velocity x pipe area linearisation was applied. In other words, by using the linearised hydrodynamics the GBWLM results matched better with the hydrodynamic results for low and high rainfall intensities.

If the flow velocity in the network was known and more or less uniform, the Tuindorp network showed that the velocity × surface of a pipe (v x A) can be a good substitute for linearised hydraulic information. Applying the linearisation to estimate the pipe capacity made the GBWLM more generally applicable.
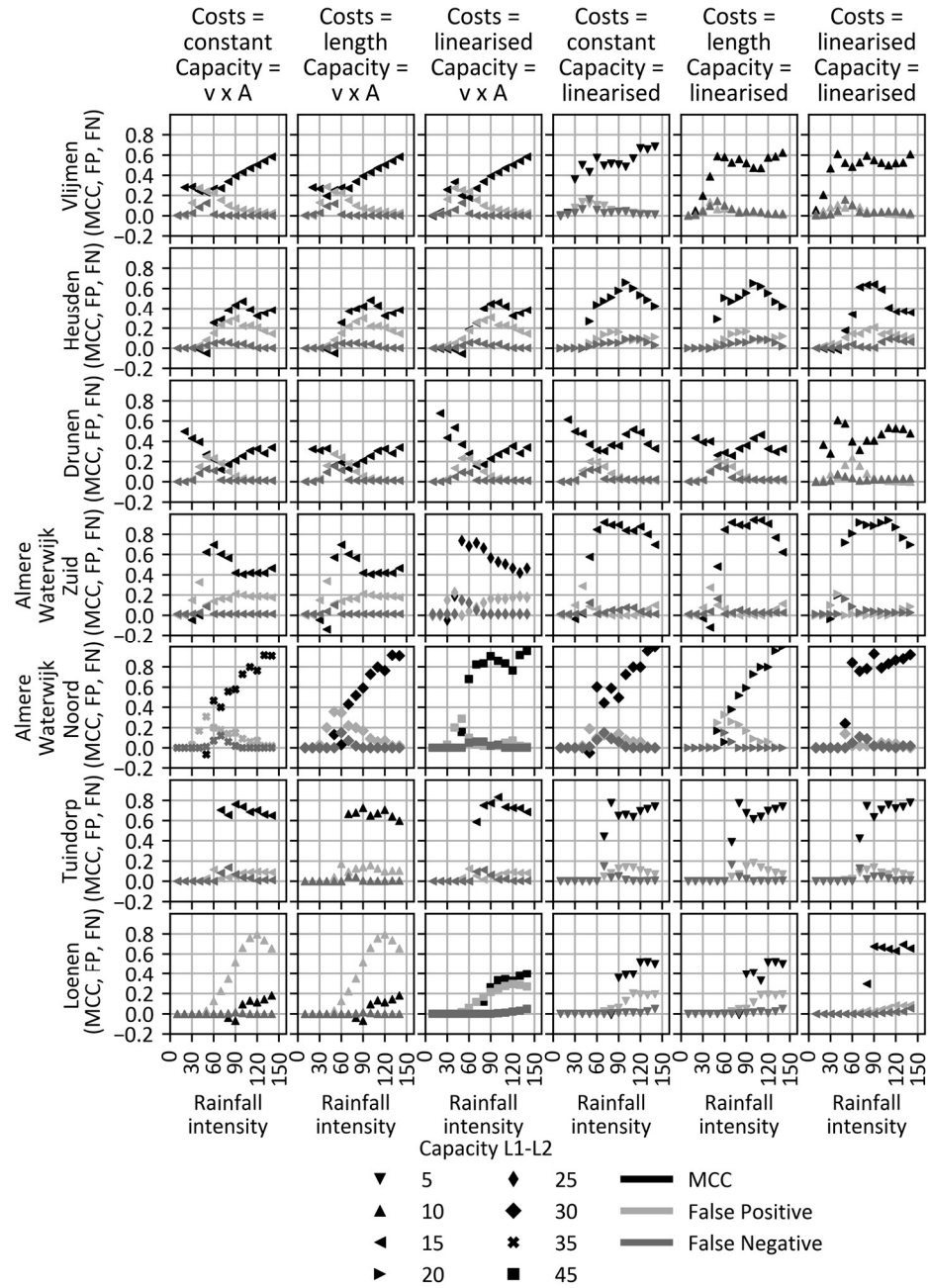
Figure 7.5   Matthews correlation coefficient and the% False Positive (FP) and False Negative (FN) for seven networks, six variants of hydraulic information and 14 storm intensities. Capacity L1–L2 indicates the applied and optimal capacity for the connection between layer-1 and layer-2 of the layered graph.

7.2.5 Applicability of the GBWLM for increased rainfall intensities

As stated in Section 3.5, the equilibrium between the discharge and storage capacity of the subsystems can be affected due to either a change in load or capacity of the networks. In this subsection, the focus is on network capacity.

A comparison was made between the freeboard (freeboard is the distance between ground level and water level) at a doubling of the precipitation intensity and at a halving of the discharge capacity for a storm sewer system. Three sets of calculations were performed:
1. The storm sewer system was tested with 2 stationary events of 4 mm/h and 8 mm/h.
2. The intensity of the events was doubled and the storm sewer system was tested with 2 stationary events of 8 mm/h and 16 mm/h.
3. The discharge capacity of the storm sewer system was halved and tested with 2 stationary events of 4 mm/h and 8 mm/h.

The storm sewer network reacted similarly to a capacity reduction of the pipe diameter and an increased storm intensity. Figure 7.6 shows that when the storm intensity increased by a factor of two (Figure 7.6, bottom-left) or the available capacity decreased by a factor two (Figure 7.6, bottom-right), the changes in freeboard were as expected and on the same order of magnitude (Figure 7.6, top-right). This means that the GBWLM can be used to analyse the impact of both a decrease in capacity of the system and an increase in load on the system.
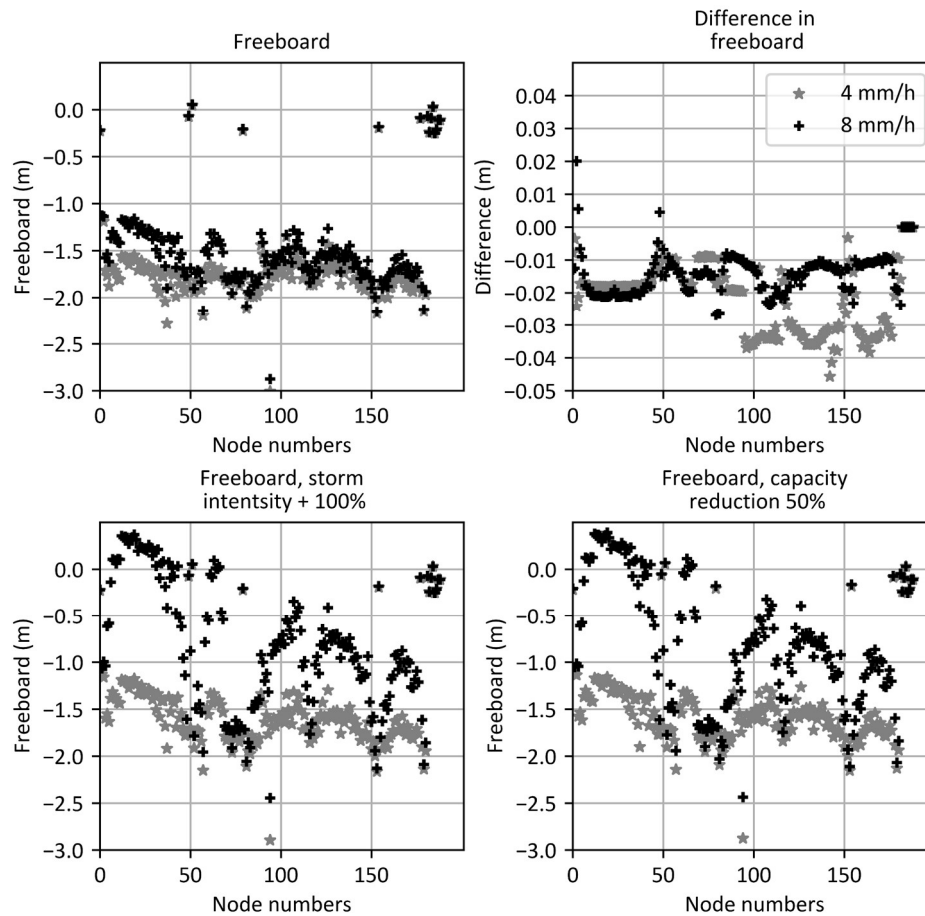
Figure 7.6   Comparison of the freeboard in the event of an increase of the storm intensity and a decrease of the available capacity for a storm event of 4 mm/h and 8 mm/h. Note: A different Y-scale has been used for the graph top right.

The rainfall intensities of storm events with return periods of 0.5–1000 years and a duration of 10 min–12 hours are expected to increase by 17.1–21.3% as a result of climate change (Beersma et al., 2019). This is expected to correspond to a capacity reduction of approximately 20% (see Figure 7.6). Figure 7.1 and Figure 7.2 show that such a capacity reduction had little impact on the flood frequency and extent caused by gully pots and surface water. However, it could lead to a 50% increase in the storm sewer flood frequency and to an increase in the extent of flooding.

7.3   Discussion

The objective of the GBWLM is to assess the potential functional limitations due to degradation-induced capacity losses and changes in network load of different subsystems of an urban drainage system. The GBWLM can be used to balance between required data, effort and accuracy. In this section, these aspects of the GBWLM are discussed.

7.3.1   Required input data and effort

The GBWLM is more accessible than the HBWLM because fewer data and less computational effort are needed. The computational effort required for the HBWLM is approximately 30 times greater than that for the GBWLM.

Correct representation of the network structure and geometry is important in both approaches; however, in the GBWLM, hydrodynamic models are replaced by path analysis of digraphs. As a result, the GBWLM requires less information about manholes and structures when compared to the HBWLM. Table 7.3 shows the data not included in the GBWLM.

Table 7.3   Overview of the required data per subsystem included in hydrodynamic model-based weakest link method but not in the graph-based weakest link method.

Rainfall runoff models	Gully pots	Storm sewers	Surface water system
Runoff parameters	Inlet parameters	Street level manhole	Thalweg (centre line of the water system)
Differentiation of roof types	z-coordinate	Dimensions manholes	Cross sections
Differentiation of paved area types		Weir characteristics (except height)	Weir characteristics (except capacity)
Differentiation of unpaved area types		Pump characteristics (except capacity)	Pump characteristics (except capacity)

Collecting data regarding structures normally requires significant effort, particularly when the sewer must be accessed to obtain these data. Information about manholes can be collected relatively easily and is often combined with sourcing characteristics that are necessary for both the HBWLM and the GBWLM.

For surface water systems, an important difference between the two methods is the detailed cross sections that are needed for the HBWLM as opposed to the GBWLM. The boundaries of the watercourses are sufficient for the GBWLM to determine the storage capacity.

7.3.2 Sensitivity of the GBWLM

The purpose of the GBWLM is to identify potential functional limitations due to degradation-induced capacity losses and changes in network load. The GBWLM should be able to assess the functioning of the system under different conditions. For these conditions, the results should show mutually significant differences.

The τ_b and F1 score (see Table 7.1) have indicated a relationship between the outcomes of the HBWLM and the GBWLM. However, these tests have also hinted at some differences caused by the simplification of hydrodynamics in the GBWLM.

The application of linearised hydrodynamics in the GBWLM results in over- and underestimations of the discharge capacity of elements (see Figure C.2.). In the GBWLM, the capacity of a conduit is estimated based on the geometry of the conduit and the hydraulic gradient. Simplifications are made by assuming that hydraulic gradients are the same for all conduits in one path (see Subsection 3.5.2).

With the GBWLM, the flood locations could be determined reasonably well. For most precipitation intensities, the F1 was greater than 0.6 (see Figure C.5). However, at the transitions from non-flooded to flooded regions, the number of flooded locations was overestimated. The size of the flooding extent was sometimes overestimated and sometimes underestimated, but for Almere the locations matched up well (see Figure C.3 and Figure C.4).

In case of sewer systems with a large storage capacity, the storage could be included in the storm or combined sewer graph, in a similar manner to that applied to the surface water component of the GBWLM. For the tested storm sewers of Almere, storage was not included in schematisation because the systems are directly connected (in open access) to the surface water and the majority of the pipes are always surcharged.

7.3.3 The degree of similarity between Hydrodynamic model Based Weakest Link Method (HBWLM) and GBWLM

The results of the GBWLM can be considered to be representative for the HBWLM. The comparison (see Subsection 7.2.2 and Appendix C) demonstrated a relationship in the development of the flood volume at different precipitation intensities between the HBWLM and the GBWLM (storm sewer $R^2 > 0.9$ and $\tau_b > 0.9$; see Table 7.1). A relationship between the HBWLM and the GBWLM was also observed in the calculated rise in surface water level due to storms (surface water $R^2 > 0.9$; see Appendix 9.2.2C.2.4). The minimum

overall F1 score was 0.69. This means that although the GBWLM results did not fully match those of the HBWLM, the overall impression was similar in terms of both the number of flooding locations and the locations themselves (see Table 7.1 and Figures in Appendix C.2.2. and C.2.3.).

The largest differences occurred at the transitions from non-flooded to flooded regions. They occurred at the beginning of a flood event and at the edges of the flooded area. Especially at the beginning of a flood event, when the number of flooded manholes in both the HBWLM and the GBWLM was low, relatively small deviations could result in a low F1 score.

7.3.4   An integrated analysis with the GBWLM

The interaction between subsystems is included in the GBWLM. The backwater effects of the surface water system on a storm sewer are included in the GBWLM by reducing the capacity of the storm sewers based on the occurring surface water levels. The GBWLM allows for an analysis of the overall functioning of an urban drainage system using a multiyear rainfall series. A multiyear analysis is necessary because event selection in advance is difficult due to the differences in storage and drainage characteristics of subsystems. The combination of storage and discharge capacity determines the time it takes for the system to return to its initial status after a storm event.

The drainage capacity of a gully pot connection becomes critical at approximately the same time as flooding occurs in the sewer system. In the GBWLM, this was labelled as storm sewer flooding. Gully pots and storm sewers are connected through pipes that are usually relatively short (i.e. length < 10 m, diameter 125 mm). A difference in water level of 1 cm results in a gradient of 0.1% and a discharge capacity of the connection pipe between gully pot and sewer of approximately 2.5 l/s (neglecting inflow and outflow losses). The average runoff surface per gully pot in Almere is < 120 m^2. Therefore, even when the water level in the storm sewer is close to ground level, the discharge capacity of a connection is still 215 l/(s.ha) and is therefore not a limiting factor.

7.3.5   Application options

Section 7.2.2. shows that the results of the GBWLM and HBWLM were consistent in this study. The added value of the GBWLM compared to the HBWLM is that:
- The GBWLM allows the analysis of urban drainage systems with multiyear rainfall series.
- The GBWLM allows for a combined analysis of subsystems of urban water subsystems.

- The GBWLM facilitates sensitivity analysis of urban drainage systems due to ageing or climate change.
- The GBWLM permits comparing flood frequency and flood extent caused by capacity reduction of urban water subsystems.

7.4   Conclusions

The GBWLM was used to compare the overall performance of urban drainage systems in terms of flood frequency and flood extent making use of relatively limited resources. The GBWLM is an integrated method to analyse the robustness of water networks consisting of gully pots, storm sewers and surface water networks with full (multiple decade) rainfall series. This method was used to analyse urban drainage systems at different levels of detail, ranging from gully pots to complete surface water systems. The subsystems could be analysed separately, but also in conjunction, including the corresponding interactions between the subsystems using multi-decade precipitation series.

The GBWLM differs from the HBWLM in that the former relies on the structure of the network and the different subsystems while the latter requires the application of full hydrodynamics. The advantages of the GBWLM approach can be summarised as:
- A full and integrated analysis of urban drainage systems (gully pots, storm sewers and surface water).
- An analysis with full (multiyear) rainfall series consisting of multiple events.
- Less required computational effort, resulting in a significant reduction of simulation run times.
- Determination of the effects of both reduced (sub)system capacity and increased rainfall intensities.

The parameters "flood extent" and "flood frequency" were used to assess the system's performance. Both are an indication of the severity of floods. These can be used as a basis to determine the impact in terms of impact such as damage or health risk.

The outcomes of the analysis can be used to prioritise maintenance activities and system rehabilitation. For the system of Almere, it was clear that the storm sewer system is the weakest link and most prone to capacity reduction. Due to climate change, the flood frequency could increase by approximately 50% in 2050.

8 Topological characterisation of looped drainage networks

8.1 Introduction

The Graph-Based Weakest Link Method (GBWLM) discussed in Chapters 3 and 7 combines elements of graph theory with linearised hydraulics. In order to test the applicability of the GBWLM to a storm or combined sewer network, measures are needed to characterise the networks. For this purpose, 22 topological characteristics to characterise networks were evaluated. The topology of seven Urban Drainage Networks (UDNs; see Chapter 4) was analysed based on these characteristics to evaluate whether existing methods provide indicators that distinguish networks for which the results of the Hydrodynamic model-Based Weakest Link Method (HBWLM) and the GBWLM do or do not coincide. The seven UDNs were also characterised using the Network Linearisation Parameter (NLP; see Subsection 3.5.4). Section 8.2 presents the results of classifying these looped drainage networks based on network structure, linearised hydraulics and bottlenecks (pipes with larger hydraulic gradients at high flows than adjacent upstream pipes) in the drainage paths to the outfalls. The results are discussed in Section 8.3, and the conclusions are presented in Section 8.4.

8.2 Results and interpretation

8.2.1 Reflection on the applicability of the topological parameters for urban drainage systems

Underground piped systems, as UDNs, are examples of planar graphs. They have spatial constraints, and connections between distant nodes normally do not occur (Buhl et al., 2004). UDNs have some typical characteristics that distinguish them from other spatial networks:

- UDNs are supply-driven.
- UDNs have multiple origins and few destinations.

- UDNs are mainly gravity-driven. Both free surface and pressurised flows may occur during a storm event.

Because of spatial constraints, the characteristics of UDNs do not correspond to the characteristics of small-world and scale-free networks (Barthélemy, 2011). The topological features mentioned in Subsection 2.4.4 to describe networks can be applied to describe UDNs, but these turn out to be very specific for each network (see Figure 8.1 and Table 8.1). In Figure 8.1 , values have been normalised based on the minimum and maximum values of the parameters for the seven networks.

Parameters 1 and 2 are measures for the size of the network. The larger networks Vlijmen and Drunen, holding many nodes and pipes, have a high score.

Parameters 3–6 describe the structures of the UDNs. The differences in the parameter values for the tested networks are limited. The average degree of the less-looped system of Loenen is slightly lower than that of the other looped networks. The parameter values "node closeness" and "density" of the Almere UDNs are slightly higher than those of the other networks. This may be related to the fact that the Almere networks are smaller (less nodes and pipes) and more looped than the other networks.

Parameters 8–10 are indicators for redundancy. As expected, the meshedness parameters for the partly branched and partly looped UDN of Loenen are slightly less than those of the other networks. The clustering coefficient indicates the absence of triangle loops in six of the seven tested networks.

The robustness parameters (11–16) contain three parameters (density of bridges and articulation points and inverse spectral radius) that have an inverse relationship with the meshedness parameters. The UDN of Loenen scores highly for these parameters. The smaller and more meshed networks of Almere have high values for algebraic connectivity and spectral gap. This is consistent with the characteristic that a relatively large number of links should be deleted to generate a bipartition (characteristic of algebraic connectivity) and the relatively short distance between nodes (characteristic of spectral gap). The central point dominance of the UDNs of Loenen, Vlijmen and Heusden is relatively high. These networks are either partly branched (Loenen) or made of different parts connected by a few pipes only (see Figure 4.8). The distance parameters (17–20) and the centrality parameters (21–22) are high for the larger tested networks and low for the smaller ones.

In summary, there are three distinguishing features for the tested networks:
1. The size of the network (number of nodes and pipes).

2. The degree of meshedness.
3. The structure of the network (central point dominance).
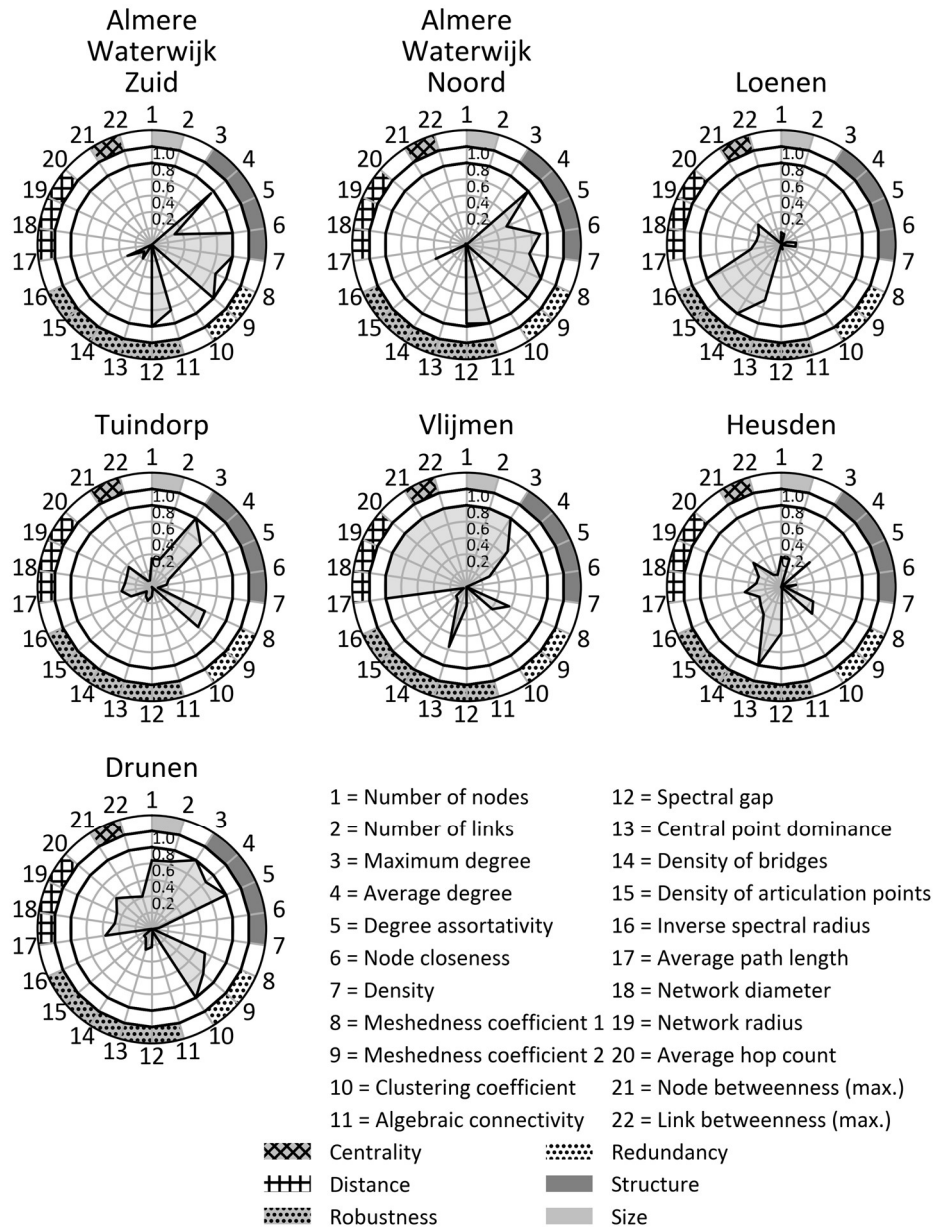
Figure 8.1   Normalised values of 22 different network parameters for seven urban drainage networks. For each parameter, the normalisation is based on the minimum and maximum values of the seven networks.

1 = Number of nodes
2 = Number of links
3 = Maximum degree
4 = Average degree
5 = Degree assortativity
6 = Node closeness
7 = Density
8 = Meshedness coefficient 1
9 = Meshedness coefficient 2
10 = Clustering coefficient
11 = Algebraic connectivity
12 = Spectral gap
13 = Central point dominance
14 = Density of bridges
15 = Density of articulation points
16 = Inverse spectral radius
17 = Average path length
18 = Network diameter
19 = Network radius
20 = Average hop count
21 = Node betweenness (max.)
22 = Link betweenness (max.)

Centrality   Redundancy
Distance   Structure
Robustness   Size

Table 8.1   Overview of 22 parameters of seven sewer networks.

	Almere Waterwijk Zuid	Almere Watewijk Noord	Loenen	Tuindorp	Vlijmen	Heusden	Drunen
Number of nodes	80	102	337	684	1,843	722	1,556
Number of links	92	118	352	778	2,053	787	1,776
Maximum degree	4	4	4	5	5	4	5
Average degree	2.3	2.31	2.07	2.26	2.23	2.18	2.28
Degree assortativity	-0.11	-0.08	-0.14	-0.12	-0.11	-0.15	-0.02
Node closeness	0.13	0.12	0.04	0.04	0.02	0.04	0.03
Density	0.0291	0.0229	0.0061	0.0033	0.0012	0.003	0.0015
Meshedness coefficient 1	0.08	0.09	0.02	0.07	0.06	0.05	0.07
Meshedness coefficient 2	0.23	0.23	0.11	0.2	0.16	0.17	0.21
Clustering coefficient	0	0	0	0	0	0	0.01
Algebraic connectivity	0.0161	0.0193	0.0012	0.0008	0.0001	0.0007	0.0007
Spectral gap	0.1724	0.1673	0.0289	0.0456	0.0624	0.1102	0.0607
Central point dominance	0.24	0.25	0.48	0.3	0.5	0.58	0.33
Density of bridges	0.26	0.2	0.5	0.24	0.26	0.32	0.24
Density of articulation points	0.25	0.22	0.46	0.24	0.26	0.3	0.25
Inverse spectral radius	0.3616	0.3661	0.3961	0.3591	0.3468	0.3599	0.3449
Average path length	7.96	8.71	23.99	23.95	50.84	27.24	32.53
Network diameter	21	22	62	65	154	62	82
Network radius	11	11	31	33	77	31	42
Average hop count	7.96	8.71	23.99	23.95	50.84	27.24	32.53
Node betweenness (maximum)	1,013	1,641	31,052	80,025	901,142	159,114	417,366
Link betweenness (maximum)	1,069	1,323	16,933	70,599	837,172	130,312	346,459

8.2.2   Results of the network linearisation parameter

The NLP was determined for the seven UDNs. Table 8.2 and Figure 8.2 present the results. In Figure 8.2, each dot represents a bottleneck. The size and greyscale colouring visualise the number of nodes of the UDN that discharge via the bottleneck (see % affected manholes in Figure 8.2). The larger and darker the dot, the higher is the percentage of affected manholes. On the *x*-axis is the applied threshold for the bottleneck. The bottlenecks per combined sewer outfall or storm sewer outflow of the UDN have been plotted side by side for each threshold. The position of the bottleneck is on the *y*-axis. The position has been normalised per outfall based on the maximum path length to the outfall. The numbers on top of each plot indicate the number of bottlenecks per threshold for the outfall with the highest number of bottlenecks.

For Tuindorp's UDN, Figure 8.2 shows that there is one major bottleneck that affects approximately 40% of the manholes that drain to one of the outflow locations if the "bottleneck threshold" is smaller than three. The bottleneck is located at approximately 0.25 of the maximum path length. The other bottlenecks only influence a few percent of the manholes. For Heusden's UDN, there is a relatively large bottleneck (impacting 60% of the manholes) at a threshold value of 100 relatively close to an outfall. At a threshold value of 50, a second bottleneck can be identified with similar characteristics.
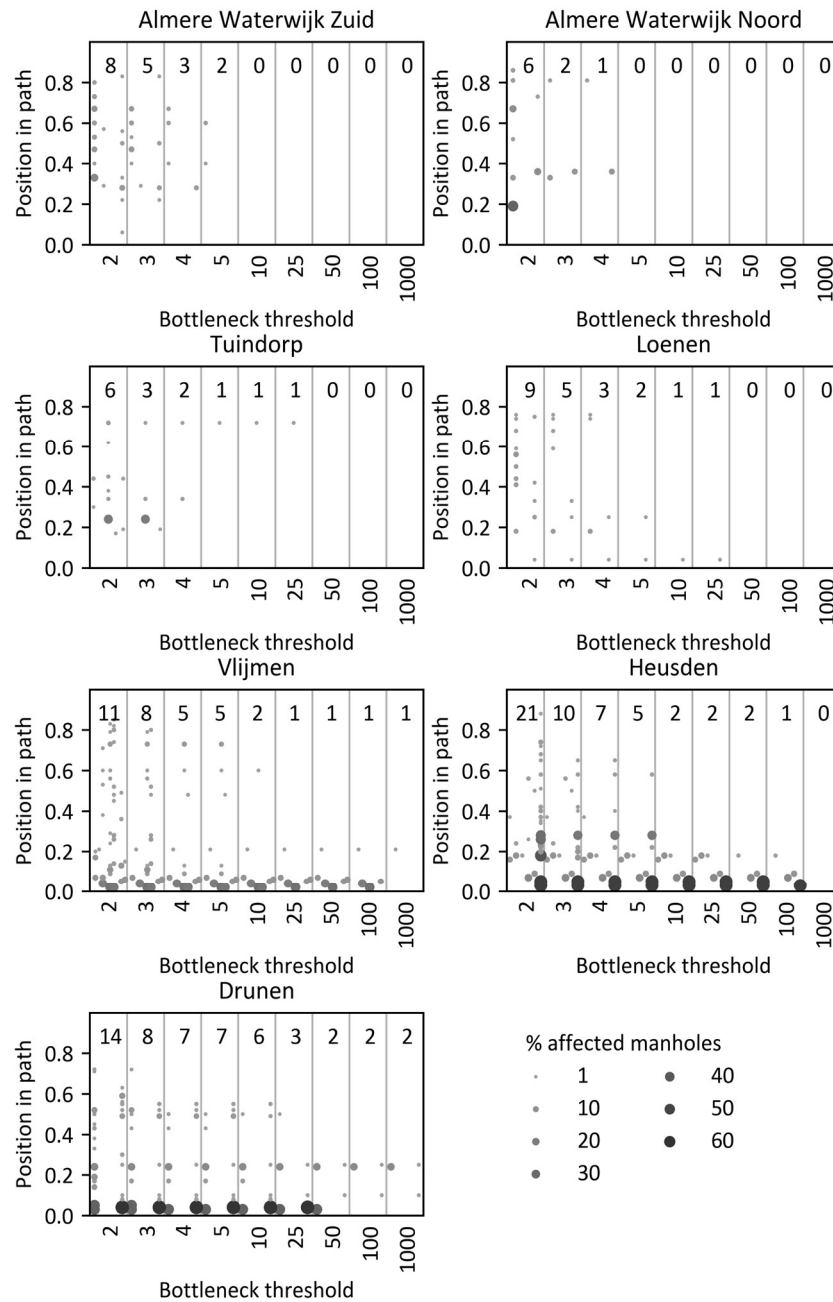
Figure 8.2   Bottlenecks in seven Urban Drainage Networks (UDNs) that affect more than 1% of the manholes of the UDN. The applied threshold is on the *x*-axis, and the normalised position is on the *y*-axis. The numbers in top of each plot indicate per threshold the number of bottlenecks for the outfall with the highest number of bottlenecks.

Table 8.2 presents an overview of the maximum thresholds at which more than 1% of the manholes of an outflow catchment would be affected by a bottleneck. It also includes the corresponding position of the bottleneck, the percentage of manholes influenced by the bottleneck and the number of catchments.

The table shows the following:

- For the UDNs of Vlijmen, Heusden and Drunen, the maximum threshold is higher than that for the networks of Almere, Loenen and Tuindorp.
- The percentage of affected manholes of the UDNs of Heusden and Drunen is larger than that of the other networks.
- The bottlenecks of the UDNs of Almere Zuid, Almere Noord and Tuindorp are situated at a greater distance from the outflow than those of the other networks.

Table 8.2   Overview of Urban Drainage Networks (UDNs) with a threshold at which more than 1% of a catchment of the UDN is affected by a bottleneck including the location, the percentage affected manholes and the number of bottlenecks.

	Threshold at which > 1% of manholes are affected by a bottleneck	Bottleneck location in path (0 = downstream, 1 = upstream)	% of affected manholes	Total number of bottlenecks
Almere Waterwijk Zuid	5	0.4	1	2
Almere Waterwijk Noord	4	0.36	7	2
Tuindorp	25	0.3	1	1
Loenen	25	0.04	4	1
Vlijmen	1000	0.07	7	1
Heusden	100	0.03	57	4
Drunen	1000	0.1	14	3

For precipitation intensities between 10 and 140 l/(s.ha), in steps of 10 l/(s.ha), the HBWLM and the GBWLM were used to identify flooding. The results were mutually compared using the Matthews Correlation Coefficient (MCC; see Figure 7.3).

For each catchment, the calculated MCC values of the different precipitation intensities for which the MCC was not equal to zero were analysed. The mean 95% confidence interval and median of the MCC values were calculated. Table 8.3 summarises the results of the MCC analysis. Please note that the confidence interval is based on a small sample and should therefore be regarded as an indication, at best.

Table 8.3 shows that the mean, the median and the lower and upper limit of the 95% confidence interval of the MCC values of the UDNs of Vlijmen, Heusden and Drunen were lower than those of the other four UDNs. Based on this observation, it can be concluded that for the UDNs of Almere Waterwijk Zuid, Almere Waterwijk Noord, Tuindorp and Loenen, the results of GBWLM were more in agreement with the HBWLM results than those for the UDNs of Vlijmen, Heusden and Drunen.

Table 8.3   The mean, 95% confidence interval and median of the available Matthews correlation coefficient values for 14 rainfall intensities in seven urban drainage networks.

Catchment	Mean	95% confidence interval	Median
Almere Waterwijk Zuid	0.714	[0.517, 0.911]	0.839
Almere Waterwijk Noord	0.784	[0.641, 0.926]	0.836
Tuindorp	0.687	[0.591, 0.783]	0.728
Loenen	0.610	[0.481, 0.739]	0.656
Vlijmen	0.478	[0.388, 0.568]	0.523
Heusden	0.343	[0.195, 0.490]	0.364
Drunen	0.453	[0.392, 0.514]	0.471

When the results of the NLP and the comparison of the GBWLM with the HBWLM were compared, the following observations could be made:

- The mean MCC of Heusden's UDN was the lowest, and the NLP showed several major bottlenecks close to an outfall.
- The mean MCC values for the UDNs of Vlijmen, Heusden and Drunen were relatively small, and the NLP showed multiple bottlenecks for high thresholds (i.e. 100, 1000).
- The UDNs of Almere, Loenen and Tuindorp had relatively high MCC values and a relatively small number of bottlenecks, occurring at smaller threshold values and affecting fewer manholes.

8.3   Discussion

8.3.1   Value of the topological network parameters

Many parameters have been proposed in literature to describe the topological features of networks. The seven networks tested exhibit three distinctive features, each of which can be described by one or more parameters.

1. Size of the network (parameters are e.g. number of nodes, number of pipes, network diameter or network radius).

2. Meshedness of the network (parameters are e.g. meshedness coefficient, density of bridges, density of articulation points and inverse spectral radius).
3. Structure of the network (parameters are e.g. central point dominance).

Even using a combination of the above parameters, it is not possible to describe the characteristics of a UDN in an unambiguous manner. The parameters describe the structure and not the flow (hydrodynamics) in the network. Special characteristics of UDNs that are not taken into account by the parameters mentioned are:

1. The flow directions (multiple origins, few destinations).
2. The capacity (geometry) of the pipes.
3. The transportation "costs" (required energy, head loss).

UDNs that produce more or less similar results in the GBWLM may have very different network parameter values. Therefore, other indicators are needed to characterise UDNs in order to predict whether or not the GBWLM can be applied successfully.

8.3.2   Network Linearisation Parameter (NLP)

The NLP combines linearised hydraulics and network structure to classify networks. There was no general value for the NLP for all tested networks. There were differences in the following:

- The threshold at which bottlenecks might occur.
- The position of the bottlenecks in the paths.
- The percentage of manholes affected by the bottlenecks.

The importance of these three sub-parameters is not yet entirely clear. The threshold value is an indication of the severity of the bottleneck. The higher the value, the larger is the difference in capacity between two adjacent pipes. However, the consequences also depend on the position. The consequences are smaller if the bottleneck occurs in the upstream parts of the network than in the downstream parts. The consequences are larger if the block is in a "main path" to an outflow location rather than in a path used only to discharge water from a few manholes. More networks should be analysed to determine the importance of the three sub-parameters more precisely and to determine whether or not these parameters set specific boundaries for the successful implementation of the GBWLM.

8.4 Conclusions and recommendations

The existing topological features used to describe networks can be applied to describe UDNs but prove to be very specific for each individual network (see Subsection 8.2.1). On the other hand, special characteristics of UDNs (multiple origins but few destinations, required transport energy, etc.) are not (fully) taken into account. Although the 22 parameters mentioned in this chapter are all different, there are only three main distinguishing features among them:

1. The size of the network (number of nodes and pipes).
2. The degree of meshedness.
3. The structure of the network (central point dominance).

Seven UDNs with different topological features (see Figure 8.1 and Table 8.1) were analysed using the GBWLM and the HBWLM. The results of the GBWLM and HBWLM were compared based on the MCC. The mean MCC values for four of the seven UDNs (Almere Zuid, Noord, Tuindorp and Loenen) were greater than 0.6, indicating a relatively strong correlation between the outcomes of the GWBLM and the HBWLM (see Table 8.3).

The seven UDNs exhibited different characteristics based on the NLP. The UDNs that matched well with the outcomes of hydrodynamic models according to the MCC met the following NLP criteria (Figure 8.2):

- A low bottleneck threshold (< 5) for bottlenecks that affect more than 10% of the manholes.
- No large bottlenecks (impact on > 5% of manholes) close to outfalls (< 20% path length).

More networks must be analysed to more precisely determine the importance of the sub-parameters (e.g. bottleneck threshold, bottleneck position, percentage of affected manholes or number of bottlenecks [see Figure 8.2]) and to assess the applicability of the NLP to other networks.

9 Conclusions and recommendations

Network managers face a major challenge in maintaining the desired service levels with "static" networks in a "dynamic" urban environment. Climate change, urbanisation and deterioration due to ageing have a negative impact on the performance of their networks. In addition, the impact of failure of networks is increasing, because cities and citizens have become increasingly dependent on numerous networks. In addition, due to co-location and network interdependence, the failure of one network can lead to the failure of other nearby networks. Limited available resources (time and budget) determine the scope of maintenance and rehabilitation activities that can be realised. Therefore, network operators must prioritise their activities.

To assist managers in prioritising, this thesis has provided and demonstrated methodologies to identify critical elements and weakest links in urban water infrastructure networks. This information contributes to a better understanding of the performance of these networks. Which can be used by managers of water networks as one of the pieces to solve the maintenance and rehabilitation puzzle.

9.1   General conclusions

In order to maintain the current performance of water networks, investments in maintenance and rehabilitation are necessary. In order to enhance the efficacy of the investments, information on the criticality of individual assets is necessary. The criticality of elements can be used to determine the maintenance sequence or to apply different minimum quality classes for elements with different levels of criticality. Knowledge about the criticality of the elements that make up networks can contribute to effective and efficient asset management strategies.

It requires a different approach to determine the criticality of elements in looped networks in flat areas or branched networks. The former requires a comprehensive analysis. The network managers should analyse the geometry (dimensions and height position), the network structure and bypass options. The criticality can be determined

with algorithms that analyse these features. However, for branched networks (in sloping areas), simpler analyses may suffice. The importance of pipes in branched systems can be based on the network structure. This can be done manually based on a map of the network or with algorithms that determine which part of a network is closed due to a blockage or leakage.

Hydrodynamic models can be used to determine the criticality of elements. Urban drainage systems consist of multiple subsystems. Changes in system type (e.g. combined sewers to separate systems or nature-based solutions), changes in requirements for storage and discharge capacity and climate change influence the interactions between systems. The network characteristics (i.e. storage and discharge capacity) determine whether storm events can be seen as mutually dependent or independent. Because the sewer and surface water characteristics are different, the dependency between events also differs. Independent sewer or storm water storm events could become dependent events because of the surface water system characteristics. Events that are independent in the design phase can become dependent if load and or capacity of the system changes. This implies that, in order to quantify the probability of flooding, an integrated analysis with multiyear rainfall series are required.

The calculation efforts of existing methods for determining the criticality of elements in networks is significant. These depend on:
1. The number of elements making up a network.
2. The hydraulic load (series vs design events).
3. The process description of the physical processes (i.e. rainfall runoff and hydrodynamic processes).

The Graph Theory Method (GTM) that has been presented and demonstrated here for pressurised systems and the GTM for gravity-driven systems is an example of models with simplified process descriptions. It offers the possibility to analyse the criticality of elements without simplifying the network structure. The outcomes are event-independent. The Graph-Based Weakest Link Method (GBWLM) can also be used for full networks and enables the analysis of urban drainage systems with multiyear rainfall series. Both methods consider network structure and geometry and flow path analysis based on graph theory.

> **Principles of graph theory**
>
> Graph theory has been applied in this research to replace hydrodynamic calculations by "flow path analysis". A graph $G = (V, E)$ is a set V of nodes and a set E of links. A path in a graph between a source node and a target node is a route between these nodes without a node occurring more than once. Each link has a cost. Costs are a metric for determining the shortest paths. For water systems, the necessary amount of energy to transport the water (head loss) is utilised as costs. The shortest path is a path between two nodes (manholes, connection nodes) in a graph such that the sum of the costs of the edges is minimised (see Section 3.3).

Because no unambiguous measure to characterise networks was found in literature, the Network Linearisation Parameter (NLP) was developed. The NLP provides an indication of whether or not a simplification of the process description, through linearisation of the hydraulics, is feasible and if the GBWLM methods can be applied successfully to a network. "Bottlenecks" (connections with a larger head loss than the adjacent ones) in the paths from manhole to outfall are used as indicators. The combination of the number, location and size of the bottlenecks and the percentage of affected manholes proves to be an indication of the applicability of the GBWLM on a specific network. In other words, the more homogeneous the hydraulic gradients, the smaller the deviations between the results of the hydrodynamic model-based weakest link model (HBWLM) and the GBWLM.

In the following three sections, the research questions formulated in Chapter 1 are addressed:

1. Which factors contribute to the criticality of an element in a water network?
2. What are the effects of simplifying hydrodynamic processes when evaluating the criticality of elements in networks?
3. What is the contribution of the network geometry, the network structure, the hydraulic load and the hydrodynamic processes to the functioning of a water network?

9.1.1 Factors affecting the criticality of an element in a network

In this thesis, the criticality of network elements has been described from the perspective of network performance. In the application of the GTM for pressurised systems, the network was tested for leaks. The system was evaluated on the number of locations for which the head loss to the leak is smaller than to head loss to the pumping station. For the GTM for gravity-driven systems, the network was tested for blockages. Networks were evaluated based on the required amount of energy to transport the water to outfalls. In

9 Conclusions and recommendations

the GBWLM, the network was tested for capacity reduction. The performance was evaluated based on the extent of flooding and flood frequency.

The effects of element failure on the network and the behaviour of the system were investigated for both pressurised systems and gravity-driven systems. According to the results of the analyses conducted on water distribution networks (WDNs) and the urban drainage networks (UDNs), the criticality observed depends on a combination of factors.

Because WDNs are evaluated based on the number of locations for which the head loss to the leak is smaller than to the pumping station, factors that influence the criticality include:
- The position of the element in the network structure:
  - Distance to a water pumping station.
  - Proximity of major pipes (pipe that is part of the shortest path [in terms of required pressure head loss] for a relatively large number of connection points).
- The connection to the network (through pipes with relatively high or low transportation costs).

The GTM for UDNs analyses whether, in the event of a failure of a connection, water can be transported from all locations to an outfall and what the costs of this would be. Factors that influence the criticality of elements in a UDN include:
- Will a blockage result in a disconnection between a part of the network and an outfall? The network graph is split into two graphs in which one of the graphs is no longer connected to an outfall. If all storage in this graph is fully used, extra water results in flooding.
- Is the blockage located in a pipe that is part of the shortest path (in terms of required pressure head loss) to an outfall or pumping station for a relatively large number of manholes?
- Are bypasses available? If so, what is the capacity, and what are the additional transportation costs?

The GTM and GBWLM can be used to determine the criticality of network elements for both branched and looped networks in sloping and flat areas. However, the criticality is easier to estimate for branched networks in sloping areas than for looped networks in flat areas.

Besides network performance, there are other factors that influence the criticality of elements from a network manager's perspective, for example the risk of malfunctioning,

170

expressed as the product of the likelihood of failure and the consequence of failures (see Section 2.2). The likelihood of failure has not been addressed in this thesis.

The GBWLM is used to calculate flood locations, flood extent and frequency. In flat areas, water will remain relatively close to the locations where it leaves the system. In sloping areas, it is necessary to use terrain models to analyse where the water flows, as it flows across the surface. When the flood locations are known, a GIS analysis could be used to determine the impact. The impact may result in a reassessment of the criticality.

9.1.2 Effects of simplifying hydrodynamic processes on the criticality in urban drainage systems

In the GTM and the GBWLM, the hydrodynamic process description has been simplified. Simplified hydrodynamics are used to calculate the "costs" (GTM and GBWLM) and capacity (GBWLM) of network connections. The costs are an indication of the energy needed to transport the water through the connection. They are derived from the head loss and consist of a static and a dynamic part (see Subsection 3.4.2).

The characteristics of the catchment area, the invert levels of the pipes and the crest levels influence the static part of the costs. Typical differences for determining pipe costs and capacity between networks in sloping and flat areas are:

- In sloping areas, the invert levels of some of the pipes are higher than the crest levels of the weirs; however, in flat areas the invert levels of almost all pipes are lower than the crest levels of weirs. If the invert levels of the pipes are lower than the crest level of the Combined Sewer Outfall (CSO) in a combined system or the surface water in a storm water system, the static costs are zero (because a water level equal to the lowest CSO in the network is applied) and the pipe costs are fully determined by the dynamic part.
- In sloping areas, networks are designed based on a surcharge percentage, while in flat areas fully surcharged pipes are assumed.
- In sloping areas, the terrain gradients, the pipe gradients and the hydraulic gradients run towards the outfalls (CSO, Storm Sewer Outflow [SSO]) and pumping stations while in flat areas, pipes slope down only towards pumping stations and the hydraulic gradients slope down towards the outfalls during storm events.
- In flat areas, the flow in pipes can be reversed. In sloping areas, this is only possible if there is an alternative flow path in which the ground level of the downstream manhole of the original flow path is higher than the highest invert level in the modified flow route.

171

9 Conclusions and recommendations

The dynamic head loss is dependent on the pipe characteristics and the flow rate or velocity in a pipe. Since the discharge and velocity are not known, the dynamic head loss can only be approximated assuming a uniform discharge or velocity. In this research a uniform discharge has been chosen. This discharge is a scaling factor of the pipes' costs. For fully surcharged systems in flat areas, the static costs are approximately zero and the results are more or less independent of the applied discharge. For fully surcharged systems in sloping areas and for partly surcharged systems, the applied discharge affects the ratio between static and dynamic costs. If the discharge is too high, dynamic costs outweigh static costs. If the variation in pipe diameters is large, the application of a uniform discharge can lead to large differences in flow velocity in the pipes and therefore to large differences in costs. This causes an imbalance in costs.

In the GTM, the costs in combination with the network structure are used to perform a "shortest path analysis". Based on changes in transport costs in case of blockages or leaks, the criticality of elements can be determined.

In the GBWLM, the costs and shortest paths are also used to determine the capacity of the pipes. If the networks are designed based on the surcharge ratio in sloping catchments, the capacity of the edges can be determined from the surcharge in combination with the invert levels of the pipe and the pipe diameter. This is not possible in flat areas because the gradient of the pipes runs towards the pumping station and the hydraulic gradient runs towards the outfalls. Therefore, for these areas the description of the hydrodynamic processes in the GBWLM is a simplified (linearised) momentum balance.

Simplifying the hydraulics may have the following effects on determining the criticality:
- If large differences occur in the hydraulic gradients (heterogeneous gradients) within a network, the capacity of the pipes is not correctly estimated by the GBWLM. The results of the GBWLM are then less reliable or not reliable at all.
- Static and dynamic cost ratios may be disturbed if the actual flows or velocities are incorrectly estimated. This may distort the interrelationship in the cost of the pipes. If this happens, the calculated shortest paths no longer correspond to the paths that the water follows in practice, and the results of the criticality analysis are unreliable.
- Simplified hydraulics sometimes produce an incorrect result when a blockage causes a significant flow change. The changes in head loss due to changing flows are not included in the dynamic costs of the pipes in the GTM and the GBWLM.

The above observations mean that for each network, an assessment must be made as to whether linearisation can be applied. The NLP can be used for this purpose.

172

9.1.3   Importance of the components of hydrodynamic models

The flow in both gravity-driven water networks and pressurised systems can be simulated with hydrodynamic models. In this research, UDNs were used as examples of gravity-driven systems and WDNs of pressurised systems. The criticality of elements in a UDN is quantified based on a 100% loss of transport capacity (blockage or complete structural collapse). In a WDN, a pressure-drop as a result of a leakage or pipe burst is considered as the dominant failure mechanism. WDNs and UDNs are further distinguished by the following facts (see Section 3.4):

- A WDN is driven by water demand, while a UDN is driven by supply.
- In a WDN, water flows from a limited number of points to many connection points. In a UDN, this is exactly the opposite.

In the following paragraphs, the functioning of the network has been considered from the main components of hydrodynamic model (see Section 1.4):

- System (network structure and geometry [dimensions of the pipes]).
- Hydraulic load.
- Hydraulic processes.

Network structure and geometry of UDNs
Pipes can become partially or completely blocked due to ageing or lack of maintenance. Blockage influences the available cross section (geometry). Pipes may be partially blocked due to sediment accumulation or root intrusion. If no maintenance is carried out, this can lead to completely blocked pipes over time. Pipes can also be completely blocked if they collapse. Fully blocked pipes reduce the transport capacity to zero. This corresponds to a change in the network structure. Partly blocked pipes reduce the capacity to a lesser extent and are considered as a change in the network geometry. Blockage can occur at any time and any location within the network. Therefore, this can strongly affect the functioning of the network.

The analyses conducted on the UDNs showed that a blockage in some cases could lead to a noticeable change in system behaviour. The larger the system change, the more critical the pipe. The extent of this change depends on the location and a combination of factors (see Subsection 6.2) such as the following:

1. Does the blockage result in the disconnection of part of the network and an outfall?
2. Is the main transport route to the outfall disrupted by the blockage?
3. Are diversion possibilities available, and if so, at what cost?

Relatively small deviations in geometry can result in significant changes in the behaviour of the system. This is because both the relationship between discharge and diameter and the relationship between discharge and gradient contain a power term. The impact of changes in geometry depends on the degree of the changes and on the location of the obstructed pipes in the network.

Hydraulic load on UDNs
The GTM analysis is load-independent, and in the GBWLM a series of events are analysed. The analysis is based on changes in transportation costs rather than flood locations in the GTM, and with the GBWLM it is possible to use multiyear rainfall series due to the limited computational effort required.

Network performance of UDNs is often assessed on the change in number of flooded locations or flood volume with hydrodynamic models. Both criteria are influenced by hydraulic load. The effect of a blockage depends on the overcapacity of the system. If a system has a certain overcapacity for a given load, a reduced capacity of pipes far from an outfall in the upstream part of the network could lead to more flooded manholes than a reduced capacity of a main transport pipe with bypass options close to an outfall. By contrast, if the load on the entire system is critical, a reduced capacity of the main transport pipes close to an outfall will have a larger effect on the number of flooded locations than a reduced capacity of pipes in the upstream part of the network. Therefore, other pipes will be marked as critical. This means that the hydraulic load affects the results of a criticality analysis (see Subsection 6.2.1).

Section 7.2 has shown that networks with different storage and discharge capacities react differently to a change in capacity or load (see Subsection 7.2.5). If networks are interrelated, an analysis of the entire system is needed with (multiyear) precipitation series to understand the effects of changes in load or system characteristics.

Hydraulic load on WDNs
A leak results in an additional water demand in a WDN and can be considered as a change in load. The size of the pressure drop has little influence on the ranking of the criticality of the elements. However, the impact of a leak strongly depends on the size of the pressure drop. A higher pressure drop in the event of a leak will lead to more people suffering from low water pressure. If more water flows out of the WDN into the street, the chance of nuisance is also higher.

Hydrodynamic processes
The transport of water is described using hydrodynamics equations. There are many examples of well-calibrated hydrodynamic models for surface water and sewage systems

that accurately describe flows and water levels. These models quantify static and dynamic flows for a variety of events. However, the exact parameters are not usually known. In this case, conservative parameter value estimates are often used to prevent the models from being overly optimistic and networks from being under-dimensioned. The more complex the models, the more parameters are required, and the greater the uncertainties are in the absence of calibration.

The linearisation of hydrodynamic processes is more complex for looped networks in flat areas than for branched networks in hilly areas because in flat areas there is little or no relationship between the gradient of the ground level or the pipe and the hydraulic gradient (see Subsection 9.1.2),. Moreover, in looped systems in flat areas, the flow direction may reverse during storm events.

In the GBWLM, the hydrodynamic processes are linearised based on a maximum available hydraulic gradient between the crest level and the ground level and the corresponding maximum discharge. The analysis of seven UDNs (see Chapter 7) demonstrates that despite the linearisation, the results of the GBWLM still match the results of hydrodynamic models reasonably well.

The more homogeneous the gradients are in an area that drains into an outfall in a network, the better the results correspond to a model with a complete hydrodynamic process description. The NLP can be used to determine whether there are differences in gradients for each overflow in a network. The NLP is used to determine whether the head loss in a connection is larger than the adjacent upstream pipe ("bottleneck"). By analysing whether and where these bottlenecks occur for each sub-catchment that drains into one outfall, the NLP indicates whether linearisation can be applied in such a way that the results are representative of the real situation.

Large differences in the hydraulic gradient occur if there are large differences in the amount of energy required to transport the water through pipes. This depends on pipe geometry and the flow and also explains why network features that focus only on the geometry or structure of a network and not on the flow rates that occur are unreliable criteria for determining whether linearisation can be applied.

In case of large differences in discharge or storage capacity in a network, hydrodynamic equations are necessary to describe the water transport. Unless the network can be properly subdivided into sub-networks, each with its own uniform storage and drainage characteristics, linearisation will lead to results that differ potentially greatly from practice such that the results of the criticality analyses cannot be used.

9.2 Recommendations for future research and applications

9.2.1 General recommendations

The GTM, the GBWLM and the NLP have been applied in a limited number of case studies. For these case studies, statistical tests have shown that there is a clear correlation with the results of methods based on hydrodynamic models. However, more tests are needed before these methods can be widely applied in practice. The most urgent questions are the following: What requirements must a network meet exactly in order for the GTM or GBWLM to be successfully applied? In addition, is it possible to develop an unambiguous parameter to classify networks? The NLP can be used for a first estimation of the probability of a successful application of the GBWLM; However, more case studies are needed to tighten the criteria.

Validation method
In order to further validate the methods presented, it is recommended to apply them at other UDNs and WDNs as well taking into account the following steps:
1. Validate the input data.
2. Determine the NLP-factor.
3. Calculate the criticality of the elements.
4. Visualise the results.
5. Evaluate the plausibility of the criticality.
6. If the results are plausible, then use the results. If not:
   a. Select the most critical elements according to the GTM.
   b. Select the pipes with the largest pipe diameters from the network.
   c. Run a hydrodynamic model and adjust the selected elements one by one.
   d. Visualise the results.
   e. Evaluate the plausibility of the results.

After more networks have been analysed, one can determine whether the derived relationship for determining the capacity of the connection between the sewer system and the ground level (L1–L2 connection) can be generally applied.

Dynamic costs based on uniform velocity instead of uniform discharge
In this study, the dynamic part of the costs of the edges was based on a uniform discharge through the system. If the variation in pipe diameters is large, the application of a uniform discharge can lead to large differences in flow velocities and therefore to large differences in dynamic costs. Using a uniform velocity is probably a more realistic assumption and may

lead to dynamic costs that are more in line with practice. It is therefore recommended for follow-up research to examine whether the results can be further improved by applying a uniform velocity (equal to the design velocity).

9.2.2   Recommendations for possible applications

There are several applications for graph-based analysis that could be further explored, such as the following:

- Developing cleaning strategies.
- Developing monitoring strategies.
- Increasing the robustness of (storm water and combined sewer) networks during (re)design by adapting the structure or geometry.
- Impact analyses of hydraulic failure of systems by combining the results of the GTM and GBWLM with GIS analyses.
- Application of the GTM, GBWLM and NLP to other networks.

Developing cleaning strategies
The GTM could be applied as described in Chapter 3 to develop new cleaning strategies for (combined) sewer systems. The impact of partly blocked pipes could be analysed. Instead of removing a pipe from the graph to simulate a blockage, a "resistance factor" could be added by increasing the costs of the pipes one by one. Possible options include the following:

1. Recalculate the head loss where it is assumed that the pipe is 50% blocked.
2. Add a constant resistance factor to each pipe.
3. Increase the weight of the pipes by a certain percentage.

Different weather conditions may be simulated by choosing different target nodes. The pumping stations could be used as targets to evaluate dry weather conditions, and the combined sewer outflow structures could be used to assess wet weather conditions.

The results of fully blocked and partly blocked pipes for the two conditions could be visualised in a GIS system. For example, the 25–30% most critical pipes identified with the GTM could be used as basis for the cleaning strategy. If this process were to result in small sections spread across the network, this could be inefficient because moving to another location and restarting takes a relatively long time. In that case, the information from the GTM could be combined with information about major traffic routes, previous blockages and existing inspection and cleaning reports to optimise the cleaning routes.

Developing monitoring strategies
The results of the GTM could also be used to design a monitoring network in two ways. Measuring points could be located in the most critical pipes based on the GTM, as changes in flows and water levels will affect a relatively large part of the network. Another approach would be to select the manholes with the most frequent or largest differences from the results of the GTM. These points would be the most sensitive to changes in the network and possible act as accurate predictors of changes in maintenance conditions. More research is needed to determine the best approach.

Increasing network robustness and removing bottlenecks
The GTM, GBWLM and the NLP-factor could be used to identify critical elements, weakest links and bottlenecks in (looped) networks. If these are identified in the network, structure or geometry can be adjusted to reduce or remove these obstacles to increase the robustness of the network.

The robustness of networks can often be increased by adjusting network structure or network geometry. Bottlenecks sometimes occur at locations where the capacity of the downstream pipe is not aligned with the capacity of the upstream pipes. Another common bottleneck is the situation in which the redirection costs are high in case of a blockage or where there is no bypass route (branched parts of networks).

After the bottlenecks have been identified, improvement measures can be designed to reduce them. These measures can be tested to determine whether the robustness has increased or if the bottlenecks have been removed.

Impact of failure
The criticality can be combined with the consequences of failure (see Subsection 2.2.2). Failure of (sewer) systems has an impact on the service level (drainage of water) and on the environment (health risks, floods, blocked roads, damage to other infrastructure or pollution). The degree of criticality can therefore be used as a basis for risk-based asset management. In addition, it can be used to analyse the robustness of a network and to evaluate measures to increase its robustness.

The results of the GBWLM could be combined with a 2D overland model. For each pipe where a blockage would result in one or more flooded locations, a 2D simulation can be run by adding a constant discharge, during a limited period, to the 2D model. A GIS analysis could be used to determine the impact of the flooding.

Other networks

The GTM has only been tested on UDNs and WDNs, the GBWLM on urban drainage systems and the NLP on UDNs. However, there are other networks to which these methods might be applied, such as district heating, pressurised pipe systems, surface water networks and gas distribution networks. More research is needed to verify the applicability of the methods described and the characteristics which these networks must meet to apply the methods successfully.

References

Albert, R., & Barabási, A.-L. (2002). Statistical mechanics of complex networks. Reviews of Modern Physics, 74(1), 47–97. https://doi.org/10.1103/RevModPhys.74.47

Ale, B. J. M. (2005). Risk is of all time. Die Küste, 70, 173–184. https://henry.baw.de/bitstream/20.500.11970/101551/1/k070113.pdf

Ale, B. J. M. (2009). Risk: An introduction: The concepts of risk, danger and chance. Routledge. https://doi.org/10.4324/9780203879122

American Society of Civil Engineers. (2017). Infrastructure Report Card, 2017. https://www.infrastructurereportcard.org/cat-item/drinking_water/

Anbari, M. J., Tabesh, M., & Roozbahani, A. (2017). Risk assessment model to prioritize sewer pipes inspection in wastewater collection networks. Journal of Environmental Management, 190, 91–101. https://doi.org/10.1016/j.jenvman.2016.12.052

Arthur, S., & Crow, H. (2007). Prioritising sewerage maintenance using serviceability criteria. Proceedings of the Institution of Civil Engineers - Water Management, 160(3), 189–194. https://doi.org/10.1680/wama.2007.160.3.189

Arthur, S., Crow, H., Pedezert, L., & Karikas, N. (2009). The holistic prioritisation of proactive sewer maintenance. Water Science & Technology, 59(7), 1385–1396. https://doi.org/10.2166/wst.2009.134

Ashley, R. M., Bertrand-Krajewski, J.-L., Hvitved-Jacobsen, T., & Verbanck, M. (Eds.). (2004). Solids in sewers: Characteristics, effects and control of sewer solids and associated pollutants (Scientific and Technical Report No. 14). IWA Publishing.

Baah, K., Dubey, B., Harvey, R., & McBean, E. (2015). A risk-based approach to sanitary sewer pipe asset management. Science of the Total Environment, 505, 1011–1017. https://doi.org/10.1016/j.scitotenv.2014.10.040

Bach, P. M., Rauch, W., Mikkelsen, P. S., McCarthy, D. T., & Deletic, A. (2014). A critical review of integrated urban water modelling – Urban drainage and beyond. Environmental Modelling & Software, 54, 88–107. https://doi.org/10.1016/j.envsoft.2013.12.018

Balekelayi, N., & Tesfamariam, S. (2019). Graph-theoretic surrogate measure to analyze reliability of water distribution system using Bayesian belief network-based data

fusion technique. Journal of Water Resources Planning and Management, 145(8).
https://doi.org/10.1061/(ASCE)WR.1943-5452.0001087

Barthélemy, M. (2011). Spatial networks. Physics Reports, 499(1–3), 1–101.
https://doi.org/10.1016/j.physrep.2010.11.002

Beersma, J., Hakvoort, H., Jilderda, R., Overeem, A., & Versteeg, R. (2019).
Neerslagstatistiek en -reeksen voor het waterbeheer 2019 [Rainfall statistics and
series for water management 2019] (STOWA Report No. 2019-19). Stichting
Toegepast Onderzoek Waterbeheer.
https://www.stowa.nl/sites/default/files/assets/PUBLICATIES/Publicaties%20201
9/STOWA%202019-19%20neerslagstatistieken.pdf

Bolle, A., Demuynck, A., Bouteligier, R., Bosch, S., Verwey, A., & Berlamont, J. (2006).
Hydraulic modelling of the two-directional interaction between sewer and river
systems. In A. Delectic & T. Fletcher (Eds.), 7th International Conference on Urban
Drainage Modelling and the 4th International Conference on Water Sensitive
Urban Design; Book of proceedings (Vol. 1, pp. 896–903). Monash University.
https://search.informit.org/doi/10.3316/informit.784926267780303

Bos, G. S. (1942). De Rekenliniaal Voor Rioleeringsberekeningen systeem Kasper [The slide
rule for sewerage calculation system Kasper]. Publieke Werken, 1942/12.

Broadbent, S. R., & Hammersley, J. M. (1957). Percolation processes: I. Crystals and mazes.
Mathematical Proceedings of the Cambridge Philosophical Society, 53(3), 629–
641. https://doi.org/10.1017/S0305004100032680

Buhl, J., Gautrais, J., Solé, R. V., Kuntz, P., Valverde, S., Deneubourg, J. L., & Theraulaz, G.
(2004). Efficiency and robustness in ant networks of galleries. The European
Physical Journal B, 42(1), 123–129. https://doi.org/10.1140/epjb/e2004-00364-9

Burian, S. J., & Edwards, F. G. (2002). Historical perspectives of urban drainage. In E. W.
Strecker & W. C. Huber (Eds.), Global solutions for urban drainage: Proceedings of
the Ninth International Conference on Urban Drainage. American Society of Civil
Engineers. https://doi.org/10.1061/40644(2002)284

Butler, D., & Davies, J. W. (2004). Urban drainage (2nd ed.). Spon Press.

Carriço, N., Covas, D. I. C., Céu Almeida, M., Leitão, J. P., & Alegre, H. (2012). Prioritization
of rehabilitation interventions for urban water assets using multiple criteria
decision-aid methods. Water Science & Technology, 66(5), 1007–1014.
https://doi.org/10.2166/wst.2012.274

Chicago Architecture Editor. (2016, February 22). 39 things you probably don't know about
the Old Main Post Office. Chicago Architecture.
https://www.chicagoarchitecture.org/2016/02/22/30-things-you-probably-dont-
know-about-the-old-main-post-office/

Chinchor, N. (1992). MUC-4 evaluation metrics. In MUC4 '92: Proceedings of the 4th
Conference on Message Understanding (pp. 22–29). Association for

Computational Linguistics. https://doi.org/10.3115/1072064.1072067

Clark, J., & Holton, D. A. (1991). A first look at graph theory. World Scientific. https://doi.org/10.1142/1280

Coördinatiecommissie Integraal Waterbeleid. (2012). Code van goede praktijk voor het ontwerp, de aanleg en het onderhoud van rioleringssystemen [Code of good practice for the design, construction and maintenance of sewer systems]. https://www.integraalwaterbeleid.be/nl/publicaties/code-goede-praktijk-rioleringssystemen/Code%20Van%20Goede%20Praktijk%20Rioleringssystemen.pdf

Cross, H. (1936). Analysis of flow in networks of conduits or conductors. University of Illinois Bulletin, 34(22), 1–33.

de Man, H., & Leenen, I. (2014). Water in de openbare ruimte heeft risico's voor de gezondheid [Water in public spaces poses health risks] (Report No. 2014-28). STOWA; Sichting RIONED. https://www.stowa.nl/sites/default/files/assets/PUBLICATIES/Publicaties%202014/STOWA%202014-28.pdf

Davies, J., Clarke, B., Whiter, J., Cunningham, R., & Leidi, A. (2001). The structural condition of rigid sewer pipes: a statistical investigation. Urban Water, 3(4), 277–286. https://doi.org/10.1016/s1462-0758(01)00036-x

Diao, K., Farmani, R., Fu, G., Astaraie-Imani, M., Ward, S., & Butler, D. (2014). Clustering analysis of water distribution systems: identifying critical components and community impacts. Water Science and Technology, 70(11), 1764–1773. https://doi.org/10.2166/wst.2014.268

Dijkstra, E. W. (1959). A note on two problems in connexion with graphs. Numerische Mathematik, 1(1), 269–271. https://doi.org/10.1007/BF01386390

Donetti, L., Neri, F., & Muñoz, M. A. (2006). Optimal network topologies: Expanders, cages, Ramanujan graphs, entangled networks and all that. Journal of Statistical Mechanics: Theory and Experiment, 2006(8), Article P08007. https://doi.org/10.1088/1742-5468/2006/08/P08007

European Commission, Directorate-General for environment. (2018). Commission Decision (EU) 2019/61 of 19 December 2018 on the sectoral reference document on best environmental management practices, sector environmental performance indicators and benchmarks of excellence for the public administration sector under Regulation (EC) No 1221/2009 on the voluntary participation by organisations in a Community eco-management and audit scheme (EMAS). https://eur-lex.europa.eu. Geraadpleegd op 24 december 2021, van https://eur-lex.europa.eu/legal-content/EN-NL/ALL/?uri=CELEX:32019D0061&from=EN

European Parliament, Council of the European Union. (2018). Directive (EU) 2020/2184 of the European Parliament and of the Council of 16 December 2020 on the quality

of water intended for human consumption (recast). https://eur-lex.europa.eu. Geraadpleegd op 24 december 2021, van https://eur-lex.europa.eu/legal-content/EN-NL/ALL/?uri=CELEX:32020L2184&from=EN

Friedl, F., Möderl, M., Rauch, W., Liu, Q., Schrotter, S., & Fuchs-Hanusch, D. (2012). Failure Propagation for Large-Diameter Transmission Water Mains Using Dynamic Failure Risk Index. World Environmental and Water Resources Congress 2012. https://doi.org/10.1061/9780784412312.310

F-score. (2000, 1 januari). In Wikipedia. https://en.wikipedia.org/wiki/F-score

Fuchs-Hanusch, D., Möderl, M., Sitzenfrei, R., Friedl, F., & Muschalla, D. (2014). Systematic estimation of discharge water due to transmission mains failure by the means of Epanet2. In *Water Loss* (pp. 75-75). https://graz.pure.elsevier.com/en/publications/systematic-estimation-of-discharge-water-due-to-transmission-main

Geels, F. W. (2006). The hygienic transition from cesspools to sewer systems (1840–1930): The dynamics of regime transformation. Research Policy, 35(7), 1069–1082. https://doi.org/10.1016/j.respol.2006.06.001

Gemeentewet, Art. 174 [Municipality act]. (2021). https://wetten.overheid.nl. Geraadpleegd op 19 november 2021, van https://wetten.overheid.nl/BWBR0005416/2021-07-10#TiteldeelIII

Giudicianni, C., Di Nardo, A., Di Natale, M., Greco, R., Santonastaso, G. F., & Scala, A. (2018). Topological taxonomy of water distribution networks. Water, 10(4), Article 444. https://doi.org/10.3390/w10040444

Gormley. (2006). MASS [1.6 mm stainless steel rod, 102 x 302.4 x 206 cm]. Museum Voorlinden, Wassenaar, the Netherlands. Photograph by Stephen White & Co. © the artist

Gujer, W., Krejci, V., Schwarzenbach, R., & Zobrist, J. (1982). Von der Kanalisation ins Grundwasser - Charakterisierung eines Regenereignisses im Glattal [From the sewer system into the groundwater - characterisation of a rainfall event in the Glattal valley]. Gas-Wasser-Abwasser, 62(7), 298–311. https://www.dora.lib4ri.ch/eawag/islandora/object/eawag%3A2313/datastream/PDF/Gujer-1982-Von_der_Kanalisation_ins_Grundwasser-%28published_version%29.pdf

Hagberg, A. A., Schult, D. A., & Swart, P. J. (2008). Exploring network structure, dynamics, and function using NetworkX. In G. Varoquaux, T. Vaught, & J. Millman (Eds.), Proceedings of the 7th Python in Science Conference (SciPy2008) (pp. 11–15).

Halfawy, M. R., Dridi, L., & Baker, S. (2008). Integrated decision support system for optimal renewal planning of sewer networks. Journal of Computing in Civil Engineering, 22(6), 360–372. https://doi.org/10.1061/(ASCE)0887-3801(2008)22:6(360)

Hall, E. L., & Dietrich, A. M. (2000). A brief history of drinking water. Opflow, 26(6), 46–49.

https://doi.org/10.1002/j.1551-8701.2000.tb02243.x

Hamlin, C. (1992). Edwin Chadwick and the Engineers, 1842-1854: Systems and
	Antisystems in the Pipe-and-Brick Sewers War. Technology and Culture, 33(4),
	680–709. https://doi.org/10.2307/3106586

Harary, F., & Norman, R. Z. (1960). Some properties of line digraphs. Rendiconti del Circolo
	Matematico di Palermo, 9(2), 161–168. https://doi.org/10.1007/BF02854581

Harju, T. (2012). Lecture notes on graph theory. University of Turku.
	https://users.utu.fi/harju/graphtheory/graphtheory.pdf

Hele week gasstoring Apeldoorn [Gas failure Apeldoorn entire week]. (2014, June 1). NOS.
	https://nos.nl/artikel/655469-hele-week-gasstoring-apeldoorn.html

Hoagland, S., Schal, S., Ormsbee, L., & Bryson, S. (2015). Classification of water distribution
	systems for research applications. In K. Karvazy & V. L. Webster (Eds.),
	Proceedings of the 2015 World Environmental and Water Resources Congress:
	Floods, droughts, and ecosystems (pp. 696–702). American Society of Civil
	Engineers. https://doi.org/10.1061/9780784479162.064

Huizen Apeldoorn dagenlang zonder gas [Apeldoorn houses without gas for days]. (2014,
	December 7). NOS. https://nos.nl/artikel/2007798-huizen-apeldoorn-dagenlang-
	zonder-gas

International Organization for Standardization. (2014). Asset management – Overview,
	principles and terminology (ISO Standard No. 55000:2014).

International Organization for Standardization. (2017). Systems and software engineering
	– Vocabulary (ISO/IEC/IEEE Standard No. 24765:2017).

International Water Association Publishing. (n.d.). A brief history of water and health from
	ancient civilizations to modern times.
	https://www.iwapublishing.com/news/brief-history-water-and-health-ancient-
	civilizations-modern-times

Jha, A. K., Bloch, R., & Lamond, J. (2012). Cities and flooding: A guide to integrated urban
	flood risk management for the 21st century. The World Bank.
	https://doi.org/10.1596/978-0-8213-8866-2

Johnson, C. A., Flage, R., & Guikema, S. D. (2019). Characterising the robustness of coupled
	power-law networks. Reliability Engineering & System Safety, 191, Article
	106560. https://doi.org/10.1016/j.ress.2019.106560

Johnson, C. A., Reilly, A. C., Flage, R., & Guikema, S. D. (2021). Characterizing the
	robustness of power-law networks that experience spatially-correlated failures.
	Proceedings of the Institution of Mechanical Engineers, Part O: Journal of Risk
	and Reliability, 235(3), 403–415. https://doi.org/10.1177/1748006X20974476

Kalapala, V., Sanwalani, V., Clauset, A., & Moore, C. (2006). Scale invariance in road
	networks. Physical Review E, 73(2), Article 026130.
	https://doi.org/10.1103/PhysRevE.73.026130

Kendall, M. G. (1945). The treatment of ties in ranking problems. Biometrika, 33(3), 239–251. https://doi.org/10.2307/2332303

Kessener, H. P. M. (2017). Roman water distribution and inverted siphons – Until our days [Doctoral dissertation, Radboud University Nijmegen]. Radboud Repository. https://hdl.handle.net/2066/178805

Kesztenbaum, L., & Rosenthal, J.-L. (2017). Sewers' diffusion and the decline of mortality: The case of Paris, 1880–1914. Journal of Urban Economics, 98, 174–186. https://doi.org/10.1016/j.jue.2016.03.001

Kingdom, B., Liemberger, R., & Marin, P. (2006). The challenge of reducing non-revenue water (NRW) in developing countries: How the private sector can help: A look at performance-based service contracting (Water Supply and Sanitation Sector Board Discussion Paper Series, Paper No. 8). The World Bank Group. http://documents.worldbank.org/curated/en/385761468330326484/pdf/394050 Reducing1e0water0WSS81PUBLIC1.pdf

Klinkhamer, C., Krueger, E., Zhan, X., Blumensaat, F., Ukkusuri, S., & Rao, P. S. C. (2017). Functionally fractal urban networks: Geospatial co-location and homogeneity of infrastructure. arXiv. https://doi.org/10.48550/arXiv.1712.03883

Klinkhamer, C., Zischg, J., Krueger, E., Yang, S., Blumensaat, F., Urich, C., Kaeseberg, T., Paik, K., Borchardt, D., Silva, J. R., Sitzenfrei, R., Rauch, W., McGrath, G., Krebs, P., Ukkusuri, S., & Rao, P. S. C. (2019). Topological convergence of urban infrastructure networks. arXiv. https://doi.org/10.48550/arXiv.1902.01266

König, D. (1936). Theorie der endlichen und unendlichen Graphen: Kombinatorische Topologie der Streckenkomplexe [Theory of finite and infinite graphs: Combinatorial topology of line complexes]. AMS Chelsea Publishing.

Korving, J., & Clemens, F. (2005). Impact of dimension uncertainty and model calibration on sewer system assessment. Water Science & Technology, 52(5), 35–42. https://doi.org/10.2166/wst.2005.0103

Krueger, E., Klinkhamer, C., Urich, C., Zhan, X., & Rao, P. S. C. (2017). Generic patterns in the evolution of urban water networks: Evidence from a large Asian city. Physical Review E, 95(3), Article 032312. https://doi.org/10.1103/PhysRevE.95.032312

Kuichling, E. (1889). The relation between the rainfall and the discharge of sewers in populous districts. Transactions of the American Society of Civil Engineers, 20(1), 1–56. https://doi.org/10.1061/TACEAT.0000694

Laakso, T., Ahopelto, S., Lampola, T., Kokkonen, T., & Vahala, R. (2018). Estimating water and wastewater pipe failure consequences and the most detrimental failure modes. Water Supply, 18(3), 901–909. https://doi.org/10.2166/ws.2017.164

LaBrecque, S. (2015, March 2). Water loss: Seven things you need to know about an invisible global problem. The Guardian. https://www.theguardian.com/sustainable-business/2015/mar/02/water-loss-

eight-things-you-need-to-know-about-an-invisible-global-problem

Langeveld, J. (2004). Interactions within wastewater systems [Doctoral thesis, Delft University of Technology]. https://repository.tudelft.nl/islandora/object/uuid:c0e869ee-b376-42e4-b733-2fbe23c6add6/datastream/OBJ/download

Langeveld, J., & Schilperoort, R. (2019). Stedelijk Water 2040: hemelwater verbindt! [Urban water 2040: Rainwater connects!] [White paper]. Partners4UrbanWater. https://www.urbanwater.nl/Files/190604_Whitepaper_hemelwater_verbindt.pdf

Langeveld, J., Veldkamp, R. G., & Clemens, F. (2005). Suspended solids transport: An analysis based on turbidity measurements and event based fully calibrated hydrodynamic models. Water Science & Technology, 52(3), 93–101. https://doi.org/10.2166/wst.2005.0065

Le Gauffre, P., Joannis, C., Vasconcelos, E., Breysse, D., Gibello, C., & Desmulliez, J.-J. (2007). Performance indicators and multicriteria decision support for sewer asset management. Journal of Infrastructure Systems, 13(2), 105–114. https://doi.org/10.1061/(ASCE)1076-0342(2007)13:2(105)

Lloyd-Davies, D. E. (1906). The elimination of storm-water from sewerage systems. Minutes of the Proceedings of the Institution of Civil Engineers, 164(1906), 41–67. https://doi.org/10.1680/imotp.1906.16637

Lukas, A., & Merrill, S. (2006). Scraps: An expert system for prioritizing sewer inspections. No-Dig-2006, Nashville, North American.

Mair, M., Sitzenfrei, R., Kleidorfer, M., Möderl, M., & Rauch, W. (2012). GIS-based applications of sensitivity analysis for sewer models. Water Science & Technology, 65(7), 1215–1222. https://doi.org/10.2166/wst.2012.954

Mair, M., Zischg, J., Rauch, W., & Sitzenfrei, R. (2017). Where to find water pipes and sewers?—On the correlation of infrastructure networks in the urban environment. Water, 9(2), Article 146. https://doi.org/10.3390/w9020146

Mala-Jetmarova, H., Barton, A., & Bagirov, A. (2015). A history of water distribution systems and their optimisation. Water Supply, 15(2), 224–235. https://doi.org/10.2166/ws.2014.115

Mancuso, A., Compare, M., Salo, A., Zio, E., & Laakso, T. (2016). Risk-based optimization of pipe inspections in large underground networks with imprecise information. Reliability Engineering & System Safety, 152, 228–238. https://doi.org/10.1016/j.ress.2016.03.011

Marlow, D. R., Beale, D. J., & Burn, S. (2010). A pathway to a more sustainable water sector: Sustainability-based asset management. Water Science & Technology, 61(5), 1245–1255. https://doi.org/10.2166/wst.2010.043

Masucci, A. P., Stanilov, K., & Batty, M. (2013). Limited urban growth: London's street

network dynamics since the 18th century. PLoS ONE, 8(8), Article e69469. https://doi.org/10.1371/journal.pone.0069469

McDonald, S. E., & Zhao, J. Q. (2001). Condition assessment and rehabilitation of large sewers. In M. Knight & N. Thomson (Eds.), Underground infrastructure research: Municipal, industrial and environmental applications (pp. 361–370). CRC Press. http://doi.org/10.1201/9781003077480

McKeown, T., Brown, R. G., & Record, R. G. (1972). An interpretation of the modern rise of population in Europe. Population Studies, 26(3), 345–382. https://doi.org/10.2307/2173815

McMath, R.E. (1887). Determination of the size of sewers. Transactions of the American Society of Civil Engineers, 16, 179-190.

Meng, F., Fu, G., Farmani, R., Sweetapple, C., & Butler, D. (2018). Topological attributes of network resilience: A study in water distribution systems. Water Research, 143, 376–386. https://doi.org/10.1016/j.watres.2018.06.048

Mesman, G. (2018). KWR, Cavlar. Download Test Models. http://waterware.kwrwater.nl/Cavlar/Testmodels/

Metcalf, L., & Eddy, H.P. (1914). American sewerage practice. McGraw-Hill Book Company, Inc.

Metcalfe, C. A. (2020). Contributions to improved risk and vulnerability assessment of critical infrastructure [Doctoral thesis, University of Stavanger]. UiS Brage. https://hdl.handle.net/11250/2688801

Michaud, D., & Apostolakis, G. E. (2006). Methodology for Ranking the Elements of Water-Supply Networks. Journal of Infrastructure Systems, 12(4), 230–242. https://doi.org/10.1061/(asce)1076-0342(2006)12:4(230)

Möderl, M., Kleidorfer, M., Sitzenfrei, R., & Rauch, W. (2009). Identifying weak points of urban drainage systems by means of VulNetUD. Water Science & Technology, 60(10), 2507–2513. https://doi.org/10.2166/wst.2009.664

Möderl, M., & Rauch, W. (2011). Spatial risk assessment for critical network infrastructure using sensitivity analysis. Frontiers of Earth Science, 5(4), 414–420. https://doi.org/10.1007/s11707-011-0202-1

Moore, E. C. S. (1898). Sanitary engineering. a practical treatise on the collection, removal and final disposal of sewage and the design and construction of works of drainage and sewerage. [s.n.]

Moors, J., Scholten, L., van der Hoek, J. P., & den Besten, J. (2018). Automated leak localization performance without detailed demand distribution data. Urban Water Journal, 15(2), 116–123. https://doi.org/10.1080/1573062X.2017.1414272

Mulvany, T. J. (1851). On the use of self-registering rain and flood gauges, in making observations of the relations of rain fall and of flood discharges in a given catchment. The Transactions and Minutes of Proceedings of the Institution of

Civil Engineers of Ireland, 4(2), 18–33.

NetworkX Developers. (n.d.). min_cost_flow. NetworkX.
https://networkx.org/documentation/stable/reference/algorithms/generated/ne
tworkx.algorithms.flow.min_cost_flow.html

Nederlands Instituut Bedrijfshulpverlening (2016). 15 miljoen liter water teisterde VUmc
[15 million litres of water damaged VUmc]. http://www.technisch-
tekstwerk.nl/wp-content/uploads/2016/11/%0ANIBHV-Veiligheid-67-
wateroverlast-VUMc.pdf

Ostfeld, A. (2015). Water distribution networks. In E. Kyriakides & M. Polycarpou (Eds.),
Intelligent monitoring, control, and security of critical infrastructure systems
(pp. 101–124). Springer. https://doi.org/10.1007/978-3-662-44160-2_4

Papadakis, G. A. (1999). Major hazard pipelines: a comparative study of onshore
transmission accidents. Journal of Loss Prevention in the Process Industries,
12(1), 91–107. https://doi.org/10.1016/s0950-4230(98)00048-5

Pederson, P., Dudenhoeffer, D., Hartley, S., & Permann, M. (2006). Critical infrastructure
interdependency modeling: a survey of US and international research. Idaho
National Laboratory, 25, 27.

Pienaar, M. (2013). Outcomes from a sewer maintenance backlog investigation. In
Proceedings of the 77th Annual Conference of the Institute of Municipal
Engineering of South Africa (pp. 163–168). 3S Media.
https://www.imesa.org.za/wp-content/uploads/2015/08/Paper-19-Outcomes-
from-a-Sewer-Backlog-Study-Morne-Pienaar.pdf

Pocock, R. G., Lawrence, G. J. L., & Taylor, M. E. (1980). Behaviour of a shallow buried
pipeline under static and rolling wheel loads (Transport and Road Research
Laboratory Report No. 954). Transport and Road Research Laboratory.

Porta, S., Crucitti, P., & Latora, V. (2006). The network analysis of urban streets: A dual
approach. Physica A: Statistical Mechanics and Its Applications, 369(2), 853–866.
https://doi.org/10.1016/j.physa.2005.12.063

Post, J. A. B. (2016). A statistical approach to guide the management of the anterior part
of the sewer system [Doctoral thesis, Delft University of Technology]. TUDelft.
https://doi.org/10.4233/uuid:8cb16d1a-44e0-4798-b638-88b5b74d6bd6

Preston, S. H., & van de Walle, E. (1978). Urban French mortality in the nineteenth
century. Population Studies, 32(2), 275–297. https://doi.org/10.2307/2173562

Raphson, J. (1697). Analysis aequationum universalis seu ad aequationes algebraicas
resolvendas methodus generalis, & expedita, ex nova infinitarum serierum
methodo, deducta ac demonstrata [Analysis of universal equations, or general
method for solving algebraic equations, has been developed and demonstrated
from a new method of infinite series] (2nd ed.). Typis Tho. Braddyll, prostant
venales apud Johannem Taylor. https://doi.org/10.3931/e-rara-13516

References

Rauch, W., Bach, P. M., Brown, R., Deletic, A., Ferguson, B., de Haan, F. J., McCarthy, D. T., Kleidorfer, M., Tapper, N., Sitzenfrei, R., & Urich, C. (2012, September 4–6). Modelling transitions in urban drainage management [Paper presentation]. 9th International Conference on Urban Drainage Modelling, Belgrade, Serbia.

Reyes-Silva, J. D., Helm, B., & Krebs, P. (2020). Meshness of sewer networks and its implications for flooding occurrence. Water Science & Technology, 81(1), 40–51. https://doi.org/10.2166/wst.2020.070

Rinaldi, S. M., Peerenboom, J. P., & Kelly, T. K. (2001). Identifying, understanding, and analyzing critical infrastructure interdependencies. IEEE Control Systems Magazine, 21(6), 11–25. https://doi.org/10.1109/37.969131

Rodrigue, J.-P. (with Comtois, C., & Slack, B.). (2017). The geography of transport systems (4th ed.). Routledge.

Sahimi, M. (1994). Applications of percolation theory. Taylor & Francis.

Salman, B., & Salem, O. (2012). Risk assessment of wastewater collection lines using failure models and criticality ratings. Journal of Pipeline Systems Engineering and Practice, 3(3), 68–76. https://doi.org/10.1061/(ASCE)PS.1949-1204.0000100

Schuitema, I. (1998). Kasper and his sewerage rule. The Journal of the Oughtred Society, 7(2), 54–56.

Sitzenfrei, R., Mair, M., Möderl, M., & Rauch, W. (2011). Cascade vulnerability for risk analysis of water infrastructure. Water Science & Technology, 64(9), 1885–1891. https://doi.org/10.2166/wst.2011.813

Snow, J. (1855). On the mode of communication of cholera (2nd ed.). John Churchill. https://books.google.nl/books?hl=nl&lr=&id=-N0_AAAAcAAJ&oi=fnd&pg=PA1&dq=On+the+mode+of+communication+of+cholera.&ots=mXNdIrMqOV&sig=qA7hI-REPp_LNirAg9KOeqI8AXQ#v=onepage&q=On%20the%20mode%20of%20communication%20of%20cholera.&f=false

Stauffer, D., & Aharony, A. (1991). Introduction to percolation theory (Rev. 2nd ed.). Taylor & Francis. https://doi.org/10.1201/9781315274386

Stevenson, R. L. (2013). Robert Louis Stevenson's Admiral Guinea: "Don't judge each day by the harvest you reap but by the seeds that you plant." A Word To The Wise. (Original work published 1884)

Stichting RIONED. (2004). Leidraad Riolering, Module C2100: Rioleringsberekeningen, hydraulisch functioneren [Sewerage guideline, Module C2100: Sewage calculations, hydraulic performance]

Stichting RIONED. (2020, September 8). Composietbuien beschikbaar in de Kennisbank Stedelijk Water [Composite storm event available in the Urban Water Knowledge Base]. https://www.riool.net/nieuws/composietbuien-beschikbaar-in-de-kennisbank-stedelijk-water

Stockmayer, W. H. (1944). Theory of molecular size distribution and gel formation in branched polymers: II. General cross linking. The Journal of Chemical Physics, 12(4), 125–131. https://doi.org/10.1063/1.1723922

Symons, I. F., Chard, B., & Carder, D. R. (1982). Ground movements caused by deep trench construction. In Restoration of sewerage systems (pp. 87–104). Thomas Telford. https://doi.org/10.1680/ross.01459.0013

Szreter, S. (1997). Economic growth, disruption, deprivation, disease, and death: On the importance of the politics of public health for development. Population and Development Review, 23(4), 693–728. https://doi.org/10.2307/2137377

ten Veldhuis, J. A. E., & Clemens, F. H. L. R. (2011). The efficiency of asset management strategies to reduce urban flood risk. Water Science & Technology, 64(6), 1317–1324. https://doi.org/10.2166/wst.2011.715

Todini, E. (2000). Looped water distribution networks design using a resilience index based heuristic approach. Urban Water, 2(2), 115–122. https://doi.org/10.1016/S1462-0758(00)00049-2

Tscheikner-Gratl, F., Bellos, V., Schellart, A., Moreno-Rodenas, A., Muthusamy, M., Langeveld, J., Clemens, F., Benedetti, L., Rico-Ramirez, M. A., Fernandes de Carvalho, R., Breuer, L., Shucksmith, J., Heuvelink, G. B. M., & Tait, S. (2019). Recent insights on uncertainties present in integrated catchment water quality modelling. Water Research, 150, 368–379. https://doi.org/10.1016/j.watres.2018.11.079

Tscheikner-Gratl, F., Caradot, N., Cherqui, F., Leitão, J. P., Ahmadi, M., Langeveld, J. G., Le Gat, Y., Scholten, L., Roghani, B., Rodríguez, J. P., Lepot, M., Stegeman, B., Heinrichsen, A., Kropp, I., Kerres, K., do Céu Almeida, M., Bach, P. M., Moy de Vitry, M., Marques, A. S., . . . Clemens, F. (2019). Sewer asset management – State of the art and research needs. Urban Water Journal, 16(9), 662–675. https://doi.org/10.1080/1573062X.2020.1713382

Tscheikner-Gratl, F., Sitzenfrei, R., Rauch, W., & Kleidorfer, M. (2016). Integrated rehabilitation planning of urban infrastructure systems using a street section priority model. Urban Water Journal, 13(1), 28–40. https://doi.org/10.1080/1573062X.2015.1057174

United Nations Department of Economic and Social Affairs. (2019). World urbanization prospects: The 2018 revision. United Nations. https://doi.org/10.18356/b9e995fe-en

United Nations Development Programme. (2006). Human development report 2006: Beyond scarcity: Power, poverty and the global water crisis. https://hdr.undp.org/system/files/documents//human-development-report-2006-english.human-development-report-2006-english

Vaes, G., Feyaerts, T., & Swartenbroekx, P. (2009). Influence and modelling of urban runoff

on the peak flows in rivers. Water Science & Technology, 60(7), 1919–1927. https://doi.org/10.2166/wst.2009.638

Vaes, G., Luyckx, G., & Berlamont, J. (n.d.). Nieuwe tendensen in het rioleringsontwerp [New trends in sewer design] [Workshop summary]. https://bwk.kuleuven.be/hydr/downloads/adwel7-2.pdf

van Bijnen, M., Korving, H., & Clemens, F. (2012). Impact of sewer condition on urban flooding: An uncertainty analysis based on field observations and Monte Carlo simulations on full hydrodynamic models. Water Science & Technology, 65(12), 2219–2227. https://doi.org/10.2166/wst.2012.134

van Bijnen, M., Korving, H., Langeveld, J., & Clemens, F. (2017). Calibration of hydrodynamic model-driven sewer maintenance. Structure and Infrastructure Engineering, 13(9), 1167–1185. https://doi.org/10.1080/15732479.2016.1247287

van Bijnen, M., Korving, H., Langeveld, J., & Clemens, F. (2018). Quantitative impact assessment of sewer condition on health risk. Water, 10(3), Article 245. https://doi.org/10.3390/w10030245

van Riel, W. (2016). On decision-making for sewer replacement [Doctoral thesis, Delft University of Technology]. TUDelft. https://doi.org/10.4233/uuid:92b10448-795d-43ac-8071-d779af9d374d

Vereniging van Nederlandse Gemeenten. (2021). Kernbeleid Veiligheid 2021: Handreiking voor gemeenten [Core Safety Policy 2021: Guide for municipalities]. https://vng.nl/sites/default/files/2021-03/kernbeleid-veiligheid-2021_def.pdf

Voor tientallen miljoenen schade aan VUmc door wateroverlast [For tens of millions of damage to VUmc by flooding]. (2015, September 9). NU.nl. https://www.nu.nl/binnenland/4122553/tientallen-miljoenen-schade-vumc-wateroverlast.html

Voronoï, G. (1908). Nouvelles applications des paramètres continus à la théorie des formes quadratiques : Deuxième mémoire : Recherches sur les parallélloèdres primitifs [New applications of continuous parameters to the theory of quadratic forms: Second dissertation: Research on primitive paralleloids]. Journal für die reine und angewandte Mathematik, 1908(134), 198–287. https://doi.org/10.1515/crll.1908.134.198

Walski, T. M. (2006). A history of water distribution. Journal AWWA, 98(3), 110–121. https://doi.org/10.1002/j.1551-8833.2006.tb07611.x

Wang, H., & Van Mieghem, P. (2010). Algebraic connectivity optimization via link addition. In M. Murata & O. Akan (Eds.), 3rd International ICST Conference on Bio-Inspired Models of Network, Information, and Computing Systems, BIONETICS 2008. ICST. https://doi.org/10.4108/icst.bionetics2008.4691

Ward, B., & Savić, D. A. (2012). A multi-objective optimisation model for sewer rehabilitation considering critical risk of failure. Water Science & Technology,

66(11), 2410–2417. https://doi.org/10.2166/wst.2012.393

Wasserman, S., & Faust, K. (1994). Social network analysis: Methods and applications. Cambridge University Press. https://doi.org/10.1017/CBO9780511815478

Watanabe, T., & Masuda, N. (2010). Enhancing the spectral gap of networks by node removal. Physical Review E, 82(4), Article 046102. https://doi.org/10.1103/PhysRevE.82.046102

Watts, D. J. (1999). Small worlds: The dynamics of networks between order and randomness. Princeton University Press.

Watts, D. J., & Strogatz, S. H. (1998). Collective dynamics of 'small-world' networks. Nature, 393(6684), 440–442. https://doi.org/10.1038/30918

Welsh, J. (2014, December 16). Here's what's causing the disgusting London sewer blockages. Insider. https://www.businessinsider.com/fatbergs-causing-london-sewer-blockages-2014-12?international=true&r=US&IR=T

Wirahadikusumah, R., Abraham, D., & Iseley, T. (2001). Challenging issues in modeling deterioration of combined sewers. Journal of Infrastructure Systems, 7(2), 77–84. https://doi.org/10.1061/(ASCE)1076-0342(2001)7:2(77)

Yazdani, A., Otoo, R. A., & Jeffrey, P. (2011). Resilience enhancing expansion strategies for water distribution systems: A network theory approach. Environmental Modelling & Software, 26(12), 1574–1582. https://doi.org/10.1016/j.envsoft.2011.07.016

Yen, C. B. (1987). Urban drainage hydraulics and hydrology; From art to science. In Proceedings of 4th International Conference on Urban Storm Draiange, IUCUSD, Lausanne, Switzerland (pp. 135–154).

Yerri, S. R., Piratla, K. R., Matthews, J. C., Yazdekhasti, S., Cho, J., & Koo, D. (2017). Empirical analysis of large diameter water main break consequences. Resources, Conservation and Recycling, 123, 242–248. https://doi.org/10.1016/j.resconrec.2016.03.015

Zischg, J., Klinkhamer, C., Zhan, X., Krueger, E., Ukkusuri, S., Rao, P. S. C., Rauch, W., & Sitzenfrei, R. (2017). Evolution of complex network topologies in urban water infrastructure. In C. N. Dunn & B. Van Weele (Eds.), Selected papers from the World Environmental and Water Resources Congress 2017: Hydraulics and waterways and water distribution systems analysis (pp. 648–659). American Society of Civil Engineers. https://doi.org/10.1061/9780784480625.061

Zischg, J., Klinkhamer, C., Zhan, X., Rao, P. S. C., & Sitzenfrei, R. (2019). A century of topological coevolution of complex infrastructure networks in an alpine city. Complexity, 2019, Article 2096749. https://doi.org/10.1155/2019/2096749

194

A   Abbreviations

BEMP   Best Environmental Management Practices
CARL   Current Annual Real Losses
CoF   Consequence of Failure
CSS   Combined Sewer System
CSO   Combined Sewer Outfall
EU   European Union
GTM   Graph Theory Method
GBWLM   Graph-Based Weakest Link Method
HBWLM   Hydrodynamic Model-Based Weakest Link Method
ICBMs   Integral Component-Based Models
ILI   Infrastructure Leakage Index
IUDMs   Integral Urban Drainage Models
IUWCMs   Integral Urban Water Cycle Models
IUWSMs   Integral Urban Water System Models
LoF   Likelihood of Failure
NLP   Network Linearisation Parameter
SSO   Storm Sewer Outflow
SWS   Storm Water Systems
UARL   Unavoidable Annual Real Losses
UDN   Urban Drainage Network
WDN   Water Distribution Network
WPS   Water Pumping Station

B   Results and analysis of water distribution networks

B.1   Tuindorp water distribution network

Figure B.1 presents the correlation between the outcomes and the F1 score of the Hydrodynamic model-Based Weakest Link Method (HBWLM) and the graph theory method (GTM) for Tuindorp's Water Distribution Network (WDN) for the connection points with water consumers.
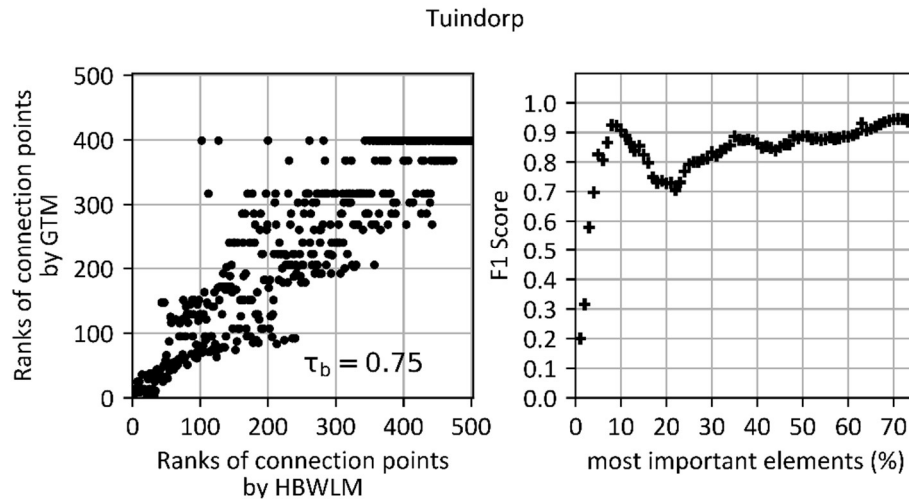

Figure B.1   Overview of the correlation between the outcomes and the F1 score of the hydrodynamic model-based weakest link method and the graph theory method for the water distribution network of Tuindorp, with a pressure drop of 20 m for the connection points with water consumers. The figure shows that for the 1–5% most critical elements, the F1 score increases from 0.17 to 0.79. The other F1 scores are greater than 0.69.

B.2   Leimuiden water distribution network

Figure B.2 presents the correlation between the outcomes and the F1 score of the HBWLM and the GTM for Leimuiden's WDN for the connection points with water consumers.
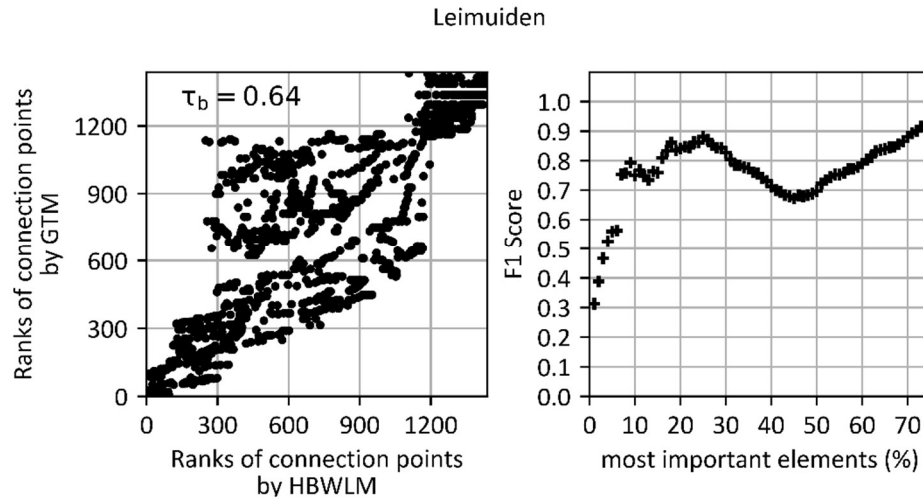
Leimuiden

Figure B.2   Overview of the correlation between the outcomes and the F1 score of the hydrodynamic model-based weakest link method and the graph theory method for the water distribution network of Leimuiden with, a pressure drop of 20 m for the connection points with water consumers.

Figure B.3 presents the correlation between the outcomes and the F1 score of the HBWLM and the GTM for Leimuiden's WDN for the connection points with water consumers, based on the weighting evaluation method.
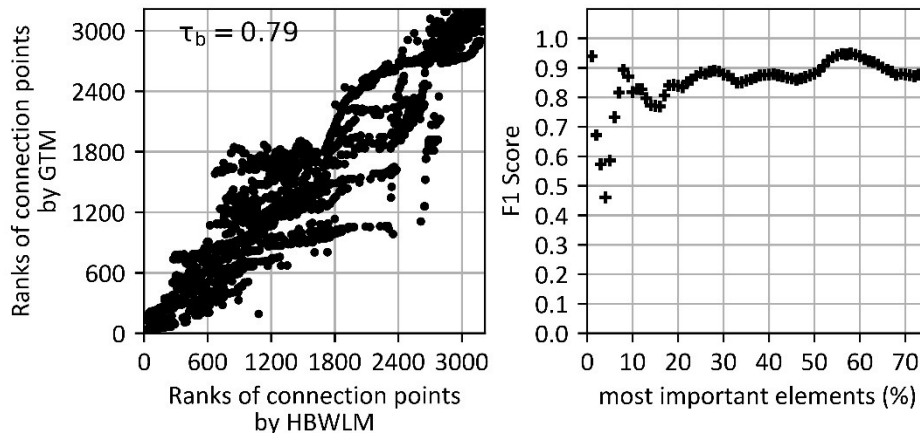
Leimuiden

Figure B.3   Overview of the correlation between the outcomes and the F1 score of the hydrodynamic model-based weakest link method and the graph theory method for the Leimuiden water distribution network with a pressure drop of 20 m for the connection points with water consumers. The criticality is based on sum of (costs to water pumping station)$^{-1}$ for the nodes where the costs to the leak is less than to the water pumping station.

B.3   Analysis of the criticality for different head losses

Figure B.4–Figure B.6 present comparisons between the results of the HBWLM (pressure drop of 20 m in leak) for the WDNs of Cavlar, Tuindorp and Leimuiden, respectively, ranked by the number of nodes with a pressure below a threshold (11, 15, 20 and 25 m or 16, 20, 25 and 30 m), and the GTM for those WDNs.

Figure B.4   Overview of the comparison of the results of the hydrodynamic model-based weakest link method (pressure drop in leak is 20 m) ranked on the number of nodes with a pressure below a threshold (11, 15, 20 and 25 m) and the graph theory method (evaluation method 1) for the Cavlar water distribution network.
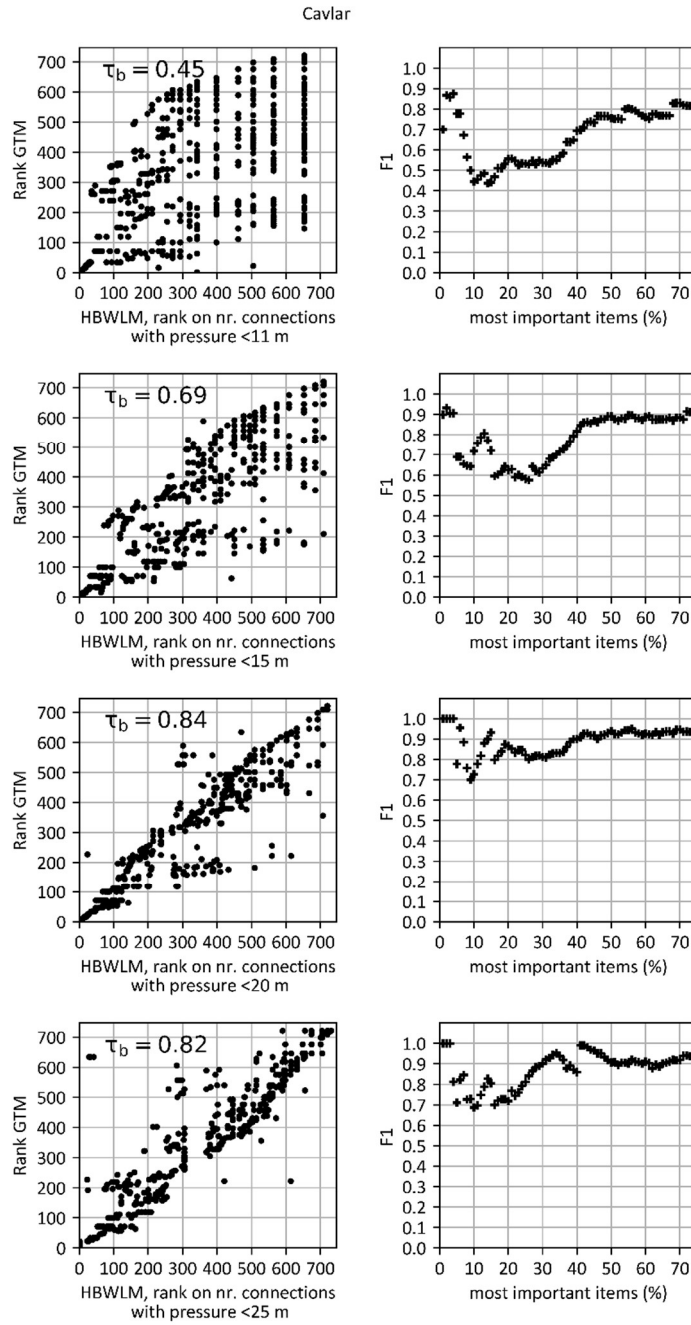
Figure B.5   Overview of the comparison of the results of the hydrodynamic model-based weakest link method (pressure drop in leak is 20 m) ranked on the number of nodes with a pressure below a threshold (16, 20, 25 and 30 m) and the graph theory method (evaluation method 1) of Tuindorp's water distribution network.
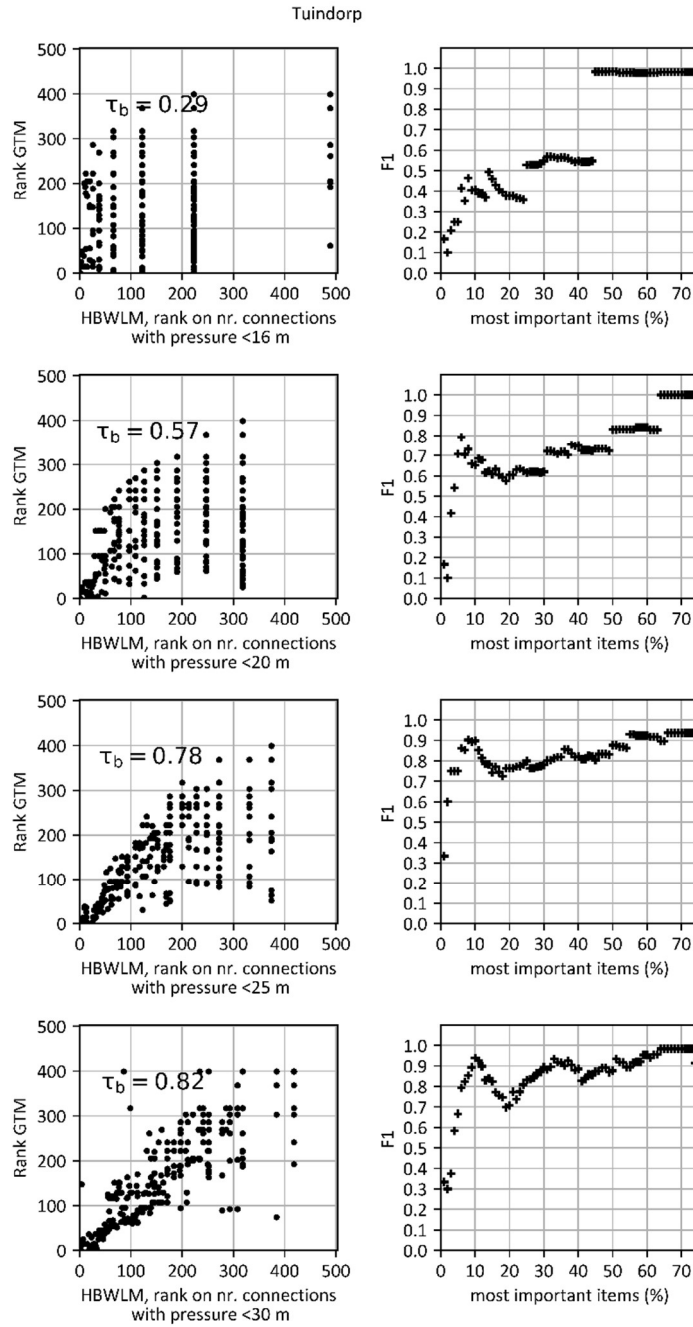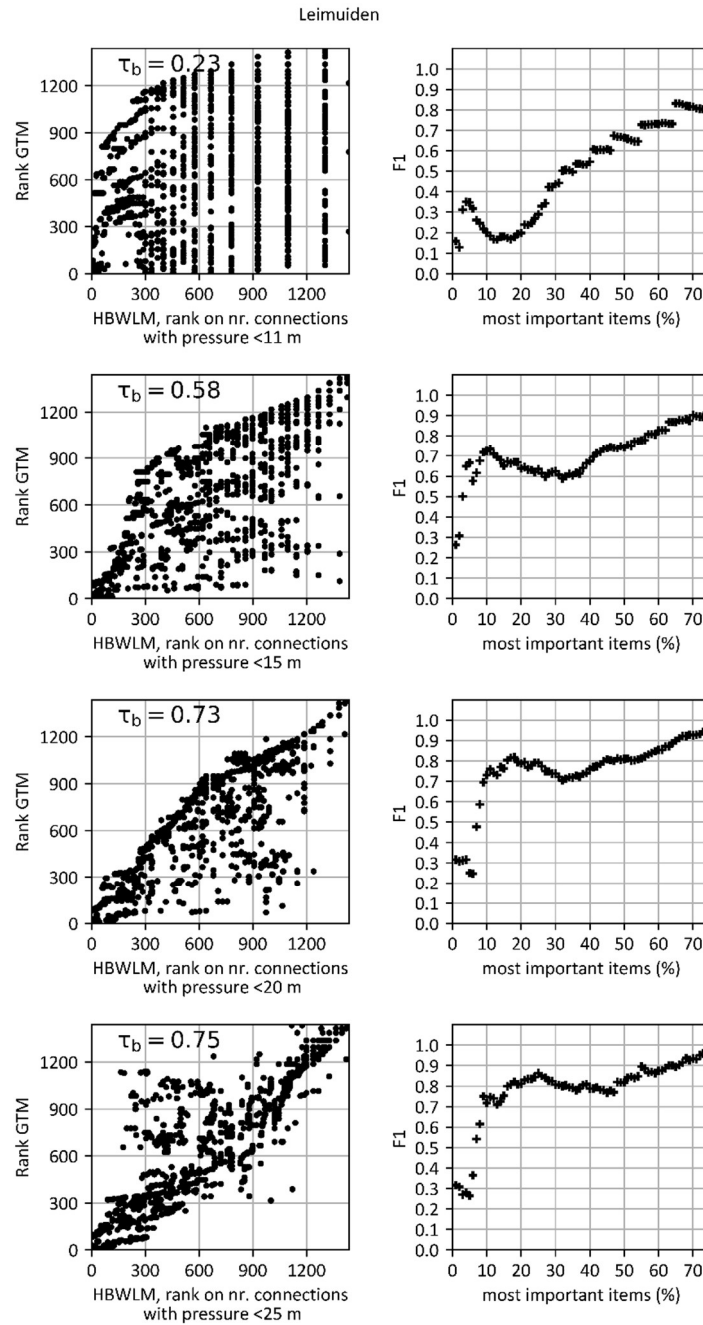
Leimuiden

Figure B.6   Overview of the comparison of the results of the hydrodynamic model-based weakest
link method (pressure drop in leak is 20 m) ranked on the number of nodes with a
pressure below a threshold (11, 15, 20 and 25 m) and the graph theory method
(evaluation method 1) of the water distribution network of Leimuiden.

B.4   Effect of number of iterations

Figure B.7 presents the criticality of elements of the WDN of Cavlar based on 2, 5, 10 and 25 iterations, compared with the base scenario of 100 iterations.
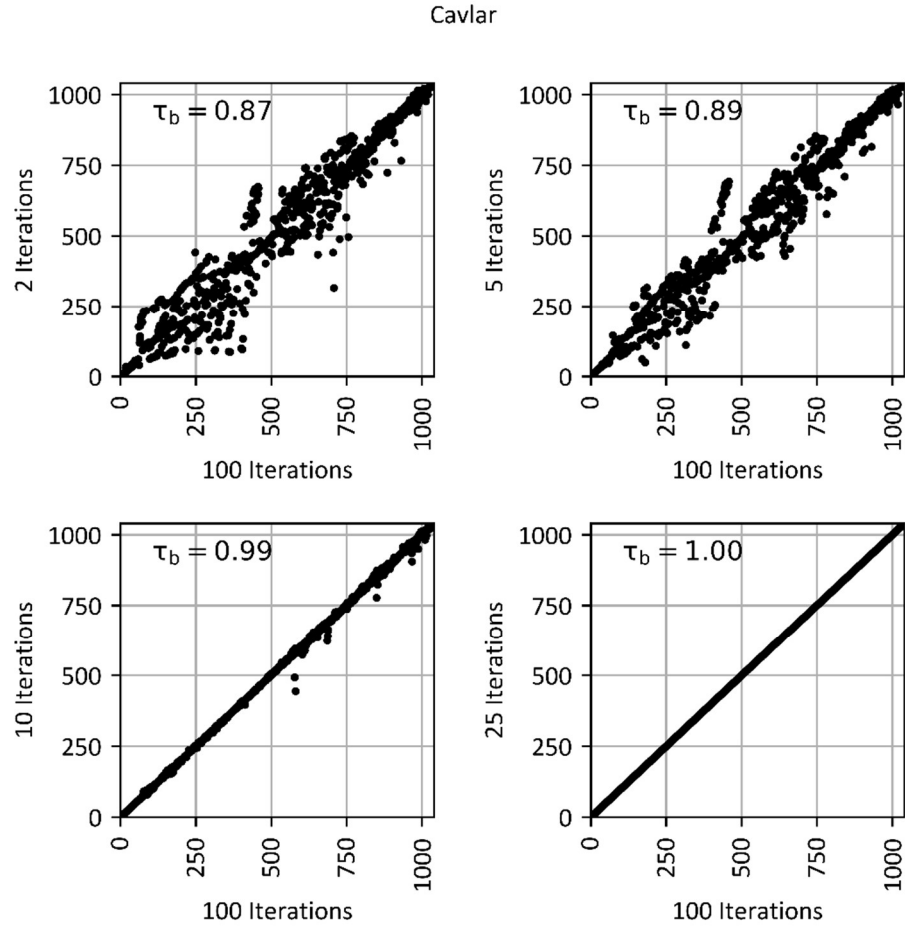
Cavlar

Figure B.7   Overview of the criticality of the elements of the water distribution network of Cavlar, based on 2, 5, 10 and 25 iterations, compared with the base scenario of 100 iterations.

C Load on the GBWLM and validation results

C.1 Inflow of the subsystems

The load on a gully pot is equal to the precipitation intensity multiplied by the connected paved surface (Equation C.1).

$$Q_{in\ gully\ pot} = A * \frac{P \times \Delta t}{1000} \qquad (C.1)$$

where $Q_{in\ gully\ pot}$ is the inflow in the gully pot (m³/s), A is the paved area connected to a gully pot (m²), Δt is time interval (s) and P is the precipitation (mm/s).

The outflow of the gully pots depends on the inflow, available storage volume and the outflow capacity. This is described with Equations C.3.

$$\left.\begin{array}{c} \Delta t \times Q_{in} + S_{t-1} > \Delta t \times Q_{structure} \rightarrow Q_{out} = Q_{structure} \\ S_t = S_{t-1} + \Delta t \times (Q_{in} - Q_{out}) \\ \Delta t \times Q_{in} + S_{t-1} \leq \Delta t \times Q_{structure} \rightarrow Q_{out} = Q_{in} + S_{t-1} \\ S_t = S_{t-1} + \Delta t \times (Q_{in} - Q_{out}) \end{array}\right\} \qquad (C.2)$$

where Q_{out} is the outflow of a gully pot (m³/s), $Q_{out\_capacity}$ is the discharge capacity of a gully pot (m³/s), Δt is time interval (s), S_t is the storage on timestep t (m³) and S_{t-1} is the storage on timestep $t-1$ (m³).

The inflow in the storm sewer network varies per event and manhole. The inflow consists of two components (Equation C.3):
- Runoff from paved areas via the gully pots.
- Runoff from roofs.

The total inflow is derived from the outflow of the gully pots connected to a manhole and the ratio between the paved area and the total runoff connected to a manhole.

$$Q_{in\ manhole\ j} = \left(\frac{\sum_1^n Q_{out\ i}}{\sum_1^n A_{paved\ area\ i}} \right) * \left(\left(\sum_1^n A_{paved\ area\ i} \right) + A_{roofs\ j} \right) \qquad \text{(C.3)}$$

where $Q_{in\ manhole\ j}$ is the inflow in a manhole j for an event k (m³/s), $Q_{out\ i}$ is the maximum outflow of gully pot i for an event k (m³/s), $A_{paved\ area\ i}$ is the paved runoff area connected to gully pot i (m²), $A_{roofs\ j}$ is the runoff area of the roofs connected to manhole j (m²) and n is the number of gully pots connected to the manhole j.

The load of the surface water system consists of two components:
- Runoff from roofs and paved areas.
- Discharge of unpaved areas (Equations C.4 and C.5).

$$Q_{in\ sws\ i,t} = \frac{P_t}{1000} \times A_{p-areas\ i} + \alpha \times \left(\frac{S_{i,t-1}}{\Delta t} + \frac{P_t}{1000} \times A_{unp-areas\ i} \right) \qquad \text{(C.4)}$$

$$S_{i,t} = (1 - \alpha) * \left(S_{i,t-1} + \frac{\Delta t \times P_t}{1000} * A_{unp-areas\ i} \right) \qquad \text{(C.5)}$$

where $Q_{in\ sws\ i,\ t}$ is the inflow to the surface water system component i at time step t (m³/day), $A_{p-areas\ I}$ is the runoff of roofs and paved areas connected to component i (m²), $A_{unp-areas\ I}$ is the runoff of unpaved areas connected to component i (m²), Δt is time interval (day), $S_{i,\ t}$ is the storage in the soil in the area of component i, time step t (m³), α is a delay factor (-) and P_t is the daily precipitation, time step t (mm/day).

C.2   Validation results

C.2.1 Validation of the severity of flooding at system level of a storm sewer

The severity of floods, calculated with the GBWLM, was compared with the outcomes of the HBWLM for rainfall intensities, varying from 1–30 mm/h. The flood volume quantified with a hydrodynamic model was tested against the amount of water that cannot be transported by digraph-1 in the GBWLM, for 1 hour. The total maximum stored flood volume of all manholes was compared with the flow through the last edges of digraph-2 before the outfalls (see Figure C.1).
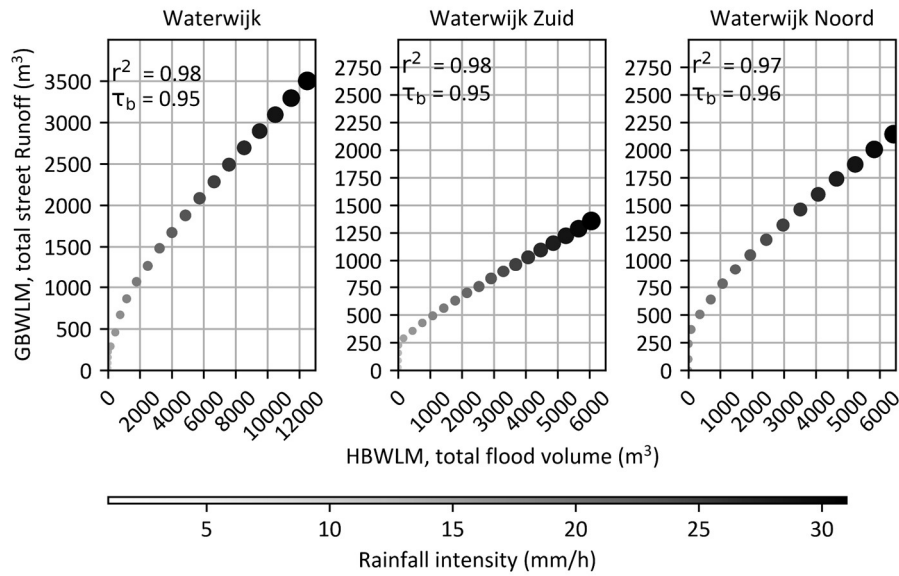
Figure C.1   Comparison of the results of a hydrodynamic model with the graph-based weakest link method storm sewer component, based on the flood volume for various rainfall intensities. The larger and darker the dots, the higher the rainfall intensity.

C.2.2 Validation of the number of flooded manholes

The number of flooded manholes according to the HBWLM was compared with the number according to the GBWLM. Figure C.2 provides an overview of the number of false positives and false negatives. A false positive is defined as a manhole labelled as flooded by the GBWLM when the hydrodynamic model indicated the opposite. The reverse situation is defined as a false negative.
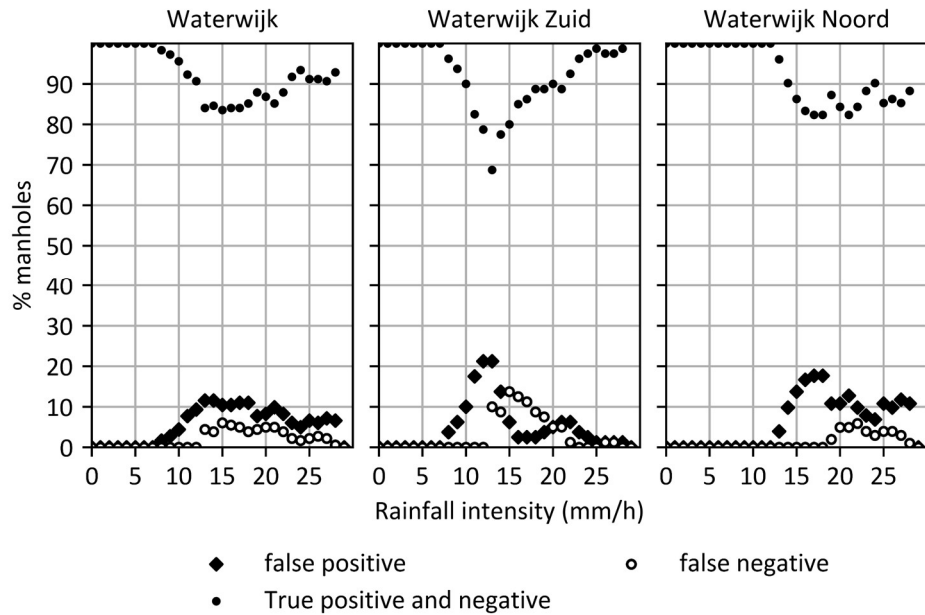
Figure C.2   Overview of the false positives and false negatives of the number of flooded locations with the graph-based weakest link method storm sewer component. In the hydrodynamic model, flooding in Waterwijk Zuid starts at 14 mm/h and in Waterwijk Noord at 17 mm/h.

C.2.3   Validation of the location of flooded manholes

Figure C.3 and Figure C.4 present an overview of the locations of true positives, false positives and false negatives for rain intensities of 15, 20 and 25 mm/h. The figures show that for low rainfall intensity (15 mm/h), the GWBLM tended to overestimate flooding. When the rainfall intensity increased (25 mm/h), the differences became smaller and the GWBLM occasionally underestimated flooding at the transitions from flooded to non-flooded areas.

Overview flooded nodes, rainfall intensity = 15 mm/h

Hydraulic model　　　　　　GBWLM　　　　　　Difference

　　●　Not flooded　　▲　True positive or negative　　■　False negative
　　●　Flooded　　　　✕　False positive

Overview flooded nodes, rainfall intensity = 20 mm/h

Hydraulic model　　　　　　GBWLM　　　　　　Difference

　　●　Not flooded　　▲　True positive or negative　　■　False negative
　　●　Flooded　　　　✕　False positive

Overview flooded nodes, rainfall intensity = 25 mm/h

Hydraulic model　　　　　　GBWLM　　　　　　Difference

　　●　Not flooded　　▲　True positive or negative　　■　False negative
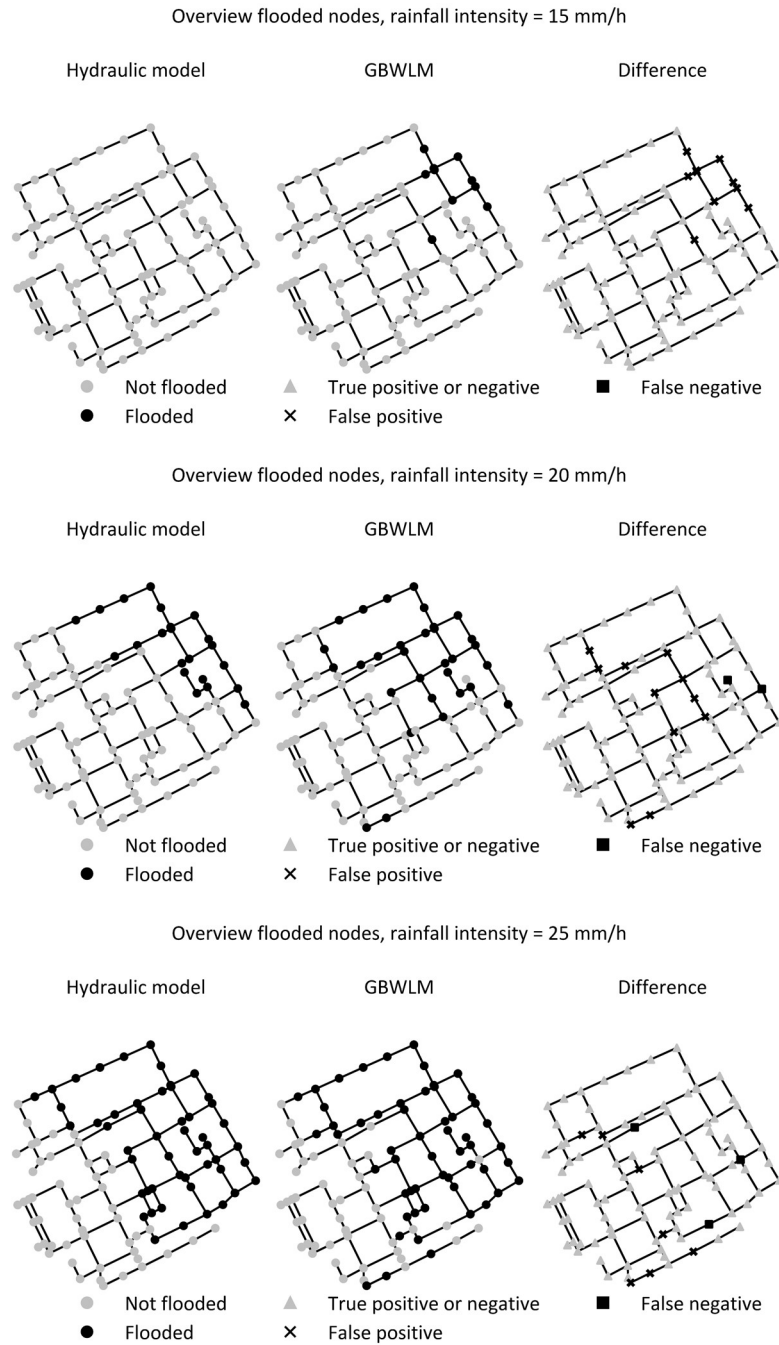　　●　Flooded　　　　✕　False positive

Figure C.3　　Overview of the locations of the hits, false positives and false negatives of Waterwijk Noord for rainfall intensities of 15, 20 and 25 mm/h.

Overview flooded nodes, rainfall intensity = 15 mm/h

Hydraulic model   GBWLM   Difference

● Not flooded   ▲ True positive or negative   ■ False negative
● Flooded   ✕ False positive

Overview flooded nodes, rainfall intensity = 20 mm/h

Hydraulic model   GBWLM   Difference

● Not flooded   ▲ True positive or negative   ■ False negative
● Flooded   ✕ False positive

Overview flooded nodes, rainfall intensity = 25 mm/h

Hydraulic model   GBWLM   Difference

● Not flooded   ▲ True positive or negative   ■ False negative
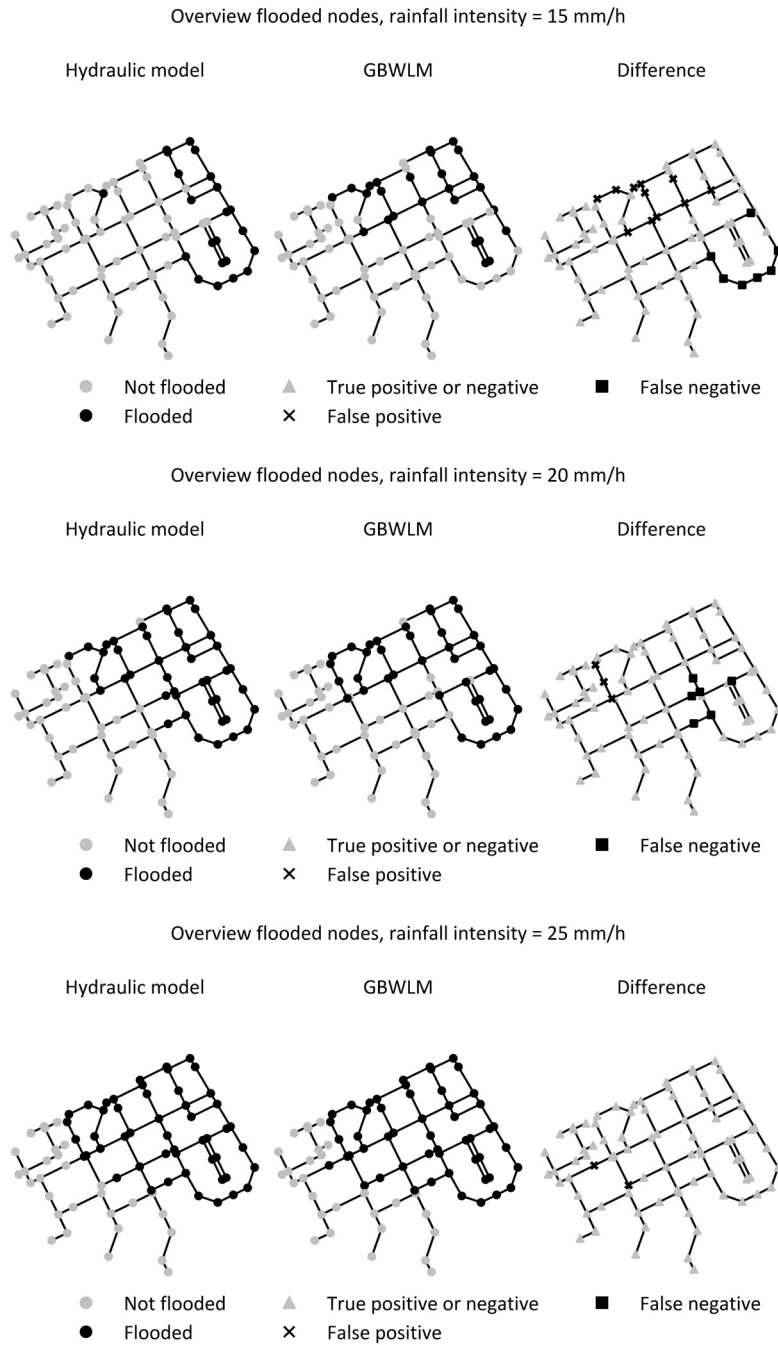● Flooded   ✕ False positive

Figure C.4   Overview of the locations of the hits, false positives and false negatives of Waterwijk Zuid, for rainfall intensities of 15, 20 and 25 mm/h.

Based on the recall and precision, an F1 score was calculated for the various separate rainfall intensities. Furthermore, an overall F1 score for all the simulated intensities was determined. Figure C.5 shows the results. The precision, recall and F1 score were low when the HBWLM only indicated a few flooded nodes and flooding starts.
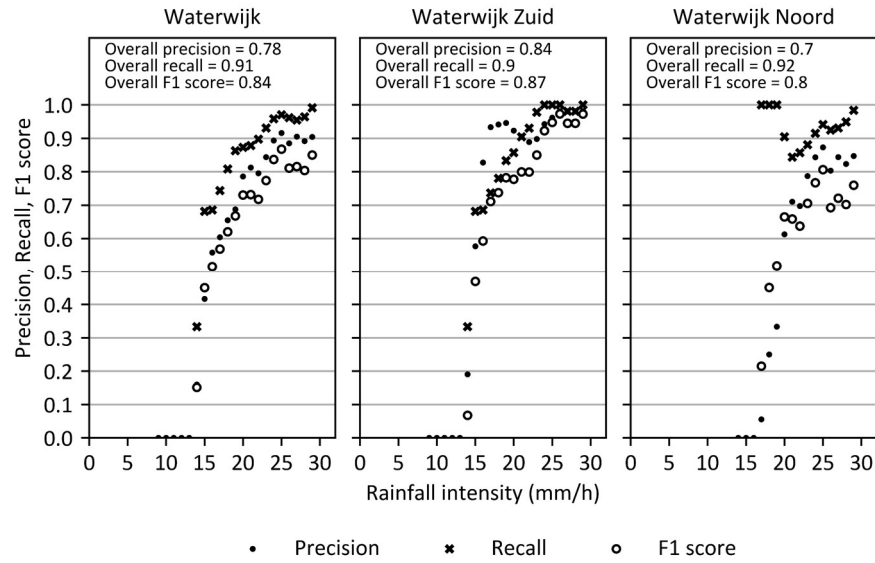

Figure C.5   Overview of the F1, recall and precision of the graph-based weakest link method for the storm sewers of Waterwijk.

C.2.4 Validation of surface water component of the GBWLM

The increase in water levels of the surface water component of the GBWLM were calculated. The results were compared with the results of the HBWLM (see Figure C.6).
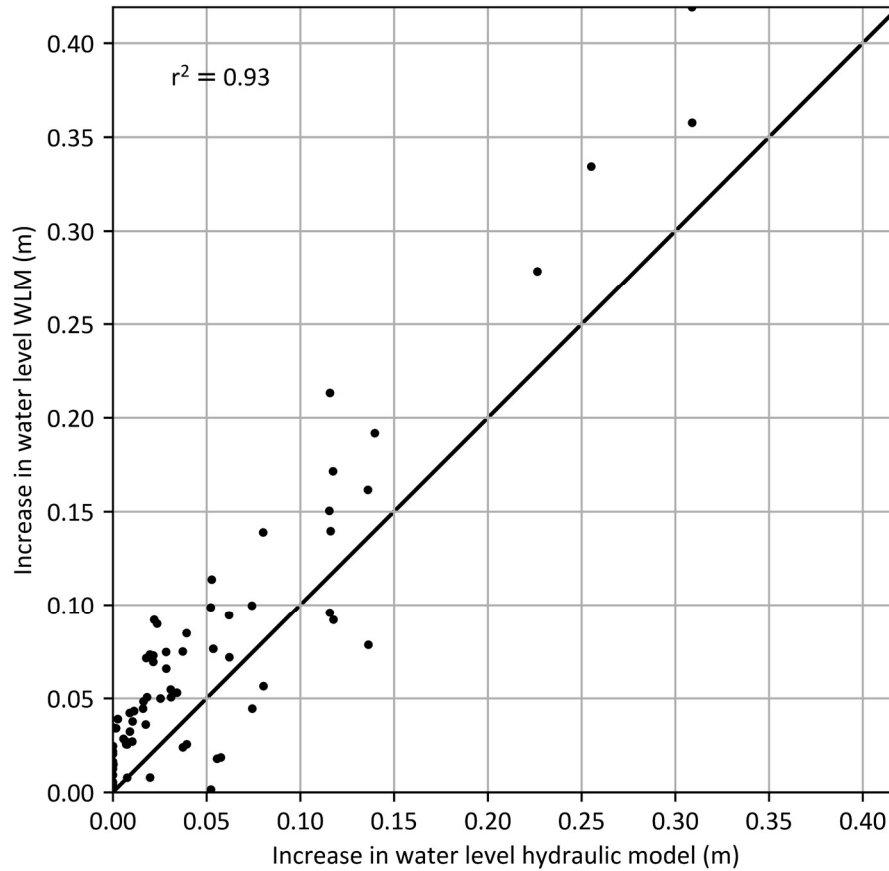

Figure C.6   Relationship between the increase in levels, as a result of storms, of a hydrodynamic bases weakest link method and the graph-based weakest link method for the main part of the surface water system (with a water level of −5.5 m) of Almere.

List of publications

Peer-reviewed journals

Meijer, D., Korving, H., & Clemens-Meyer, F. (2022). A topological characterisation of looped drainage networks. Structure and Infrastructure Engineering, 1–14. https://doi.org/10.1080/15732479.2022.2152464

Meijer, D., Korving, H., Langeveld, J., Clemens, F. (2023). A method to identify the weakest link in urban drainage systems. (submitted to Water Science & Technology under review)

Meijer, D., Post, J., van der Hoek, J.P., Korving, H., Langeveld, J., & Clemens, F. (2020). Identifying critical elements in drinking water distribution networks using graph theory. Structure and infrastructure engineering. doi.org/10.1080/15732479.2020.1751664

Meijer, D., Van Bijnen, M., Langeveld, J., Korving, H., Post, J., & Clemens, F. (2018) Identifying Critical Elements in Sewer Networks Using Graph-Theory. Water, 10(2), 136, doi:10.3390/w10020136

Winsemius, H. C., Ward, P. J., Gayton, I., Ten Veldhuis, M. C., Meijer, D., & Iliffe, M. (2019). Commentary: The Need for a High-Accuracy, Open-Access Global DEM. Frontiers in Earth Science, 7. https://doi.org/10.3389/feart.2019.00033)

Conference papers

Meijer, D., & Clemens, F. (2016). A Fast Method to Identify the Criticality of Individual Components in Water Related Network Systems. In Proceedings of the 8th International Conference on Sewer Processes and Networks. The 8th IWA International Conference on Sewer Processes and Networks, Rotterdam, the Netherlands

Meijer, D., & Clemens, F. (2017). A fast method to identify the criticality of individual components in water supply networks. CCWI 2017 Computing and Control for the Water Industry, Sheffield, UK. https://doi.org/10.15131/shef.data.5363896.v1

National publications

Henckens, G., Bos, R., van Bijnen, M., & Meijer, D. (2008). Meten in de riolering (deel 1). Van aanleiding naar meetprogramma. Vakblad Riolering, 15/1. 19-20.

Henckens, G., Bos, R., van Bijnen, M., & Meijer, D. (2008). Meten in de riolering (deel 2). Van meetplan naar bestek. Vakblad Riolering, 15/2. 18-19.

Meijer, D. & Hartemink, J.W. (2012). Financiering van investeringen in de riolering. Vakblad Riolering, 18/11.

Meijer, D. & Hartemink, J.W. (2012). Perceptiekosten rioolheffing. Vakblad Riolering, 18/11.

Meijer, D. & Smits, J. (2011). WION: een stimulans voor revisieverwerking? Vakblad Riolering, 17/2.

Meijer, D. & Veurink, J. (2014). Afvalwatersysteem geoptimaliseerd. Vakblad Riolering, 20/3. 7-9.

Meijer, D., Bos, R. & Veurink, J. (2012). Gemaaldata, bruikbaar voor meetprojecten? Vakblad Riolering, 18/10. 12-14.

Meijer, D., de Niet, A., Clemens, C., Vruggink, M. & Borghuis, W (2014). Meten in de Riolering: Kosten versus Baten. Vakblad Riolering, 20/1. 30-31.

Meijer, D., Henckens, G., Bos, R. & van Bijnen, M. (2008). Meten in de riolering (deel 3). Van bestek naar uitvoering. Vakblad Riolering, 15/3. 18-19.

Meijer, D., Henckens, G., Bos, R. & van Bijnen, M. (2008). Meten in de riolering (deel 4). Van uitvoering naar bruikbare data. Vakblad Riolering, 15/4. 11-13.

Meijer, D., Henckens, G., Bos, R. & van Bijnen, M. (2008). Meten in de riolering (deel 5). Van data naar informatie. Vakblad Riolering, 15/5. 11-13.

Smits, J. & Meijer, D. (2011). Het beperken van schade bij incidenten. Vakblad Riolering, 17/2.

Stegeman, B., Clemens, F., van Bijnen, J., Korving, J., & Meijer, D. (2013). Hydraulische vingerafdruk als indicator voor de noodzaak van onderhoudsmaatregelen aan riolering. WT-Afvalwater , 13/2. 121-130

van Mameren, H., Klein, J., Meijer, D. Lanfermeijer, B. & Baars, S. (2020). Meten stedelijk watersysteem geeft inzicht en bespaart flink. Land en water, 2020/11.

Wannyn, R., Meijer, D., Te Beest, C., &n Baars-Van der Kraan, S. (2019). Investeer pas in riool als je weet hoe het werkt. Land en Water, 2019/9. 7-9.

About the author

Didrik Meijer was born on 1 September 1977 in Zevenaar, the Netherlands. He pursued his secondary education (VWO) at Greydanus College in Zwolle, the Netherlands. In 1995 Didrik started the study of Civil Engineering and Management at the University of Twente in Enschede, the Netherlands and received his M.Sc. degree in 2000. After his graduation, Didrik moved to Cotahuasi, Peru. During the period of May 2001–February 2004, he was employed at AEDES in Cotahuasi, in the field of irrigation and water management. In October 2004 he started working at Witteveen+Bos, an engineering consultancy company in Deventer, the Netherlands. At Witteveen+Bos, he focussed on the field of hydraulic modelling of sewer systems, sewer monitoring networks and management of sewer systems. Since June 2014 Didrik has been working at Deltares in Delft, the Netherlands, specialising in urban drainage. In 2017, next to his full-time job, he started as a PhD candidate at Delft University of Technology in the section of Sanitary Engineering. His research focussed on the identification of critical elements in urban water infrastructure.